



US Army Corps  
of Engineers

TECHNICAL REPORT GL-87-15

(2)

# COMPARATIVE STUDY OF NONDESTRUCTIVE PAVEMENT TESTING MACDILL AIR FORCE BASE, FLORIDA

AD-A186 082

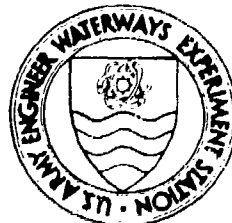
by

Jim W. Hall, Jr.

Geotechnical Laboratory

DEPARTMENT OF THE ARMY  
Waterways Experiment Station, Corps of Engineers  
PO Box 631, Vicksburg, Mississippi 39180-0631

DTIC  
ELECTED  
OCT 14 1987  
S D

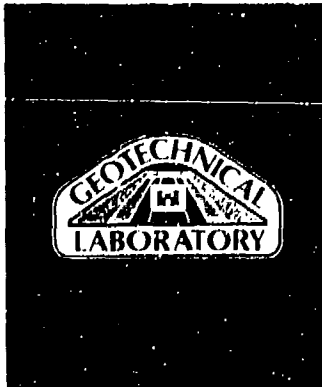


July 1987  
Final Report

Approved For Public Release, Distribution Unlimited

Prepared for Air Force Engineering and Services Center  
Tyndall Air Force Base, Florida 32403

Under Project No. F-82-74



**BEST**

**AVAILABLE**

**COPY**

Unclassified

SECURITY CLASSIFICATION OF THIS PAGE

REPORT DOCUMENTATION PAGE													
1a. REPORT SECURITY CLASSIFICATION Unclassified		1b. RESTRICTIVE MARKINGS											
2a. SECURITY CLASSIFICATION AUTHORITY		3. DISTRIBUTION/AVAILABILITY OF REPORT Approved for public release; distribution unlimited.											
2b. DECLASSIFICATION/DOWNGRADING SCHEDULE													
4. PERFORMING ORGANIZATION REPORT NUMBER(S)  Technical Report GL-87-15		5. MONITORING ORGANIZATION REPORT NUMBER(S)											
6a. NAME OF PERFORMING ORGANIZATION USAEWES Geotechnical Laboratory	6b. OFFICE SYMBOL (If applicable) WESGP-1	7a. NAME OF MONITORING ORGANIZATION											
6c. ADDRESS (City, State, and ZIP Code) PO Box 631 Vicksburg, MS 39180-0631		7b. ADDRESS (City, State, and ZIP Code)											
8a. NAME OF FUNDING/SPONSORING ORGANIZATION Air Force Engineering and Services Center	8b. OFFICE SYMBOL (If applicable)	9. PROCUREMENT INSTRUMENT IDENTIFICATION NUMBER											
8c. ADDRESS (City, State, and ZIP Code) Tyndall Air Force Base, FL 32403		10. SOURCE OF FUNDING NUMBERS  PROGRAM ELEMENT NO.      PROJECT NO.      TASK NO.      WORK UNIT ACCESSION NO. F-82-74											
11. TITLE (Include Security Classification)  Comparative Study of Nondestructive Pavement Testing, MacDill Air Force Base, Florida													
12. PERSONAL AUTHOR(S) Hall, Jim W., Jr.													
13a. TYPE OF REPORT Final report	13b. TIME COVERED FROM Aug 82 TO Sep 83	14. DATE OF REPORT (Year, Month, Day) July 1987	15. PAGE COUNT 271										
16. SUPPLEMENTARY NOTATION Available from National Technical Information Service, 5285 Port Royal Road, Springfield, VA 22161.													
17. COSATI CODES  <table border="1"><tr><th>FIELD</th><th>GROUP</th><th>SUB-GROUP</th></tr><tr><td></td><td></td><td></td></tr><tr><td></td><td></td><td></td></tr></table>		FIELD	GROUP	SUB-GROUP							18. SUBJECT TERMS (Continue on reverse if necessary and identify by block number)  See reverse		
FIELD	GROUP	SUB-GROUP											
19. ABSTRACT (Continue on reverse if necessary and identify by block number)  This project is the most comprehensive single undertaking to date which is directed toward an evaluation of the validity of concepts of nondestructive evaluation of the load-carrying capacity of airfield pavements. Seven nondestructive test devices tested five sections of airfield pavements at MacDill Air Force Base (AFB) which consisted of two rigid, two flexible, and one composite pavements, ranging from 20-in. portland cement concrete (PCC) to 5.5-in. asphaltic concrete. Analytical treatments of the test data included empirical correlation analyses, and layered-elastic and finite element computer analyses. Six private firms each with a different nondestructive testing (NDT) evaluation method provided evaluation results in terms of allowable aircraft loads and overlay thicknesses. The Air Force produced one set of results using its new nondestructive pavement testing method, and Waterways Experiment Station provided three sets of results.													
(Continued)													
20. DISTRIBUTION/AVAILABILITY OF ABSTRACT <input checked="" type="checkbox"/> UNCLASSIFIED/UNLIMITED <input type="checkbox"/> SAME AS RPT <input type="checkbox"/> DTIC USER		21. ABSTRACT SECURITY CLASSIFICATION Unclassified											
22a. NAME OF RESPONSIBLE INDIVIDUAL Jim W. Hall, Jr.		22b. TELEPHONE (Include Area Code) 601/631-2203	22c. OFFICE SYMBOL WESGP-1										

DD FORM 1473, 84 MAR

83 APR edition may be used until exhausted.

All other editions are obsolete.

SECURITY CLASSIFICATION OF THIS PAGE

Unclassified

Unclassified

SECURITY CLASSIFICATION OF THIS PAGE

18. SUBJECT TERMS (Continued).

Airfield pavement evaluation  
Elastic modulus  
Finite element theory

Layered-elastic theory  
Nondestructive testing  
Pavements deflection measurements

19. ABSTRACT (Continued).

The NDT evaluation methods characterize the pavement structural layers based on the response measured with the NDT devices. Most procedures produce moduli values for the pavement layers and subgrade. Most of the evaluation methods used a back-calculating technique whereby moduli are determined through an iterative process of matching calculated deflection basins to measured basins. The Air Force method determines the velocity of waves propagated through the pavement layers and converts these to moduli.

However, as carefully as the project was planned and conducted, the results are not conclusive. There is a lack of agreement between the allowable load ratings and overlay thickness predictions of the NDT evaluation methods to the standard test pit rating, and a lack of agreement among results from the NDT evaluation methods themselves.

None of the NDT evaluation methods agree perfectly with the standard test-pit method in terms of allowable loads or overlay thicknesses. However, the standard test-pit results make assumptions as to factors such as the quality of base and subbase material, load transfer at joints, condition of the existing pavement, and traffic distribution that might be different from the manner that the NDT evaluation methods treated the same variables. Conventional tests such as California Bearing Ratio and plate-bearing tests are performed on partially disturbed materials because the pavement must be excavated to perform the tests. In contrast, the NDT is a truly in situ test that evaluates the pavement without any disturbance or modification. The allowable aircraft loads from the NDT evaluation methods appear to agree better with the test-pit method than do the predicted overlay thicknesses. The reason for this is not readily apparent since the same basic approaches are used by most evaluation methods for both sets of results.

This study has shown that NDT technology exists for evaluation of airfield pavements. For the pavements at MacDill AFB, some NDT evaluation methods agreed better with the standard test-pit method than others. However, the pavements at MacDill AFB are rather nontypical, and those NDT evaluation methods that did not give good results at MacDill may give more agreeable results on different pavements. The lack of agreement between results of the NDT evaluation methods does justify concern and may point to the need for a standard evaluation method.

Unclassified

SECURITY CLASSIFICATION OF THIS PAGE

## EXECUTIVE SUMMARY

This project, which is directed toward an evaluation of the validity of concepts of nondestructive evaluation of the load-carrying capacity of airfield pavements, has been the most comprehensive single undertaking to date. Seven nondestructive test devices were used to test five sections of airfield pavement at MacDill Air Force Base (AFB), consisting of two rigid, two flexible, and one composite pavements and ranging from 20-in. portland cement concrete (PCC) to 5.5-in. asphaltic concrete (AC). Analytical treatments of the test data included empirical correlation analyses, and layered-elastic and finite-element computer analyses. Six private firms each with a different nondestructive testing (NDT) evaluation method provided evaluation results in terms of allowable aircraft loads and overlay thicknesses. The Air Force produced one set of results using its new nondestructive pavement testing (NDPT) method, and the US Army Engineer Waterways Experiment Station (WES) provided three sets of results with the Dynamic Stiffness Modulus method and layered-elastic analysis using data from the WES 16-kip vibrator and a Dynatest Model 8000 Falling Weight Deflectometer (FWD) using layered-elastic analysis. The participants in the project and the NDT equipment used by each were:

Participant	NDT Equipment
ARE, Inc.	Dynaflect
Louis Berger International	Pavement Profiler Model 2000
Dynatest Consulting	Dynatest Model 8000 FWD
ERES Consultants, Inc.	Dynatest Model 8000 FWD*
Reinard W. Brandley	Dynatest Model 8000 FWD*
	Brandley Centilever Beam
Pavement Consultancy Services	Shell FWD
WES	WES 16-kip vibrator
	Dynatest Model 8000 FWD
Air Force Engineering and Services Center (AFESC)	NDPT wave velocity van

\* Tests were conducted by Dynatest Consulting for these participants.

The tests were conducted on pavement sections where test pits for density and California Bearing Ratio (CBR) had been placed 2 years earlier by the AFESC.

However, as carefully as the project was planned and conducted, the results are not conclusive. There is a lack of agreement between the allowable load ratings and overlay thickness predictions of the NDT evaluation methods to the standard test-pit rating, and a lack of agreement between results from the NDT evaluation methods themselves.

The pavement materials such as limerock base and the sand subgrade at MacDill AFB are not typical of most other airfield pavements. The standard test-pit data were collected 2 years prior to the NDT, although conditions and material strengths probably had changed little. The test-pit measurements reported by AFESC were suspected in the area of flexural strength ( $R$ ) of PCC and plate-bearing measurements. Standard test-pit measurements in terms of CBR and subgrade modulus  $k$  in a cohesionless material such as the sand subgrade are difficult to obtain accurately. For the standard rating based on test-pit measurements, test data collected in the 1940's were used to supplement the AFESC test-pit data. The pavement properties used for the standard evaluation were:

<u>Test Area</u>	<u>Pavement Properties</u>
1	20-in. PCC, $R = 750$ psi 6-in. stabilized subbase, $k = 300$ pci Subgrade (SP-SM)
2	11-in. AC 8-in. limerock base, CBR = 80 7-in. stabilized subbase, CBR = 30 Subgrade (SP) CBR = 25
3	5.5-in. AC 8.0-in. limerock base, CBR = 80 7.0-in. stabilized subbase, CBR = 30 Subgrade (SP), CBR = 25
4	7.5-in. AC 6.0-in. PCC, $R = 650$ psi Subgrade (SP), $k = 250$ pci
	<u>Alternate as flexible pavement</u>
5	7.5-in. AC 6.0-in. base, CBR = 80 Subgrade (SP), CBR = 25  10.5-in. PCC, $R = 650$ psi Subgrade (SP), $k = 250$ pci

The NDT evaluation methods characterize the pavement structural layers based on the response measured with the NDT devices. Most procedures produce moduli values for the pavement layers and subgrade. Most of the evaluation methods used a back-calculating technique whereby moduli are determined through an iterative process of matching calculated deflection basins to measured basins. The Air Force method determines the velocity of stress waves propagated through the pavement layers and converts these to moduli.

A critical part of each pavement evaluation method is the relationship  $v$  to performance. The link to performance in this study has been of a measured or calculated parameter in the form of limiting stress or strain in the pavement components, limiting deflection of the subgrade, and as correlations to established pavement parameters such as CBR and  $k$ . All of these factors are somehow related to the number of load repetitions to cause failure of the pavement system. The performance criteria must be based on real-world performance of airfield pavements. The evaluation methods involved in this study included such features as considerations of existing pavement conditions, seasonal effects, load transfer at joints, and other important items. Some evaluation methods make predictions of rut depth and cracking as a function of applied traffic. However, the performance predictions can only be as good as the limiting criteria on which the predictions are based. This performance criteria must be compatible with the evaluation method in which it is used; i.e., it must be a closed system in that the computed moduli, limiting criteria, and predicted performance have been derived and validated against true performance standards. Different performance criteria may account for the major differences in the evaluations of the test areas at MacDill AFB.

None of the NDT evaluation methods agreed perfectly with the standard test-pit method in terms of allowable loads or overlay thicknesses. However, the standard test-pit results make assumptions as to factors such as the quality of base and subbase material, load transfer at joints, condition of the existing pavement, and traffic distribution that might be different from the manner which the NDT evaluation methods treated the same variables. Conventional tests such as CBR and plate-bearing tests are performed on partially disturbed materials, because the pavement must be excavated to perform the tests. In contrast, the NDT is a truly in situ test that evaluates the pavement without any disturbance or modification. The allowable aircraft loads from the NDT evaluation methods appear to agree better with the test-pit

method than do the predicted overlay thicknesses. The reason for this is not readily apparent since the same basic approaches are used by most evaluation methods for both sets of results.

This study has shown that NDT technology exists for evaluation of airfield pavements. For the pavements at MacDill AFB, some NDT evaluation methods agreed better with the standard test-pit method than others. However, the pavements at MacDill AFB are rather nontypical, and those NDT evaluation methods that did not give good results at MacDill may give more agreeable results on different pavements. The lack of agreement between results of the NDT evaluation methods does justify concern and may point to the need for a standard evaluation method.

This study has also indicated that further comparisons of the NDT evaluation methods should be made on an airfield with pavements more representative of typical conditions such as on a clay subgrade. The clay subgrade would allow more exact CBR and  $k$  measurements with higher confidence. Test-pit measurements should be made concurrently with the NDT. The airfield should be of a medium-load design so that the allowable loads would not be at the maximum-design loads, and the required overlay thicknesses would be produced for comparison. This would provide for a better comparison to the NDT results, and a more definite assessment of the validity of NDT.

## PREFACE

This report was prepared by the Pavement Systems Division (PSD), Geotechnical Laboratory (GL), of the US Army Engineer Waterways Experiment Station (WES) under Air Force Project Order No. F-82-74. The work was sponsored by the Air Force Engineering and Services Center, Tyndall Air Force Base, Fla. The Project Monitor was LTC Bill Tolson.

The work reported herein was performed during the period August 1982-September 1983. WES engineers actively engaged in the project were Messrs. Jim W. Hall, Jr., and Don R. Alexander. This report was prepared by Mr. Hall. The work was performed under the direction of Dr. T. D. White, Chief, PSD, and Dr. W. F. Marcuson III, Chief, GL.

COL Allen F. Grum, USA, was the previous Director of WES. COL Dwayne G. Lee, CE, is the present Commander and Director. Dr. Robert W. Whalin is Technical Director.

## CONTENTS

	<u>Page</u>
EXECUTIVE SUMMARY.....	1
PREFACE.....	5
CONVERSION FACTORS, NON-SI TO SI (METRIC) UNITS OF MEASUREMENT.....	7
PART I: INTRODUCTION.....	8
Background.....	8
Purpose and Scope.....	10
Site Selection.....	11
Description of Test Areas.....	11
Physical Properties of Test Pavements.....	13
Project Requirements.....	15
PART II: NONDESTRUCTIVE TESTING EVALUATION METHODS.....	17
Selection of NDT Evaluation Methods.....	17
Field Demonstrations.....	18
Description of NDT Equipment.....	18
Summary of NDT Evaluation Methods.....	22
PART III: COMPARISON OF RESULTS.....	26
Test Data Comparisons.....	26
Comparison of Predicted In Situ Moduli.....	28
Comparison of Performance Criteria.....	30
Comparison of Allowable Load Predictions.....	31
Comparison of Overlay Thickness.....	33
PART IV: CONCLUSIONS.....	36
PART V: RECOMMENDATIONS.....	38
REFERENCES.....	39
TABLES 1-17	
FIGURES 1-45	
APPENDIX A: DESCRIPTION OF NONDESTRUCTIVE TESTING EVALUATION METHODS.....	A1
APPENDIX B: TEST DATA.....	B1
APPENDIX C: PCC JOINT EFFICIENCY TEST DATA.....	C1

CONVERSION FACTORS, NON-SI TO SI (METRIC)  
UNITS OF MEASUREMENT

Non-SI units of measurement used in this report can be converted to SI (metric) units as follows:

<u>Multiply</u>	<u>By</u>	<u>To Obtain</u>
degrees (angle)	0.01745329	radians
Fahrenheit degrees	5/9	Celsius degrees or Kelvins*
feet	0.3048	metres
inches	2.54	centimetres
kips (force)	4.448222	kilonewtons
kips (force) per square inch	6.894757	megapascals
miles (US statute)	1.609347	kilometres
mils	0.0254	millimetres
pounds (force)	4.448222	newtons
pounds (force) per square inch	6.894757	kilopascals
pounds (mass)	0.4535924	kilograms
pounds (mass) per cubic foot	16.01846	kilograms per cubic metre
pounds (mass) per cubic inch	27.6799	grams per cubic centimetre
square feet	0.09290304	square metres
square inches	6.4516	square centimetres

---

\* To obtain Celsius (C) temperature readings from Fahrenheit (F) readings, use the following formula:  $C = (5/9)(F - 32)$ . To obtain Kelvin (K) readings, use  $K = (5/9)(F - 32) + 273.15$ .

COMPARATIVE STUDY OF NONDESTRUCTIVE PAVEMENT TESTING,  
MACDILL AIR FORCE BASE, FLORIDA

PART I: INTRODUCTION

Background

1. The Air Force Engineering Services Center (AFESC), Tyndall Air Force Base, (AFB) Fla., requested that the US Army Engineer Waterways Experiment Station (WES) conduct a study of various pavement evaluation techniques based on nondestructive testing (NDT). In the 1982 statement of work for the project the following background was given:

During recent years several nondestructive (NDT) pavement evaluation systems have been developed by government agencies and civilian firms to analyze the load-carrying capability of airfield pavements. The use of NDT devices is seen as a great advance over costly and time-consuming destructive evaluation techniques. Although the NDT devices do not allow the same analysis as destructive testing, the benefits of minimal operational impact and reduced effort to produce a final report are particularly attractive. The use of NDT by the Air Force for airfield evaluation is now feasible and desirable; however, the newness of the systems and the disparities in data reporting format (between NDT systems and destructive testing) make a prudent selection of any type of NDT system difficult. To insure the Air Force receives the kind of information it needs in a given situation, familiarity with the NDT systems and the data they produce is needed. A side-by-side field comparison of available NDT systems which could be contracted by the Air Force would allow USAF personnel to make intelligent decisions about which system to use in any given situation. This side-by-side comparison will be conducted at an airfield designated by AFESC that has been evaluated by destructive techniques which will provide comparison of NDT results with the traditional system results.

2. The NDT of pavements was begun as early as 1933 by the German Research Society for Soil Mechanics and was further developed by the Royal Dutch Shell Laboratory in The Netherlands and the Road Research Laboratory in the United Kingdom. This early work used vibratory devices generally consisting of counter-rotating eccentric masses arranged to produce vertical

loadings. Within the past 10 years or so, more advanced equipment such as the electrohydraulic and electromagnetic vibrators and falling weight impulse devices have been introduced.

3. WES has kept current in the advancement of NDT technology, particularly as related to airfield pavements. WES followed the early work of the Shell researchers and participated in joint efforts during the 1950's (Heukelom and Foster 1960; Maxwell 1960a, 1960b). As part of this early WES work, wave propagation measurements were conducted at the American Association of State Highway Officials (AASHO) Road Test (WES 1963) at Foss Field (WES 1964), and on military airfields (Maxwell and Joseph 1967) and roadways. The Air Force sponsored early work (Hall 1970, 1972, 1973) at WES that led to the development of the present WES NDT procedures. Additional work funded by the Army, the Air Force, and the Federal Aviation Administration (FAA) produced the present WES equipment and WES NDT evaluation method called the Dynamic Stiffness Modulus (DSM) method (Ahlvin 1971, Green and Hall 1975). The DSM method has been adopted by the FAA (1976) and the Department of the Army (Hall 1978). WES also conducted studies based on layered-elastic theory and developed procedures for NDT (Green 1978, Weiss 1980, Bush 1980a). In a study conducted by WES for the FAA, several NDT devices were evaluated for use on light airport pavements, and comparisons were made of the measurements made by each (Bush 1980b). However, no attempt was made in that study to compare analytical methodologies.

4. During the past 10 to 15 years, much effort has been applied by various research organizations to the area of NDT, and as a result, numerous methods have been developed using a range of equipment. The Transportation Research Board (TRB) made a review of nondestructive evaluation of pavements in 1978, and TRB formed a Task Force (A2T56) in January 1981 to make a state-of-the-art review of NDT of airfield pavements (Moore, Hansen, and Hall 1978). Some 15 different procedures have been brought before the Task Force of which the author is a member. Table 1 gives a list of the evaluation methods presented to the Task Force. The information and procedures being reviewed by the Task Force provided some of the background for selection of the participants in this project. The evaluation methods selected for the study and reported herein were those complete evaluation procedures that had been demonstrated on airfield evaluation projects. Also selected were those methods providing the full range of available NDT equipment and analysis techniques.

### Purpose and Scope

5. The primary purpose of this study was to provide the AFESC with an assessment of the nondestructive approach to pavement evaluation so that the Air Force can make sound decisions as to the possible uses and benefits of NDT pavement evaluation methods. It was not the purpose of this investigation to identify any "best method" but rather to assess the state of the art, demonstrate differences in test and analysis methods, and study the impact of these differences on results at one airfield. Because it is possible to obtain the best answer for the wrong reason (accidentally compensating mistakes), a comparative evaluation at a single airfield (that is, a single type of subgrade and base course) could never be used as a basis for defining one method as best (Hadala 1975). Comparative evaluation of different methods will give the decision maker a reasonably good exposure to the differences in the methods, their individual strengths and weaknesses, their areas of commonality, and a feel for the effect of the differences on practical engineering decisions.

6. The scope of the project involved comparisons of selected NDT equipment and procedures on representative airfield pavements and a comparison of the NDT results with those obtained from the standard Air Force evaluation procedures based on test-pit measurements. WES selected six leading firms with demonstrated NDT capabilities. These firms are believed to represent the state of the art or terms of commercial NDT equipment and available analytical evaluation methods. In addition, WES demonstrated three NDT procedures that it had developed and the AFESC demonstrated its new NDT evaluation method. The field demonstrations were conducted on five selected test areas at MacDill AFB, Tampa, Fla., during October and November 1982. The test areas at MacDill AFB had each been evaluated in March 1980 by test-pit measurements in each of the five test areas. Each participant made an evaluation of the test areas and independently submitted a report to WES. Allowable gross aircraft loadings were computed for each test area for the 13 aircraft groups and 4 pass intensity levels as given in Air Force Regulation AFR 93-5 (Headquarters, Department of the Air Force 1981). Also, overlay thickness requirements were determined for the KC10A (DC-10-30) aircraft at a total of 1,000 passes and for the E4 (B-747) aircraft at 10,000 passes. This report contains results presented by each of the participants and makes comparisons with the standard Air Force evaluation procedure based on test-pit measurements.

### Site Selection

7. The AFESC selected MacDill AFB as the demonstration site. A visit was made to MacDill AFB on 30 August 1982 by LTC Bill Tolson and CPT Paul Foxworthy of AFESC and Mr. Jim W. Hall, Jr., of WES. Five test areas were selected to provide a range of pavement types and strengths. Figure 1 shows a layout of the airfield at MacDill AFB indicating the five test areas. A test pit had been placed in each of the test areas during a pavement evaluation conducted by AFESC in March 1980. The information obtained from each test pit as reported in the pavement evaluation report is shown in Figure 2 (AFESC 1980). Note that the subgrade material was classified as an SP sand\* in Test Areas 2-5 and as an SP-SM sand in Test Area 1; therefore, the subgrade was nearly the same for all test areas. A construction history for each of the test areas is shown in Table 2.

### Description of Test Areas

8. Each of the test areas contained approximately 50,000 sq ft\*\* of pavement. This size was selected to be large enough to provide a representative amount of pavement and yet permit all five test areas to be studied in 1 day by each participant. The test areas were selected so as to provide the least interference with MacDill AFB's daily aircraft operations. Each test area was outlined and marked so that location of all tests could be identified.

#### Test Area 1

9. The pavement in Test Area 1 consisted of a 20-in. portland cement concrete (PCC) pavement. The 25- by 20-ft slabs constructed in 1959 were in excellent condition. The test area, located on Taxiway 33 at MacDill AFB, was 3 slabs wide (75 ft) by 28 slabs long (700 ft). A layout of the area is shown in Figure 3; the marking system was used to locate all NDT measurements. Test Area 1 contained no observable surface distress. An overall view of Test Area 1 is shown in Figure 4.

---

\* Classified according to the Unified Soil Classification System (USCS).

\*\* A table of factors for converting non-SI units of measurement to SI (metric) units is presented on page 7.

### Test Area 2

10. Test Area 2 was located on the Parallel Taxiway (Taxiway 3B) to the Main Runway and was constructed in 1943. An asphalt concrete (AC) overlay was placed in the center 18 ft of the taxiway in 1956, and additional overlays were placed in 1963 and 1971. The pavement was in good condition, but contained longitudinal and transverse cracking. This test area, shown in Figure 5, was 75 ft wide and 700 ft long. Station numbers, beginning with 0+00 at the south end of the test area, were marked every 100 ft along the center line. Figure 6 is an overall view of this test area.

### Test Area 3

11. Test Area 3 was along the same parallel taxiway as Test Area 2 but farther north. This pavement was also constructed in 1943 and was originally identical to Test Area 2. The original asphalt surface had been overlayed with AC in 1956 and again in 1969. This area was considered in fair condition, although exhibiting considerable distress in the form of block cracking. This test area shown in Figure 7 was 40 ft wide by 1,000 ft long. This area was confined to the 40-ft width because the pavement outside this width was apparently not the same thickness. Station numbers were marked at 100-ft intervals beginning with 0+00 at the south end. Figure 8 gives an overall view of Test Area 3.

### Test Area 4

12. Test Area 4 was a composite section located in Apron 1-A-1. The original 6-in. PCC pavement was constructed in 1941 with a slab size of 25 by 25 ft. An AC overlay was placed on this pavement in 1952 followed by a slurry seal in 1966. Considerable reflective cracking of the joints and cracks in the underlying slabs had occurred. The overall condition was considered good. The layout in Figure 9 shows the identification scheme used. Letters A-E were marked every 50 ft along one side and station numbers were marked every 50 ft along the other direction. The area was 200 by 250 ft. Test Area 4 is shown in Figure 10.

### Test Area 5

13. Test Area 5 was a 10.5-in. PCC pavement with 15- by 12.5-ft slabs. The pavement, constructed in 1975, consists of the slabs placed directly on the sand subgrade. This apron area, designated Apron 1-A, is actively used for F-16 aircraft parking. The pavement was in excellent condition with only minor distress in the form of corner spalls and joint spalls. Figure 11 gives

a layout of this test area and shows the identification scheme used. The rectangular area consisted of a total of 270 slabs with 18 slabs along the 12.5-ft slab dimension and 15 slabs along the 15-ft-slab dimension. Letters A-O were used to identify the slabs along the 15-ft slab dimension and numbers 1-18 were used to label the side with the 12.5-ft-slab dimension. Figure 12 is an overall view of Test Area 5.

#### Physical Properties of Test Pavements

14. The pavement properties (California Bearing Ratio (CBR), subgrade modulus  $k$ , flexural strength) used by AFESC for evaluation differed from those reported in earlier pavement evaluation reports (US Engineer Office, Jacksonville, Fla. 1944; Office, District Engineer, Savannah, Ga. 1947; US Army Engineer District, Jacksonville, Fla. 1960) and condition survey reports (US Army Engineer, Ohio River Division Laboratories 1954; the Rigid Pavement Laboratory, Ohio River Division Laboratories 1960; Construction Engineering Laboratory, Ohio River Division Laboratories 1964). Table 3 compares these pavement properties for the pavements located in each of the five test areas. Two primary differences are the flexural strength  $R$  of the PCC and the subgrade modulus  $k$ .

15. For Test Areas 1, 4, and 5, AFESC reports flexural strengths of 480, 580, and 470 psi, respectively (Table 3 (AFESC 1980)). Earlier reports showed flexural strengths of 750 psi for Area 4 (Table 3, US Engineer Office, Jacksonville, Fla. 1944; US Army Engineer District, Jacksonville, Fla. 1960; US Army Engineer, Ohio River Division Laboratories 1954). The AFESC used results from tensile-split tests on 4-in.-diam cores and obtained the flexural strength from correlations of tensile-split test results to flexural strengths. Generally, fairly good correlation results by using 6-in.-diam cores, but the correlation with 4-in.-diam cores is poor (Hammitt 1974). Flexural strength generally does not decrease with time; therefore, the values given in the earlier reports are probably more representative of actual flexural strengths.

16. Some subgrade strengths in terms of subgrade modulus  $k$  are not consistent with values reported in the earlier evaluations. Subgrade modulus  $k$  of 85 and 80 pci for Test Areas 4 and 5 are in disagreement with values ranging between 250 and 400 pci measured in the earlier evaluations. CBR

values of 35 and 30 were measured by AFESC on the sand subgrade in Test Areas 2 and 3, respectively. The sand subgrade, classified as a poorly graded sand (SP), appears to be fairly uniform throughout the airfield. According to the correlation between CBR and  $k$ , a CBR of 30 corresponds to a  $k$  value of 300 pci or greater, and a CBR of 25 corresponds to a  $k$  of approximately 250 pci (Hall and Elsea 1974). Therefore, the  $k$  values of 80 and 85 pci seem unreasonably low for these conditions.

17. Also, some discrepancy exists as to the thickness of pavement layers. Thicknesses reported by AFESC for evaluation (Table 3, (AFESC 1980)) are not the same as indicated by AFESC test-pit data (Figure 2). Thicknesses given by earlier pavement studies are also somewhat different (US Engineer Office, Jacksonville, Fla. 1944; Office, District Engineer, Savannah, Ga. 1947; US Army Engineer District, Jacksonville, Fla. 1960; US Army Engineer, Ohio River Division Laboratories 1954; the Rigid Pavement Laboratory, Ohio River Division Laboratories 1960; Construction Engineering Laboratory, Ohio River Division Laboratories 1964). The AFESC report gives additional thickness measurements made from core borings (AFESC 1980). All of the available thickness information was used to select a set of values for each of the five test areas for use in the study reported herein.

18. Based on the above considerations and a review of all available information on the test area pavements, the following properties have been selected for the standard test-pit analysis for this study:

<u>Test Area</u>	<u>Pavement Properties</u>
1	20-in. PCC, $R = 750$ psi where $R$ denotes flexural strength 6-in.-stabilized subbase, $k = 300$ pci Subgrade (SP-SM)
2	11-in. AC 8-in. limerock base, CBR = 80 7-in. stabilized subbase, CBR = 30 Subgrade (SP), CBR = 25
3	5.5-in. AC 8.0-in. limerock base, CBR = 80 7.0-in. stabilized subbase, CBR = 30 Subgrade (SP), CBR = 25

(Continued)

<u>Test Area</u>	<u>Pavement Properties</u>
4	7.5-in. AC 6.0-in. PCC, R = 650 psi Subgrade (SP), k = 250 pci  <u>Alternate as Flexible Pavement</u>
5	7.5-in. AC 6.0-in. base, CBR = 80 Subgrade (SP), CBR = 25  10.5-in. PCC, R = 650 psi Subgrade (SP), k = 250 pci

Project Requirements

19. The specific requirements of the project were to (a) select several of the better NDT procedures and equipment for demonstration, (b) have each procedure demonstrated through field tests on each of the five test areas at MacDill AFB, (c) obtain pavement evaluation reports from each procedure giving allowable loadings and overlay requirements for each test area, and (d) compare the results from each method with the standard Air Force evaluation based on test-pit measurements. The original plan was to use the test-pit data collected in 1981 by AFESC; however, some changes were made to these data as previously discussed.

20. Each participant in this demonstration project was given a full day at MacDill AFB to test all five test areas. With the exception of the AFESC, who performed tests for several days, only one participant was on the field for any given day of the demonstration. At the completion of the field tests, each participant provided WES a copy of the field test data.

21. Each participant prepared an evaluation report of the five test areas. This evaluation required the assessment of the allowable gross aircraft loads (AGAL's) for all 13 military aircraft groups at four specified pass intensity levels as given in AFR 93-5 (Headquarters, Department of the Air Force 1981). A pass intensity level is a specified number of aircraft passes (operational movements) for which the AGAL is to be determined. Therefore, the AGAL for pass intensity I would be less than the AGAL for pass intensity II, etc., since pass intensity I requires more passes than pass intensity II. The 13 aircraft groups and the various aircraft in each group are

shown in Table 4. Table 5 shows the controlling aircraft (primary aircraft to be considered) in each group and gives the number of passes for each group for each of four pass intensity levels. Note that the number of passes for a given pass intensity level is not the same for all 13 aircraft groups. The characteristics of the controlling aircraft in each of the 13 aircraft groups to be used for pavement evaluations are shown in Table 6. The evaluation by each participant also included overlay thickness requirements for each of the five test areas for two design loads: (a) 1,000 passes of the DC-10-30 aircraft (KC 10A), and (b) 10,000 passes of the B-747 aircraft (E-4).

## PART II: NONDESTRUCTIVE TESTING EVALUATION METHODS

### Selection of NDT Evaluation Methods

22. In the selection of the NDT evaluation methods to be demonstrated, both equipment and analytical procedures were considered. The participants selected were those with a unique and demonstrated capability (experience in evaluating airfield pavements). Because several types of NDT equipment were available for nondestructive pavement testing (NDPT), attempts were made to include evaluation methods that would demonstrate all equipment types. Evaluation methods in use included a range of analytical treatments, and again, effort was made to include a cross section of various analysis schemes. Six private firms, WES, and AFESC were selected to participate, and sole-source contracts were negotiated with each private firm. WES also contracted with the New Mexico Engineering Research Institute (NMERI) to have its representative assist in the demonstration of the AFESC methodology. The NMERI was the developer of the AFESC procedure. The following is a list of the participants and the equipment used by each:

Participant	NDT Equipment
ARE, Inc.	Dynaflect
Louis Berger International (Berger)	Pavement Profiler Model 2000
Dynatest Consulting (Dynatest)	Falling weight deflectometer (FWD) Dynatest Model 8000
ERES Consultants, Inc.	Dynatest Model 8000 FWD*
Reinard W. Brandley (Brandley)	Dynatest Model 8000 FWD* Brandley Centilever Beam
Pavement Consultancy Services (PCS)	Shell FWD
WES	WES 16-kip vibrator Dynatest Model 8000 FWD
AFESC	NDPT wave velocity van

\* Tests were conducted by Dynatest Consulting for these participants.

23. Each participant demonstrated its analytical procedure using test data from the NDT device used. Ten different analysis schemes were considered in the study. These consisted of six evaluation methods from the six private firms, the AFESC evaluation method, and three evaluation methods from WES.

### Field Demonstrations

24. The field tests were conducted during the period 26 October to 3 November 1982. The date on which the areas were tested by each participant were:

<u>Participant</u>	<u>Date</u>
PCS	27 October 1982
ARE	28 October 1982
Dynatest	29 October 1982
ERES	30 October 1982
Berger	31 October 1982
Brandley	1 November 1982
WES	2 November 1982
AFESC	27 October- 3 November 1982

25. The field tests were coordinated with MacDill AFB operations. All test areas were fairly free of aircraft movement during the 6-day test period except Test Area 5. In this area, which is the parking apron for F-16 aircraft, some delays in the testing were experienced because of frequent aircraft movements. Test Area 4 was used as a parking apron for F-111 aircraft on 2 November, making some of this area unavailable to WES.

### Description of NDT Equipment

26. Seven NDT devices were used in the project and characteristics of each are presented in Table 7. Three devices--the WES 16-kip vibrator, the Berger Pavement Profiler, and the ARE Dynaflect--operate with a vibratory loading. All of the other devices use an impulse (drop-weight) loading. All devices except the Air Force NDPT device measure the deflection response of the pavement surface to the applied load. The Air Force NDPT device operates on the principle of wave propagation. A brief description of each NDT equipment used in the project is given.

#### ARE Dynaflect

27. The Dynaflect is an electromechanical system for measuring the dynamic deflection of a pavement caused by an oscillatory load. It is manufactured by SIE, Inc., Fort Worth, Tex. This trailer-mounted device (Figure 13) applies a 1,000-lb peak-to-peak sinusoidal load to the pavement. The load is generated by two counterrotating masses that rotate at a constant

frequency of 8 Hz. The force is transmitted to the pavement through two 4-in.-wide, 16-in.-outside-diam polyurethane-coated steel wheels spaced 20 in. apart. The Dynaflect applies a 2,000-lb static weight to the pavement.

28. The pavement response to the dynamically applied load is measured with 210- $\Omega$ , 4.5-Hz geophones that are shunted to a damping factor of approximately 0.7. One geophone is located directly between the two steel wheels. The other four geophones are spaced at 1-ft intervals toward the front of the trailer.

#### Berger Pavement Profiler Model 2000

29. This device is a Road-Rater Model 2000 manufactured by Foundation Mechanics, Inc., El Segundo, Calif. The Model 2000 applies a peak-to-peak cyclic load of 4.5 kip at a frequency of 25 Hz. The trailer-mounted device (Figure 14) is an electrohydraulic system. The Model 2000 has a self-contained power supply. The gasoline engine supports the hydraulic and electrical systems of the device. The reaction mass of the Model 2000 is 2,000 lb.

30. Three load cells mounted on the load plate monitor the force. The three load cells are summed for total-force output. Deflection is monitored by four velocity sensors. The first is located in the center of the 18-in.-diam load plate, and the other three are at 12, 24, and 36 in. or 12, 24, and 60 in. from the center of the load plate.

#### Dynatest FWD

31. The Dynatest 8000 FWD is an impact load device that applies a single-pulse transient load of approximately 25-30 msec duration. This trailer-mounted device (Figure 15) measures both applied load and seven deflection points on the pavement with the maximum distance of the deflection point being 7 ft from the center of the load plate. The load is adjustable to a maximum of 24,000 lb and is applied through a 300-mm (approximately 12-in.) diam load plate. The system is controlled with a Hewlett-Packard HP-85 computer that also records the output data. This equipment is shown in Figure 16.

#### Brandley deflection beam

32. The Brandley deflection beam (Figure 17) is used for testing joints in PCC pavement sections to determine the effectiveness of the load transfer at the joints. The test procedure consists of placing a cantilever deflection beam on the slab with two linear potentiometers located at the free end of the

beam. The beam is set on the slab such that one of the potentiometers is located on one side of the joint and the other potentiometer is located on the other side of the joint. A rubber-tired wheel, which imposes approximately the same total load as the aircraft using the pavements, is then pulled or driven across the joint perpendicular to the joint and passes immediately adjacent to the location of the potentiometers. In this manner, the total relative deflection of the slab at the joint and the relative movement of one slab with respect to the other slab (slab rocking) as the wheel moves over the joint can be measured and recorded. A test vehicle with 50,000 lb per single wheel would normally be used, but the only equipment available at MacDill AFB was a truck-mounted crane with three axles. The rear axles had dual wheels, and each of dual wheels was loaded to 7,000-8,000 lb. Because this was the only equipment available, the tests were conducted using these loads.

PCS FWD

33. The PCS FWD applies a pulse load to the pavement surface by dropping a mass on a baseplate that is connected to the load plate by a set of springs. The maximum force is 22.4 kips, and the force is varied by adjusting the drop height. Both force and deflection are electronically recorded. Velocity transducers, which are electronically integrated to measure deflection, are located at the center of the load plate and at three radial distances of 60, 100, and 200 cm. This trailer-mounted device is shown in Figure 18, and the data recording equipment is shown in Figure 19.

WES 16-kip vibrator

34. The WES 16-kip vibrator shown in Figures 20 and 21 is an electro-hydraulic vibratory loading system. The unit is contained in a 36-ft semi-trailer along with supporting power supplies and automatic data recording equipment. A 16,000-lb preload is applied to the pavement with a superimposed dynamic load ranging up to 30,000 lb peak-to-peak. The dynamic load can be applied over a frequency range of 5 to 100 Hz but the standard test frequency is 15 Hz. The dynamic load is measured with a set of three load cells mounted on an 18-in.-diam load plate. Velocity transducers located on the load plate and at points away from the plate are calibrated to measure deflection. Test results are recorded on X-Y plotters and a digital printer.

35. Data collected with the WES 16-kip vibrator are the DSM and deflection basins. DSM is the slope (load/deflection) of the dynamic load versus deflection curve obtained by sweeping the force from zero to maximum at a

constant frequency of 15 Hz. This slope is taken at the maximum force levels. The deflection basin is obtained by measuring deflections at distances of 0, 18, 36, and 60 in. from the center of the load plate. The deflection ratio  $\Delta 60/\Delta 18$  (obtained by taking the deflection at 60 in. and dividing by the deflection at 18 in.) is used to determine the radius of relative stiffness  $k$  for rigid pavements using the developed correlations.

WES FWD

36. The FWD used by WES is a Model 8000 manufactured by Dynatest (Figure 22). A dynamic force is applied to the pavement surface by dropping a 440-lb weight onto a set of rubber cushions, resulting in an impulse loading. The applied force and pavement deflections are measured with load cells and velocity transducers, respectively. The drop height can be varied from 0 to 15.7 in. to produce a force from 0 to 15,000 lb. The load is transmitted to the pavement through an 11.8-in.-diam plate. The signal-conditioning equipment displays the resulting average pressure in kilopascals and the maximum peak displacement in micrometers. As many as three displacement sensors may be recorded at one time.

37. FWD data collected were deflection basin measurements. Displacements were measured on the load plate and at distances of 12, 24, 36, and 48 in. from the center of the load plate. Because this particular model has only two transducers for deflection basin measurements, the four deflection points were obtained by dropping the weight twice and shifting the transducers to the additional spacings.

Air Force NDPT device

38. The AFESC NDPT device is an impact hammer used to excite the pavement system to measure wave velocity response. The hydraulically operated hammer can be dropped from 6 to 36 in. and the drop weight varied from 220 to 500 lb. The assembly is equipped with grippers that lift the hammer, release it, and then catch the hammer after the first impact to prevent the hammer from striking the pavement more than once. A 12-in.-diam loading plate is used with a rubber mat on PCC pavement and without the mat on AC surfaces. Accelerometers are generally placed on the pavement surface at 1, 2, 4, 8, and 16 ft from the edge of the load plate. Signals from the accelerometers are collected through a Hewlett-Packard HP-6942 multiprogrammer and transferred to an HP-9845B computer for analysis and stored on an HP-9895 floppy disk.

39. The computer is primarily used to compute fast Fourier transforms

(FFT) for phase angle versus frequency and wave velocity versus wavelength (dispersion) plots immediately after the data are acquired. When sufficient data are collected for interpretation of the dispersion curve (based on operator experience), the data are stored on the floppy disk and a hard copy is made.

40. It is from this hard copy that the operator selects the velocity values that will ultimately be used in the computer analysis for load-carrying capability of the pavement. The van containing the NDPT device is shown in Figure 23. A close-up of the impact hammer and load plate is shown in Figure 24.

#### Summary of NDT Evaluation Methods

41. A brief description of the analytical procedures used by each evaluation method is given here. Table 8 gives a summary of some important characteristics of the methods. A more detailed description is given in Appendix A.

#### ARE, Inc. (1983)

42. Deflection basin data from the Dynaflect are used with the BASFIT program, which is a deflection-basin fitting program that predicts moduli of the pavement layers and subgrade. A layered-elastic program AIRPOD is used in a fatigue analysis to predict remaining pavement life and allowable loadings. Another layered-elastic program ELSYM-5 is used to compute overlay thickness requirements.

#### Louis Berger International Inc. (1983)

43. The evaluation method used by Berger is a combination of layered-elastic theory and a modified version of the WES DSM method (Hall 1978). Test data were collected with the Model 2000 pavement profiler. Deflection basin data were used to back-calculate elastic moduli of the pavement layers and subgrade. These moduli were used for an apparent quality assessment of the pavement materials. A correlation was used to convert the DSM's measured with the pavement profiler to the DSM that would be obtained with the WES 16-kip vibrator. Then the DSM procedure with some modifications was used to evaluate the load capacity. For flexible pavements, a subgrade CBR was determined from both the DSM procedure and from the calculated subgrade moduli. The CBR values were then used with the CBR design curve to determine allowable load

and overlay requirements. The DSM was used to determine allowable loadings for rigid pavements using a modified relationship of DSM to allowable gross load. Load transfers at joints in rigid pavements were evaluated with the pavement profiler.

Dynatest Consulting (1983)

44. Dynatest uses the Dynatest 8000 FWD to measure deflection basins, and these measurements are the input for a computer program called ELMOD developed for an HP-85 microcomputer. The ELMOD program includes the method of equivalent thicknesses (MET) to calculate the elastic modulus of up to four pavement layers (Ullidtz 1973, 1977). Nonlinearity of the subgrade is considered in these calculations. Evaluations of joints and corners of rigid-pavement slabs are made with the FWD tests and Westergaard equations (Westergaard 1948). The ELMOD program allows consideration of seasonal temperature effects in the load evaluation. The performance criteria used by Dynatest are permissible normal stress in unbound materials and subgrade, horizontal strain at the bottom of AC, and a fatigue relationship based on flexural strength for PCC (Herholdt et al. 1979).

ERES Consultants, Inc. (1982)

45. The ERES procedure for NDT evaluation uses the Dynatest Model 8000 FWD test results; three load magnitudes are used including the maximum of 24 kips. Pavement layer stiffness values are back-calculated from the measured deflection basins using a layered-elastic program for flexible pavement and a finite element program (ILLISLAB) for rigid pavement. The method for flexible pavements is to model the pavement as a two-layered system to determine the subgrade modulus, and then to calculate other layer moduli that match the theoretical deflection basin to the measured basin (Hoffman and Thompson 1981). Failure criteria for flexible pavement includes radial strain in the asphalt and vertical strain in the subgrade; both rutting (Chou 1976) and fatigue (Bonnaure, Gravois, and Udrone 1980) are considered. Fatigue life of the limerock base course was also part of the flexible pavement analysis (Larson and Nussbaum 1967). For rigid pavements, an E modulus of the concrete and a subgrade k modulus are calculated by matching the area of the center slab deflection basin and the maximum deflection. Failure criteria are a relationship of aircraft coverages to concrete modulus of rupture stress ratio. The modulus of rupture is estimated from the E of the slab. Measured load transfer at joints is accounted for in the evaluation.

Reinard W. Brandley (1983)

46. Brandley used test results from the Dynatest 8000 FWD, the WES 16-kip vibrator, and the cantilever deflection beam. Two loads were applied with the FWD, 830 and 1,500 kPa. Test data from both the FWD and the 16-kip vibrator were used with the Dynatest programs of the ELMOD and ISSEM4. These programs, along with the Chevron layered elastic model program, were used to calculate moduli of the pavement layers and subgrade from the FWD deflection data. These moduli were used to compute subgrade deflection under different aircraft loadings; these were compared to the Brandley limiting subgrade deflection criteria to obtain the evaluation results (Brandley 1975). Joint conditions in rigid pavements were evaluated using the cantilever beam. It is the opinion of Brandley that neither the FWD nor the 16-kip vibrator can adequately load joints to measure load transfer.

PCS (1983)

47. The general approach of PCS demonstrated in this project is the collection of deflection data with the PCS FWD, input of these measured deflection basins into the BISAR layered-elastic computer program, and back-calculated elastic moduli ( $E$ ) for the pavement layers. These moduli are then translated to CBR and/or subgrade  $k$  modulus from correlations such as

$$E = 1,500 \text{ CBR}$$

$$E = 10^x \text{ where } x = 1.415 + 1.284 \log k$$

$E$  in units of psi and  $k$  in units of pci

The values of CBR were used for flexible pavements, while  $k$  values were obtained on the rigid pavements, and these values were used with the conventional Air Force load evaluation procedures to determine the allowable aircraft loadings and overlay thickness requirements (Headquarters, Department of the Air Force 1981). The method used by PCS for load evaluation used the flexible pavement design equation developed by WES and the equivalent single-wheel analysis (Yoder and Witczak 1975). For rigid pavements the evaluations were based on the Westergaard free-edge stress.

WES DSM method  
(Hall and Alexander 1983)

48. The DSM procedure is based on correlations between DSM (load/deflection) measurements with the WES 16-kip vibrator and the allowable single-wheel load (ASWL) as determined from test-pit measurements. DSM is a

ratio of dynamic load:deflection. The correlations were developed from tests on a large number of inservice airfield pavements. The procedure for NDT evaluation provides for correction of deflection measurements on AC for temperature effects, calculation of the effective subgrade CBR for flexible pavement, and determination of the radius of relative stiffness for rigid pavement (Asphalt Institute 1969). Existing analytical relationships from the standard US Army Corps of Engineers design procedures convert the ASWL to AGAL and compute overlay thicknesses (Headquarters, Departments of the Navy, Army, and Air Force 1978; Headquarters, Departments of the Army and Air Force 1979). A load reduction factor based on joint load transfer measurements is included in the procedure.

WES layered-elastic method (Hall and Alexander 1983)

49. This evaluation method (Bush 1980a, Alexander 1982) uses deflection basin measurements from the WES 16-kip vibrator or FWD as input to layered-elastic computer programs (Bush 1980a, Alexander 1982). The program used is BISDEF, which is a modification of the BISAR program (Bush 1980a, Peutz 1968). Elastic moduli of the pavement layers and subgrade are back-calculated, and these moduli are then used in the AIRPAV layered-elastic program to determine allowable loads and overlay thicknesses (Alexander 1982). Failure criteria consists of limiting tensile stress in the bottom of PCC slabs, and limiting horizontal tensile strain in AC and vertical subgrade strain in flexible pavement subgrade. A load reduction factor based on joint load-transfer measurements is included in the procedure.

AFESC (1983)

50. Data from the Air Force NDPT impulse load device are interpreted to give shear wave velocity values for each pavement layer and subgrade. These velocity values are converted to elastic moduli, which are used with the PREDICT computer program to determine allowable aircraft loads. Performance criteria are based on tensile stress or strain in the pavement surface layer and subgrade compressive strain. Overlay thicknesses are not presently determined by the method. Load transfer at joints is not measured.

### PART III: COMPARISON OF RESULTS

#### Test Data Comparisons

51. The scope of this project does not provide for an indepth study of NDT equipment capabilities and comparison but, instead, concentrates on the complete evaluation method. However, some comparisons of results from different equipment that are readily available are offered here. Test data collected with each NDT device are presented in Appendix B. Some study of pavement response in terms of measured parameters, such as deflections, deflection basin, applied load, loading frequency, and wave velocity, may aid understanding of NDT equipment requirements.

52. Most of the NDT evaluation methods make use of the deflection basin (shape of deflected pavement surface) for calculation of layer moduli. A comparison of the deflection basins measured with each of the test devices near the 1980 test-pit locations is presented in Figures 25 through 29. The Air Force NDPT device does not measure deflection, and is, therefore, not included. These figures show the relative magnitude of displacements corresponding to the maximum dynamic/impulse force for each particular test device. These deflection data were then normalized in terms of a unit force of 1,000 lb by dividing measured deflection by applied force; the resulting value is termed unit deflection. The static load (preload) applied by some devices (WES 16-kip vibrator, Berger Pavement Profiler, and ARE Dynaflect) is not considered in these comparisons; only the applied dynamic load was used. Unit deflections in mils per 1,000 lb of applied force are presented in Figures 30 through 34. The Dynaflect, which has the smallest measured deflection at all test areas, gives the largest unit deflection for Test Areas 1, 4, and 5. Test Areas 1 and 5 are rigid pavements and Test Area 4 is a composite pavement.

53. A quantity often used to express the pavement response to nondestructive testing is a ratio of load/deflection or stiffness. To make additional comparisons of the pavement response with the NDT devices used in the project, a comparison of stiffness measurements is presented in Table 9. Table 9 gives an average stiffness for each test area for each NDT device. The number of tests conducted on each test area and used for the average stiffness is shown. Also shown is an average stiffness for each test area

which was obtained by averaging the average stiffness for each NDT device for that test area. The standard deviation and coefficient of variation are shown for each set of data. The coefficient of variation is of interest because it gives some indication of the variability of each NDT test device on the different test areas. A graphical comparison of the stiffness measured by each NDT device is a ratio of the average stiffness from all devices (Figure 35). Differences in load plate diameter, static preload, and dynamic load may produce different stiffness values, and these factors are not considered in Figure 35. However, a study of Figure 35 shows how the measurements vary from the average as a function of pavement strength. The PCS FWD and Dynaflect FWD have very similar characteristics, yet these do not closely agree in this comparison. The two devices manufactured by Dynatest (Dynatest FWD and WES FWD) do agree well even though the dynamic load magnitude is different. The greatest variation occurred in Test Area 3, the composite pavement. No consistent trend developed as to which device had greater or lesser variation in Figure 35, and maximum variation of results from all test areas combined is a factor of approximately 2 (maximum stiffness divided by minimum stiffness).

54. Because the stiffness value can be used with the WES DSM evaluation method to determine allowable load, that method was used to indicate the significance of the range in stiffness values from the NDT devices. Allowable gross aircraft loads were computed for three aircraft using the upper and lower limits of the stiffness range. The following comparison was made for only two of the test areas and three aircraft but gives a representative set of results.

<u>Test Area</u>	<u>Pavement Type</u>	<u>Range in Stiffness, kips/in.</u>	<u>Aircraft</u>	<u>Range in Allowable Load, kips</u>	<u>Increase from Lower Value, percent</u>
3	Flexible	509-1,139	F-4	26-60	131
			C-141	110-291	165
			B-52	143-379	165
5	Rigid	1,924-3,200	F-4	52-60	15
			C-141	249-345	39
			B-52	231-385	67

55. The range of stiffness values is highly significant on the weaker flexible pavement (Test Area 3) and not as significant on the rigid pavement (Test Area 5). On pavements with high stiffness values, such as Test Areas 1,

2, and 4, the range is not important since the low side of the range evaluates the pavement at a high allowable load level.

56. The WES computer program BISDEF was used to calculate modulus values for each of the five test areas using the deflection basins in Figures 25 through 29. Because most evaluation methods use a back-calculating technique to obtain layer moduli, this comparison is of interest. The moduli obtained using BISDEF and deflection data from all six devices are provided in Table 10. The Dynaflect loading area was difficult to model in this program, and values presented for that device in Table 10 may be suspect. Table 10 does show that the back-calculated moduli can vary considerably as a function of the deflection basin.

#### Comparison of Predicted In Situ Moduli

57. All evaluation methods characterized the pavement sections through prediction of the moduli of the pavement layers and subgrade except the WES DSM procedure. Table 11 summarizes these predicted moduli. A graphical comparison of the subgrade moduli for each of the five test areas is presented in Figure 36. By some evaluation methods, the subgrade modulus for Test Area 1 was treated as a composite of the 6-in. subbase and the sand subgrade with a single modulus computed for the composite materials. This causes the appearance of a large variation in predicted subgrade moduli of Area 1 until this is understood; i.e., that the subgrade modulus for Test Area 1 was not computed on the same basis by all methods. Brändley, ARE, and AFESC were the participants making the separation of a subbase and subgrade, and therefore computing a modulus for each material. All others treated the material beneath the PCC slab in Test Area 1 as subgrade only and did not identify the subbase as a separate layer. The procedure of ERES gives only a subgrade modulus  $k$  for the subgrade beneath rigid pavements and, therefore, no elastic moduli for the subgrade by that method are available for Test Areas 1, 4, and 5.

58. An analysis of the elastic moduli of the subgrade predicted by all methods for all five test areas gives the following (Area 1 includes data from only Brändley, ARE, and AFESC):

Area	Subgrade Moduli, psi		
	Mean	Standard Deviation	Spread of Data
1	20,250	9,820	19,250
2	30,910	12,550	39,450
3	22,570	8,640	29,250
4	21,450	5,170	15,800
5	21,210	7,570	22,850

The mean value shows approximately the same subgrade moduli for all areas except Test Area 2, but the spread of data indicates the significant range in the individual values by each evaluation method. The spread of data is defined as the maximum value less the minimum value.

59. With the exception of Test Area 1, the highest moduli of the subgrade were determined by PCS, and in all areas the lowest values came from the AFESC method. For Test Area 1, Brandley, ARE, and AFESC gave E values for both the subgrade and subbase, whereas the other evaluation methods combined the subbase and subgrade; however, for Test Area 1 only the moduli from Brandley, ARE, and AFESC were used for the above statistics.

60. Only ARE predicted modulus values for the subbase layers of Test Areas 2 and 3; the other participants determined a combined modulus of the base and subbase. A presentation of the base course moduli is shown in Figure 37. By all evaluation methods (except by Brandley where both areas have the same value), the base course in Test Area 3 was rated with a lower modulus than the base course of Test Area 2. A significant range in the base course moduli occurs as shown.

Area	Base Course Moduli, psi		
	Mean	Standard Deviation	Spread of Data
2	74,700	47,950	148,000
3	42,280	25,620	75,000

61. Because the modulus of AC is temperature-dependent, values were selected from temperature-modulus relationships by most participants. However, a fairly wide range of values was used for the AC. The moduli for the AC surface from all test areas combined gave the following.

AC Moduli, psi		
Mean	Standard Deviation	Spread of Data
410,000	217,000	852,000

The value of 1,391,000 psi predicted by AFESC for Test Area 4 was not included in the above statistics.

62. For design and evaluation purposes, most evaluation methods provide for a variable moduli of the AC layer (as well as the subgrade) to allow for changing seasonal conditions throughout the design life. This appears to be an important feature since the layered-elastic procedures use the limiting stress/strain concept to predict number of aircraft passes, and the strain is a function of the seasonal/environmental fluctuations in the layer moduli.

63. It is of interest to note in Table 11 the values of subgrade modulus  $k$  were determined from some evaluation methods (Dynatest, ERES, Berger). The  $k$  values range from 195 to 500 pci, which tends to confirm the value of 250 pci selected earlier in this report for the standard evaluation procedure. As could be expected, the moduli determined for the PCC layers were more consistent with most values being in the range of  $4 \times 10^6$  to  $5 \times 10^6$  psi. The AFESC did predict a low value of  $2.1 \times 10^6$  psi for Test Area 5.

64. In addition to the moduli values presented for the evaluation analysis, both Brändley and Berger offered additional comparisons. These values are of interest because some moduli are computed with deflection basin data from the same equipment using different analytical procedures; whereas, some moduli are computed with the same analytical procedure using deflection measurements from different NDT equipment. These results are shown in Table 12. Similar comparisons can be made by looking at the two columns in Table 11 where WES made computations with the same analytical procedure using deflection data from two NDT devices.

#### Comparisons of Performance Criteria

65. Performance criteria are the link between pavement characterization and evaluation in terms of predicted allowable loadings and remaining pavement life. The evaluation methods demonstrated in this project use several approaches to performance criteria. Some methods such as PCS, Berger, and WES DSM correlate the NDT-pavement characterization to conventional parameters of CBR and  $k$  and then apply the standard relationships in terms of design curves from existing Air Force manuals (or use computer codes using these criteria). Other methods, such as Dynatest, ERES, ARE, and AFESC, use allowable stress/strain levels in the various pavement components to predict when pavement failure will occur. Another approach is the use of limiting levels of subgrade deflection, such as Brändley. Table 13 summarizes the various

performance criteria used in the evaluation method demonstrated in this study. These criteria differ considerably in format, and, therefore, a direct comparison is difficult.

66. The existing pavement evaluation procedure used by the Air Force uses test-pit measurements based on many years of performance data collected on both inservice pavements and special test sections which were trafficked to failure. This approach uses values of CBR and  $k$  to characterize the strength of subgrade and of base and subbase layers. Moisture and density are accounted for as well as other important material properties such as gradation and plasticity. Failure of pavements in this system is characterized by cracking and/or rutting. This method has been validated through the years and is considered as the standard (Headquarters, Departments of the Navy, Army, and Air Force 1978; Headquarters, Departments of the Army and Air Force 1979).

67. Those evaluation methods using the standard Air Force evaluation curves make use of this established performance criteria. However, the relationships used to predict the CBR and  $k$  values become the critical elements. PCS used a direct correlation between predicted modulus and CBR or  $k$ . The Berger and WES DSM methods also used correlations to the existing Air Force procedure, but, by making correlations to ASWL as obtained from CBR or  $k$ , the methods are more indirect.

68. Other methods, such as Dynatest, ERES, ARE, and AFESC, have limiting criteria placed on critical elements of the pavement structure such as the AC, PCC, and subgrade. PCS states that they have a similar evaluation method, but it was not demonstrated for this project. Brandley bases the link to the performance on subgrade deflection criteria. Although the subgrade deflection criteria are presented in graphical form by Brandley, the curves have been converted to an equation that approximates the curves for inclusion in Table 13.

#### Comparison of Allowable Load Predictions

69. The project requirements called for evaluation of the five test areas in terms of AGAL's for each of the 13 aircraft groups, each at four pass-intensity levels. Each aircraft group has a controlling aircraft (the most critical aircraft for the group), and the evaluations are actually made for these controlling aircraft. These controlling aircraft for each group and

pass-intensity level are presented in Table 5. The aircraft characteristics including maximum design loads and empty loads are shown in Table 6.

70. The AGAL's for the 13 aircraft groups were computed using the standard Air Force method based on test-pit measurements. The test-pit data used for the standard evaluation have been previously discussed. The rigid pavement AGAL's were determined using extended traffic (shattered slab) criteria as set forth in TM 5-827-1 (Headquarters, Departments of the Army and Air Force 1981) and TM 5-827-3 (Headquarters, Department of the Army 1982). The flexible pavement AGAL's were determined as set forth in TM 5-827-2 (Headquarters, Departments of the Army and Air Force 1981). The AGAL's based on the standard are shown in Table 14. Overlay thicknesses, which are discussed later, are also shown in Table 14. Pavement properties used for evaluation are also shown in this table. Test Areas 1 and 2 rate as adequate to support the maximum design loads for all 13 aircraft groups at all pass intensity levels. (Note that + indicates the allowable load is greater than maximum weight of the aircraft.) Test Areas 3 and 4 rate adequate for the maximum load at pass intensity levels III and IV. Test Area 5 has the lowest load rating of all the five areas, but it too has a fairly high load rating.

71. Allowable loads and overlays were also computed for Test Areas 1 and 5 using test-pit data reported in the 1980 AFESC Evaluation Report (AFESC 1980). These results are shown in Table 15. Test Area 4 was evaluated as an equivalent flexible pavement in Table 14, and therefore the discrepancy between 1980 AFESC test-pit data and the values selected for use in Table 14 would not change the results for Test Area 4. The allowable loads and overlays in Table 15 can be compared with those in Table 14. No significant change occurs for Test Area 1; however, a significant difference results for Test Area 5.

72. Each participant was furnished a copy of pages 5-16, 21-22, and 24-51 of the 1980 AFESC Pavement Evaluation Report (AFESC 1980). These pages contain the data summarized in the first column of Table 3.

73. The allowable load results from each NDT evaluation method are compared to the standard rating, as shown in Table 16. The comparisons are made only for three aircraft, the F-4, C-141, and B-52, which represent light-, medium-, and heavy-load aircraft, respectively. Because the allowable loads represented by + mean that the rating exceeds the maximum design load (see Table 6 for maximum values), a comparison of these ratings could be

misleading. This is because, in this case, the amount that the predicted load rating exceeds the maximum design load is not known. Obviously, most of the test area pavements were more than adequate for all aircraft. This fact makes the comparisons difficult.

74. Figures 38 through 43 graphically display the allowable load comparisons. Figures 38, 39, and 40 are for Test Area 3; whereas, Figures 41, 42, and 43 show results for Test Area 5. The three aircraft, F-4, C-141, and B-52, are shown for pass intensity level I. Test Areas 3 and 5 were selected for these comparisons because the allowable loads from the NDT evaluation methods for these areas are not all at the maximum design loads. Similar comparisons for the other three test areas are not possible because the allowable loads are at the maximum.

75. Figures 38, 39, and 40 show that all NDT evaluation methods predicted the allowable loads for Test Area 3 to be generally lower than the standard load rating. The pattern, however, varies with the different aircraft, and this may indicate some difference in the way the evaluation methods consider multiple-wheel gear configurations. The evaluation methods agree better with the standard load rating for the rigid pavement of Test Area 5 (Figures 41, 42, and 43). The distribution is very similar for the F-4 and C-141 but somewhat different for the B-52.

76. The fatigue relationships inherent in all the evaluation methods adjust the allowable loads as a function of number of passes (load repetitions). Figures 44 and 45 show the relationship of allowable load to passes for flexible (Test Area 3) and rigid (Test Area 5) pavements, respectively.

#### Comparison of Overlay Thickness

77. Overlay thickness computations were made using the standard Air Force procedure and each of the NDT evaluation methods. The overlays were computed for two design load conditions--1,000 passes of KC-10A (DC-10-30) aircraft, and 10,000 passes of an E-4 (B-747) aircraft. Table 17 shows the predicted overlay thicknesses from the standard procedure (minimum overlay criteria has not been included) and from the various NDT evaluation methods. The AFESC NDT procedure does not presently produce overlay thicknesses, so it is absent from the table. Some evaluation methods presented only AC overlays; whereas, others gave both AC and PCC options.

78. By the standard procedure, overlay thicknesses were only required for Test Area 5 because all other test areas evaluated as adequate to support the design aircraft. The overlay calculations (for Test Area 5 which is PCC pavement) were performed as set forth in TM 5-824-3/AFM 88-6 (Headquarters, Departments of the Army and Air Force 1979). All overlay designs are based on initial failure criteria. Thickness of nonrigid (AC) overlay on a rigid pavement,  $t_{ac}$ , is determined by

$$t_{ac} = 2.5 [F(h_d) - Ch]$$

where

F = factor that projects the cracking that may be expected to occur in the base pavement

$h_d$  = required single slab thickness, in.

C = condition factor (0.5 to 1.0)

$h$  = existing rigid slab thickness, in.

Rigid overlays to be placed directly on the existing rigid base pavement were designed using the partial bond equation

$$h_o = 1.4 \sqrt{h_d^{1.4} - Ch^{1.4}}$$

and for the base where the rigid slab is to be placed on a flexible leveling course or bond breaker the unbonded equation was used.

$$h_o = h_d^2 - Ch^2$$

where

$h_d$  = required single slab thickness, in.

C = condition factor (0.35 to 1.0)

$h$  = existing rigid slab thickness, in.

For the overlay designs for Test Area 5, the condition factor C in the above equations was taken as 1.0 because of the excellent condition of the existing pavement. The F factor was also 1.0.

79. Most NDT evaluation methods showed little, if any, overlay needed for Test Areas 1 and 2. The methods indicated some overlay for Test Area 3. AC overlays predicted for Test Areas 4 and 5 ranged considerably. Statistics

from all evaluation methods indicate the following.

AC Overlays, in.					
<u>Test Area</u>	<u>Design Aircraft</u>	<u>Mean</u>	<u>Standard Deviation</u>	<u>Spread of Data</u>	<u>Standard Air Force Test-Pit Method, in.</u>
1	KC10A	0	0	0	0
	E4	0.30	0.90	0-2.7	0
2	KC10A	0.20	0.60	0-1.8	0
	E4	0.41	1.23	0-3.7	0
3	KC10A	5.94	9.62	0-31.1	0
	E4	8.71	8.45	0-26.1	0
4	KC10A	2.74	3.27	0-8	0
	E4	4.05	5.98	0-17	0
5	KC10A	4.58	6.39	0-18.9	1.8
	E4	8.40	8.67	0-21.0	4.5

80. This same type of information cannot be presented for PCC overlays, because not all evaluation methods give PCC overlays; not enough information is available for the statistical computations.

#### PART IV: CONCLUSIONS

81. As earlier stated, the main purpose of the study reported herein was to assess several NDT evaluation methods and to provide the Air Force with information to make sound decisions for the possible uses and benefits of NDT. The results of this study led to the following conclusions:

- a. The study did not set out to identify any best method for NDT, and no best method for general application at all airfields was identified as a result of the data collected and comparisons made.
- b. It appears that the site selected (MacDill AFB) proved to be a poor choice for the following reasons: (1) unusual subgrade (sand) and base course (limerock) materials are nontypical; (2) the pavements were strong enough so that most evaluated as being adequate for all loading conditions using the current standard method which reduced one's ability to compare the results of evaluation techniques (Headquarters, Department of the Air Force 1981); and (3) the baseline test-pit data were not collected concurrently with the NDT results (test-pit data were 2 years old), and some test-pit data are suspected of being in error.
- c. Based on use of the NDT evaluation method at MacDill, wide variation occurs in terms of allowable loads among the results and substantial disagreement of some methods with the standard test-pit method (Figures 38 through 43). Some NDT methods predicted overlay thicknesses that were in agreement with the overlay thickness predicted by the test-pit standard; others did not agree (Table 17). Some methods agreed well on some pavement test areas, but did not agree on other test areas. In general, the various NDT evaluation methods produced inconsistent results for the pavement areas evaluated. However, in almost all cases, the NDT methods gave results more conservative (i.e., smaller allowable load and thicker overlay) than those from the test-pit standard method. Overlay thicknesses from some methods generally agreed with the standard. Because of the unusual base course and subgrade conditions, the relative ranking of the various methods in terms of overlay thickness prediction should not be generalized to other airfields.
- d. Significant differences were noted in measurements made by the various NDT devices, and no one device can be said to give the best results on the pavement test areas studied. Deflection basin data from the various NDT devices were compared (Figures 25 through 29). The devices with higher load magnitudes, i.e., WES 16-kip vibrator, PCS FWD, and Dynatest FWD, produced larger deflections and steeper deflection basins than did the smaller ARE Dynaflect and Berger Pavement Profiler devices. Input of deflection basin data from each device into a common layered-elastic theory analysis gave inconsistent and variable elastic moduli using the back-calculating technique (Table 10).

- e. Stiffness values (maximum load divided by maximum deflection) from each device on each test area were compared. The overall range of stiffness values was a factor of approximately two with no consistent trends of high or low mean value from any device common to all or nearly all of the five test areas. The Berger Pavement Profiler consistently gave the highest coefficient of variation in terms of stiffness value.
- f. All evaluation methods, except the WES DSM method, determine elastic moduli for the pavement layers and subgrade. Considerable variation in these moduli occurred from one technique to another (Figures 36 and 37).
- g. The performance criteria, which translates the NDT measurements to evaluated load-carrying capacity and overlay requirements, were quite different for the various NDT evaluation methods (Table 13). The performance criteria were given in terms of limiting stress or strain for pavement components, limiting subgrade deflection, and correlations to existing Air Force criteria and are functions of pass intensity level. No direct comparisons could be made of the performance criteria from different methods because of fundamental differences in the nature of the criteria. A comparison of predicted allowable loads at different pass intensities indicated that the rate of change in allowable load with pass intensity was significantly different by some methods (Figures 44 and 45). Because the performance criteria are the only parts of the methods which are functions of pass intensity, a conclusion is drawn that the performance criteria used in some of the methods are more sensitive to the number of passes than others for the conditions at MacDill AFB.
- h. Most of the NDT procedures provide for testing of the load transfer capacity at joints in PCC pavement. This was typically done by applying a load on one slab near the joint, and measuring the deflection of each slab at the joint. Not all methods used the load transfer measurements in the allowable load and overlay computations. The standard Air Force evaluation method for PCC pavement assumes an average load transfer of 25 percent at the joints, which may not be true for all pavement conditions. This may account for some of the variation in results, particularly for Test Area 5.
- i. Use of the NDT procedures to evaluate the load transfer capacity of joints in PCC pavements appears to be a viable approach and is an important aspect of any structural evaluation. Further work needs to be devoted to development of this concept to validate the various methods demonstrated in this project.

## PART V: RECOMMENDATIONS

82. The following recommendations are made:

- a. The study reported herein should be repeated at other sites to produce more conclusive results. These sites should cover more typical pavements over fine-grained soils (clays and silts), test-pit data should be collected concurrently with the NDT data, and the pavements should be of such design that a range of allowable loads and overlay thicknesses would be anticipated so that a better comparison of results could be made. What is needed is a set of test areas where the standard method predicts some areas are in danger of incipient failure under common aircraft loads and other areas are not. At MacDill, this was not the case.
- b. A standard NDT evaluation method is apparently needed. The standard could be a general procedure (based on an appropriate analytical theory); the performance criteria must be compatible with the system and based on known performance of airfield pavements and the method should be validated. Such a standard could be used to assess the validity of new or more simplified methods. Further study should be made of performance criteria, such as limiting stress, strain, and deflection, and criteria should be selected for use with the standard NDT evaluation method.
- c. Further work with NDT equipment is needed to determine limitations (if any) of different NDT devices. A desirable goal is a standard analysis method that would accept input from any one of several different test devices. A sensitivity study could be made using the standard NDT evaluation method with input from various NDT devices to identify limitations.

## REFERENCES

- Ahlin, R. G., et al. 1971 (No.). "Multiple-Wheel Heavy Gear Load Pavement Tests; Basic Report," Technical Report S-71-17, Vol II, US Army Engineer Waterways Experiment Station, Vicksburg, Miss.
- Air Force Engineering and Services Center. 1980 (Jul). "Partial Airfield Pavement Evaluation Report - MacDill AFB, Florida," Tyndall Air Force Base, Fla.
- . 1982. "USAF Nondestructive Pavement Evaluation System," Tyndall AFB, Fla.
- Alexander, D. R. 1982 (Nov). "Nondestructive Pavement Evaluation, Alameda Naval Air Station, Alameda, California," (unnumbered paper) US Army Engineer Waterways Experiment Station, Vicksburg, Miss.
- ARE, Inc. 1983 (Jan). "Demonstration of ARE Inc. Pavement Evaluation Methodology at MacDill AFB," Report No. AF-8, Engineering Consultants, Austin, Tex.
- Asphalt Institute. 1969 (Nov). "Asphalt Overlays and Pavement Rehabilitation," Manual Series No. 17, College Park, Md.
- Bonnaure, F., Gravois, A., and Udrone, J. 1980. "A New Method for Predicting the Fatigue Life of Bituminous Mixes," Proceedings, Association of Asphalt Paving Technologists, Vol 49, pp. 499-529.
- Brandley, R. W. 1975 (Nov). "Fatigue-Analysis Method for Pavement Evaluation and Design," Symposium on Nondestructive Test and Evaluation of Airport Pavement, Vicksburg, Miss.
- . 1983 (Feb). "Nondestructive Test Evaluation Study, MacDill Air Force Base, Tampa, Florida," Published by Brandley, Sacramento, Calif.
- Bush, A. J., III. 1980a. "Nondestructive Testing for Light Aircraft Pavements; Phase II, Development of the Nondestructive Evaluation Methodology," Report No. FAA-RD-80-9-II, Federal Aviation Administration, Department of Transportation, Washington, DC.
- . 1980b. "Nondestructive Testing for Light Aircraft Pavements; Phase I, Evaluation of Nondestructive Testing Devices," Report No. FAA-RD-80-9-I, Federal Aviation Administration, Department of Transportation, Washington, DC.
- Chou, Y. T. 1976. "Analysis of Subgrade Rutting in Flexible Airfield Pavements," Transportation Research Record, No. 616, Washington, DC.
- . 1981. "Structural Analysis Computer Programs for Rigid Multi-component Pavement Structures with Discontinuities - WESLIQID and WESLAYER," Technical Report GL-81-6, Reports 1, 2, and 3, US Army Engineer Waterways Experiment Station, Vicksburg, Miss.
- Construction Engineering Laboratory, Ohio River Division Laboratories. 1964 (Oct). "Condition Survey Report, MacDill Air Force Base, Florida," Cincinnati, Ohio.
- Dynatest Consulting, Inc. 1983 (Jan). "Comparative NDT Study of Five Test Areas at MacDill AFB in Tampa, Florida," Final Report, Ojai, Calif.

ERES Consultants, Inc. 1982 (Dec). "Nondestructive Structural Evaluation of Airfield Pavements," Champaign, Ill.

Federal Aviation Administration. 1976 (Jun). "Use of Nondestructive Testing Devices in the Evaluation of Airport Pavements," Advisory Circular AC 150/5370-11, Department of Transportation, Washington, DC.

Green, J. L. 1978 (Mar). "Literature Review - Elastic Constants for Airport Pavement Materials," Report No. FAA-RD-76-138, Federal Aviation Administration, Department of Transportation, Washington, DC.

Green, J. L., and Hall, J. W., Jr. 1975 (Sep). "Nondestructive Vibratory Testing of Airport Pavements, Experimental Test Results, and Development of Evaluation Methodology and Procedure," Report No. FAA-RD-73-205-1, Vol I, Federal Aviation Administration, Washington, DC.

Hadala, P. E. 1975 (Jun). "Evaluation of Empirical and Analytical Procedures Used for Predicting the Rigid Body Motion of an Earth Penetrator," Miscellaneous Paper MP S-75-15, US Army Engineer Waterways Experiment Station, Vicksburg, Miss.

Hall, J. W., Jr. 1970 (May). "Nondestructive Testing of Flexible Pavements A Literature Review," Technical Report No. AFWL-TR-68-147, Kirtland Air Force Base, Air Force Weapons Laboratory, N. Mex.

\_\_\_\_\_. 1972 (Mar). "Nondestructive Testing of Pavements; Tests on Multiple-Wheel Heavy Gear Load Sections at Eglin and Hurlburt Airfields," Technical Report No. AFWL-TR-71-64, Air Force Weapons Laboratory, Albuquerque, N. Mex.

\_\_\_\_\_. 1973 (Jun). "Nondestructive Testing of Pavements; Final Test Results and Evaluation Procedure," Technical Report No. AFWL-TR-151, Air Force Weapons Laboratory, Albuquerque, N. Mex.

\_\_\_\_\_. 1978 (Jul). "Nondestructive Evaluation Procedure for Military Airfields," Miscellaneous Paper S-78-7, US Army Engineer Waterways Experiment Station, Vicksburg, Miss.

Hall, J. W., Jr., and Alexander, D. R. 1983 (Jan). "Comparative Study of Nondestructive Pavement Testing-WES NDT Methodologies," Miscellaneous Paper GL-85-26, US Army Engineer Waterways Experiment Station, Vicksburg, Miss.

Hall, J. W., Jr., and Elsea, D. R. 1974 (Feb). "Small Aperture Testing for Airfield Pavement Evaluation," Miscellaneous Paper S-74-3, US Army Engineer Waterways Experiment Station, Vicksburg, Miss.

Hammitt, G. M., II. 1974 (Dec). "Concrete Strength Relationships," Miscellaneous Paper S-74-30, US Army Engineer Waterways Experiment Station, Vicksburg, Miss.

Headquarters, Department of the Air Force. 1981 (May). "Airfield Pavement Evaluation Program," AFM 93-5, Washington, DC.

Headquarters, Department of the Army. 1982 (Mar). "Rigid Airfield Pavement Evaluation," TM 5-827-3, Washington, DC.

Headquarters, Departments of the Army and Air Force. 1979 (Aug). "Rigid Pavements for Airfields Other than Army," TM 5-824-3/AFM 88-6, Chap. 3, Washington, DC.

Headquarters, Departments of the Army and Air Force. 1981 (Mar). "Airfield Pavement Evaluation Concepts," TM 5-827-1/AFM 88-24, Chap. 1, Washington, DC.

\_\_\_\_\_. 1981 (Apr). "Flexible Pavement Evaluation," TM 5-827-2/AFM 88-24, Chap. 2, Washington, DC.

Headquarters, Departments of the Navy, Army, and Air Force. 1978 (Aug). "Flexible Pavement Design for Airfields," DM 21.3/TM 5-825-2/AFM 88-6, Chap. 2, Washington, DC.

Herholdt, A. D., et al. 1979. "Beton-bogen," Cementfabrikkernes tekniske Oplysningskontor, Denmark.

Heukelom, W., and Foster, C. R. 1960 (Feb). "Dynamic Testing of Pavements," Journal, Soil Mechanics and Foundations Division, American Society of Civil Engineers, Vol 86, No. SM1, Part 1, pp 1-28.

Heukelom, W., and Klomp, A. J. G. 1962 (Aug). "Dynamic Testing as a Means of Controlling Pavements During and After Construction," Proceedings, First International Conference on the Structural Design of Asphalt Pavements, Ann Arbor, Mich.

Hoffman, M. D., and Thompson, M. R. 1981 (Jun). "Mechanistic Interpretation of Nondestructive Pavement Testing Deflections," Report No. UILU-ENG-81-2010, University of Illinois/Illinois Department of Transportation.

Larsen, T. J., and Nussbaum, P. J. 1967 (May). "Fatigue of Soil Cement," Journal of the Portland Cement Association, Research and Development Laboratories, Skokie, Ill.

Louis Berger International, Inc. 1983 (Mar). "Airfield Pavement Evaluation, MacDill Air Force Base, Florida, Final Report," East Orange, N. J.

Maxwell, A. A. 1960a (Jan). "Nondestructive Testing of Pavements," Miscellaneous Paper No. 4-373, US Army Engineer Waterways Experiment Station, Vicksburg, Miss.

\_\_\_\_\_. 1960b. "Non-Destructive Testing of Pavements," Non-Destructive Dynamic Testing of Soils and Highway Pavements, Highway Research Bulletin No. 277, pp. 30-36, National Academy of Sciences--National Research Council, Washington, DC.

Maxwell, A. A., and Joseph, A. H. 1967. "Vibratory Study of Stabilized Layers of Pavement in Runway at Randolph Air Force Base," Proceedings, Second International Conference on the Structural Design of Asphaltic Pavements, University of Michigan, Ann Arbor, Mich.

Moore, W. M., Hanson, D. I., and Hall, J. W., Jr. 1978 (Jan). "An Introduction to Nondestructive Structural Evaluation of Pavements," Transportation Research Circular No. 189, Transportation Research Board, National Academy of Sciences, Washington, DC.

Office, District Engineer, Savannah. 1947 (Jan). "Airfield Evaluation, MacDill Field, Supplement to Final Report," Savannah, Ga.

Pavement Consultancy Services 1983. "NDT Testing, Analysis, and Evaluation of Pavement Sections at MacDill Air Force Base, Tampa, Florida," Arlington, Va.

Peutz, M. G. F. 1968. "BISTRO: Computer Program for Layered Systems Under Normal Surface Loads," Koninklijke/Shell Laboratorium, Amsterdam, Holland.

Rigid Pavement Laboratory of the US Army Engineer, Ohio River Division Laboratories. 1960 (May). "Condition Survey Report, MacDill Air Force Base, Florida," Mariemont, Ohio.

Tabatabie, A. M., and Barenberg, E. J. 1979. "Longitudinal Joint Systems in Slip-Formed Rigid Pavement: Vol III--User's Manual," Technical Report No. FAA-RRD-79-4-III, Federal Aviation Administration, Washington, DC.

Ullidtz, P. 1973. "En Studie Af to Dybdeasfaltbefaestelser," (Danish), Ph.D. dissertation, The Technical University of Denmark.

. 1977. "Overlay and Stage by Stage Design," Fourth International Conference on the Structural Design of Asphalt Pavements, Ann Arbor, Mich.

US Engineer Office, Jacksonville. 1944 (Apr). "Airfield Pavement Evaluation MacDill Field," Final Report, Jacksonville, Fla.

US Army Engineer District, Jacksonville. 1960 (Feb). "Airfield Evaluation Report, MacDill Air Force Base, Florida," Jacksonville, Fla.

US Army Engineer, Ohio River Division Laboratories. 1954 (Apr). "Report on Rigid Pavement Condition Surveys at MacDill AFB, Tampa, Florida," Mariemont, Ohio.

US Army Engineer Waterways Experiment Station. 1963 (Sep). "Analysis of Data, Non-Destructive Dynamic Soil Tests at AASHO Road Test," Contract Report No. 4-79, Vicksburg, Miss., prepared by Eustis Engineering Company, New Orleans, La.

. 1964 (Jan). "Analysis of Data, Non-Destructive Dynamic Soil Tests, Foss Field, Sioux Falls, South Dakota," Contract Report No. 4-85, Vicksburg, Miss., prepared by Eustis Engineering Company, New Orleans, La.

Weiss, R. A. 1980. "Pavement Evaluation and Overlay Design Using Vibratory Nondestructive Testing and Layered Elastic Theory; Vol 1, Development of Procedure," Report No. FAA-RD-77-186-I, Federal Aviation Administration, Department of Transportation, Washington, DC.

Westergaard, H. M. 1948. "New Formulas for Stresses in Concrete Pavements of Airfields," Transactions, American Society of Civil Engineers, New York.

Yoder, E. J., and Witczak, M. W. 1975. Principles of Pavement Design, 2nd ed., Wiley, New York.

Table 1  
NDT Method Presented to Transportation Research Board  
Task Force AZT56, August 11-14, 1981

- 
- O'Massey, R. C. and McReynolds, M. (McDonnell Douglas), "Dynamic Pavement Modeling - Preliminary Studies"
- Ilves, G. J. and Majidzadeh, K. (Resource International), "Nondestructive Evaluation of Airfield Pavements"
- Thompson, M. R. (University of Illinois), "Illi-Pave Procedure for Determining In-Situ Properties from NDT Deflection Data"
- Bush, A. J. (U. S. Army Corps of Engineers), "Pavement Evaluation Using Deflection Basin Measurements to Characterize an Elastic Layer System"
- Witczak, M. W. (University of Maryland), "Use of NDT Deflection Data to Estimate In Situ Material Moduli"
- Shahin, M. Y., Sharma, J., Smith, M. E. and Stubstad, R. N. (Dynatest - ERES) "Nondestructive Testing of Airfield Pavements"
- Visser, W., and Koole, R. C. (Pavement Consultancy Services/Shell), "Evaluation of Aircraft Pavements"
- Harr, M. E. and Elton, D. J. (Purdue), "Non Contact - Non Destructive Evaluation Using Prototype Loads"
- Hall, J. W. (WES), "Nondestructive Evaluation of Airfield Pavements - DSM Method"
- Walker, F. K. (Greiner Engineering Sciences), "Evaluation of Flexible Airfield Pavement Using the Corps of Engineers WES 16 Kip Vibratory Loading Device"
- Marien, H. R. and Baird, G. T. (U. S. Air Force), "US Air Force Nondestructive Airfield Pavement Evaluation Method"
- Irwin, L. H. and Johnson, T. C. (CRREL), "Frost-Affected Resilient Moduli Evaluated with the Aid of Nondestructively Measured Pavement Surface Deflections"
- Argue, G. H. (Transport Canada - Air), "Strength Evaluation of Airport Pavements by Static Plate Load Testing"
- McCullough, B. F. (ARE, Inc.), "Position Paper on ARE, Inc. Airport Design Method"
- Wiseman, G. and Berger, L. (L. Berger International), "Evaluation of Airfield Pavements and Subgrades Based on Deflection Basin Measurements (NDT)"

Table 2  
Construction History

<u>Area</u>	<u>Description</u>	<u>Approximate Construction Period</u>	<u>Remarks</u>
1	Taxiway 33	1959	COE Project AP 86-04-16
2	Taxiway 3B	1943	Original construction by COE
		1956	18-ft-keel overlay, MacDill Project 22-57
		1963	MacDill Project 5-62, overlay
		1971	MacDill Project 62-0, overlay
3	Taxiway 3	1943	Original construction by COE
		1956	MacDill Project 22-57, 18-ft-keel overlay
		1969	MacDill Project 8-5, overlay
4	Apron 1A-1	1941	Original construction by COE
		1952	COE Project 85-04-04, overlay
		1966	Slurry seal, MacDill Project 7-5
		1968	Seal coat, MacDill Project 214-8
5	Apron 1A	1941	Original construction by COE
		1952	COE Project 06-06-02
		1975	MacDill Project 90-3, remove existing pavement and replace

Table 3  
Summary of Pavement Physical Properties

Test Area	Air Force Engineering and Services Center (1960)	US Engineer Office, Jacksonville, Fla. (1944)	Office, District Engineer, Savannah, Ga. (1947)
1	20-in. PCC, $R = 480$ 11.5-in. subbase (SP-SM), $k = 230$ Subgrade (SP-SM), $\gamma_d = 98.3$ , $w = 23.9$	---	---
2	11-in. AC 11-in. base, CBR = 80 4-in. base, CBR = 80 Subgrade, CBR = 35, $\gamma_d = 105.4$ , $w = 6.7$	---	3-in. AC 8-in. limerock, CBR = 80 Subgrade (GP), CBR = 30
3	5.5-in. AC 6.5-in. base, CBR = 80 5.5-inet. SP-SM, CBR = 25, $\gamma_d = 107.3$ , $w = 9.1$ SP, CBR = 30, $\gamma_d = 97.0$ , $w = 10.8$	---	3-in. AC 8-in. limerock, CBR = 80 Subgrade (GP), CBR = 30
4	7.5-in. AC 6.5-in. PCC, $R = 580$ SP, $k = 85$ , $\gamma_d = 101.4$ , $w = 9.0$	$R = 591$ Subgrade (SP), $k = 440$ $\gamma_d = 110$ , $w = 7.8$ , 0-6 in. depth $\gamma_d = 106$ , $w = 9.5$ , 6-18 in. depth	8-6 in. PCC* Sand (SP), $k = 370$
Alternate for Area 4 as flexible pavement:			
7	7.5-in. AC 6.5-in. base, CBR = 80 SP, CBR = 30	8-6 in. PCC* Sand (SP), $k = 370$ psi	8-6 in. PCC* Sand (SP), $k = 370$ psi
5	10.5-in. PCC, $R = 470$ SP, $k = 80$ , $\gamma_d = 109.8$ , $w = 11.7$	$k = 360$ pci $\gamma_d = w = 107$ , 4.3, 0-6 in. depth $\gamma_d = w = 100$ , 15.8, 6-18 in. depth	8-6 in. PCC* Sand (SP), $k = 370$ psi

(Continued)

Note:  $\gamma_d$  = dry density, pci;  $w$  = moisture content, percent; SP-SM = poorly graded silty sand; SP = poorly graded sand; and GP = poorly graded gravel.  
\* Working stress of PCC = 345 psi.

Table 3 (Concluded)

Test Area	US Army Engineer District, Jacksonville, Fla. (1960)	US Army Engineer, Ohio River Laboratories (1954)	Rigid Pavement	Construction Engineering Laboratory, Ohio River Division Laboratories (1964)
			Laboratory of the Ohio River Division (1960)	
1	2)-in. PCC, R = 750 6-in. stabilized subbase, k = 300 Sand (SP)	--	--	20-in. PCC, R = 750 6-in. stabilized sub- grade, k = 300 Sand (SP-SM)
2	6-in. AC 8-in. limerock, CBR = 80 7-in. stabilized subbase, CBR = 30 Sand (SP), CBR = 25	3-in. AC 8-in. limerock base, CBR = 80 7-in. limerock stabilized subbase, CBR = 30 Sand (SP), CBR = 30	--	--
3	6-in. AC 8-in. limerock, CBR = 80 7-in. stabilized subbase, CBR = 30 Sand (SP), CBR = 25	3-in. AC 8-in. limerock base, CBR = 80 7-in. limerock stabilized subbase, CBR = 30 Sand (SP), CBR = 30	--	--
4	6-in. AC 6-in. PCC, R = 650 Sand (SP), k = 250	6-in. AC 8-6-8-in. PCC, R = 700 Sand (SP), k = 370 , CBR = 40	6-in. AC 8-6-8 in. PCC, k = 650 Sand (SP-SM), k = 250 CBR = 25	6-in. AC 8-6-8 in. PCC, R = 650 Sand (SP-SM), k = 250 CBR = 25
5	6-in. AC 6-in. PCC, R = 650 Sand (SP), k = 250	6-in. AC 8-6-8-in. PCC, R = 700 Sand (SP), k = 370 , CBR = 40	6-in. AC 9-6-9 in. PCC, R = 650 Sand (SP-SM), k = 250 , CBR = 25	6-in. AC 9-6-9-in. PCC, R = 650 Sand (SP-SM), k = 250

Table 4  
Thirteen Aircraft Groups

Aircraft Group	Aircraft
1	C-123
2	A-7, A-10, A-37, F-4, F-5, F-14, F-15, F-16, F-100, F-101, F-102, F-105, F-106, T-33, T-37, T-38, T-39, OV-10
3	F-111, FB-111
4	C-130
5	C-7, C-9, DC-9, C-54, C-131, C-140, T-29
6	737, T-45, C-119, EC-121
7	727, KC-97
8	707, E-3, C-135, KC-135, VC-137
9	C-141
10	C-5A
11	KC-10A, DC-10, L-1011
12	747, E-4
13	B-52

Table 5  
Pass Levels for Pavement Evaluation

<u>Aircraft Group</u>	<u>Controlling Aircraft</u>	Number of Passes for Four Pass Intensities			
		<u>I</u>	<u>II</u>	<u>III</u>	<u>IV</u>
1	C-123	300,000	50,000	15,000	3,000
2	F-4	300,000	50,000	15,000	3,000
3	F-111	300,000	50,000	15,000	3,000
4	C-130	50,000	15,000	3,000	500
5	C-9	50,000	15,000	3,000	500
6	T-43 (B-737)	50,000	15,000	3,000	500
7	B-727	50,000	15,000	3,000	500
8	KC-135	50,000	15,000	3,000	500
9	C-141	50,000	15,000	3,000	500
10	C-5A	50,000	15,000	3,000	500
11	KC-10A	15,000	3,000	500	100
12	E-4	15,000	3,000	500	100
13	B-52	15,000	3,000	500	100

Table 6  
Aircraft Characteristics for Pavement Evaluation

Air-craft Group	Control-ling Aircraft	Tire Spacing in.	Tire			Main Gear Load percent	Group Minimum kips	Load Range* Maximum kips
			Contact Area sq in.	Tire Pressure psi				
1	C-123	--	270	100		84.3	35	60
2	F-4	--	100	--		87.7	5	60
3	F-111	--	241	--		95.0	50	120
4	C-130	60	400	--		95.7	60	175
5	C-9	26	165	--		93.6	20	110
6	T-43	30.5	174	--		92.8	40	150
7	B-727	34	237	--		92.4	85	175
8	KC-135/ E-3	34.5 x 56	218	--		93.5	105	335
9	C-141	32.5 x 48	208	--		94.4	135	345
10	C-5A	35 x 53 x 65	265	--		94.2	325	770
11	KC-10A (DC 10-30)	54 x 64	294	--		92.2	230	590
12	E-4 (B-747)	44 x 58	245	--		93.5	300	780
13	B-52	37 x 62	267	--		52.0	175	490

\* Group Load Range is the minimum (empty) and maximum (loaded) aircraft weights used for evaluation.

Table 7  
Characteristics of Nondestructive Testing Equipment

Type of load applied	WES 16-kip Vibrator	WES FWD Impulse	Dynatest FWD Impulse	PCS FWD Impulse	Berger Pavement Profiler Vibrator	ARE Dynaflect Vibrator	AF NDPT Van Impulse
Type deflection output	Peak-Peak	Peak	Peak	Peak	Peak-Peak	Peak-Peak	#
Contact area, sq in.	254	110	110	110	254	8.6	113
Maximum dynamic/ impulse force (peak-to-peak), lb	30,000	15,000	24,000	22,400	4,500	1,000	520-lb weight dropped 30 in.
Static weight, lb	16,000	--	--	--	3,800	2,000	--
Test frequency, Hz	15	--	--	--	25	8	--
Loading time, msec	--	25-30	25-30	--	--	--	--
Number of displacement sensors	4	3	7	4	4	5	##
Location of displacement sensors, distance from center of loaded area, in.:	0	+	+	+	+	+	
	8		+				
	12	+	+		+	+	
	18	+					
	24	+	+	+	+	+	
	36	+	+	+	+	+	
	39			+			
	48	+	+				
	60	+	+		++*		
	71				++*		
	79			+			
	96		++*				

Note: # = Accelerometers spaced at 1, 2, 4, 8, and 16 ft from plate to measure wave velocity.

## = Measures phase difference between transducers.

\* = Flexible pavements only.

\*\* = Rigid pavements only.

+ = Locations of sensors.

Table 8  
Summary of NDT Evaluation Methods

Method	Data Analysis	Type Theory	Performance Criteria
PCS	Back-calculate modulus of pavement layers from deflection basin	Layered-elastic (BISAR)	Correlation of E to California Bearing Ratio and k, then use AF design curves
Dynatest	Back-calculate moduli of pavement layers from deflection basin	Layered-elastic (ELMOD) (MET)	Normal stress in unbound materials, horizontal strain bottom of AC, fatigue based on flexural strength of PCC
ERES	Back-calculate moduli of pavement layers from deflection basin (subgrade k modulus determined for sub-grade under PCC)	Finite element (ILLISLAB) for rigid pavement; layered-elastic for flexible pavement	For rigid pavement-- relationship of aircraft coverages to computed stress in concrete; for flexible pavement--radial strain in AC and vertical strain in subgrade; fatigue of base layer
Brandley	Back-calculate moduli of pavement layers from deflection basin	Layered-elastic (ELMOD) (ISSEM4) (CHEVRON)	Limiting subgrade deflection
Berger	Back-calculate moduli of pavement layers from deflection basin and correlation analysis to allowable load and overlay	Layered-elastic (CRANLAY) (GWLB-100) (COMRIGID) (COMPLAYER)	Correlation of stiffness to existing AF design criteria
ARE	Back-calculated moduli of pavement layers from deflection basin (BASFIT)	Layered-elastic (AIRPOD) (ELSYM-5)	Limiting stress in PCC; limiting strain in AC
AFESC	Elastic moduli of pavement layers from wave velocity dispersion curves	Finite element (PREDICT)	Limiting tensile strain in AC; limiting stress in PCC; limiting vertical strain in subgrade
WES DSM	DSM of composite pavement from load-deflection data; radius of relative stiffness, &, from deflection basin	Correlation relationships and analysis of computer (FLEXEVAL) (RIGEVAL)	Correlation of DSM to existing Corps of Engineers/AF design criteria
WES layered-elastic	Back-calculate moduli of pavement layers from deflection basin	Layered-elastic (BISDEF) (AIRPAV)	Limiting strain in subgrade and AC for flexible pavement; limiting tensile stress in PCC for rigid pavement

Table 9  
Comparison of Stiffness Measurements

<u>Nondestructive Testing Device</u>	<u>Number of Test</u>	<u>Average Stiffness kips/in.</u>	<u>Standard Deviation</u>	<u>Coefficient of Variation</u>
<u>Test Area 1</u>				
WES 16-kip vibrator	28	6,053	617	10.2
WES FWD	28	7,689	665	8.6
Dynatest FWD	14	8,575	582	6.8
PCS FWD	28	9,367	512	5.5
Berger Pavement Profiler	8	10,249	1,260	12.3
ARE Dynaflect	14	6,366	627	9.85
Average for Test Area	--	8,050	--	--
<u>Test Area 2</u>				
WES 16-kip vibrator	30	1,762	212	12.0
WES FWD	30	1,481	167	11.3
Dynatest FWD	16	1,304	225	17.2
PCS FWD	18	1,719	205	11.9
Berger Pavement Profiler	16	2,348	337	14.4
ARE Dynaflect	15	2,453	240	9.8
Average for Test Area	--	1,845	--	--
<u>Test Area 3</u>				
WES 16-kip vibrator	22	865	102	11.7
WES FWD	21	509	49	9.6
Dynatest FWD	22	499	55	11.1
PCS FWD	26	676	66	9.3
Berger Pavement Profiler	22	808	126	15.6
ARE Dynaflect	22	1,189	155	13.0
Average for Test Area	--	--	--	--
<u>Test Area 4</u>				
WES 16-kip vibrator	12	2,233	287	12.8
WES FWD	12	2,125	305	14.4
Dynatest FWD	12	2,230	400	18.0
PCS FWD	20	2,362	540	22.8
Berger Pavement Profiler	10	2,933	686	23.4
ARE Dynaflect	25	2,274	419	18.4
Average for Test Area	--	2,360	--	--

(Continued)

Table 9 (Concluded)

<u>Nondestructive Testing Device</u>	<u>Number of Test</u>	<u>Average Stiffness kips/in.</u>	<u>Standard Deviation</u>	<u>Coefficient of Variation</u>
<u>Test Area 5</u>				
WES 16-kip vibrator	35	2,588	186	7.2
WES FWD	34	2,762	188	6.8
Dynatest FWD	25	2,554	297	11.6
PCS FWD	28	3,200	285	8.9
Berger Pavement Profiler	22	2,896	316	10.9
ARE Dynaflect	14	1,924	181	9.4
Average for Test Area	--	2,654	--	--
<u>Variation, All Areas</u>				
WES 16-kip vibrator			10.8	
WES FWD			10.1	
Dynatest FWD			12.9	
PCS FWD			11.7	
Berger Pavement Profiler			15.3	
ARE Dynaflect			12.1	

Table 10  
Moduli Predicted from Deflection Basins  
from Different NDT Equipment

NDT Device	Elastic Modulus, psi		Subgrade Sand
	20-in. PCC	Test Area 1	
<u>Test Area 1</u>			
WES 16-kip vibrator	3,440,538		46,244
WES FWD	6,928,316		35,639
Dynatest FWD	9,117,088		31,499
PCS FWD	9,452,344		35,080
Berger Pavement Profiler	6,111,868		59,205
ARE Dynaflect	11,530,20		10,367
<u>Test Area 2</u>			
	10-in. AC	15-in. Limerock- Stabilized Base	Subgrade Sand
WES 16-kip vibrator	680,279	59,740	37,209
WES FWD	572,022	30,116	37,438
Dynatest FWD	538,205	36,649	29,799
PCS FWD	559,951	65,255	31,818
Berger Pavement Profiler	452,499	90,633	50,928
ARE Dynaflect	154,052	403,405	22,579
<u>Test Area 3</u>			
	5.5-in. AC	15-in. Limerock- Stabilized Base	Subgrade Sand
WES 16-kip vibrator	691,229	40,926	26,753
WES FWD	185,244	16,241	31,738
Dynatest FWD	185,952	20,682	20,375
PCS FWD	332,768	18,244	27,155
Berger Pavement Profiler	537,513	35,074	24,344
ARE Dynaflect	52,175	40,381	23,872

(Continued)

Table 10. (Concluded)

<u>NDT Device</u>	<u>Elastic Modulus, psi</u>		
	<u>7-in. AC</u>	<u>6-in. Limerock- Stabilized Base</u>	<u>Subgrade Sand</u>
<u>Test Area 4</u>			
WES 16-kip vibrator	1,440,817	3,227,078	25,157
WES FWD	1,982,382	2,047,265	23,242
Dynatest FWD	1,903,426	1,841,818	22,108
PCS FWD	2,334,218	1,387,285	17,160
Berger Pavement Profiler	6,878,414	248,228	23,376
ARE Dynaflect	12,030,469	716,935	10,687
<u>Test Area 5</u>			
10.5-in. <u>AC</u>			<u>Subgrade Sand</u>
WES 16-kip vibrator	3,119,032		26,580
WES FWD	3,756,947		23,448
Dynatest FWD	4,040,810		19,496
PCS FWD	6,846,501		22,938
Berger Pavement Profiler	3,652,117		24,131
ARE Dynaflect	3,562,470		11,292

**Table 11**  
**Summary of Predicted Moduli**

Test Area	Layer	Modulus of Pavement Layers, psi						WES FWD
		Dynatest*	ERES**	PCST†	Berger	ARE	AFESC	
1	PCC	4,400,000	4,000,000	4,000,000	4,000,000	5,000,000	3,150,000	3,200,000
	Base	--	--	--	60,000	--	200,000	65,000
	Subgrade	63,300 k = 345 pci	k = 450 pci	63,300	18,000 k = 500 pci	70,000	31,000	11,750
2	AC	348,000	180,000	63,000	330,000	400,000	500,000	782,000
	Base	32,000	86,000	35,300	60,000	100,000	120,000	78,000
	Subbase	--	--	--	--	--	60,000	--
3	Subgrade	26,000	23,400	51,200	16,000	37,000	34,500	11,750
	AC	401,000	156,000	635,000	330,000	300,000	200,000	1,002,000
	Base	16,000	40,000	10,000	60,000	50,000	60,000	85,000
4	Subbase	--	--	--	--	--	35,000	--
	Subgrade	20,000	19,300	41,000	13,000	24,000	27,000	11,750
	AC	533,000	400,000	635,000	330,000	800,000	300,000	1,391,000
5	PCC	4,500,000	5,800,000	900,000	4,000,000	4,000,000	6,000,000	2,796,000
	Subgrade	26,000 k = 270 pci	k = 375 pci	30,600	18,000	24,000	21,000	14,800
	AC	4,900,000	4,500,000	4,900,000	4,000,000	4,000,000	3,300,000	2,100,000
	Subgrade	15,800 k = 315 pci	k = 195 pci	34,600	18,000 k = 250 pci	30,000	17,500	11,750
	AC	--	--	--	--	--	--	--

\* For evaluation, k = 310 and CBR = 27 were selected for subgrade by PCS.

\*\* Moduli shown for Test Areas 2 and 3 are for 8 ft left of center line.

† Moduli shown for Test Area 2 are for 20 ft left of center line and 10 ft left for Test Area 3.

Table 12

## Moduli Comparison from Brandley and Berger

Test Area	Pavement Layer	Modulus of Pavement Layers, kips per square inch											
		Matching Deflection Bowls-GHLB-100*						Boussinesq Equivalent Thickness†					
		Burmister-Hogg#		WES FWD		PP		WES FWD		ELMOD**		ISSEM 4**	
		WES	16-kip	WES	FWD	WES	16-kip	WES	FWD	WES	FWD	WES	FWD
1	PCC Subgrade	4,400	2,090	2,990	4,880	2,200	3,780	4,250	62	—	—	60	42
2	AC Base Subgrade	400††	400††	400††	500	500	365	340	—	—	—	—	13
3	AC Base Subgrade	400††	400††	400††	450	400	407	446	227	27	—	—	5
4	AC PCC Subgrade	800††	800††	800††	800	800	800	140	—	—	—	—	32
5	PCC Subgrade	11,100	5,300	1,400	8,000	4,000	4,000	4,500	—	30	—	—	25

# Louis Burger International, Inc. 1983.

\*\* Both the ELMOD and ISSEM 4 are programs provided by Dynatest, Inc.

† Brandley 1983.

†† Assumed value.

Table 13  
Summary of Performance Criteria

Methodology	Rigid Pavement		Flexible Pavement		Subgrade
	ERES	Dynatest	ERES	Dynatest	
FS = $A \times (E/E_o)^d$	$\epsilon_t = 0.000228 \times VB \times N^{-0.178}$	$\epsilon_t = 0.000228 \times VB \times N^{-0.178}$	$\sigma = 0.05 \times n^{-0.0667} \times (E/E_o)^d$	$\sigma = 0.05 \times n^{-0.0667} \times (E/E_o)^d$	$\sigma = 0.05 \times n^{-0.0667} \times (E/E_o)^d$
$A = 1.18 \text{ MPa (170 psi)}$	$\epsilon_t = \text{permissible horizontal strain at bottom of AC}$	$\epsilon_t = \text{permissible horizontal strain at bottom of AC}$	$n = \text{permissible normal stress}$	$n = \text{load applications}$	$n = \text{load applications}$
$E = \text{modulus of PCC}$	$V_B = \text{volume percentage of asphalt, approximately 12}$	$V_B = \text{volume percentage of asphalt, approximately 12}$	$E = \text{modulus}$	$E_o = 160 \text{ MPa (23,000 psi)}$	$E = \text{modulus}$
$E_o = 1,000 \text{ MPa (1,450,000 psi)}$	$N = \text{load applications}$	$N = 10 [2 \times (1-\Sigma DS/FS)/(1-PS/\Sigma DS)]$	$d = \text{power equal to 1.0 where } E > E_o, \text{ otherwise 1.16}$	$\Sigma DS = \text{static + dynamic load}$	$d = \text{power equal to 1.0 where } E > E_o, \text{ otherwise 1.16}$
$\Sigma DS = \text{static + dynamic load}$	$FS = \text{flexural strength}$	$PS = \text{static load}$	$\epsilon_v = 5.511 \times 10^{-3} \frac{1}{N_{cov} 0.1532}$	$\epsilon_v = 5.511 \times 10^{-3} \frac{1}{N_{cov} 0.1532}$	$\epsilon_v = \text{vertical strain on subgrade}$
$FS = \text{flexural strength}$	$PS = \text{static load}$	$\epsilon_r = (4.102 \times PI - 0.205 \times PI \times Vb + 1.049 \times Vb - 2.707) \times S_m^{-0.28} \times N_{cov}^{-0.2}$	$\epsilon_r = (4.102 \times PI - 0.205 \times PI \times Vb + 1.049 \times Vb - 2.707) \times S_m^{-0.28} \times N_{cov}^{-0.2}$	$\epsilon_r = \text{radical strain}$	$N_{cov} = \text{number of coverages of the specified aircraft producing strain}$
$PS = \text{static load}$	$MR = \text{modulus of rupture determined from modulus FWD}$	$PI = \text{penetration index (assumed = 0)}$	$PI = \text{penetration index (assumed = 0)}$	$Vb = \text{volumetric bitumen content (15 percent)}$	$Vb = \text{volumetric bitumen content (15 percent)}$
$MR = \text{modulus of rupture determined from modulus FWD}$	$C = \text{coverage to 50 percent slab cracking}$	$S_m = \text{stiffness of mix (N/m**2)}$	$S_m = \text{stiffness of mix (N/m**2)}$	$N_{cov} = \text{number of coverages}$	$N_{cov} = \text{number of coverages}$
$C = \text{coverage to 50 percent slab cracking}$	$\sigma = \text{critical stress in slab using load transfer in ILLISLAB}$	$N_{cov} = \text{number of coverages}$	$N_{cov} = \text{number of coverages}$		

(Continued)

Table 13. (Continued)

Methodology	Flexible Pavement		Subgrade
	Rigid Pavement		
ARE	$N = a \left(\frac{f}{c}\right)^b$  $f$ = concrete flexural strength, psi $c$ = computed stress due to aircraft load on rigid pavement, psi $a, b$ = constants	$N = c \left(\frac{1}{e}\right)^d$  $e$ = computed strain due to aircraft load on flexible pavement, psi $L_R = 100 - \left(\frac{n}{N}\right) \times 100$ $L_R$ = fatigue life remaining in pavement $n$ = aircraft operations to date for an individual aircraft	$N$ = number of aircraft loads until failure (fatigue life) $N$ = allowable number of aircraft loads until failure for an individual aircraft
PCS	E-k Relationship*  $E = 10^X$ with $E$ in psi units with $X = 1.415 + 1.284 \log k$	E-CBR Relationship*  $E = 1,500$ (CBR) with $E$ in psi units	(Continued)

\*  $k$  and CBR used with standard Air Force pavement evaluation procedure.

Table 13 (Continued)

Methology	Rigid Pavement	Flexible Pavement	Subgrade
Berger	$P_G = 0.0159 \times DSM \times F_L \times T_c$ Composite pavement $P_G = 0.0162 \times DSM \times F_L \times T_c$ DSM = measured ratio of load/deflection from pavement profiler $F_L$ = load factor $T_c$ = traffic factor	$CBR = \frac{a^2 \times 1,000 \times ASML}{8.1 \times (T_t^2 + a A/s)}$ $ASML = 0.0437 \times DSM$ $T_t$ = equivalent thickness from predicted layer modulus Then CBR and $T_t$ used with standard Air Force pavement evaluation procedure DSM = measured ratio of load/deflection from pavement profiler	$C = 0.00036 T^2 - 2.88325 D - 2.8641$ C = coverages to failure T = total thickness of pavement above subgrade D = subgrade deflection, in.

Brandley

(Continued)

Table 13 (Continued)

Methodology	Rigid Pavement	Flexible Pavement	Subgrade
WES-DSH	$P_G = 0.0819(DSM)F_L T_C$ Composite pavement	$P_G = \frac{F_K(DSM)}{S(ESWL)} \times \frac{N_m}{N_c} \times 100$	
	$F_G = 0.0172(DSM)F_L T_C$	$F_K =$ load factor	
	$F_L =$ load factor	$S =$ load on road gear	
	$T_C =$ traffic factor	$ESWL =$ equivalent single-wheel load in percent	
		$N_m =$ number of main gear wheels	
		$N_c =$ number of controlling wheels	

WES Layered Elastic

$$\epsilon_{All} = \frac{R}{A + B(\log_{10} COV)}$$

R = flexural strength of PCC,  
psi

A = 0.58901  
B = 0.35486

COV = number of passes divided  
by pass to coverage ratio

$$\epsilon_{All(AC)} = \frac{10^A}{N + 2.665 \left( \frac{\log_{10} \frac{E_{AC}}{E_{AC} - 0.392}}{5.0} \right)}$$

where

A = 0.000247 + 0.000245 log  $M_R$   
 $S_s$  = vertical strain at the top of  
the subgrade  
B = 0.0658  $M_R$  0.559  
 $M_R$  = resilient modulus in pounds  
per square inch of the subgrade

(Continued)

(Sheet 4 of 5)

Table 13 (Concluded)

Methodology	Rigid Pavement	Flexible Pavement	Subgrade
AFESC	$\text{Operations} = \text{CPC} \times 10(96 - \text{PERMR})/8.0$ $\text{CPC} = \text{cycles per coverage}$ $\text{PERMR} = \frac{\text{Max. Element Stress}}{\text{Rupt or Rupt of FRC}} \times 100\%$	$\text{CONSTM} = 1.054 - \left\{ 0.1370 \times \left[ \text{ALOG}_{10}(\text{PROPY}) \right] \right\}$ $\text{CONSTL} = -4.15490 + \text{CONSTM} \times 6.60206$ $\text{PROPY} = \text{Young's modulus}$ $\text{EXZMAX} = \text{asphaltic concrete tensile strain}$	<p>Weak flexible pavement -</p> $\text{Operations} = \text{CPC} \times (4.7188 E - 22) \times \left[ \frac{\text{ABS}(\text{EV}_{\max})}{\text{ABS}(\text{EV}_{\max}) - 8.6615} \right]$ <p>Heavy multiple-wheel aircraft -</p> $\text{Operations} = \text{CPC} \times (1.448 E - 15) \times \left[ \frac{\text{ABS}(\text{EV}_{\max})}{\text{ABS}(\text{EV}_{\max}) - 6.605} \right]$ <p>Rigid pavement and strong flexible pavement -</p> $\text{Operations} = \text{CPC} \times (1.07 E - 8) \times \left[ \frac{\text{ABS}(\text{EV}_{\max})}{\text{ABS}(\text{EV}_{\max}) - 4.4} \right]$ <p><math>\text{EV}_{\max}</math> = vertical subgrade strain</p>

Table 1.  
Evaluation of Test Areas Based on Standard Air Force Test-Pit Procedures

Test Area	Pavement Properties for Evaluation	Pass Intensity Level	Overlay Thickness, in.											
			B-747, 1,000 passes						B-747, 1,000 passes					
			FC-C PCC	FC-C PCC	Partial (Rounded)	AC (Unbonded)	FC-C PCC	FC-C PCC	Partial (Rounded)	AC (Unbonded)	FC-C PCC	FC-C PCC	Partial (Rounded)	AC (Unbonded)
1	20-in. FCC 6-in. subbase Sand subgrade (SP)	I II III IV	+ + +	+ + +	+ + +	+ + +	+ + +	+ + +	+ + +	+ + +	+ + +	+ + +	+ + +	
2	15-in. AC 8-in. limerock base CBR = 8G 7-in. limerock stabilized subbase CBR = 30 Sand subgrade (SP) CBR = 25	I II III IV	+ + +	+ + +	+ + +	+ + +	+ + +	+ + +	+ + +	+ + +	+ + +	+ + +	+ + +	
3	5.5-in. AC 8-in. limerock base CBR = 80 7-in. limerock stabilized subbase CBR = 30 Sand subgrade (SP) CBR = 25	I II III IV	+ + +	+ + +	+ + +	+ + +	+ + +	+ + +	+ + +	+ + +	+ + +	+ + +	+ + +	
4*	7.5-in. AC 6-in. PCC Sand subgrade (SP) k = 250-300	I II III IV	+ + +	+ + +	+ + +	+ + +	+ + +	+ + +	+ + +	+ + +	+ + +	+ + +	+ + +	
5	10.5-in. PCC R = 650 Sand subgrade (SP) k = 250	I II III IV	+ + +	+ + +	+ + +	+ + +	+ + +	+ + +	+ + +	+ + +	+ + +	+ + +	+ + +	

Note: Plus (+) sign indicates allowable gross load was greater than maximum weight of aircraft.  
\* Evaluated as flexible pavement.

Table 15  
Evaluation of Test Areas 1 and 5 Based on Test-Pit Data From LURC AFSR Evaluation Report

Test Area	Evaluation Properties For Pavement	Intensity Level	Allowable Aircraft Loads, Kips												Overlay Thickness, in.					
			C123	F111	C130	C9	T43	H727	E4	C1M	C5A	K1D	B717	H52	AC	PC	Partial Bonded	PC	PC	PC
1 20-in. PC	R = 480	I	+	+	+	+	+	+	+	+	+	+	+	+	0	0	0	0	0	0
b-in. subgrade	k = 230	II	+	+	+	+	+	+	+	+	+	+	+	+	+	+	+	+	+	0
Sand subgrade (SP)		III	+	+	+	+	+	+	+	+	+	+	+	+	+	+	+	+	+	0
		IV	+	+	+	+	+	+	+	+	+	+	+	+	+	+	+	+	+	0
5 LURC-11-1 R/C	R = 470	I	43	36	6	108	62	65	0	144	161	524	259	351	0	19.2	13.6	16.6	20.0	13.9
Sand subgrade (SP)	k = 80	II	53	45	50	120	70	73	0	159	156	582	292	398	0					17.1
		III	60	51	57	140	82	86	92	182	178	658	340	467	0					
		IV	+	+	68	169	101	105	113	214	210	762	399	352	181					

Note: Plus (+) sign indicates allowable gross load was greater than maximum weight of aircraft.

Table 16  
Comparisons of Allowable Load  
Allowable Gross Aircraft Load, kips

Procedure	Pass Intensity											
	Level I			Level II			Level III			Level IV		
	F4	C141	B52	F4	C141	B52	F4	C141	B52	F4	C141	B52
<u>Test Area 1</u>												
Standard evaluation from test-pit data	60+	345+	490+	+	+	+	+	+	+	+	+	+
Dynatest*	60+	345+	490+	+	+	+	+	+	+	+	+	+
ERES**	60+	345+	292	+	+	+	+	+	+	+	+	+
PCST†	60+	345+	480+	+	+	+	+	+	+	+	+	+
Brandley††	60	345	490	60	345	490	60	345	490	60	345	490
Berger	60+	345+	490+	+	+	+	+	+	+	+	+	+
ARE	62	317	488	62	317	488	62	317	488	62	317	488
AFESC	60+	345+	460	+	+	490+	+	+	+	+	+	+
WES (DSM)	60+	345+	490+	+	+	+	+	+	+	+	+	+
WES (layered-elastic, 16-kip)	60+	345+	490+	+	+	+	+	+	+	+	+	+
Wes (layered-elastic, FWD data)	60+	345+	490+	+	+	+	+	+	+	+	+	+
<u>Test Area 2</u>												
Standard evaluation from test-pit data	60+	345+	490+	+	+	+	+	+	+	+	+	+
Dynatest*	60+	345+	490+	+	+	+	+	+	+	+	+	+
ERES**	60+	345+	490+	+	+	+	+	+	+	+	+	+
PCST†	45	225	240	55	250	290	60+	300	380	+	345+	480+
Brandley††	60	179	353	60	272	490	60	345	490	60	345	490
Berger	60+	345+	490+	+	+	+	+	+	+	+	+	+
ARE	62	317	488	62	317	488	62	317	488	62	317	488
AFESC	60+	345+	300	+	+	377	+	+	490	+	+	+
WES (DSM)	60+	345+	490+	+	+	+	+	+	+	+	+	+
WES (layered-elastic, 16-kip)	60+	345+	490+	+	+	+	+	+	+	+	+	+
WES (layered-elastic FWD data)	60+	345+	455	+	+	490+	+	+	+	+	+	+

(Continued)

Note: Plus (+) sign denotes allowable gross load greater than maximum gross weight of aircraft; A denotes allowable gross load less than minimum (basic) gross weight of aircraft.

\* Eighty percent of test points.

\*\* Fifty percent slab cracking for PCC pavement, 0.5-inch rutting for Asphalt Concrete pavement.

† Initial crack for PCC pavement.

†† Allowable load presented as percent of gross in report.

Table 16 (Continued)

Procedure	Pass Intensity											
	Level I			Level II			Level III			Level IV		
	F4	C141	B52	F4	C141	B52	F4	C141	B52	F4	C141	B52
<u>Test Area 3</u>												
Standard evaluation from test-pit data	60+	345+	415	+	+	451	+	+	490+	+	+	+
Dynatest*	25	A	217	28	A	241	30	137	272	34	154	303
ERES**	55	195	490+	60+	248	+	+	345	+	+	345+	+
PCSt	A	A	A	A	A	A	A	A	A	A	A	A
Brandley††	50	128	225	60	190	392	60	331	490	60	345	490
Berger	58	212	255	60+	230	245	+	280	305	+	345+	405
ARE	7	51	65	10	64	72	11	158	135	12	317	488
AFESC	27	200	A	48	295	200	60+	345+	261	60+	+	330
WES (DSM)	59	237	298	60+	261	347	+	321	433	+	345+	490+
WES (layered-elastic, 16-kip)	48	223	225	52	237	246	55	257	271	59	281	296
WES (layered-elastic data)	32	172	213	43	222	248	52	263	273	60+	287	298
<u>Test Area 4</u>												
Standard evaluation from test-pit data	60+	345+	346	+	+	400	+	+	490+	+	+	+
Dynatest*	60+	275	490+	+	295	+	+	321	+	+	345+	+
ERES**	30	165	<175	36	188	<175	42	216	210	54	318	282
PCSt	60+	345+	480+	+	+	+	+	+	+	+	+	+
Brandley††	43	100	196	60	148	343	60	262	490	60	345	490
Berger	52	241	190	60+	272	215	+	295	230	+	325	250
ARE	41	244	350	54	278	425	62	317	488	62	317	488
AFESC	60+	345+	457	+	+	490+	+	+	+	+	+	+
WES (layered-elastic, 16-kip)	60+	295	305	+	316	336	+	345+	376	+	+	415
WES (layered-elastic, FWD data)	60+	285	292	+	306	324	+	337	363	+	345+	402

(Continued)

\* Eighty percent of test points.

\*\* Fifty percent slab cracking for PCC pavement, 0.5-inch rutting for Asphalt Concrete pavement.

† Initial crack for PCC pavement.

†† Allowable load presented as percent of gross in report.

Table 16 (Concluded)

Procedure	Pass Intensity											
	Level I			Level II			Level III			Level IV		
	F4	C141	B52	F4	C141	B52	F4	C141	B52	F4	C141	B52
<u>Test Area 5</u>												
Standard evaluation from test-pit data	57	263	198	60+	280	216	+	298	233	+	321	252
Dynatest*	32	A	401	36	A	437	39	139	477	42	152	490+
ERES**	30	177	<175	37	200	<175	42	250	187	54	>345	265
PCS†	40	210	195	50	235	220	55	260	240	60	290	270
Brandley††	41	86	181	60	135	308	60	231	490	60	345	490
Berger	52	241	190	60+	273	215	+	295	230	+	325	250
ARE	51	271	385	62	317	467	62	317	488	62	317	488
AFESC	28	267	184	31	288	202	34	318	223	37	345+	241
WES (DSM)	60+	345+	315	+	+	348	+	+	386	-	+	430
WES (layered- elastic, 16 kip)	60+	245	217	+	269	248	+	309	295	+	345	357
WES (layered- elastic, FWD data)	60+	215	190	+	235	217	+	270	259	+	325	313

† Initial crack for PCC pavement.

†† Allowable load presented as percent of gross in report.

Table 17

## Comparison of Overlay Thickness, in.

Procedure	Aircraft	Test Area 1				Test Area 2				Test Area 3				Test Area 4			
		PCC*	PCC**	RCC†	AC												
Standard	KC10A	0	0	0	0	0	0	0	0	0	0	0	0	0	0	0	0
	E-4	0	0	0	0	0	0	0	0	0	0	0	0	0	0	0	0
Dynatest	KC10A	0	0	0	0	0	0	0	0	0	0	0	0	0	0	0	0
	E-4	0	0	0	0	0	0	0	0	0	0	0	0	0	0	0	0
ESS	KC10A	0	0	0	0	0	0	0	0	0	0	0	0	0	0	0	0
	E-4	2.7	0	0	0	0	0	0	0	0	0	0	0	0	0	0	0
PGS‡	KC10A	0	0	0	0	1.8	0	0	0	0	0	0	0	0	0	0	0
	E-4	0	0	0	0	3.7	0	0	0	0	0	0	0	0	0	0	0
Brantley	KC10A	0	0	0	0	0	0	0	0	0	0	0	0	0	0	0	0
	E-4	0	0	0	0	0	0	0	0	0	0	0	0	0	0	0	0
ARE	KC10A	0	0	0	0	0	0	0	0	0	0	0	0	0	0	0	0
	E-4	0	0	0	0	0	0	0	0	0	0	0	0	0	0	0	0
Berger	KC10A	0	0	0	0	0	0	0	0	0	0	0	0	0	0	0	0
	E-4	0	0	0	0	0	0	0	0	0	0	0	0	0	0	0	0
WES DSM	KC10A	0	0	0	0	0	0	0	0	0	0	0	0	0	0	0	0
Method	E-4	0	0	0	0	0	0	0	0	0	0	0	0	0	0	0	0
WES Layered-	KC10A	0	0	0	0	0	0	0	0	0	0	0	0	0	0	0	0
elastic	E-4	0	0	0	0	0	0	0	0	0	0	0	0	0	0	0	0
(lifkip)	vibrator																
WES Layered-	KC10A	0	0	0	0	0	0	0	0	0	0	0	0	0	0	0	0
elastic	E-4	0	0	0	0	0	0	0	0	0	0	0	0	0	0	0	0
(FWB)																	

\* PCC overlay, bonded.

\*\* PCC overlay, unbonded.

† Recommends a 1-in. minimum PCC overlay for load transfer at joints.

‡ Alternative is to break up existing PCC and overlay with 3.3 in. and 4.2 in., respectively.

§ PCC overlay thicknesses are based upon the use of "weakest layer concept" derived from nondestructive testing studies.

\*\* The shear of the base layer controlled the overlay and not the subgrade.

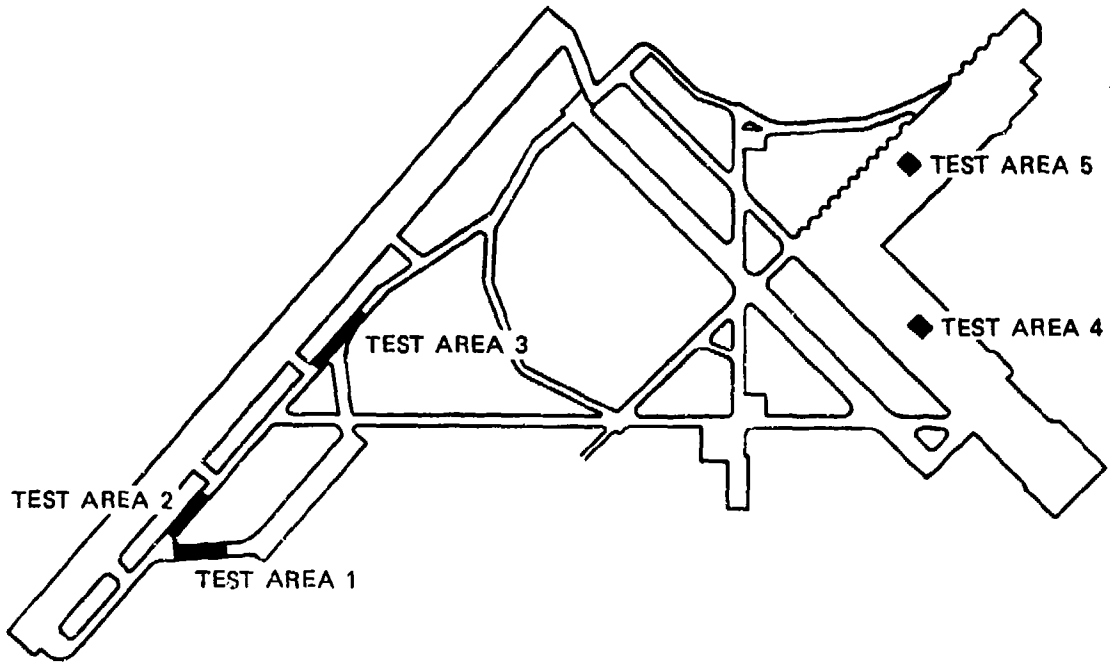


Figure 1. Airfield layout at MacDill AFB showing location of test area

TEST AREA 1								
DEPTH, IN.	MATERIAL SYMBOL CLASSIF.	$\omega$ %	$\gamma_d$ pcf	CE 55		$w_p/w_p$ %	K, psi/in.	
				% COMP	OMC			
21.5	PCC							
33.0	SP-SM	23.9	98.3	98.1	11.5	NP	230	
48.0	SP-SM	16.7			12.1	NP		
		21.8						

TEST AREA 2								
DEPTH, IN.	MATERIAL SYMBOL CLASSIF.	$\omega$ %	$\gamma_d$ pcf	CE 55		$w_p/w_p$ %	K, psi/in.	
				% COMP	OMC			
10.0	AC							
21.0	LIME ROCK	11.0	106.4	90.5	11.3	NP	30	
26.0	LR	8.1	103.1	87.7	11.3	NP	6	
36.0	SP	6.7	105.4	100.2	12.1	NP	35	
48.0		6.0						
		10.5						

TEST AREA 3								
DEPTH, IN.	MATERIAL SYMBOL CLASSIF.	$\omega$ %	$\gamma_d$ pcf	CE 55		$w_p/w_p$ %	CBR, %	
				% COMP	OMC			
5.0	AC							
13.5	LIME POCK	10.4	114.1	97.1	11.3	NP	10	
19.0	SP-SM	9.1	107.3	96.1	11.5	NP	25	
24.0	SP	10.8	97.0	92.2	12.1	NP	30	
36.0		4.7						
48.0		14.6						

TEST AREA 4								
DEPTH, IN.	MATERIAL SYMBOL CLASSIF.	$\omega$ %	$\gamma_d$ pcf	CE 55		$w_p/w_p$ %	K, psi/in.	
				% COMP	OMC			
7.5	AC							
14.0	PCC							
24.0	SP	9.0	101.4	96.4	12.1	NP	85	
36.0		7.1						
48.0		9.4						
		12.8						

TEST AREA 5								
DEPTH, IN.	MATERIAL SYMBOL CLASSIF.	$\omega$ %	$\gamma_d$ pcf	CE 55		$w_p/w_p$ %	K, psi/in.	
				% COMP	OMC			
10.5	PCC							
24.0	SP	11.7	109.8	104.4	12.1	NP	80	
36.0		9.1						
48.0		6.9						
		18.9						

#### LEGEND

- K = SUBGRADE MODULUS, PCI
- CBR = CALIFORNIA BEARING RATIO, PERCENT
- OMC = OPTIMUM MOISTURE CONTENT, PERCENT
- % COMP = FIELD DENSITY AS PERCENT OF LABORATORY DENSITY
- $\omega$  = IN-PLACE MOISTURE CONTENT, PERCENT
- $\gamma_d$  = IN-PLACE DENSITY, pcf

Figure 2. Test-pit data for each test area as presented by AFESC

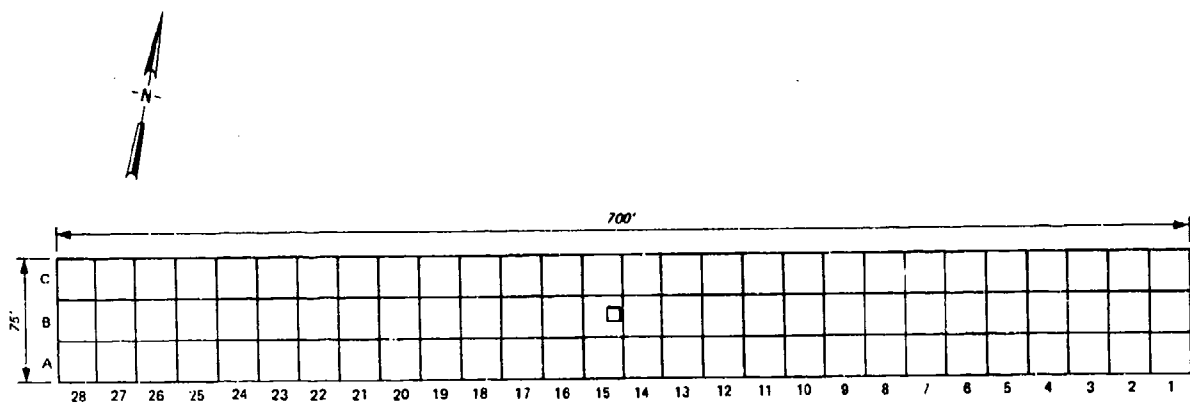


Figure 3. Layout of Test Area 1



Figure 4. Test Area 1

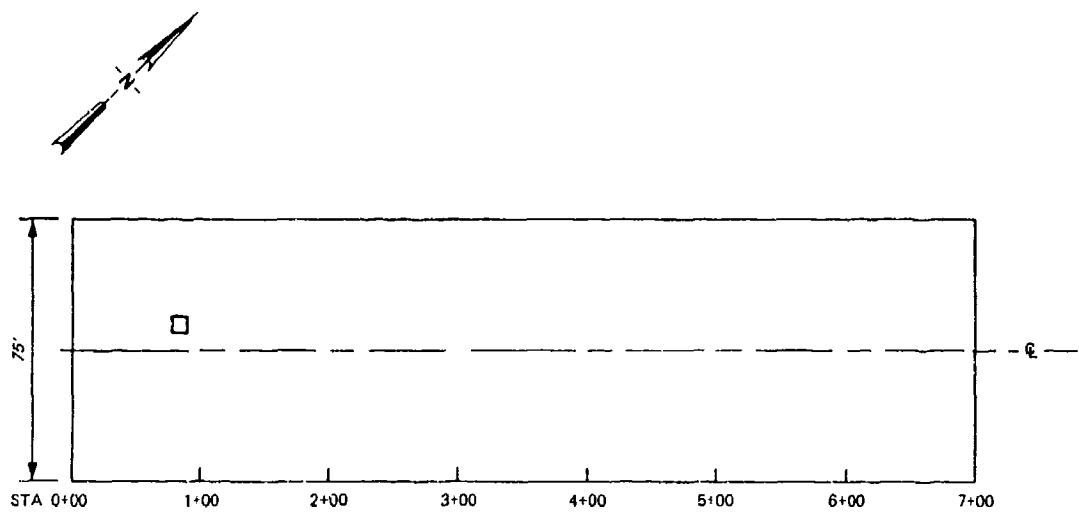


Figure 5. Layout of Test Area 2

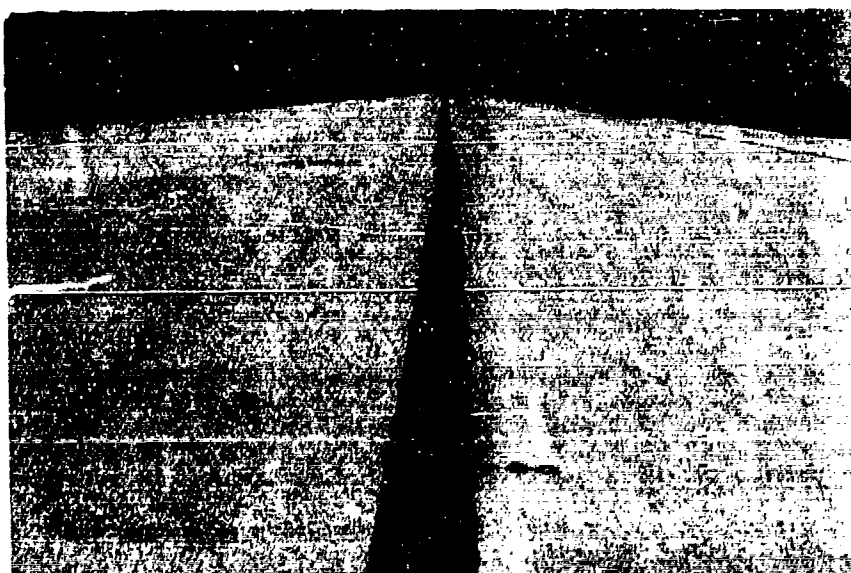


Figure 6. Test Area 2

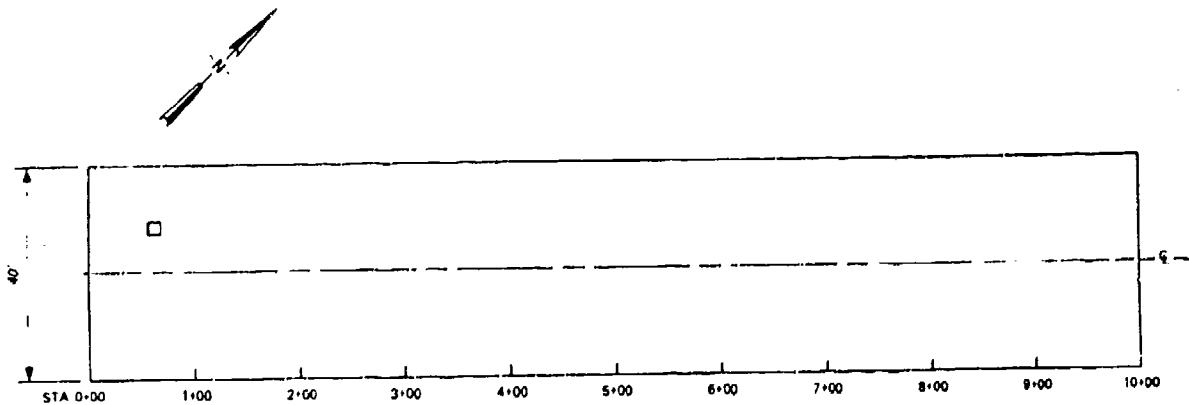


Figure 7. Layout of Test Area 3



Figure 8. Test Area 3

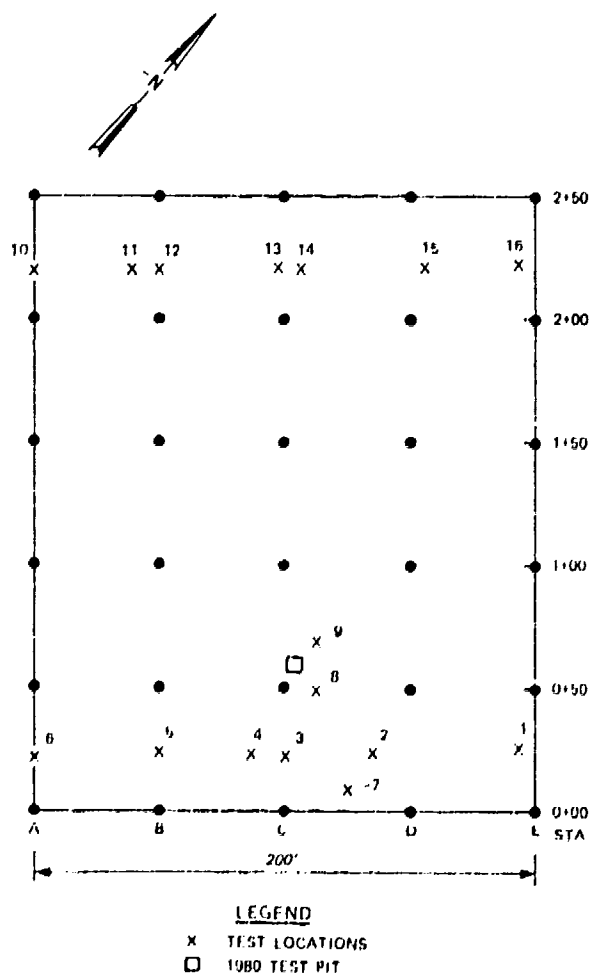


Figure 9. Layout of Test Area 4



Figure 10. Test Area 4

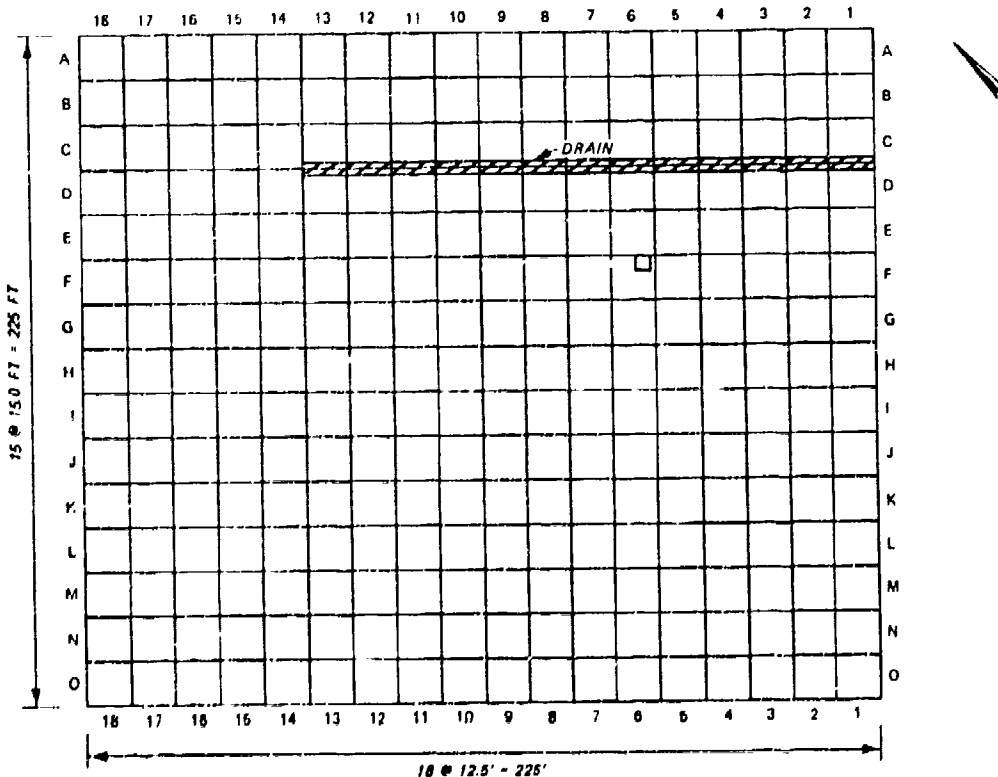


Figure 11. Layout of Test Area 5

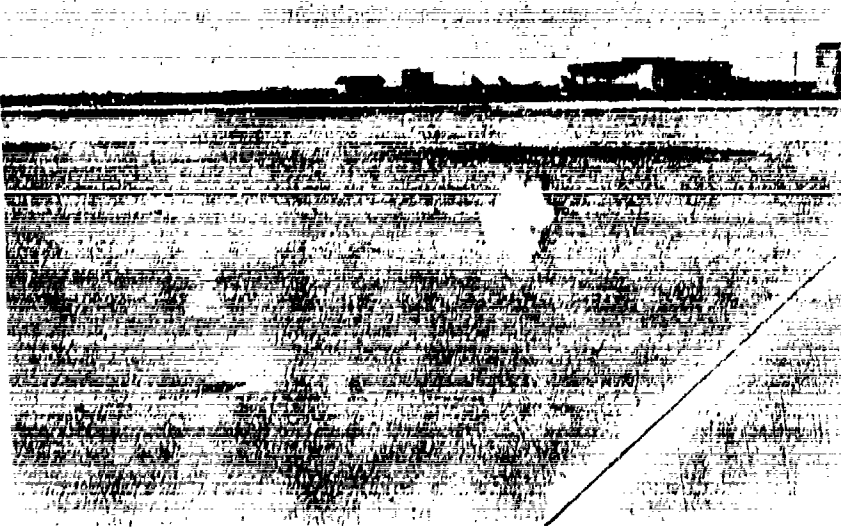


Figure 12. Test Area 5

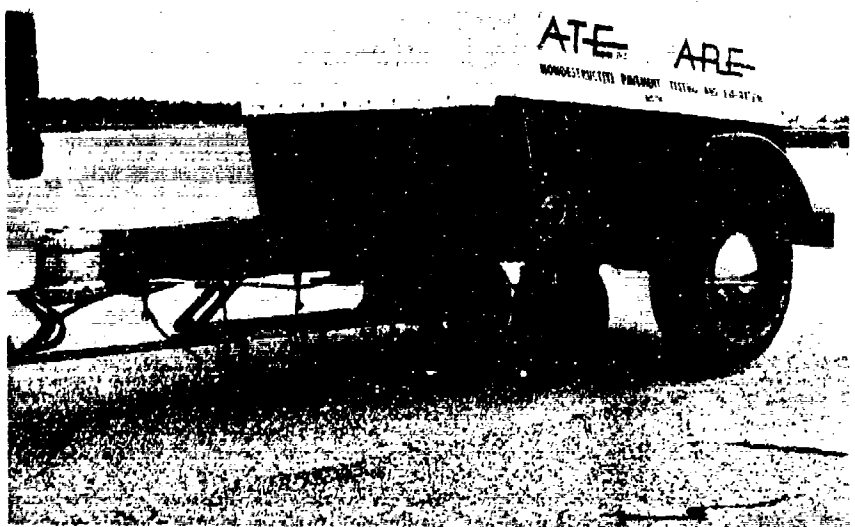


Figure 13. Dynaflect used by ARE, Inc.

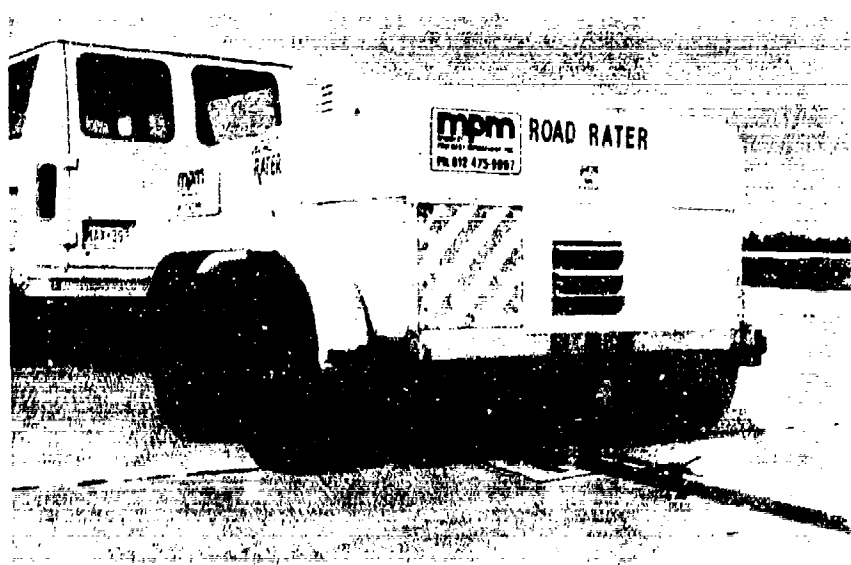


Figure 14. Road-Rater Model 2000 used by Berger

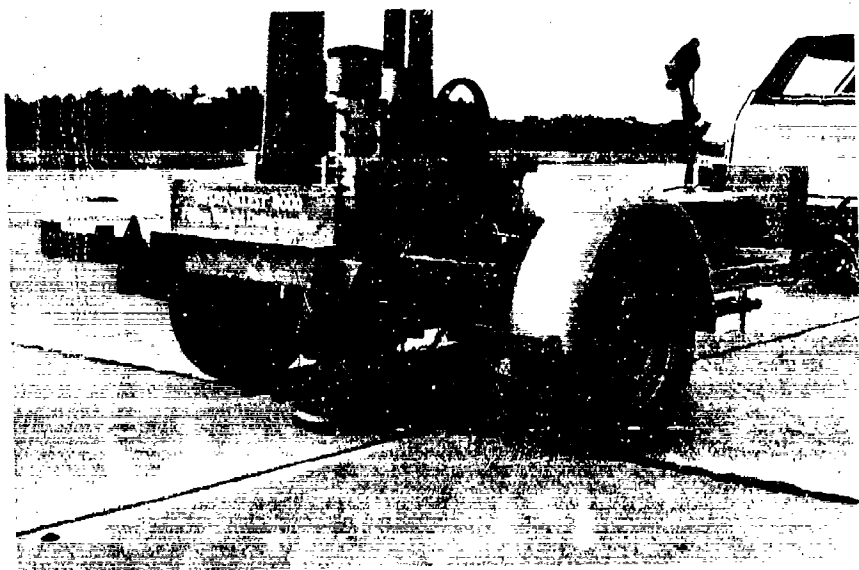


Figure 15. Dynatest Model 8000 FWD

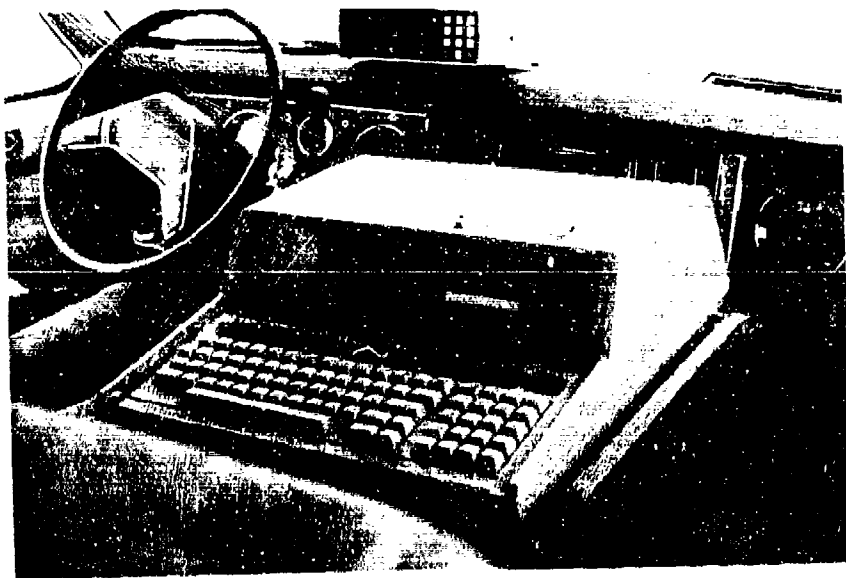


Figure 16. HP-85 computer used with  
Dynatest Model 8000 FWD

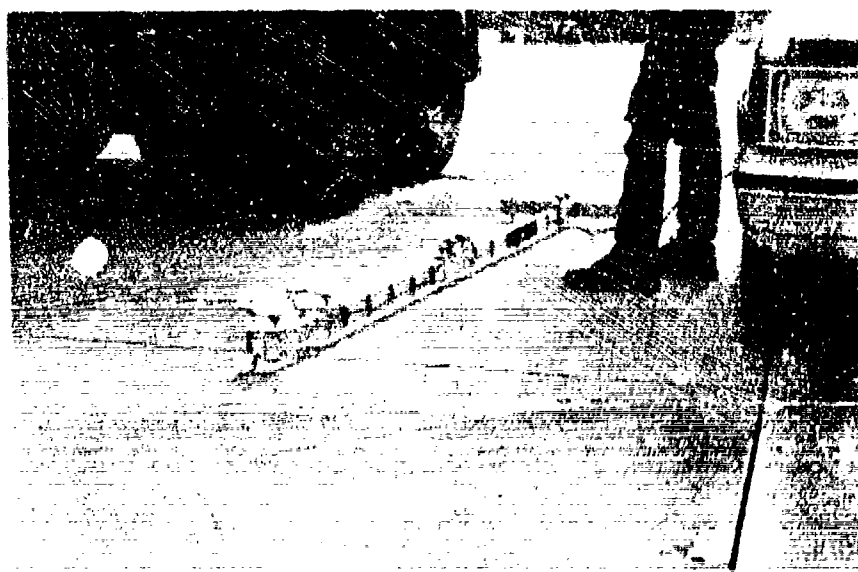


Figure 17. Brandley Cantilever Deflection Beam

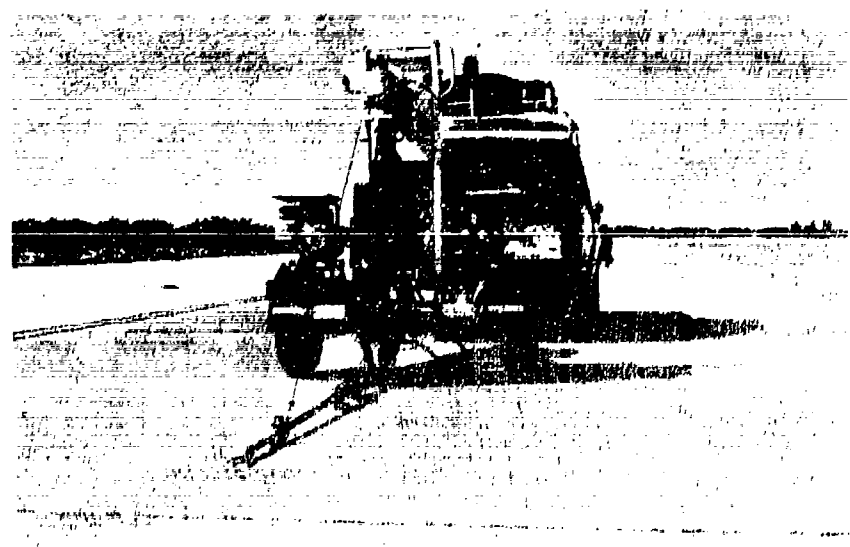


Figure 18. PCS FWD

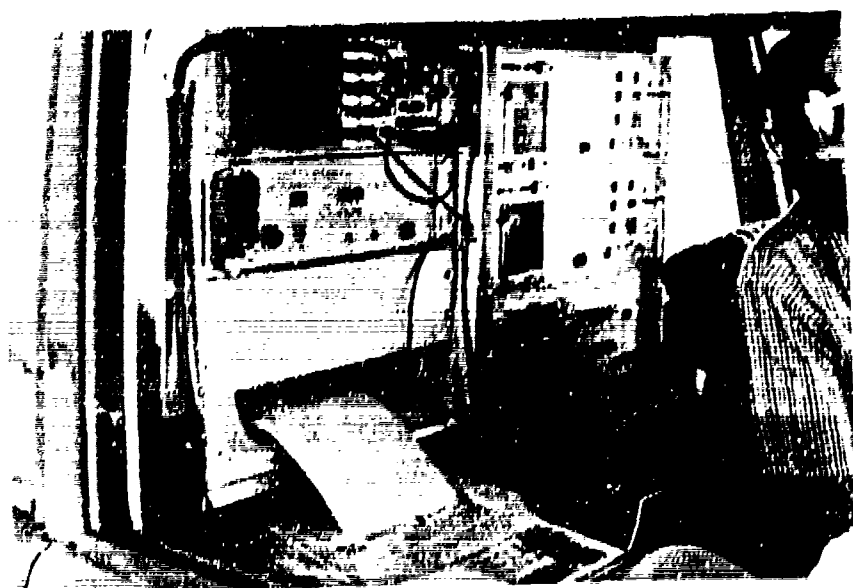


Figure 19. Data recording equipment used by PCS

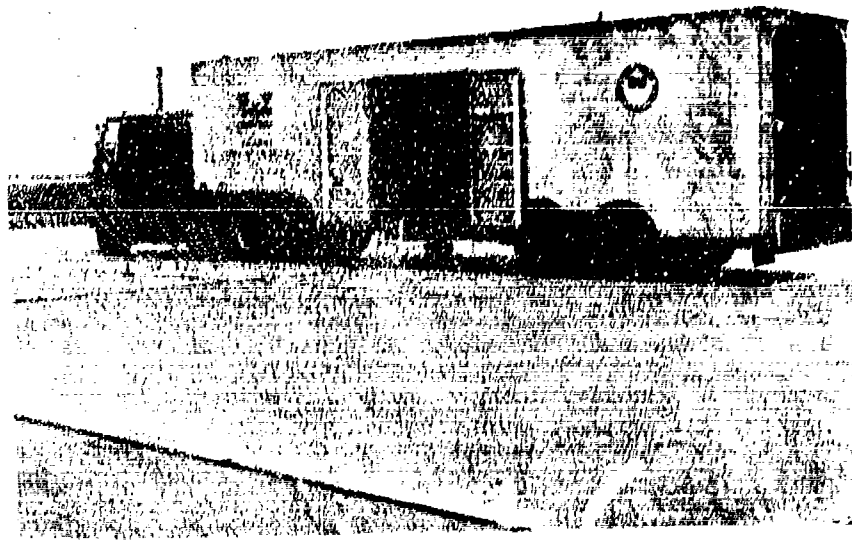


Figure 20. WES 16-kip vibrator

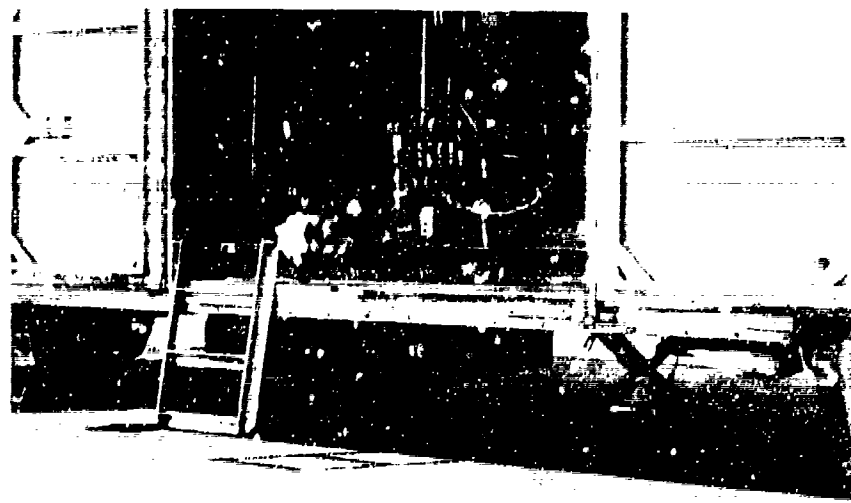


Figure 21. Load plate of WES 16-kip vibrator

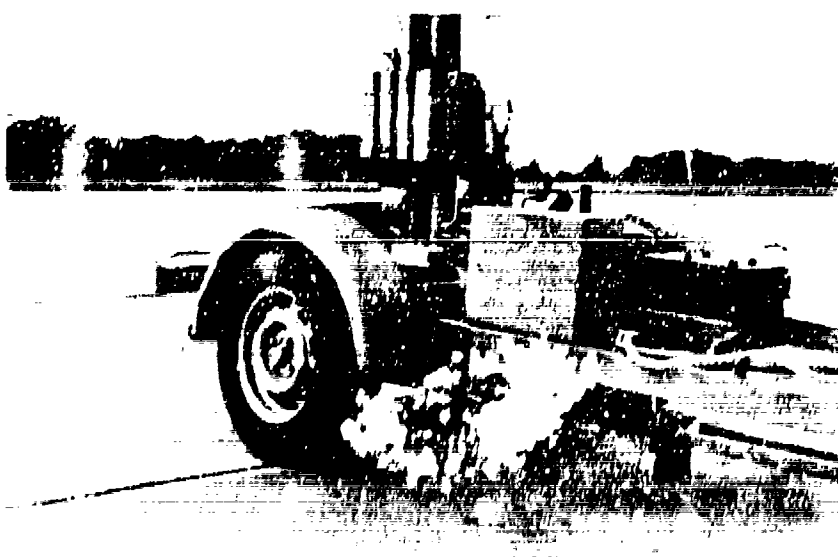


Figure 22. WES FWB (manufactured by Dynatest)

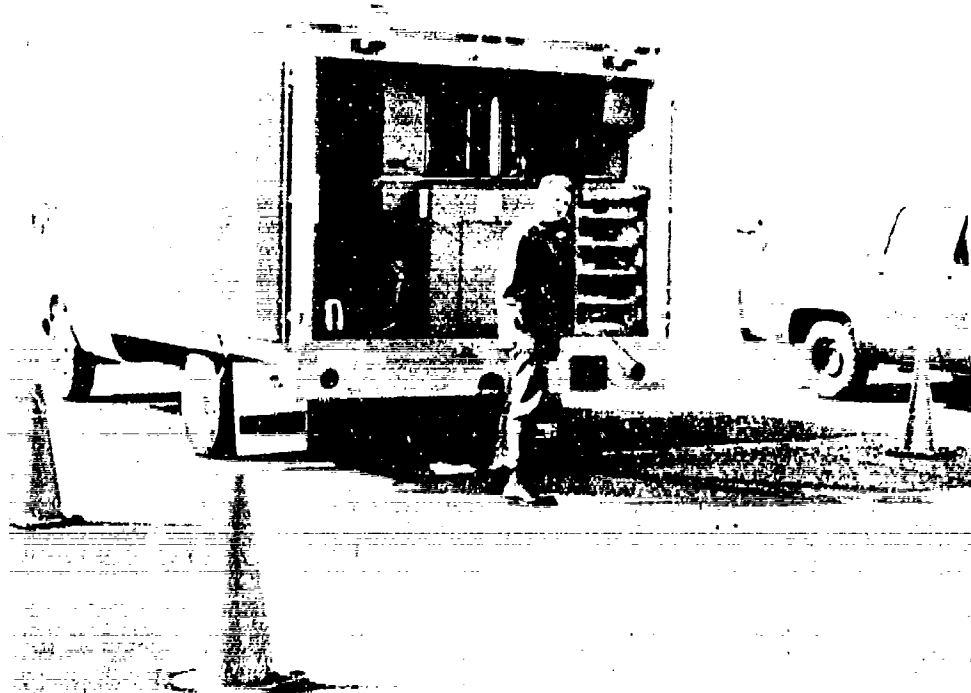


Figure 23. AFESC NDPT van

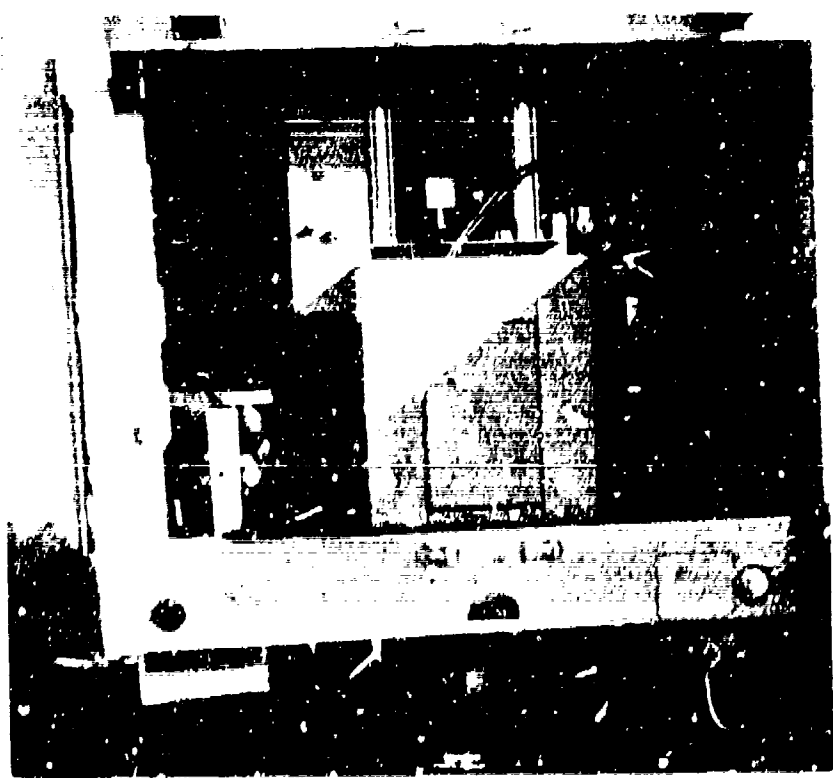


Figure 24. Lead plate and Impact hammer  
of AFESC NDPT device

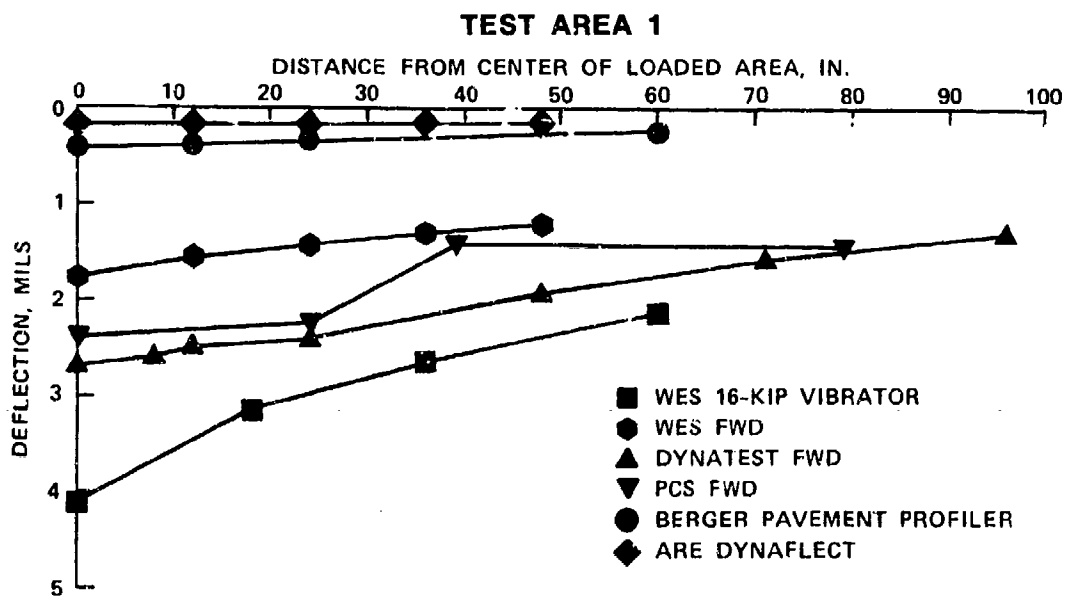


Figure 25. Comparison of measured deflector basins for Test Area 1

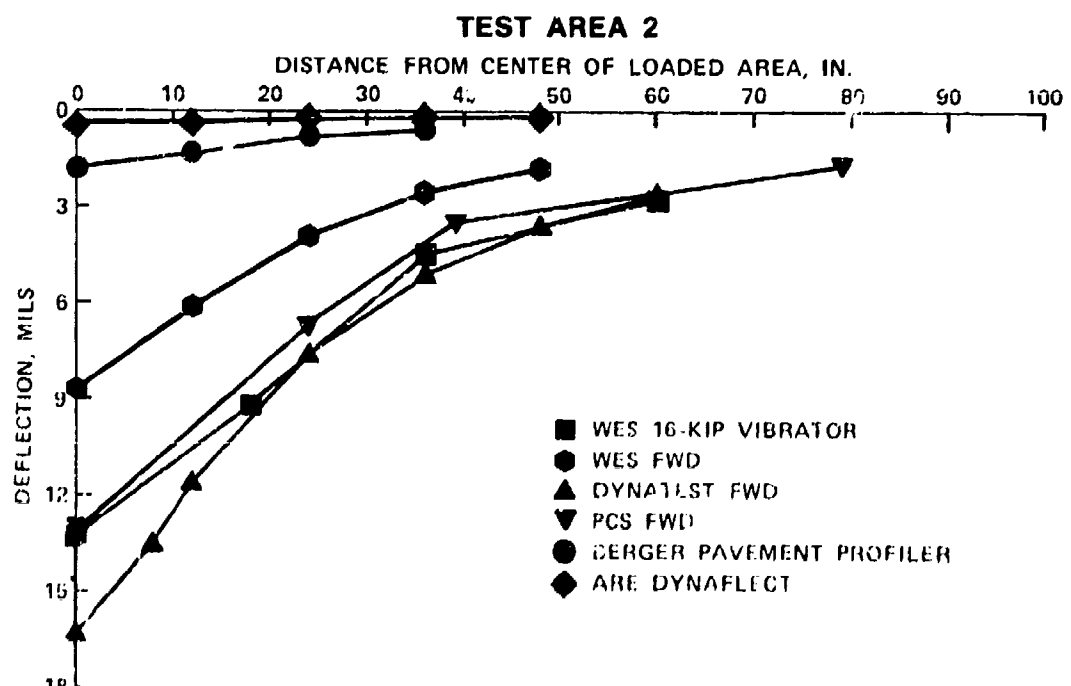


Figure 26. Comparison of measured deflector basins for Test Area 2

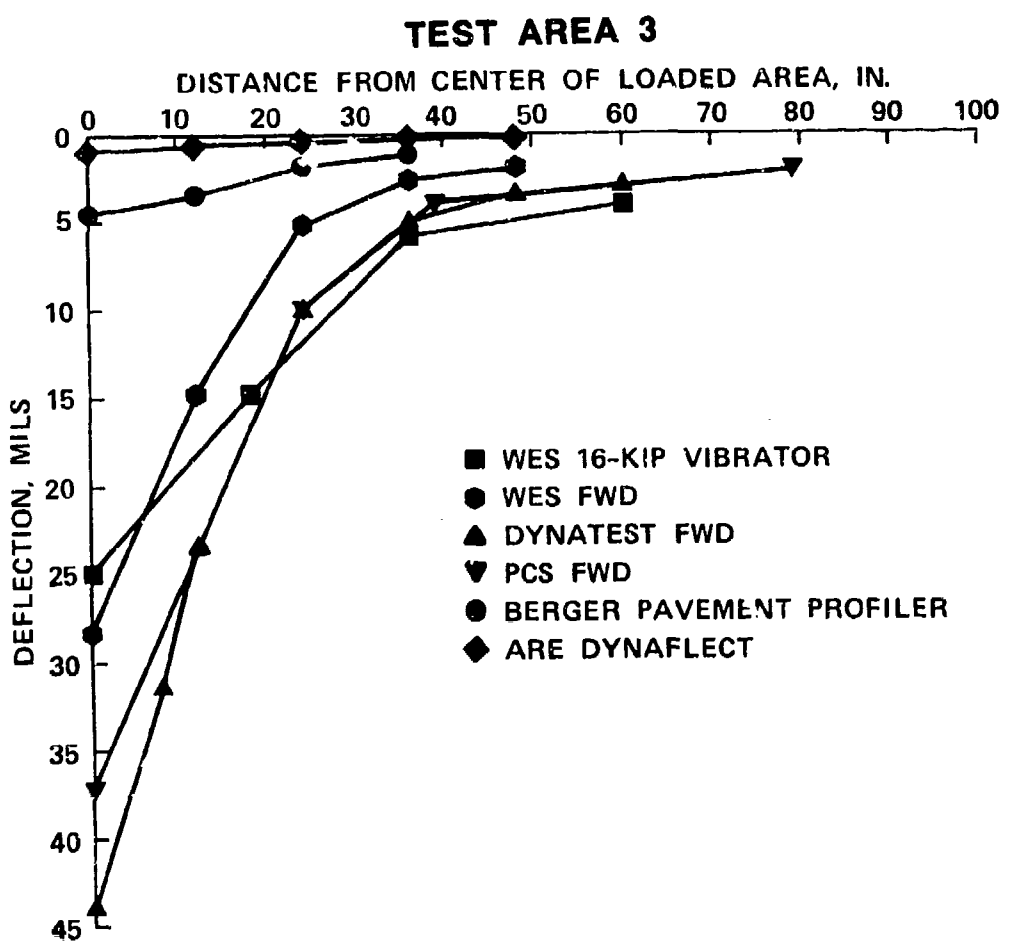


Figure 27. Comparison of measured deflector basins for Test Area 3

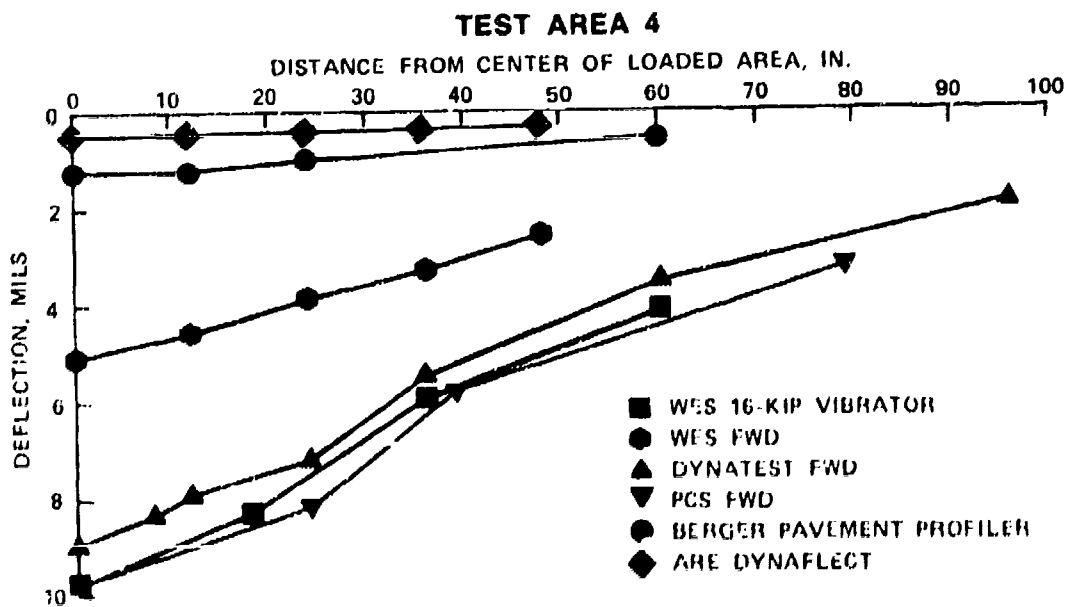


Figure 28. Comparison of measured deflector basins for Test Area 4

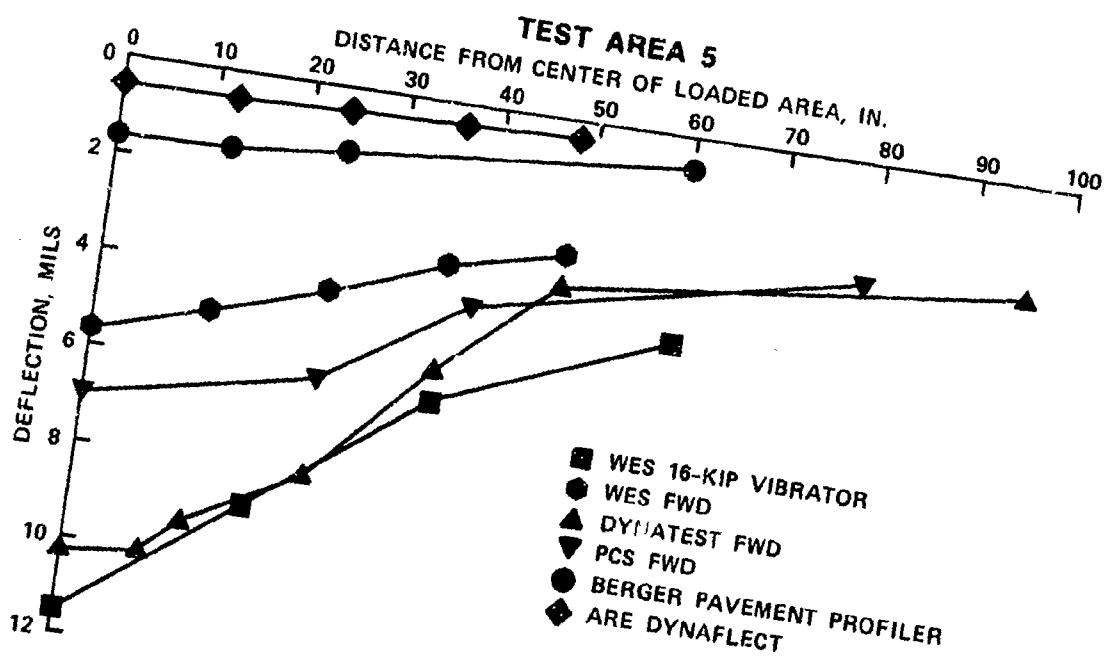


Figure 29. Comparison of measured deflector basins  
for Test Area 5

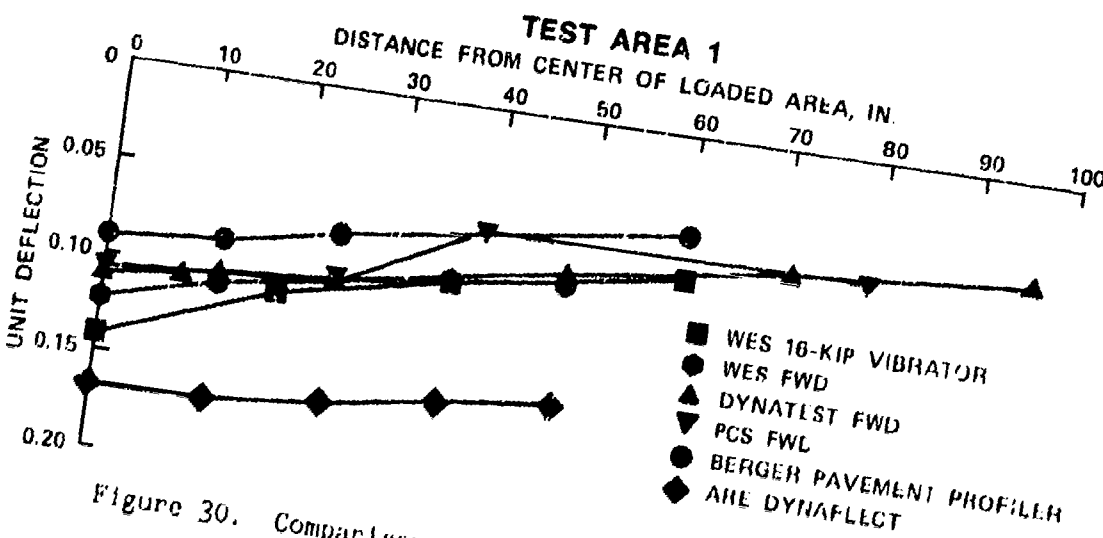


Figure 30. Comparison of normalized deflector basins  
for Test Area 1

### TEST AREA 2

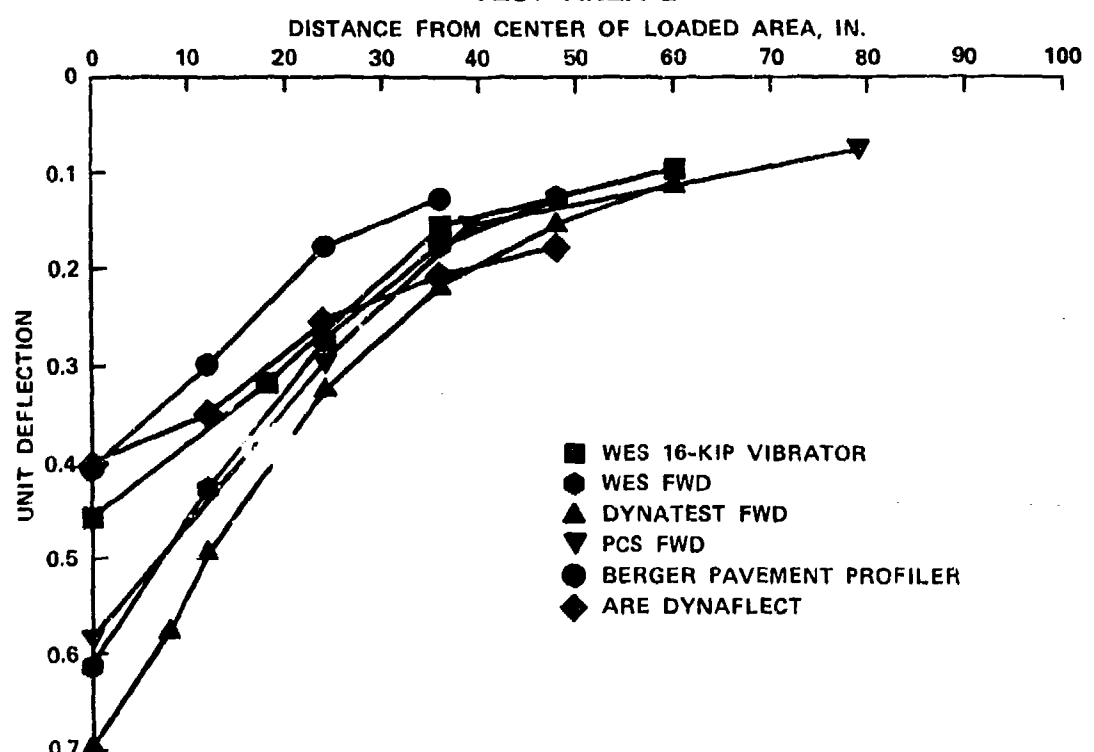


Figure 31. Comparison of normalized deflection basins for Test Area 2

### TEST AREA 3

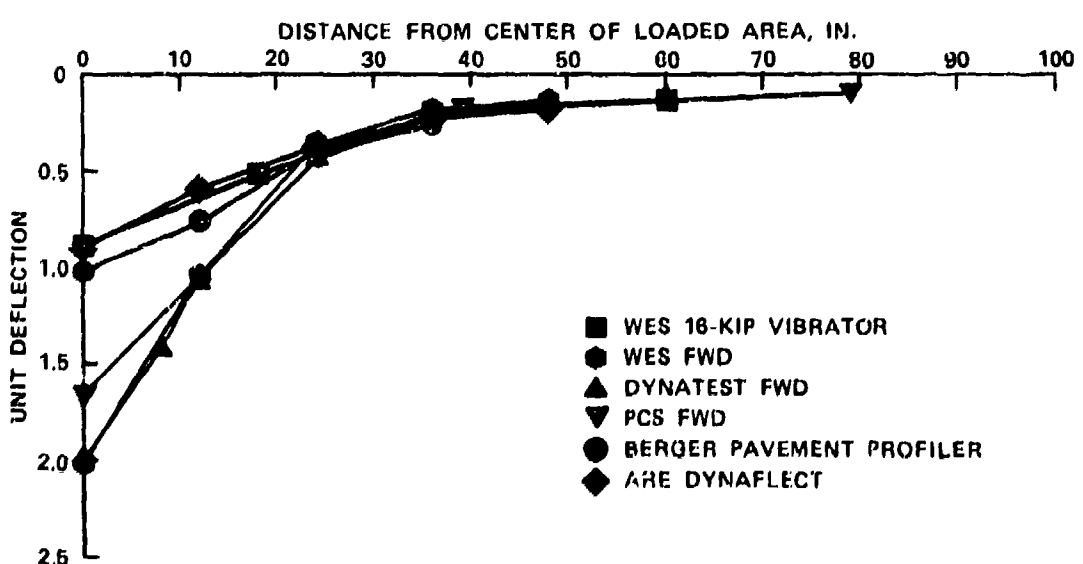


Figure 32. Comparison of normalized deflection basins for Test Area 3

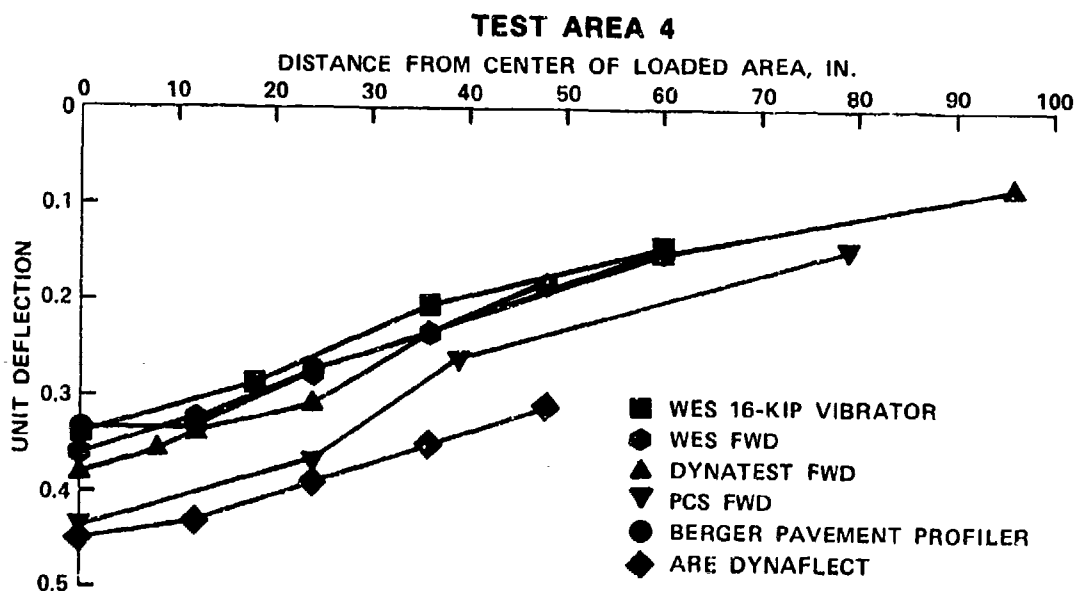


Figure 33. Comparison of normalized deflection basins  
for Test Area 4

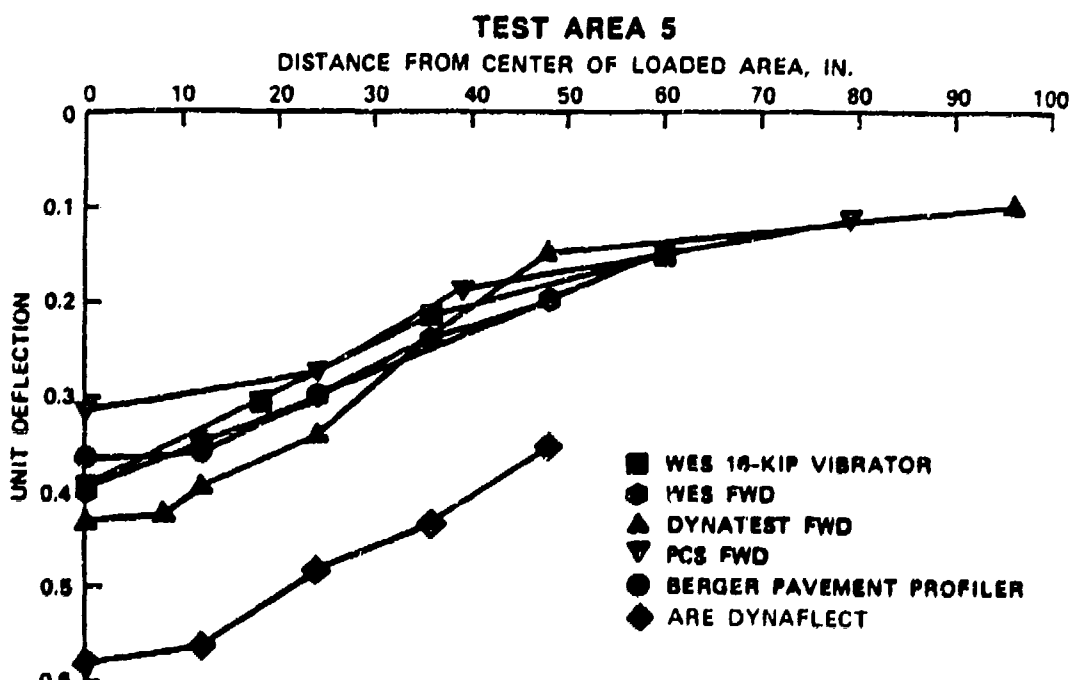


Figure 34. Comparison of normalized deflection basins  
for Test Area 5

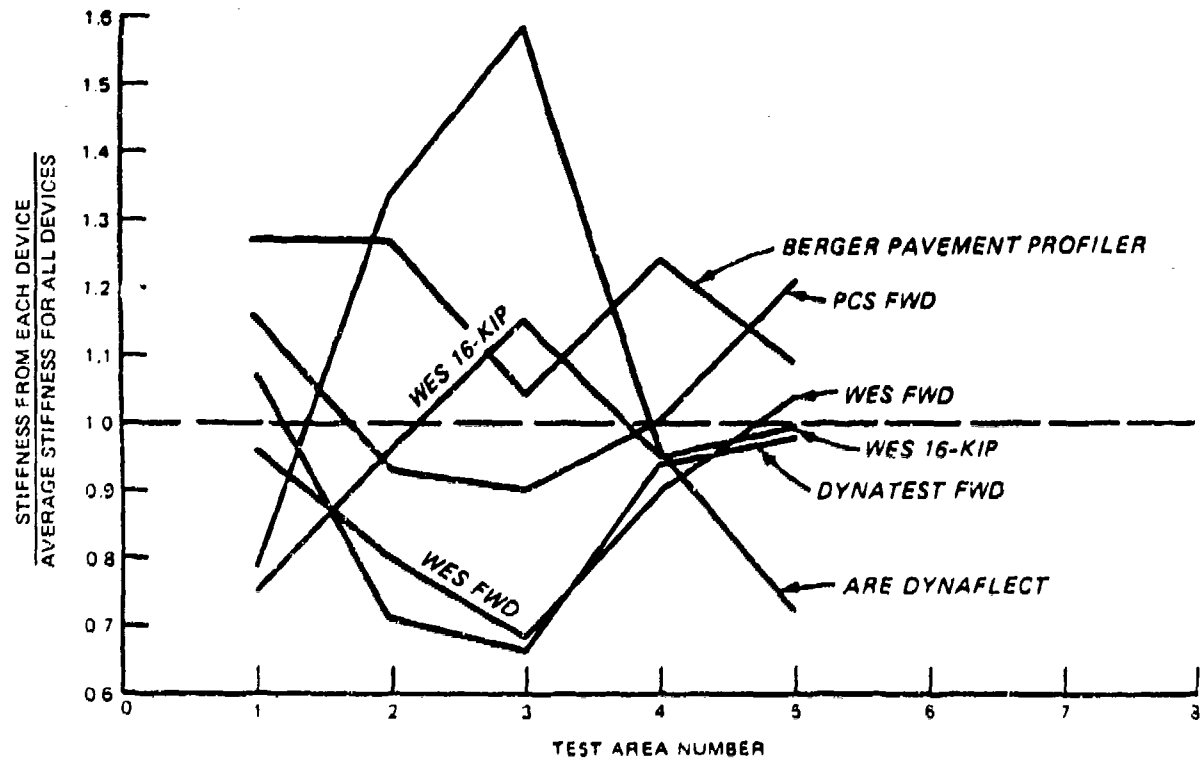
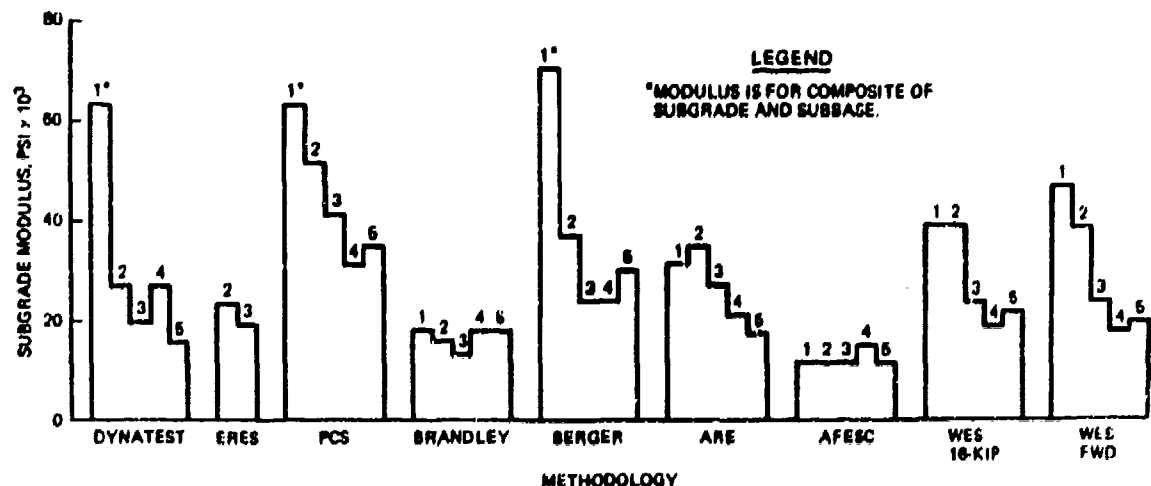


Figure 35. Comparison of stiffness measurements



NOTE: NUMBERS REFER TO TEST AREAS.

Figure 36. Presentation of predicted subgrade moduli

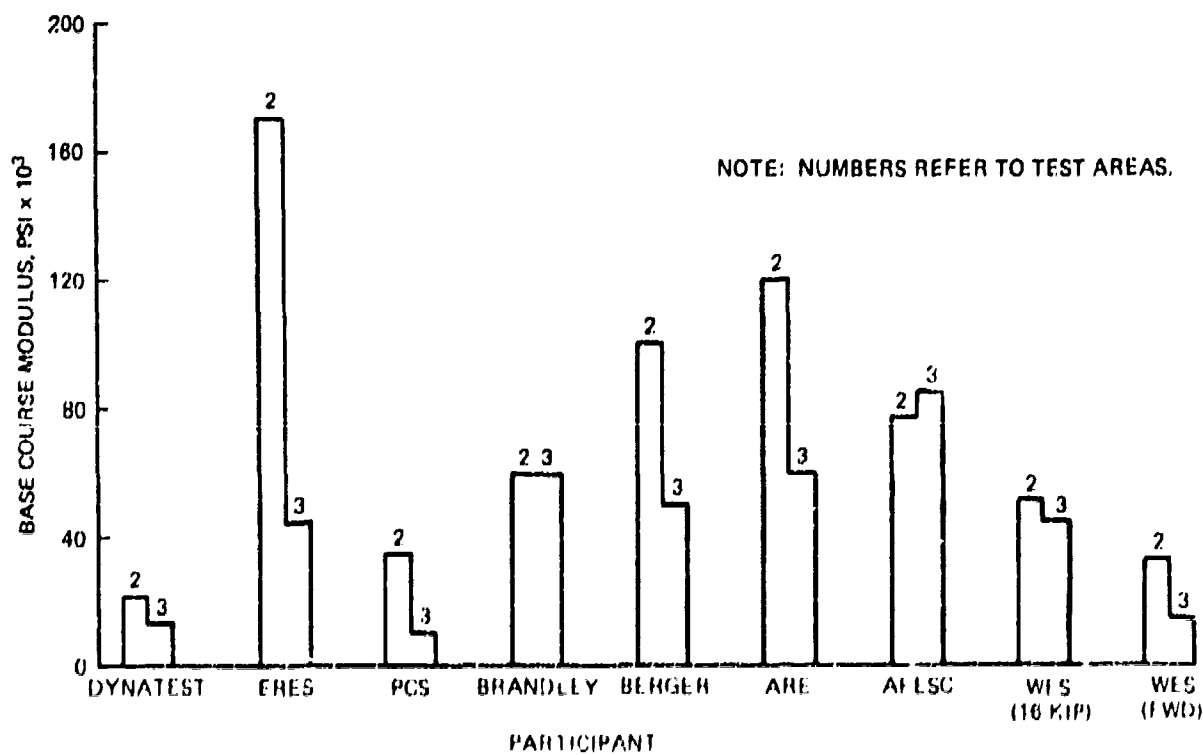


Figure 37. Presentation of predicted base course moduli

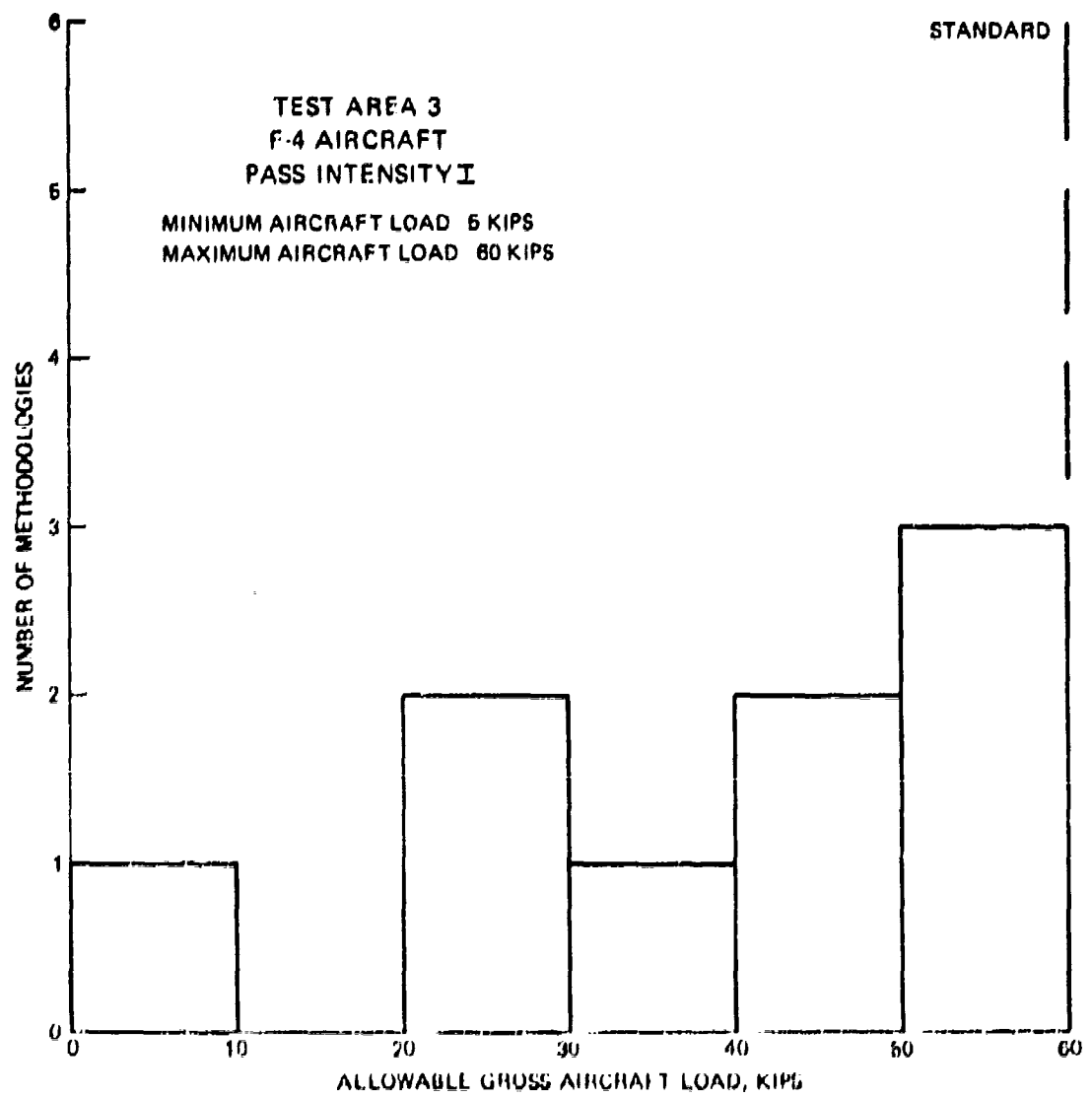


Figure 38. Comparison of predicted loads, Test Area 3, F-4 aircraft

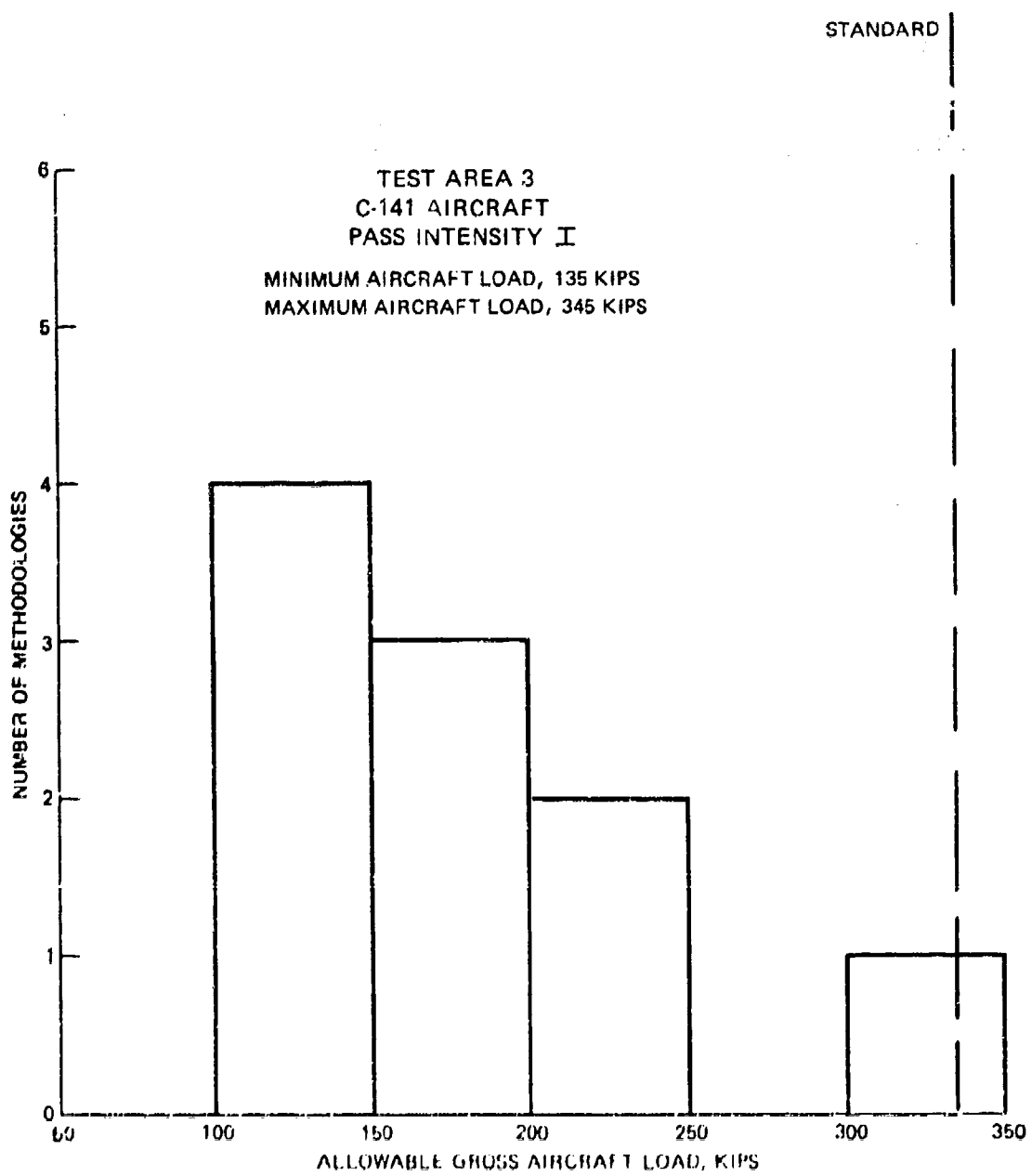


Figure 39. Comparison of predicted loads, Test Area 3, C-141 aircraft

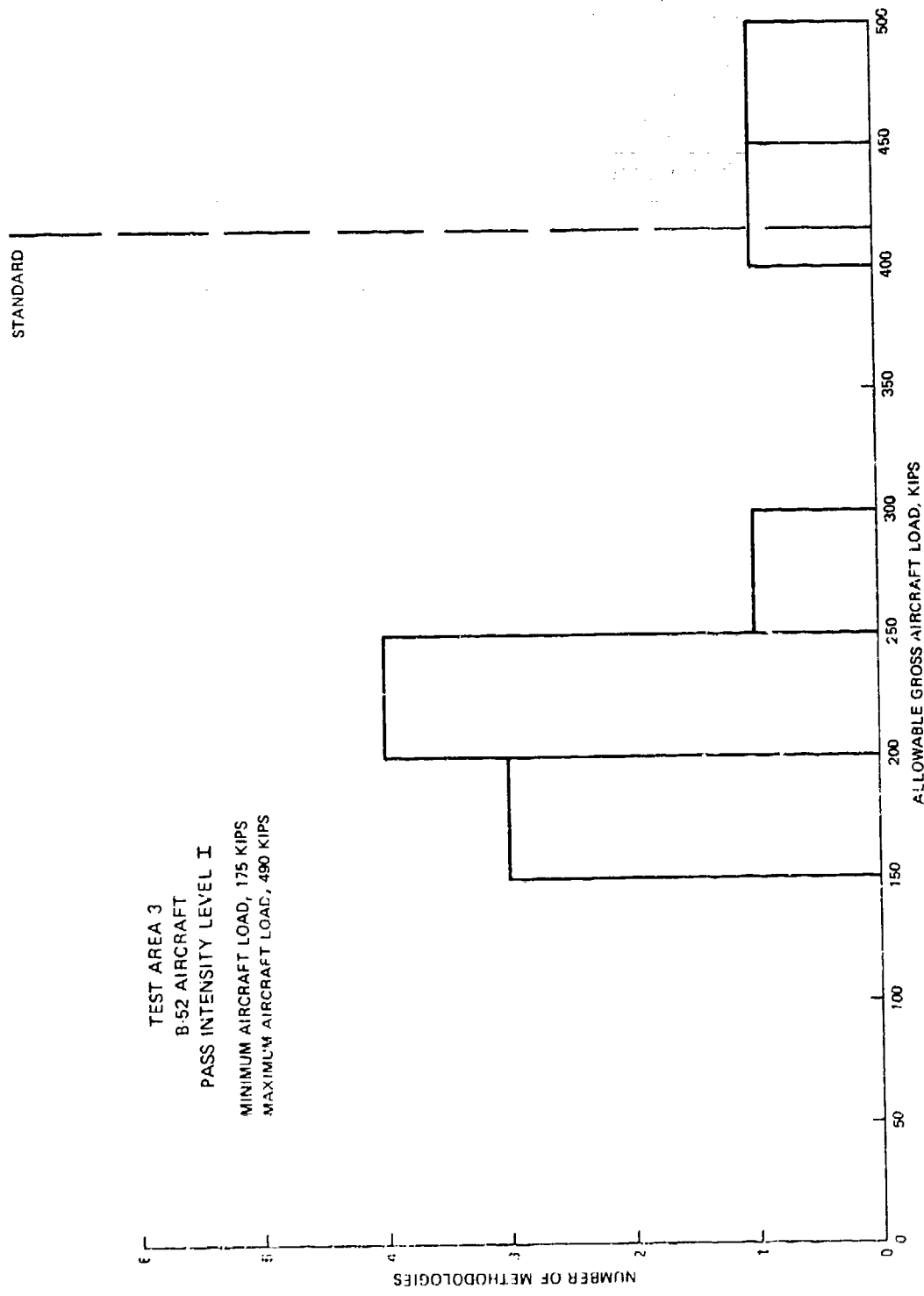


Figure 40. Comparison of predicted loads, Test Area 3, B-52 aircraft

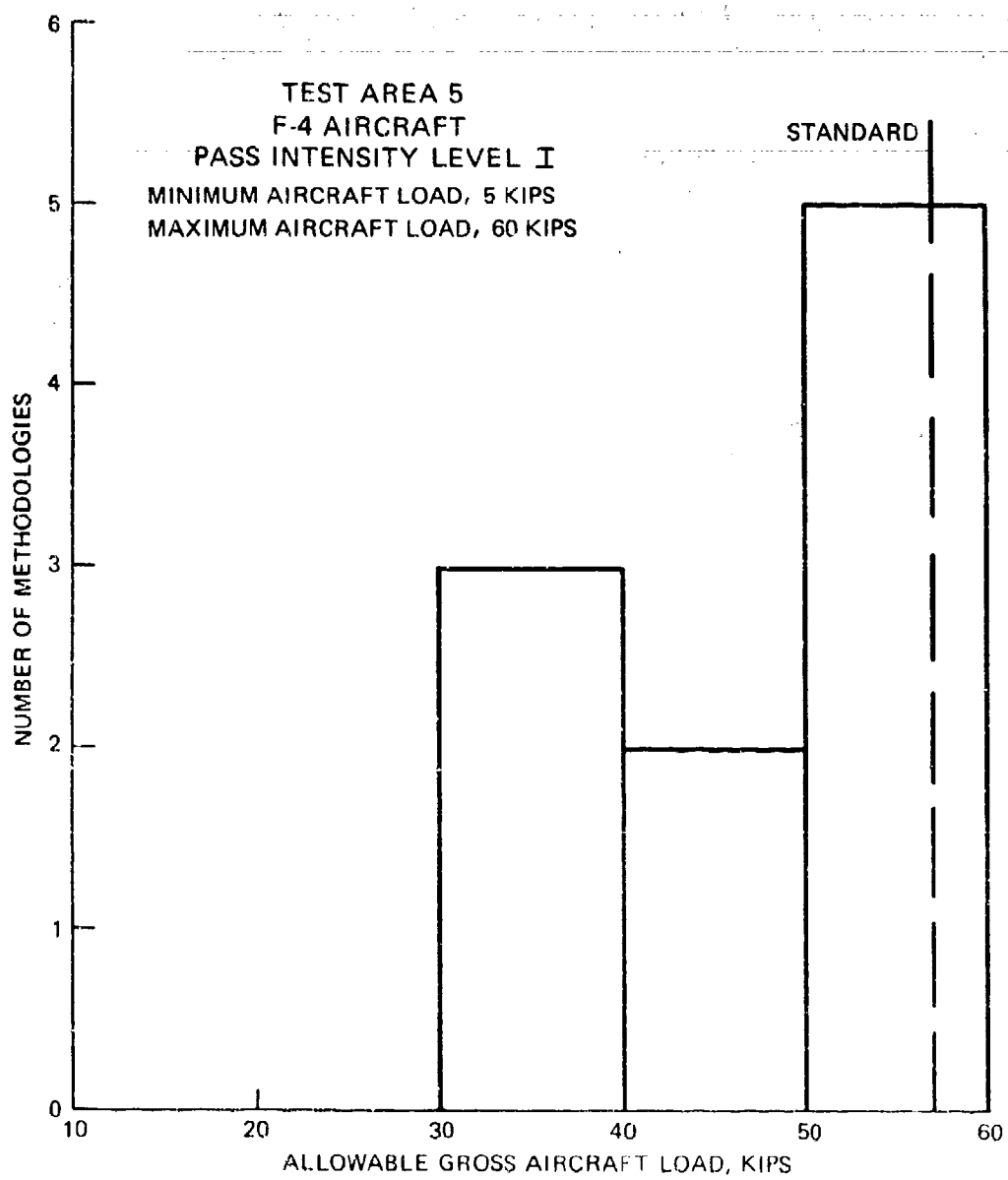


Figure 41. Comparison of predicted loads.  
Test Area 5, F-4 aircraft

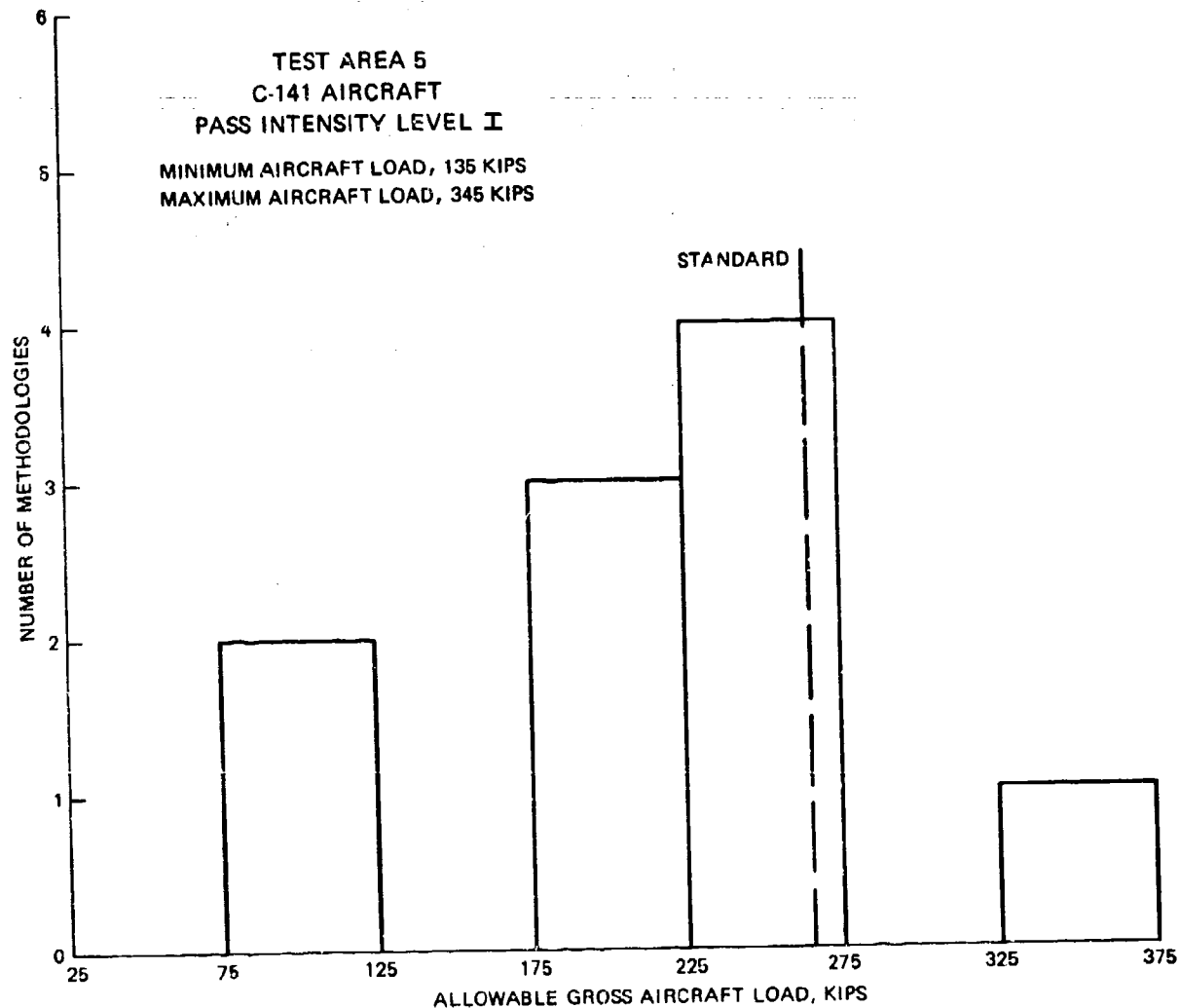


Figure 42. Comparison of predicted loads,  
Test Area 5, C-141 aircraft

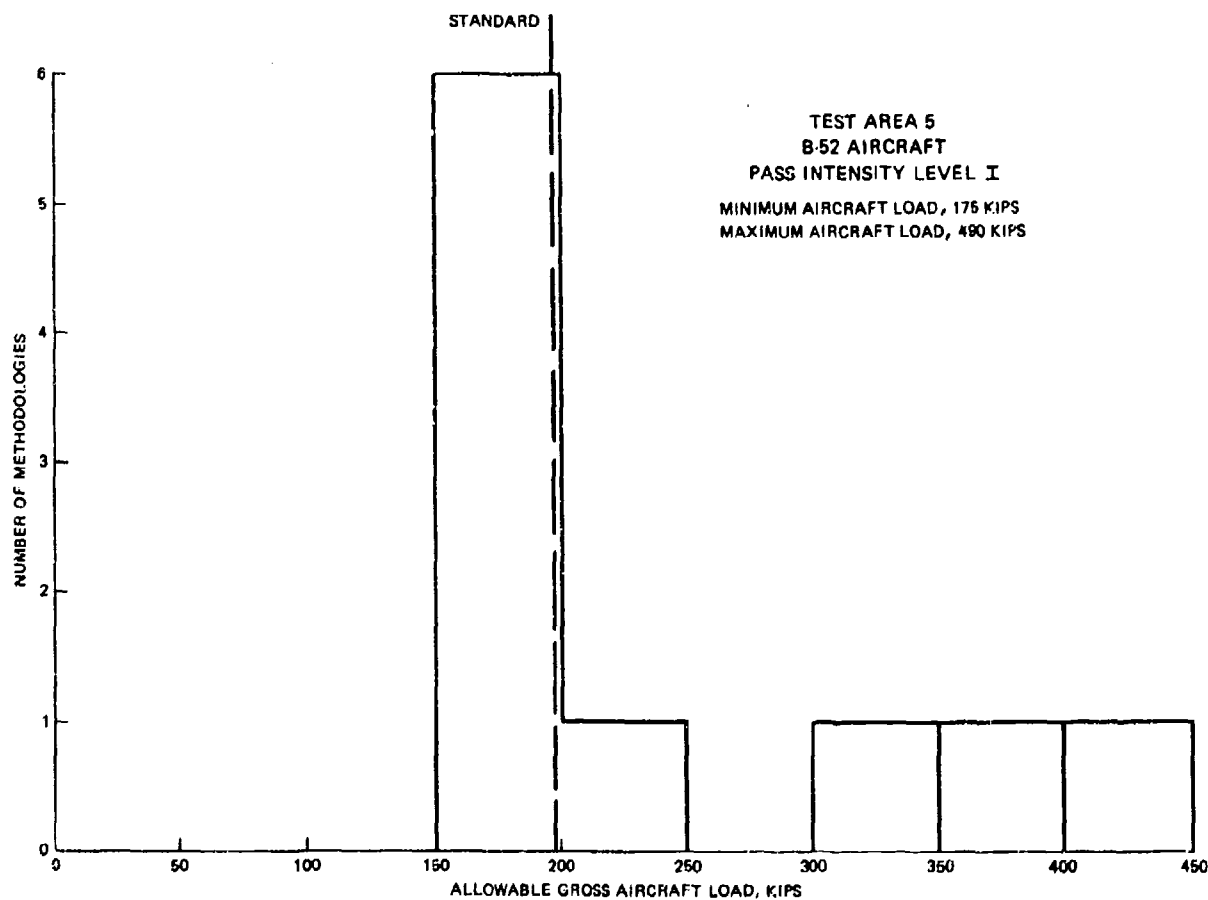


Figure 43. Comparison of predicted loads,  
Test Area 5, B-52 aircraft

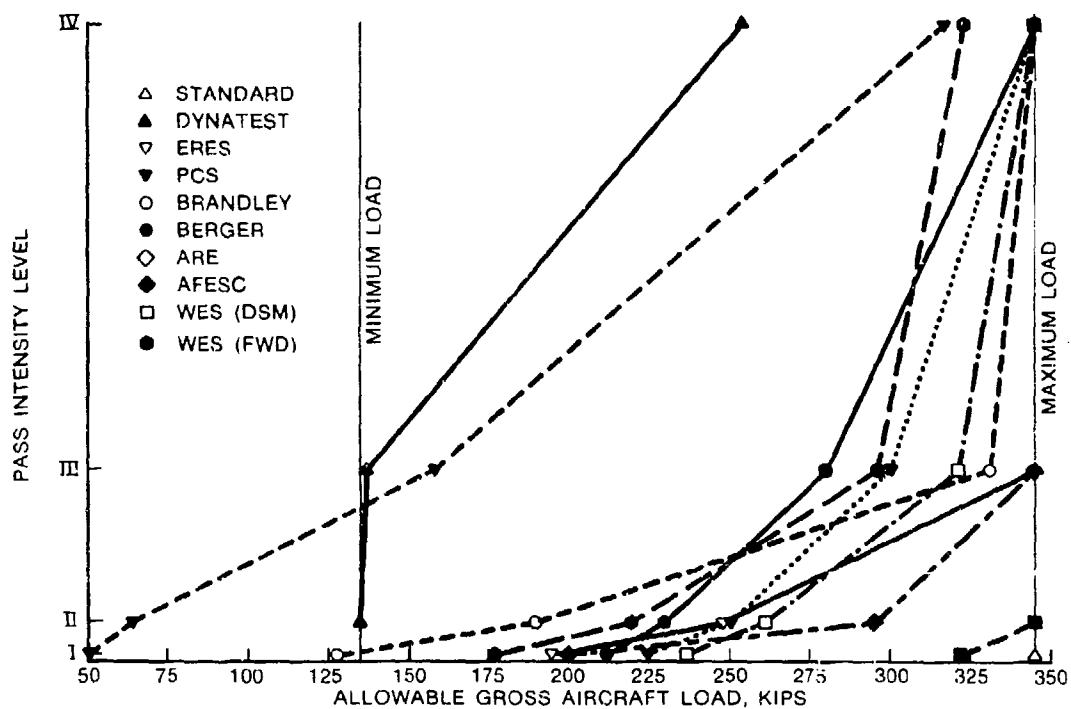


Figure 44. Relationship of allowable loads to passes for flexible pavement. (Allowable load by the standard procedure exceeded the maximum design load for all pass intensity levels)

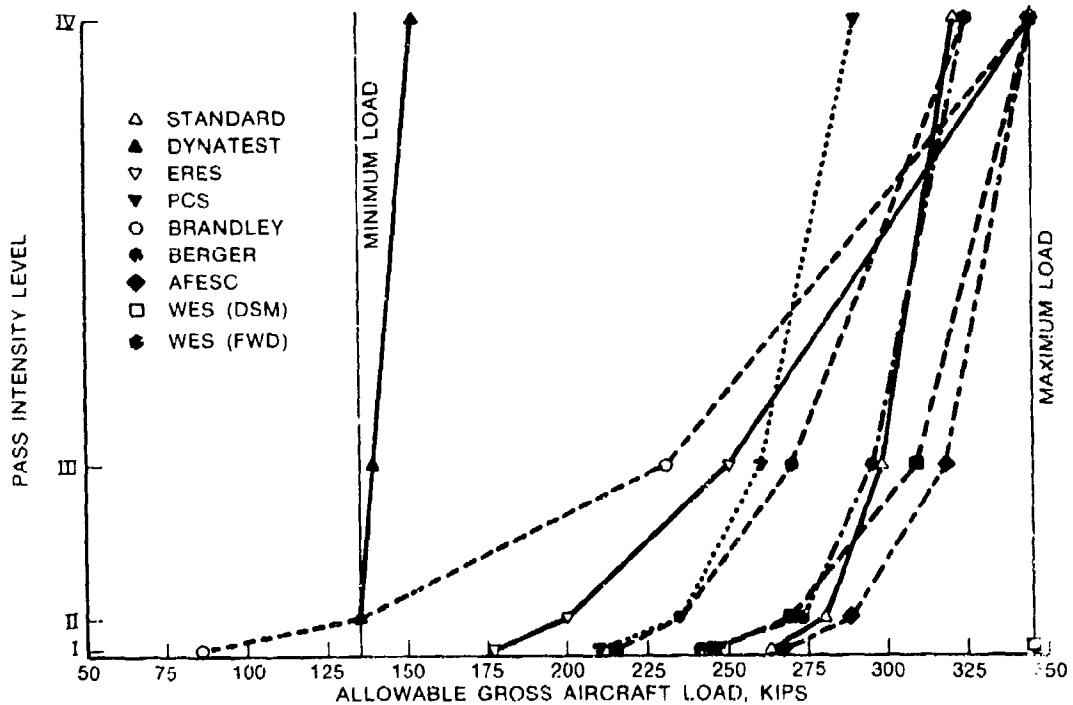


Figure 45. Relationship of allowable load to passes for rigid pavement

APPENDIX A: DESCRIPTION OF NONDESTRUCTIVE TESTING  
EVALUATION METHODS

1. The purpose of this appendix is to provide a general description of the evaluation method used by each participant in the project. This information is needed to understand the different approaches to nondestructive testing (NDT) pavement evaluation and to explain some of the differences in final results as presented in the main text of this report. These descriptions were extracted from information presented in the reports from each participant.

Pavement Consultancy Services, Inc. (PCS)

2. The basic approach of PCS is based upon the use of the Shell BISAR multilayered elastic program to evaluate the *in situ* moduli of pavement layers present. To use these results within current military design approaches, correlations relating moduli either to the modulus of subgrade reaction value (Westergaard "k") or to layer California Bearing Ratio (CBR) are necessary. The use of the current US Air Force Load Evaluation Procedure was selected by PCS to illustrate the complete system applicability of NDT testing and subsequent interpretation within current military conventional design methods (Headquarters, Department of the Air Force 1981.\*)

3. PCS uses NDT measurements performed with a heavy falling weight deflectometer (FWD) at a force level of 100 kN (22.4 kips). A mass falls on a baseplate that is connected to a 12-in.-diam rigid foot plate by means of a set of springs, thus exerting a pulse load onto the pavement surface. The duration of the pulse load is comparable to the duration of the pulse load exerted by actual traffic. The force level can be changed by adjusting the drop height. The deflection of the pavement is measured by four velocity transducers (geophones): one in the center of the foot plate ( $\delta_0$ ) and at three other radial distances--  $r_1(\delta_1)$ ,  $r_2(\delta_2)$ , and  $r_3(\delta_3)$ . At MacDill Air Force Base (AFB), the radial distances were 0, 60, 100, and 200 cm. The deflection signals are obtained by a single integration of the velocity signals from the geophones, which is performed electronically, by integrated circuits. PCS uses the BISAR computer program developed by the Koninklijke Shell Laboratory in Amsterdam in their NDT evaluation program. The BISAR is a linear-elastic multilayer computer program that is used for the calculation of

---

\* References cited in this Appendix are included in the References at the end of the main text.

stresses, strains, and displacements because of one or more uniform circular surface loads (vertical as well as surface shear loads) and allows the use of a variable degree of interface friction (smooth to rough) between any two adjacent layers within the pavement system.

4. For any given multilayer system having known thicknesses  $h_i$  and moduli  $E_i$ , the surface deflections at various radial locations (from the center of the uniformly loaded area) can be computed from the BISAR. In NDT analysis, layer thicknesses are known but layer moduli (in situ  $E_i$  and Poisson's ratio) values are unknown parameters. By assuming that the predicted deflection, at any radial distance, is equal to the measured FWD deflection at the same radial location, the BISAR can be used in a searching routine to evaluate the set of layer moduli that predict the same measured radial deflections as that determined by the FWD geophones. Thus, by measuring the surface deflection basin under a known load and known set of layer thickness, it is possible to determine the in situ response of layer material properties at the specific test location.

5. The layer moduli are developed through an existing PCS software program that sequences through several BISAR iterations until predicted deflections agree within a preselected percentage error of the FWD measured deflections. The PCS evaluation method demonstrated for this project consisted of determination of layer moduli from NDT data and conversion to conventional pavement properties through correlations between the  $E$  derived layer values and the classical CBR and  $k$  values.

6. The correlations that have been used are:

- a. E-CBR relationship.  $E = 1,500$  (CBR) with  $E$  in psi units. This is the widely known Shell Oil relationship developed by Heukelom and Foster (1960) from in situ dynamic vibratory tests.
- b. E-k relationship.  $E = 10^x$  with  $E$  in psi units with  $x = 1.415 + 1.284 \log k$  with  $k$  in pci units. This relationship has been developed by the US Army Corps of Engineers and is based upon laboratory resilient modulus results and in situ measured plate-bearing ( $k$ ) evaluations (Chou 1981).

Whereas, E-CBR relationships are valid for individual layers, the E-k correlation is only valid for subgrade.

7. The results of the NDT testing program obtained by PCS at MacDill AFB on five test sections resulted in the following general observations relative to the in situ layer properties:

- a. The sand subgrade (SP) appears to be relatively uniform, but inherently variable, within all individual sections. The most significant deviation occurs on the SP-SM subgrade of section TW-33.
- b. Using the  $E = 1,500$  (CBR) correlation equation, the average CBR of the subgrade is 27 with an associated range of 16 to 44. These NDT-predicted CBR values appear to be in excellent agreement with test-pit studies.
- c. The average NDT predicted  $k$  value is 310 pci with a general range of 210 to 450 pci. These values appear to be higher than values obtained from test-pit data.
- d. The analysis of the results of the limerock base layer material (SM) indicate that this material exhibits very poor in situ strength/response characteristics. The range of NDT-predicted CBR was found to be between 4 and 50 (overall average near 15). These NDT-predicted CBR values appear to be in excellent agreement with test-pit studies.
- e. The asphalt concrete moduli predicted from NDT results show an average  $E$  value of 635 ksi and range of approximately 300 to 900 ksi.
- f. NDT-predicted values of portland cement concrete (PCC) layer moduli indicated an average moduli of  $4.9 \times 10^6$  psi and a range from  $3.5 \times 10^6$  to  $6.2 \times 10^6$  psi.
- g. NDT analysis of the only composite pavement indicated that the existing PCC layer is severely cracked. This conclusion was based on the abnormally low PCC layer moduli that was predicted from the NDT deflection test results on this pavement section ( $\bar{E} = 1 \times 10^6$  psi).

8. The flexible pavement load evaluation used by PCS in this study was based upon the CBR equation developed by the WES. This equation is:

$$t = \alpha_i \left\{ A_c \left[ 0.0481 - 1.1562 (x) - 0.6414 (x)^2 - 0.473 (x)^3 \right] \right\} \quad (A1)$$

where

$t$  = flexible pavement thickness, in.

$\alpha_i$  = load repetition factor

$A_c$  = contact area of one tire in the known gear system, sq in.

CBR = strength of layer considered

$x = \log_{10} \text{CBR}/p_e = \log_{10} (\text{CBR} \times a_c)/p_e$

$p_e$  = equivalent tire pressure at depth  $z$  used in calculating the  $p_e$  value

$p_e$  = equivalent single-wheel load

- a. The sand subgrade (SP) appears to be relatively uniform, but inherently variable, within all individual sections. The most significant deviation occurs on the SP-SM subgrade of section TW-33.
- b. Using the  $E = 1,500$  (CBR) correlation equation, the average CBR of the subgrade is 27 with an associated range of 16 to 44. These NDT-predicted CBR values appear to be in excellent agreement with test-pit studies.
- c. The average NDT predicted  $k$  value is 310 pci with a general range of 210 to 450 pci. These values appear to be higher than values obtained from test-pit data.
- d. The analysis of the results of the limerock base layer material (SM) indicate that this material exhibits very poor in situ strength/response characteristics. The range of NDT-predicted CBR was found to be between 4 and 50 (overall average near 15). These NDT-predicted CBR values appear to be in excellent agreement with test-pit studies.
- e. The asphalt concrete moduli predicted from NDT results show an average  $E$  value of 635 ksi and range of approximately 300 to 900 ksi.
- f. NDT-predicted values of portland cement concrete (PCC) layer moduli indicated an average moduli of  $4.9 \times 10^6$  psi and a range from  $3.5 \times 10^6$  to  $6.2 \times 10^6$  psi.
- g. NDT analysis of the only composite pavement indicated that the existing PCC layer is severely cracked. This conclusion was based on the abnormally low PCC layer moduli that was predicted from the NDT deflection test results on this pavement section ( $\bar{E} = 1 \times 10^6$  psi).

8. The flexible pavement load evaluation used by PCS in this study was based upon the CBR equation developed by the WES. This equation is:

$$t = a_i \left\{ A_c [0.0481 - 1.1562 (x) - 0.6414 (x)^2 - 0.473 (x)^3] \right\} \quad (A1)$$

where

$t$  = flexible pavement thickness, in.

$a_i$  = load repetition factor

$A_c$  = contact area of one tire in the known gear system, sq in.

CBR = strength of layer considered

$x = \log_{10} \text{CBR}/p_e = \log_{10} (\text{CBR} \times a_c)/P_e$

$p_e$  = equivalent tire pressure at depth  $z$  used in calculating the  $P_e$  value

$P_e$  = equivalent single-wheel load

The alpha  $\alpha_i$  traffic factor is a function of the number of aircraft passes ( $N_p$ ) and number of tires used in the equivalent single-wheel load analysis ( $n_t$ ) (Yoder and Witczak 1975).

9. For each controlling aircraft in the Aircraft Group Index (AGI), single-wheel/load depth relationships were determined from a Chevron elastic-layered computer solution (Boussinesq solution) using the well-known principles of the equivalent single-wheel procedure of the Corps of Engineers (i.e., equal interface deflection theory). Various deflection locations were used within the gear representing the controlling aircraft of the specific AGI to determine the maximum deflection location. The results of the deflection analysis were then used to establish closed-form solutions of equivalent single-wheel load-depth relationships for each AGI.

10. Rigid-pavement evaluations were based upon the Westergaard free edge stress. The theoretical free edge stress is modified by a load-transfer factor  $\beta$  (taken in design to be  $\beta = 0.75$ ) to account for observed differences in joint load transfer, and hence actual stress, to that predicted by the Westergaard theory. Westergaard free edge stresses were computed for all 13 AGI (controlling aircraft) and closed-form solutions were developed for each aircraft. The model form used was:

$$\sigma_{fe} = \frac{1}{h^2} \left( b_0 + b_1 \ln \ell + b_2 \ell^{-1} \right) \quad (A2)$$

11. The allowable load equation, using this stress equation form, and the existing Air Force (Corps of Engineers) relationship was then:

$$P_a = \frac{P_s \times h^2 \times MR}{\beta \left[ g(k, C_f) \right] \times \left( b_0 + b_1 \ln \ell + b_2 \ell^{-1} \right)} \quad (A3)$$

where

$P_a$  = allowable load

$P_s$  = standard load used in the H-51 Westergaard stress analysis

$h$  = PCC slab thickness

MR = design flexural strength (modulus of rupture)

$\beta$  = load transfer factor

$g(k, C_f)$  = mathematical function relating the modulus of reaction  $k$  and coverage to failure level ( $C_f$ ) to the parameter called the design factor

$b_0, b_1, b_2$  = statistical regression coefficients that are functions  
of the specific AGI (aircraft type)  
 $k$  = radius of relative stiffness

12. The load evaluation summary presented in the PCS report is based upon the initial failure (first crack) criterion. Pass-to-coverage ratios which were necessary for each AGI to perform the load evaluation were calculated using taxiway conditions and assuming that 75 percent of the total traffic volume covered the assumed traffic lane. While not all test sections evaluated in this study were taxiways, this assumption was used for all sections simply for computational expediency.

Dynatest Consulting, Inc. (1983)

13. Below are listed some of the most important steps in the Dynatest procedure for evaluation and overlay design.

- a. Layer thicknesses are measured, and the modulus of each layer, including the subgrade, is calculated from deflection tests.
- b. The moduli are adjusted to correspond to the climate conditions of each season in the design procedure.
- c. The permissible stresses or strains in each material are established as a function of the condition of the material (i.e., modulus) and of the number of load repetitions.
- d. The reductions in residual life caused by previous loads are either calculated from the previous loads or are considered (indirectly) through their influence on the present structural condition.
- e. Number, size, and position of future loads are established.
- f. The needed overlay thickness of a given material to provide the desired serviceability or structural condition for the design period is calculated.

14. The Dynatest 800 FWD Test System was used for the NDT. The adjustable load was set to its maximum capacity of approximately 24,000 lb (force), and a loading plate of approximate 6-in. radius (150 mm) was used to simulate the stress level of a heavily loaded jet aircraft. The resulting stress level was somewhat in excess of 200 psi under the loading plate.

15. The FWD load is transient (as opposed to vibratory), having a time of loading of some 25-30 msec, thus corresponding to the effect of a moving aircraft wheel load. Both the load level and a series of seven simultaneous deflections are monitored for each FWD test, with the deflections measured at

the surface of the pavement from the center of the loading plate (through a small hole in the middle of it) out to a distance of more than 2 m from the center. This enables calculation of the elastic properties of each structural layer in the pavement (assuming pavement layer thicknesses are known) through the use of a reverse, iterative procedure that matches up the load and deflections measured against a unique set of material properties.

16. To obtain reasonably accurate moduli of the pavement layers, Dynatest states that it is essential to consider the nonlinearity of the subgrade. Nonlinear subgrade moduli may be considered either by using finite element methods or by using a modified version of the MET (Ullidtz 1977). If a large number of points are to be evaluated, and this is desirable because of the large variations in pavement structures and subgrades, then the use of the finite element method by Dynatest is not practical for time and cost reasons. Furthermore, MET has been found to give as good as or better agreement than the so-called exact methods (including the finite element method), when compared to actually measured stresses, strains, and deflections in road structures (Ullidtz 1973).

17. The nonlinearity of the subgrade may be determined by carrying out FWD tests at different stress levels. Another possibility is to calculate the nonlinearity from the shape of the deflection basin at one stress level. This second alternative employs the ELMOD program even though it is very easy to change stress level with the FWD, because it is preferable to include other changes in modulus with depth (e.g., layered subgrades, changes in moisture content or overburden pressure) as an "apparent" nonlinearity rather than to disregard such variations. The moduli of the pavement layers, including the subgrade, were determined with the ELMOD program, taking the nonlinearity of the subgrade into consideration.

18. MET has been incorporated into the ELMOD program (for evaluation of layer moduli and overlay design). This program has been written for the HP-85 microcomputer, the same microcomputer that controls the 8000 FWD. The ELMOD program determines the layer moduli, including the nonlinearity of the subgrade, by fitting the theoretical deflection basin to the measured deflections. When, in a later step of the calculations, the overlay thickness is to be determined, the MET is used to calculate the critical stresses and strains.

19. To consider the conditions at joints and corners of rigid

pavements, a special version of the ELMOD program is used. For the center of a slab, the same procedure as described above is used. For joints and corners, the concrete modulus is then assumed to be the same as determined at the center, and the modulus of subgrade reaction  $k$  is calculated using Westergaard's modified equations (Westergaard 1948). At joints, the degree of load transfer is calculated and considered in calculating the modulus of subgrade reaction and later when determining the required overlay thickness. Westergaard's equations are also used to calculate the modulus of subgrade reaction at the center of the slab, and, by comparing this value to the value determined at the joint, it is possible to infer the presence of voids at the joints.

20. The moduli determined from the deflection measurements obviously correspond to the climatic conditions during testing. To carry out a proper overlay design, the year should be divided into seasons of reasonably constant climatic conditions.

21. With the ELMOD program, it is possible to divide the year into up to 12 seasons. A sinusoidal relationship is used for the asphalt temperature and the asphalt modulus is determined from

$$E_T = \left[ A + B \times \log_{10} \left( \frac{T}{C} \right) \right] \times E_C \quad (A4)$$

where

$E_T$  = modulus at  $T$ , degrees Celsius

$T$  = measured temperature, °F

$E_C$  = modulus at a reference temperature  $C$ , °C

$C$  = reference temperature, °C

A and B = constants (input values)

The permissible stresses or strains will be closely related to the definition of "failure." For "bound" materials, such as PCC or asphaltic materials, "failure" may be defined as cracking of the material. In this case, the permissible stress or strain may be determined from fatigue testing in the laboratory. But a transfer function is needed between laboratory and in situ conditions.

22. Two seasons were used in the structural evaluation, each of 26 weeks. The mean temperature was assumed to be 59° F (15° C) for one season, and 94.5° F (35° C) for the other season. The subgrade modulus varies

sinusoidally with season according to the equation

$$R = \frac{1}{2} \times \left(1 + \frac{E_{\min}}{E_{\max}}\right) + \frac{1}{2} \left(1 - \frac{E_{\min}}{E_{\max}}\right) \times \sin \left[ \frac{\pi}{26} (W - WM - 13) \right] \quad (A5)$$

where

R = seasonal factor

$E_{\min}$  = minimum modulus during the wet season

$E_{\max}$  = maximum modulus during the dry season

W = week number, counted from January 1

WM = the number of the week when the modulus is at its minimum  
(for this evaluation WM = 6)

$\frac{E_{\min}}{E_{\max}}$  = 0.67 (estimated from previous FWD testing in Florida)

The seasonal correction of the modulus is applied to the subgrade only. For asphalt, the following modulus-temperature relationship has been used:

$$\frac{E(T)}{E(C)} = 1 - 2 \log_{10} \left( \frac{T - 32}{45} \right) \quad (A6)$$

where

$E(T)$  = modulus at  $T$ , °F

$E(C)$  = a reference modulus corresponding to a temperature of  
 $45 + 32 = 77$  °F

The nonlinear properties of the subgrade are expressed as:

$$E = C \times \left( \frac{\sigma_1}{\sigma'} \right)^n \quad (A7)$$

where

$\sigma_1$  = major principal stress

$\sigma'$  = reference stress (a value of 0.1 MPa (14.5 psi) has been used)

C and n = constants (n is negative)

23. For the nonlinear subgrade the modulus used in the structural evaluation  $E_m$  is the modulus corresponding to a plate-loading test on the top of the subgrade with a 450-mm- (17.7-in.-) diam slab at a magnitude of deflection of 1 mm (39 mils).

24. For composite pavements, a fixed modulus is used for the concrete and the asphalt modulus is calculated by the program.

25. A standard overlay material is used with a modulus of 650 ksi (4,500 MPa) in one season and 290 ksi (2,000 MPa) in the other season. A Poisson's ratio of 0.35 is used for all materials except concrete where Poisson's ratio is assumed to be 0.15.

26. For the unbound materials, including the subgrade, the following stress criteria has been used:

$$\sigma = 0.5 \times N^{-0.0667} \times \left(\frac{E}{E_0}\right)^d \quad (A8)$$

where

$\sigma$  = permissible normal stress for  $N$  number of load applications, MPa

$E$  = modulus of the material, MPa

$E_0$  = reference value, here equal to 160 MPa (2,300 psi)

$d$  = a power which is equal to 1 when  $E$  is greater than  $E_0$ , otherwise 1.16

This relationship has been derived from a combination of full-scale field testing and dynamic testing of permanent deformations. The  $E/E_0$  relationship was derived from the American Association of State Highway Officials (AASHO) Road Test.

27. For asphalt materials the following failure strain criteria was used:

$$\epsilon_t = 0.000228 \times VB \times N^{-0.178} \quad (A9)$$

where

$\epsilon_t$  = permissible horizontal strain at the bottom of the asphalt layer for  $N$  number of load applications

$VB$  = volume percentage of bitumen, here approximately 12

For PCC the flexural strength corresponding to static loading was determined from

$$ZP = A \times \left(\frac{E}{E_0}\right)^d \quad (A10)$$

where

ZP = flexural strength of PCC, MPa

A = a constant, here 1.18 MPa (170 psi)

E = modulus of the concrete, MPa

E<sub>o</sub> = a reference modulus, here 10,000 MPa (1,450 ksi),

d = a power, here 1 for E > E<sub>o</sub> and 0.77 for E < E<sub>o</sub>

Flexural strength, psi =  $9 \times \sqrt{\text{compressive strength, psi}}$

28. A maximum flexural strength of 610 psi was assumed, because this is the maximum value measured by the Air Force Engineering and Services Center (AFESC) at MacDill AFB.

29. The permissible number of load repetitions, when the dynamic, repeated loading is superimposed by a static load from temperature gradient is (Herholdt et al. 1979)

$$N = 10^{[12 \times (1 - \Sigma DS/FS) / (1 - PS/\Sigma DS)]} \quad (\text{A11})$$

where

$\Sigma DS$  = sum of dynamic and static load (in this analysis static load assumed to be insignificant)

FS = flexural strength

PS = static load

30. It is recommended by Dynatest that the allowable gross aircraft load be taken as the load that can be sustained by more than 80 percent of the test points.

31. A pass-to-coverage ratio of 1 is used throughout by Dynatest. Furthermore, for the concrete sections, the loading corresponds to early morning conditions. Corners and joints of concrete slabs were evaluated during the morning hours because this is the critical period from a structural point of view.

32. Test Area 1 was treated as a two-layer system, because it was impossible to distinguish the limerock-stabilized sand base from the subgrade. Test Areas 2 and 3 were both considered as three-layer systems. For both of these test areas, the subbase was included as part of the subgrade. An asphalt overlay has been assumed with a winter modulus of 650 ksi and a summer modulus of 290 ksi. The maximum gross load used for the B-747 was 825 kips and for the DC-10-30, 555 kips.

ERES Consultants, Inc. (1982)

33. The overall procedures used by ERES to evaluate the pavements were as follows:

- a. A condition survey was first conducted to determine what distress exists and the present overall condition of the pavement using the Pavement Condition Index (PCI).
- b. The pavement structural response to aircraft loads was measured with a Dynatest Model 8000 FWD; the heavy load (24,000 lb) was required to simulate the heavy aircraft wheel loads using the pavements. ERES states that the FWD closely simulates the deflection basin obtained under actual moving wheel loads. The entire deflection basin 6 ft from the load plate was measured. The load-carrying capacity of the joints was measured, and the critical load location determined.
- c. The stiffness of the pavement layers were back-calculated from the deflection basin curvature using an elastic layer model for AC pavements and a finite element model for concrete and composite pavements.
- d. The critical stresses and strains were calculated for various aircraft loads placed at the critical location on the pavement using the same elastic layer and finite element pavement models used to characterize the pavements. The measured load transfer at the joints was directly taken into account in the analysis.
- e. The number of load coverages to a selected proportion of cracking (and rutting) was then calculated using field-verified damage models for given aircraft types and loads.

34. The FWD used by ERES was manufactured by Dynatest Engineering, Ltd., of Denmark. The unit can produce loads from 1,500 to 24,000 lb with a duration of approximately 27 msec.

35. The load is applied to the loading plate by dropping a weight package on a dampening system and is measured directly by a load cell. The resulting pavement deflection is measured by seven seismic deflection transducers spaced at predetermined intervals from the loading plate (12-in. intervals in this study). The signals from the load cell and deflection transducers are fed into the system processor which selects the peak values and transfers this information to the HP-85 computer. Three different load magnitudes were used in this evaluation ranging up to 24,000 lb.

36. According to ERES, characterization of jointed concrete pavement is best modeled with a finite element model that can accurately represent the joints. ERES uses the ILLISLAB finite element program (modified) that was developed at the University of Illinois.

37. The pavement can be accurately characterized by back-calculating the modulus of elasticity of the slab and the k-value of the foundation from the measured deflection basin. ERES has used several different methods to determine the best modulus of elasticity E and k values for given pavements. The most consistent method is to use the area of the center slab deflection basin and maximum deflection. A graphical relationship of area versus maximum deflection as functions of the modulus of the concrete slab and the foundation support modulus k is then developed over a reasonable range of E modulus values and k values until the average area and maximum deflection of the pavement are bound using the ILLISLAB program. The E modulus and k value determined will normally accurately give the slab curvature measured with the FWD. The area and maximum deflection basin of individual slabs can be used to determine an E and k value, or the average of all the slabs can be used (excluding any very unrepresentative slabs). The mean area and maximum deflection were used herein to obtain an average E and k value for the pavement section.

38. The concrete modulus of elasticity E and the k value of the foundation are not the standard static E and k value measured by long-term static tests, but represent the dynamic response of the pavement to the FWD load, and consequently the moving aircraft wheel load. For example, for Test Area 5 (10.5-in. PCC), the following was obtained.

$$E \text{ modulus (dynamic)} = 4,500,000 \text{ psi}$$

$$\text{Poisson's ratio} = 0.20 \text{ (assumed)}$$

$$k \text{ value (dynamic)} = 315 \text{ pci}$$

ERES has developed an empirical relationship between the measured dynamic modulus of elasticity of a standard beam and its standard third-point loading modulus of rupture. The estimated modulus of rupture of the concrete slab is 632 psi based on a dynamic modulus of elasticity of 4,500,000 psi.

39. The pavement model characterized as described was then loaded with each of the 13 critical aircraft. The critical location for the aircraft gear is at the joints. The critical joint having the lowest load transfer was determined. The aircraft gear was positioned so as to give the critical stress in the slab. This position was normally with a wheel load parallel to the joint (similar to standard Corps of Engineers and Federal Aviation Administration (FAA) design methods).

40. The critical tensile stress in the slab was then calculated for

each aircraft. These stresses are located at the bottom of the slab and parallel to the joint. The joint was modeled with a deflection load transfer.

41. The next step was to estimate the number of stress repetitions that the slab could withstand until cracking occurs. To accomplish this difficult task, ERES used a relationship between the ratio of the modulus of rupture to the critical stress in the slab and the number of actual coverages of the aircraft gear to cracking of the slab. This relationship was developed using field data from 52 Corps of Engineers test sections that were run over the past 40 years. The critical stress in each of these pavements was calculated using the ILLISLAB finite element program for the actual loading used. The dynamic modulus of elasticity of the concrete was used and an estimate of the repeated load  $k$  value was used in the stress calculation. The damage model derived from these data is shown below.

$$\log_{10} (\text{coverages}) = 2.27 \times \frac{\text{MR}}{\text{STRESS}} + 0.056 \quad (\text{A12})$$

where

$\log_{10}$  (coverages) = number of coverages to 50 percent slab cracking

MR = third-point modulus of rupture calculated from  
dynamic modulus of elasticity from FWD, psi

STRESS = critical stress in the slab using appropriate  
load transfer in the ILLISLAB finite element  
program, psi

42. Graphs of gross aircraft load versus the number of coverages to 50-, 25-, and 10-percent slab cracking were plotted for a given aircraft. The allowable aircraft gross load can then be read from these graphs for the specified pass intensity levels.

43. Pass-to-coverage ratios calculated using the normal distribution were used to convert coverages to passes. Allowable gross aircraft loads to 50-, 25-, and 10-percent slab cracking for the given pass load intensity levels are given. It must be remembered that these loadings are for the aircraft oriented in the critical direction (parallel to the joint with the lowest load transfer for this apron). If the joint had much higher load transfer, as would occur with mechanical load-transfer devices, the load-carrying capacity would be substantially higher. The load-transfer capability of the joints will always control the load-carrying capacity of the overall jointed concrete pavement.

44. Since the overlay is to be designed for only one aircraft, a simplification of the normal ERES procedures can be made. If more than one heavy aircraft were to use the pavement, a different analysis would be conducted to analyze the need for strengthening the pavement (using the Miner's cumulative damage law).

45. If past load damage were evident, the Miner's cumulative damage law would be employed as follows.

$$\text{Total damage} = \sum_{\text{past damage}} \frac{n_p}{N_p} + \sum_{\text{future damage}} \frac{n_f}{N_f} \quad (\text{A13})$$

46. If adequate data are available, then a summation of load damage can be made using the Miner's damage law. However, if there are inadequate past traffic data, then the amount of past damage can be estimated using existing load-associated slab cracking.

47. A series of stress calculations are made using the ILLISLAB finite element program over a range of overlay thicknesses for a given pavement and aircraft. The critical stress is still in the same location at the bottom of the slab parallel to the joint for the AC and the bonded PCC overlays. The critical stress for the unbonded PCC overlay is either at the bottom of the existing slab or at the bottom of the new PCC overlay at the joint. The moduli and Poisson's ratio used for the AC and PCC overlays are as follows:

$$\text{AC overlay: } E = 350,000 \text{ psi}, \nu = 0.35 \quad (\text{A14})$$

$$\text{PCC overlay: } E = 4,000,000 \text{ psi}, \nu = 0.20 \quad (\text{A15})$$

48. The same load transfer that exists in the base slab was used for the AC and PCC bonded overlay since they will not increase the load transfer at the joint. The load transfer for the unbonded PCC overlays was increased to that normally used in new design for joints with mechanical load transfer or tied keyways (75 percent).

49. The number of aircraft coverages until slab cracking for each overlay thickness was then calculated. The allowable coverages were converted to passes. A failure criteria of 25 percent cracked slabs is believed to be

reasonable for major rehabilitation purposes.

50. For the composite pavement section, the finite element model was used to model the critical joint area. The ILLISLAB model was used with the two layers (AC and PCC) bonded together. The pavement layers and subgrade support were characterized by back-calculating the modulus of elasticity of the asphalt concrete and concrete slab and the  $k$  value from the measured deflection basin. The area method was used.

51. FWD deflection tests were conducted at the slab center, transverse joint, longitudinal joint, and slab corner. Load-transfer tests were also taken across random cracks in the overlay. Six different slab areas were tested overall. The reflective crack/joint load transfer was determined. The determination of allowable loads and overlays followed the same approach as used for jointed concrete pavement.

52. For flexible pavement characterization, the general procedures used to determine the moduli values required modeling the pavement as a two-layered system and modeling the deflection basin to determine the subgrade modulus (Hoffman and Thompson 1981). With the subgrade modulus known, a factorial design was conducted with varying moduli values to match the deflection basin. This procedure provides a unique solution for the previously selected subgrade modulus used. Relationships were developed for each pavement structural section. The FWD deflection data plotted on these relationships provide the moduli for the two layers, completing the characterization with a unique match to the deflection basin measured in the field.

53. The AC modulus was found to be very sensitive to the modulus obtained for the subgrade. The base course, however, showed little sensitivity for the pavements analyzed in this study.

54. Flexible pavements will generally fail because of permanent deformation (rutting) or fatigue cracking of the AC layer. When cement-stabilized layers are used for the base course, the problem of fatigue failure in the cement-stabilized layer must be examined. Rutting is generally characterized by the vertical stress on the subgrade, the vertical strain on the subgrade, or the vertical deflection of the pavement surface. Fatigue cracking is generally related to the radial tensile strain that develops at the bottom of the AC layer or the stabilized layer. These pavement response parameters are related to the number of loads producing a response that will cause a specified level of failure to occur.

55. Critical stresses and strains were calculated at the interfaces of the layers. The multiple-wheel load (MWL) elastic-layered program was used to analyze the multiple-wheel gears of the aircraft and calculate the stresses and strains used in the analysis. The critical values were calculated as a function of the gross aircraft load. In these calculations, the gross aircraft loads were decreased in increments with the resulting tire pressure changing to keep the contact area the same for all load levels.

56. The MWL elastic-layered system was used in this analysis because the materials in the pavement structure were primarily granular and acted linearly. Excellent deflection matches were obtained with the elastic-layered analysis used in the characterization. The outputs of the program are the vertical stresses and strains at the subgrade, the vertical deflection of the surface, and the radial strain in the AC layer.

57. The failure criteria used in this analysis include radial strain in the AC and the vertical strain on the subgrade.

58. The rutting failure criterion used in the analysis was the one developed by Chou (1976). This relationship is in the following form:

$$\epsilon_v = 5.511 \times 10^{-3} \left( \frac{1}{N_{cov}^{0.1532}} \right) \quad (A16)$$

where

$\epsilon_v$  = vertical strain on the subgrade

$N_{cov}$  = number of coverages of the specified aircraft producing that strain

59. This equation was used to calculate the allowable strain for each aircraft being analyzed as a function of the number of coverages specified for that aircraft. The allowable strain calculated in this manner was used as the failure criteria in this analysis.

60. The French Shell method of evaluating fatigue damage is one of the most flexible procedures for evaluating fatigue in different asphalt materials (Bonnaure, Gravois, and Udrone 1980). The equation is presented.

$$\begin{aligned} \epsilon_r = & (4.102 \times PI - 0.205 \times PI \times Vb + 1.049 \\ & \times Vb - 2.707) \times S_m^{-0.28} \times N_{cov}^{-0.2} \end{aligned} \quad (A17)$$

where

$\epsilon_r$  = radial strain

PI = penetration index, assumed = 0

Vb = volumetric bitumen content, 15 percent

$S_m$  = stiffness of the mix, N/m<sup>2</sup>

N = number of coverages

61. For a totally nondestructive type of analysis, typical asphalt properties can be assumed that consider the condition of the pavement, the age of the asphalt materials used, and the properties of the original materials used. The temperature variation can be accounted for in the stiffness modulus of the AC.

62. The fatigue curve developed from the French Shell method represents the median of a large number of fatigue samples, and use of this curve should produce values representative of 50 percent wheel path area cracking in the pavement. A more accepted level of fatigue cracking is approximately 10 percent cracking. Curves were also calculated representing the strain and loadings that would produce cracking levels of 10 and 25 percent.

63. The pavement response values were obtained for each aircraft for each level of loading. Graphs were then prepared showing the relationship between the response values and the gross aircraft loadings.

64. The allowable strains for rutting and fatigue were calculated from the equations using the number of coverages. Different allowable loads are calculated for conditions of rutting--fatigue 50 percent, fatigue 25 percent, and fatigue 10 percent of the area. The comparison that produces the lowest allowable gross load between fatigue and rutting should be the one selected for a particular pavement. The acceptable level of fatigue cracking is an engineering management decision.

65. The modulus value for the AC surface layer could be changed for a seasonal analysis to show temperature influences. Additionally, the subgrade modulus value could be altered to indicate seasonal variability. The values determined in October 1982 are deemed representative of the Tampa, Fla., area; over a year or so no changes were made in this analysis (no frost problem existed and the water table was relatively high).

66. Because the limerock base appears to be cemented to some extent (the modulus value is much higher than nonstabilized granular materials), an analysis was carried out to examine the fatigue life of a cement-treated

soil. The analyses conducted relate primarily to true portland cement-stabilized materials, not naturally cementitious materials. The first method of analysis used Portland Cement Association data on fatigue of soil cement using the radius of curvature of the stabilized layer (Larsen and Nussbaum 1967). The damage model for a low quality cement-stabilized material is

$$R = \frac{R_c \times N^{0.032}}{1.05 - 0.042h} \quad (A18)$$

where

R = radius of curvature

R<sub>c</sub> = critical radius of curvature = 7,000 in.

N = number of load repetitions the section will carry

h = thickness of stabilized layer

67. The second analysis used results from ERES employing AASHO road test data for the cement-stabilized layers and elastic-layer analysis to obtain appropriate critical strains. The damage model is

$$\log N_{2.5} = 8.559 - 3.488 \log \epsilon \quad (A19)$$

where

N<sub>2.5</sub> = number of loads to reduce serviceability to a failure level

ε = strain in cement-treated material

68. Because the limerock base is not a true portland cement-stabilized layer, these analyses are more approximate than the rutting and fatigue analyses. These analyses cautiously use existing pavement conditions. The results do show a substantial reduction in allowable loading.

69. For overlay design the pavement section is characterized as previously described. It is then modeled with the aircraft placed on the pavement structure at its maximum load and the pavement response values calculated by the MWL program. The thickness of the overlay is varied and the response values for each thickness calculated. The allowable strains are then calculated for each aircraft using the field-developed equations presented in the previous section for the number of coverages of each aircraft. Overlay thicknesses are selected based on the rutting and fatigue analyses. These thicknesses would be increased somewhat if the pavement showed signs of load-related distress indicating that some fatigue or rutting damage had already

been produced by the previous traffic on the pavement.

70. For multiple-aircraft loadings, the Miner's fatigue damage concept is used to compute total damage from all aircraft using the pavement. This total damage is correlated to percent cracking of the pavement to determine the limiting criteria. This procedure of directly considering existing load transfer will give reduced allowable loads and increased overlay thickness if the load transfer is poor. Poor load transfer existed on both jointed concrete test areas.

R. W. Brandley (RWB)(1983)

71. The test program conducted by RWB consisted of the following:

- a. A survey was performed to determine the condition of the existing pavements by visual observations.
- b. Dynatest FWD tests using the Dynatest 24-kip unit were conducted.
- c. Joint efficiency tests using loaded vehicles and cantilever deflection beam were carried out.
- d. Tests using the WES 16-kip vibrator were conducted.

72. Each test site was visually inspected in some detail to determine the existing conditions of pavement at each test area. The purpose of this condition survey was to provide information on distress that had occurred in the pavements as the result of traffic.

73. The Dynatest FWD test equipment was used to conduct the FWD tests. At each location tested, the test load was dropped from such a height as to provide a load of approximately 830 kPa and a load of 1,500 kPa on a 5.91-in.-radius plate. Deflection readings were measured directly under the plate at distances of 200, 305, 610, 914, 1,524, and 2,438 mm away from the plate. These deflection measurements were automatically recorded.

74. On the PCC pavement sections, tests were conducted in the center of the slab, at the edge of the slab, and at the corner of the slab to determine the effect of load transfer in the slab itself. The tests conducted at the edge and corner of the slab were conducted in such a manner that the joint was located between the gauges set at 200 and 305 mm from the plate.

75. On the AC pavement sections, the tests were conducted both along the center line of the test section and 18 ft on each side of the test section. Representative values of deflection at each distance measured from

the center of the plate were determined. These data were used in a computer program for evaluation of the pavement sections.

76. On Test Areas 2 and 3, considerable variation occurred between the pavement section at the center of the taxiway and the section at the edge of the taxiway. To obtain information as to the relative effect of this change in section, a series of FWD tests was conducted across the taxiways, which provided a cross section of deflection across these taxiways.

77. The test data obtained on the PCC pavement sections were such as to determine the support characteristics of the pavement section at the center of the slab and also to get some indication of the load transfer at the joints. This was accomplished by applying the load adjacent to a joint and measuring the induced deflections on both sides of the joint.

78. WES made data from the WES 16-kip vibrator available for evaluation. The 16-kip vibrator test data were evaluated in a manner similar to that for the FWD data in that profiles were plotted of the deflections obtained and representative values of deflection at each test location and at each distance from the applied load were determined.

79. In all of the WES 16-kip vibrator tests, dynamic loads were applied and the imposed deflections were measured under the plate at a distance of 18, 36, and 60 in. from the plate. The plate diameter for the WES 16-kip vibrator was 18 in.

80. The office of RWB had developed a method of testing joints in PCC pavements sections to determine the effectiveness of the load transfer at the joints and the resistance to deflection at the joints under load. The test procedure consists of placing a cantilever deflection beam on the slab with two linear potentiometers located at the free end of the beam. The beam is set on the slab such that one of the potentiometers is located on one side of the joint and the other potentiometer is located on the other side of the joint. A rubber-tired wheel which imposes approximately the same total load as the aircraft using the pavements is then pulled or driven across the joint perpendicular to the joint and passes immediately adjacent to the location of the potentiometers. In this manner, the total relative deflection of the slab at the joint and the relative movement of one slab with respect to the other (slab rocking) as the wheel moves over the joint can be measured and recorded.

81. This type of testing was undertaken at Test Areas 1 and 5, which had a PCC pavement. The Air Force had agreed to furnish a loaded vehicle of

approximately 50,000 lb per single wheel; however, the only equipment available was a truck-mounted crane which had three axles. The rear axles had dual wheels, and each pair of duals was loaded to 7,000 to 8,000 lb. These loads were very light and did not adequately represent the wheel loadings on any of the design aircraft other than perhaps the F-16. Because this was the only equipment available, the tests were conducted using this equipment.

82. RWB used the fatigue analysis method (Brandley 1975) for pavement evaluation and design for subgrade support, the standard CBR method for flexible pavements, and the Westergaard method for rigid pavements for evaluation of the pavement section itself. The nondestructive test data were used at MacDill AFB to obtain modulus of elasticity values for each material within the pavement section and for the subgrade soils at each test location.

83. The moduli of elasticity calculations were made using the data from both the FWD tests and the WES 16-kip vibrator tests. Using the data from the FWD tests, the entire deflection basin was evaluated using the ELMOD and the ISSEM 4 programs employed by Dynatest Consulting, Inc. In addition, the program for the Boussinesq theory using the equivalent thickness theory was put to use. The N-layer theory as developed by Chevron Asphalt Institute was also utilized, in which the center deflection and the edge deflection are used in the N-layer computer program to compute the modulus of elasticity of the subgrade layers. The values assumed for the pavement layers were those obtained from the ELMOD or ISSEM 4 evaluations.

84. For the WES 16-kip vibrator, the Boussinesq equivalent thickness program and the N-layer theory were used with the deflections obtained from this test procedure to calculate modulus of elasticity values. Part of these variations in subgrade E-values calculated by each method can be accounted for by the fact that the Boussinesq equivalent thickness theory and the N-layer theory assume a linear elastic condition for the support materials; whereas, the ELMOD and ISSEM 4 programs allow stress-dependent characteristics. Applying a factor of 2 to 3 to the E-values obtained for the subgrade soils in the concrete sections at MacDill AFB produces subgrade E-values which are reasonably uniform throughout the site.

85. Using this type of evaluation, soil and pavement section parameters to be used in the evaluation and design were determined. The E-values for the pavement section itself used in the analysis were those obtained in evaluating the deflection basin data taken from the FWD tests. Using the modulus of

elasticity values and the aircraft loading at each pavement section, subgrade deflections for each aircraft were calculated using the N-layer theory. After subgrade deflection under each aircraft loading at each pavement section had been determined, the limiting subgrade deflection criteria were used to determine the allowable aircraft coverages to failure for each aircraft. One coverage is obtained on the critical pavement section for each two passes of aircraft over the pavement section depending on type of aircraft and location, i.e., taxiway or runway.

86. The pavement evaluation by the fatigue analysis method was then determined by comparing the allowable coverages to failure with the pass levels for each of the four levels of operation established for this study. Knowing the pass level required for each aircraft type at each test location, it is now a simple matter to determine the ability of the pavement section to carry the aircraft loading and to determine what overlays are required to strengthen the deficient pavement sections enough to carry the anticipated number of aircraft operations for each aircraft.

87. This same type of analysis can be used to determine the allowable load at which each aircraft can operate without failure of the subgrade for each pass level. All of this evaluation with the fatigue analysis method is for subgrade protection only and assumes that the pavement section is adequate to distribute the loads to the subgrade without failure of these materials themselves. It is necessary to evaluate the adequacy of the pavement section itself for support of the aircraft without failure in this pavement section. This analysis was conducted using standard procedures with CBR analysis for flexible pavement and the Westergaard analysis for rigid pavement. The minimum PCC overlay presented in this analysis is 12 in., even where a thinner section theoretically would perform. It is considered that a minimum 12-in. section is required to install the necessary load transfer at the joints.

88. Joint efficiency tests were conducted using the FWD, the WES 16-kip vibrator, and a moving wheel load with a cantilever-type deflection beam. Research conducted by RWB has shown that pavements 12 in. thick can tolerate slab rocking up to 0.020 in. without inducing stresses sufficient to cause failures. However, any slab rocking or relative deflection of magnitude greater than this will contribute to early failure. This 0.020-in. maximum slab rocking or deflection criteria for the edge of the slab has been determined for 12-in. concrete slabs. For thicker slabs, less deflection can

be tolerated; and for thinner slabs, more deflection can be tolerated.

89. It appears that the amount of movement measured under the FWD test when joint efficiency tests are conducted is so small that the joint efficiency cannot be properly evaluated. All joints move a certain amount, and it has been shown that joints can move up to 0.020 in. with 12-in. slabs without imposing serious stresses. The light loading of the FWD does not produce enough movement at the joint to determine whether adequate load transfer exists. The same analysis holds true for the WES 16-kip vibrator.

90. Full-scale testing is apparently still required for joint efficiency. While the data are not adequate because of lack of loading to confidently predict adequacy of load transfer, the data do indicate that adequate load transfer is available in Test Area 1 but that there are sections of Test Area 5 in which adequate load transfer will not be available.

Louis Berger International, Inc. (1983)

91. The report submitted by Berger consisted not only of the requested pavement evaluation in terms of allowable loads and overlays but also provided results of comparisons with different NDT equipment and different layer analyses. The method used by Berger for NDT evaluation is a combination of layered-elastic theory and a modified version of the WES DSM method (Hall 1978). This method can be implemented with the pavement profiler, FWD, or the WES 16-kip vibrator, and similar results would be obtained. The description given here will briefly discuss some of the Berger results using information from the report submitted by Berger.

92. The method used in the Berger report for determining the allowable gross aircraft load (AGAL) is the CBR method for flexible pavements and the Westergaard analysis for edge loading for rigid pavements. These methods are also the basis for the current DSM procedure, as outlined by Hall (1978).

93. The NDT data used to perform the pavement evaluation were collected with the Model 2000 pavement profiler which applied a peak-to-peak cyclic load of 4.5 kips at a frequency of 25 Hz. Deflection sensors are placed either 12, 24, and 36 in. or 12, 24, and 60 in. from the center of the load plate. One sensor is mounted at the center of the 18-in.-diam plate. Berger also made use of the data collected by WES with the WES 16-kip vibrator and the Model 8000 FWD (15 kip). The WES data were not used for upgrading the pavement

systems but for comparisons of the elastic parameters obtained for the sub-grade and pavement.

94. For flexible pavements, the critical strain concept shows promise, but it is Berger's opinion that, in view of the range of critical strain values, this method requires site calibration. This can be done when past traffic records are available and when an opportunity is provided for NDT testing of both areas with satisfactory pavement sections and traffic-induced failures.

95. The method for determining a representative DSM value for each pavement based on measurements with the WES 16-kip vibrator is described in detail by Hall (1978). The DSM can be determined from measurements made with the pavement profiler using the following expression:

$$DSM = 0.8 \times \frac{P}{\Delta_0} \quad (A20)$$

where

P = peak-to-peak load for Model 2000 pavement profiler (about 4.5 kips)

$\Delta_0$  = double amplitude of the pavement center deflection on an 18-in. diam plate

This is the design DSM which is equivalent to WES DSM ksi. In determining the representative  $(P/\Delta_0)$  values to use for the pavement evaluation of the five test areas, the 50-percentile values obtained on both the center line and near wheel path were considered.

#### Flexible Pavements

$$ASWL = 0.0437 \times (DSM) \quad (A21)$$

#### Rigid Pavements

$$ASWL = 0.01896 \times (DSM) \quad (A22)$$

#### Composite Pavements

$$ASWL = 0.0172 \times (DSM) \quad (A23)$$

where allowable single-wheel load (ASWL) is in kips and (DSM) is in ksi.

The following values of allowable single-wheel load were obtained:

<u>Values, Single-Wheel Load</u>	
<u>Test Area</u>	<u>ASWL, kips</u>
1	150
2	87
3	35
4	40
5	44

96. Because the CBR method was used in determining the ASWL in the WES study on flexible pavements, it is pertinent to compute the implied CBR of the subgrade associated with the ASWL for Test Areas 2 and 3. This requires converting the existing pavement thickness to an equivalent pavement thickness,  $T_t$ , having 3 in. of AC and 6 in. of high-quality base. Assuming that the AC has a 1.7 equivalency to subbase and a 1.4 equivalency to high-quality base (as assumed in the original WES study),  $T_t$  can be computed for the two flexible pavements if equivalencies are assigned for the existing AC and base materials. Based on the NDT moduli, it seems reasonable to assign an equivalency factor of 1.7 to the existing AC, 1.15 for the existing base in Test Area 2, and 1.05 for the existing base in Test Area 3. The representative values of the elastic moduli for the base course in Test Areas 2 and 3 are 100,000 and 50,000 psi, respectively.

97. Using the CBR equation and the ASWL determined from the DSM as outlined above, one can compute the associated CBR.

$$CBR = \frac{\alpha^2 \times 1,000 \times (ASWL)}{8.1 \times (T_t^2 + \alpha^2 A/\pi)} \quad (A24)$$

where

$\alpha$  = 0.94, for 24,000 sites

ASWL = allowable single-wheel load, kips

$T_t$  = equivalent thickness, sq in.

$A$  = 254 sq in.

This gives a subgrade CBR of 9 for Test Area 2 and a CBR of about 14 for Test Area 3. These results are not consistent with the subgrade modulus  $E_3$  of about 37,000 psi for Test Area 3 determined from the NDT testing.

98. An implied linear relationship between ASWL and DSM indicates that the measured DSM would increase proportionately to the square of the pavement thickness. This has not been observed at various sites. Therefore, for the

purposes of pavement evaluation, a better procedure is to evaluate the CBR of the subgrade using deflection bowls to determine the subgrade modulus  $E_3$  and then evaluate the CBR using this subgrade modulus. The elastic modulus of the base  $E_2$  and the asphalt layer  $E_1$  determined from the interpretation of the deflection bowl are used to estimate the equivalency factors. These are used to determine the equivalent flexible pavement thickness  $T_t$ . The ASWL bowl is then computed using the CBR equation. This procedure yields a subgrade CBR of about 25 for Test Area 2 (as compare to 9) and a CBR of about 15 for Test Area 3 (as compared to 14). The equivalent flexible pavement thickness equals 31 and 14 for Test Areas 2 and 3, respectively. Consequently, the DSM procedure for determining ASWL for flexible pavement in Test Area 2 is very conservative; whereas, for Test Area 3 this procedure appears to be more reasonable.

99. The deflection bowls measured on rigid pavements can be used directly to determine all the parameters necessary for determining the ASWL if the flexural strength of the concrete is known. The following results were obtained.

<u>Test Area</u>	<u>Thickness in.</u>	<u>DSM kips/in.</u>	<u><math>E_1</math> psi</u>	<u>k pci</u>	<u><math>\ell</math> in.</u>
1	20.0	8,000	4,000,000	500	48
5	10.5	2,300	4,000,000	250	36

Using the above values for Test Area 5 with a C-141 aircraft, one can calculate the allowable gross load for 24,000 passes:

$$P_G = 0.0189 \times (\text{DSM}) \times (F_L) \times (T_C) \quad (\text{A25})$$

where

$P_G$  = allowable gross load aircraft, kips

$F_L$  = load factor, which depends on the characteristic length  $\ell$

$T_C$  = traffic factor, which depends on the aircraft gear configuration and the required number passes

For Test Area 5,  $\text{DSM} = 2,300$ ,  $\ell = 36$ ,  $F_L = 7.4$ , and  $T_C = 0.95$ , and

$$P_G = 0.0189 \times (\text{DSM} = 2,300) \times (F_L = 7.4) \times (T_C = 0.95) \approx 310 \text{ kips} \quad (\text{A26})$$

100. Using the rigid pavement evaluation curve for the same aircraft (C-141), an allowable gross load of 310 kips, 24,000 departures, and 10.5 in. of PCC pavement (with a  $k = 250$  pci) yields a concrete flexural strength of 780 psi. PCC cores tested by splitting and converted to flexural strength by an empirical relationship produced flexural strengths ranging from 420 to 610 psi (AFESC 1980). Fifty percent of the reported flexural strengths were 500 psi or less. In view of the above and in the absence of a direct determination of the flexural strength, a flexural strength of 650 psi was assumed for the rigid pavement evaluation. The allowable gross load is therefore 260 kips from the C-141 evaluation curve. Therefore, the following expression was used for evaluating the rigid pavement of Areas 1 and 5.

$$P_G = 0.0159 \times (\text{DSM}) \times (F_L) \times (T_C) \quad (\text{A27})$$

where  $0.0159 = 0.0189 (260/310)$ . The allowable gross load is determined using this equation which has been developed for flexural strength of 650 psi.

101. Based on the similarity of the deflection bowls and the same design DSM for Test Areas 4 and 5 ( $\text{DSM} = 2,300$ ), the same parameters can be used for pavement evaluation of Test Area 4 (composite pavement); i.e.,  $k = 250$  pci and  $(t = 36.0$  in.), where determined previously for Test Area 5.

102. The equivalent thickness of PCC pavement is given by the following expression.

$$h_e = \frac{1}{F} (h + 0.4t) = 11.0 \text{ in.} \quad (\text{A28})$$

where

$$F = 0.8$$

$$h = 6 \text{ in. (thickness of PCC)}$$

$$t = 7 \text{ in. (thickness of AC overlay)}$$

Following the same procedure outlined for Test Area 5,

$$P_G = 0.0172 \times (2,300) \times (7.4) \times 0.95 = \text{ kips} \quad (\text{A29})$$

103. This implies a concrete flexural strength of 690 psi for an equivalent thickness of PCC of 11 in. Following the same procedure as outlined for Test Areas 1 and 5, the following expression was used for evaluating the rigid pavements of Test Area 4.

$$P_G = 0.0162 \times (\text{DSM}) \times (F_L) \times (T_C) \quad (\text{A30})$$

where  $0.0162 = 0.0172 (650/690)$ .

104. The AGAL for flexible pavements is computed using the evaluation curves for flexible pavements for 13 aircraft groups. When using these curves,  $T_t$  values were used for thickness (e.g.,  $T_t = 31$  in. for Test Area 2 and 14 in. for Test Area 3). The subgrade CBR values were those determined from the subgrade modulus  $E_3$  values found from interpretation of the deflection bowls (i.e., CBR = 25 for Test Area 2 and CBR = 15 for Test Area 3). Based on these CBR design curves, no load limitations exist for the 13 aircraft groups at all pass intensity levels for Test Area 2.

105. The load limitations for Test Area 3 are based on the design curves for each pass level. For example, the allowable gross load of aircraft group 11 (DC-10-30) and 3,000 passes is 430 kips.

106. In Test Area 3, the CBR of the subgrade associated with the DSM method is 14. The CBR of the subgrade from  $E_3$  is 15. Because these two values are similar, it is of interest to determine the AGAL for Test Area 3 using the DSM method as outlined. The AGAL is determined by the following expression.

$$P_G = \frac{F_K \times (\text{DSM})}{S \times (\% \text{ESWL})} \times \frac{N_m}{NC} \times 100 \quad (\text{A31})$$

where

$F_K$  = load factor depending on the number of wheels and the total aircraft coverages;  $F_K$  depends on the total number of passes and on the pass-to-coverage ratio for the aircraft

$S$  = main gear load, percent

$\% \text{ ESWL}$  = percent equivalent single-wheel load depends on equivalent flexible pavement thickness the aircraft

$N_m$  = number of controlling wheels for computing (percent ESWL)

The following overlay thickness recommendations for each test area were determined.

#### Areas 1 and 2

107. No upgrading is required for the rigid pavement of Test Area 1 (20-in. concrete) and the flexible pavement of Test Area 2 (15-in. base plus 11-in. AC) to accommodate the design traffic of the B-747 or the DC-10-30.

### Area 3

108. The design subgrade CBR is 15, and the equivalent thickness  $T_t = 14$  in. Using the CBR curves, a total required flexible pavement thickness of  $T_t = 20$  in. is determined for the B-747. In other words,  $DT_t = 20 - 14 = 6$  in. of subbase. Based on an equivalency factor of 1 in. of AC = 1.7 to 2.0 in. of subbase, an overlay of 3.5 in. of AC is recommended for this aircraft. The actual overlay thickness will be based on the pavement elevation profile and the minimum overlay should be 3.0 in. For the DC-10-30 aircraft, the total required flexible pavement thickness is 17 in. Therefore, a minimum 1.75 to 2.0 in. of AC is recommended.

### Area 4

109. The most economical overlay design is based on the flexible pavement analysis. The design subgrade CBR is 15. The existing 6.0 in. of PCC is assumed to be equivalent to 6.0 in. of high-quality base course. The equivalent existing pavement thickness  $T_t$  is therefore  $T_t = (6 \text{ base} + 3 \text{ asphalt}) + (7 - 3) \times 1.7 = 15.8$  in. Using the CBR design curve, a total required flexible pavement thickness of  $T_t = 20$  in. is determined for the B-747. Therefore, the recommended overlay thickness is  $(20.0 - 15.8)/(1.8) = 2.3$ , say 2.5 in. Following this same design procedure for the DC-10-30 results in a required AC overlay thickness of less than 1.5 in. In conclusion for Test Area 4, 2-1/2 and 1-1/2 in. of AC are recommended for the B-747 and DC-10-30, respectively.

### Area 5

110. Based on the FAA design procedures for rigid pavements, the required total thickness of the PCC for Test Area 5 is 13 in. and 12 in. for the B-747 and DC-10, respectively. Because the existing pavement slabs are distress-free, the bonded or monolithic PCC overlay is recommended. In this case, the required thickness of the PCC is  $13 - 10.5 = 2.5$  in. and  $12 - 10.5 = 1.5$  in. for the B-747 and D-10-30, respectively. The joints in the overlay must be matched to the joints in the existing pavement by both location and type.

111. Measurements of deflection bowls near joints were performed in Test Areas 1 and 5. The tests included:

- a. Measurement of deflection bowls on the same side of the joint where the load was applied.

b. Measurement of the deflection bowls on two sides of the joint.

The results are analyzed using the Westergaard theory, as summarized below. The load transfer efficiency of a joint is defined as

$$Z_j - Z'j = (1 - j)(Z_e - Z'e) \quad (A32)$$

where

$Z_j$  = deflection of loaded slab at joint with  $j$ -efficiency

$Z'j$  = deflection of adjacent slab

$j$  = joint efficiency

$Z_e$  = deflection of loaded slab at joint with zero efficiency (free edge)

$Z'e$  = deflection of adjacent slab with zero efficiency at joint

When the load is applied on only one side of the joint,  $Z'e = 0$ . Therefore

$$j = 1 - \left( \frac{Z_j - Z'j}{Z_e} \right) \quad (A33)$$

The free edge deflection  $Z_e$  can be either measured wherever a free edge condition exists or computed using the approximate Westergaard formulas as follows.

$$Z_e = \frac{P \sqrt{2 + 1.2\mu}}{\sqrt{Eh^3k}} \left[ 1 - (0.76 + 0.4\mu) \frac{\bar{Y}}{i} \right] \quad (A34)$$

where

$P$  = load

$\mu$  = Poisson's ratio of concrete

$E$  = modulus of elasticity of concrete

$h$  = slab thickness

$k$  = subgrade modulus of reaction

$\bar{Y}$  = distance of center of gravity of load edge

$$i = Eh^3 / [12(1 - \mu^2)k]$$

112. According to Westergaard, the deflections at the edge of a joint with efficiency  $j$  can also be computed using these equations:

$$Z_j = \left(1 - \frac{1}{2}j\right) Z_e + \frac{1}{2} j Z'e \quad (A35)$$

$$Z'J = \frac{1}{2} j Ze + \left(1 - \frac{1}{2} j\right) Z'e \quad (A36)$$

In the case of the load being applied on one side of the joint  $Z'e = 0$ , the joint efficiency can be computed using either the first or second equation.

$$j = 2 \frac{(Ze - Zj)}{Ze} \quad (A37)$$

$$j = 2 \frac{Z'j}{Ze} \quad (A38)$$

Dividing the equation for  $Zj$  by the equation for  $Z'j$  gives

$$j = \frac{2 Z'j}{Zj + Z'j} \quad (A39)$$

113. Two cases are dealt with for evaluating joint efficiency:

- a. The deflection bowl is measured on one side of the joint where the load is applied. Equation A37 is used to compute the joint efficiency. The free edge deflection  $Ze$  is computed using Equation A34 and material properties ( $h, k$ ) derived from pavement evaluation (Hertz theory) of the center load of the same slab. The deflection at the joint  $Zj$  is found from extrapolation of the measured deflections.
- b. The deflection bowl is measured on both sides of the joint. The joint efficiency can be computed using:
  - (1) Equation A33 which comes from the definition of joint efficiency (Equation A1). (In this case, the free edge deflection  $Ze$  is computed using Equation A3 and material properties ( $h, k$ ) derived from pavement evaluation (Hertz theory) of the center load of the same slab.)
  - (2) Equation A32 which comes from the approximate Equations A35 and A36 (In this case,  $Ze$  is not needed). The deflections  $Zj$  and  $Z'j$  at the edge are found from extrapolation of the measured deflection. The main conclusion of the joint transfer analysis, both in Test Areas 1 and 5, is that the load-transfer efficiency of the joints may be taken as 0.5.

114. The following conclusions were made by Berger:

- a. The pavement profiler, the 16-kip vibrator, and the WES FWD all have satisfactory instrumentation for measuring both applied force and resulting deflections. This was indicated by the almost identical deflection bowls for the 10.5-in. concrete pavement of Test Area 5 when normalized with respect to applied load.

- b. The coefficient of variation of the normalized deflections is approximately 10 percent for each of the three NDT devices.
- c. The shapes of the deflection bowls produced by the three NDT devices are sufficiently close to those predicted by the Hogg model, so that the model can be used in pavement evaluation.
- d. Generally, good agreement was obtained between the moduli of the pavement layers as computed by the various methods outlined. The Hogg model can be used for determining the subgrade modulus  $E_3$  and of the concrete  $E_1$  for rigid pavements. For flexible pavements,  $E_1$ ,  $E_2$ , and  $E_3$  can be determined using the method of equivalent thicknesses. If  $E_1$  is known,  $E_2$  may be determined using the center deflection and the Burmister two-layer model, when combined with the determination of  $E_3$  using the Hogg model. Reasonable results were obtained using these methods for analyzing deflection bowls produced by all three NDT devices.
- e. The three NDT devices gave similar layer moduli for PCC, AC, and the subgrade. The moduli for the base course determined from the deflection bowls produced by the FWD were significantly lower than those obtained from analyzing the deflection bowls produced by either the pavement profiler or the 16-kip vibrator.
- f. All of the layer moduli values for the five test areas obtained with the three NDT devices are reasonable.

ARE, Inc. (1983)

115. The data gathered for this project included physical property data or construction history data on the five pavement sections, traffic data as furnished by the sponsor, and NDT data acquired on location at MacDill AFB.

116. The only actual tests made on location at MacDill AFB were the NDT deflection tests. These tests were performed using a Dynaflect which is a rapid mobile NDT machine available since the early 1960's. The data include deflection readings for each of the five sensors which are part of the standard Dynaflect apparatus, sensor 1 being midway between the load test wheels and the other four sensors being spaced 1 ft apart on a radius from the center between the two load wheels. The test points were located for each of the five test areas using a grid pattern on the apron areas, and on the taxiways test points were located on each side of the center line on flexible pavements. On the rigid pavements, tests were performed at transverse joints and in the center of the same slab on which the test was done at the joint.

117. The numerical computation of elastic properties for each of the

five pavement cross sections includes the stress-strain analysis and the prediction of critical aircraft.

118. Normally, the first step in the analysis is a visual and graphical evaluation of the NDT deflection data, a process used to delineate different areas of pavement response to load. However, because these pavement areas were designated and are only approximately 1,000 ft in length, the technique of dividing pavement into various response sections was bypassed. For each of the areas, various statistical parameters were computed for further use in the analysis. The mean standard deviation and coefficient of variation were computed for each of the data groupings. The mean values of the deflections at all five sensors are the most important data elements that are used in the development of the materials properties for each of the five cross sections.

119. The next step in the analysis was to analytically characterize the elastic materials properties for each of the major layers in each of the five pavement cross sections. This is accomplished using a computer program called BASFIT. BASFIT is a deflection basin fitting program that predicts deflection values under a known load and loading conditions using the cross-section geometry furnished by the sponsor, which included known layer thicknesses together with construction history and word description of the materials. Approximate values of Poission's ratio were assigned along with approximate values of elastic moduli as the initial input to the program BASFIT. The program predicts the deflection basin response. Moduli are adjusted until the predicted basin sufficiently accurately simulates the measured basin using whatever field testing device is specified. In the case of this application the Dynaflect loading was used. This process is an iterative one and is generalized; i.e., it is not unique to any particular type of NDT load but could be used with any one that can be adequately described in terms of load and geometry.

120. Normally, the ARE design procedure takes into account the relative load magnitude of the NDT apparatus and the larger magnitude of actual aircraft load. As for clay or fine-grained soils, it is believed and has been shown from extensive laboratory work that as the loads increase, the elastic moduli decrease. However, the subgrade materials that prevail on all five sections at MacDill AFB are classified as sands, thus indicating that there would be no stress sensitivity characteristics associated with the subgrade soils. For this reason, further adjustments to the elastic

properties determined in the deflection basin fitting through the use of a BASFIT program need not be made.

121. Pavement evaluation computations were next accomplished using a series of computer programs referred to as ELSYM-5 and AIRPOD. ELSYM-5 is a five-layer elastic-layered analysis program publicly available, and AIRPOD is a first-generation airport pavement overlay design procedure in the form of a computer program developed in the late 1970's by ARE for use on civil airport evaluation and runway design projects. This program likewise is based on elastic-layered theory and uses fatigue criteria for the assessment of pavement damage and the remaining life under specified traffic circumstances. ELSYM-5 and AIRPOD have been used on many past projects. A brief description of the pavement life analysis built into the AIRPOD program follows.

122. The present amount of life remaining in the pavement and the projected future life are determined with the computer program AIRPOD. The program determines the allowable number of aircraft operations for the pavement using the following fatigue equations.

$$N = a \left( \frac{f}{\sigma} \right)^b \quad (A40)$$

or

$$N = c \left( \frac{1}{\epsilon} \right)^d \quad (A41)$$

where

N = number of aircraft loads until failure (fatigue life)

f = concrete flexural strength, psi

$\sigma$  = computed stress due to aircraft load on rigid pavement, psi

$\epsilon$  = computed strain due to aircraft load on flexible pavement, psi

a, b, c, d = constants

123. The program AIRPOD computes the stress and strain in the pavement using an elastic-layered theory subroutine. This computation requires the aircraft load and materials property inputs previously discussed. The number of aircraft passes until failure is determined for each individual aircraft.

124. The percentage of life remaining in the pavement is computed using an equation of the following form.

$$L_R = 100 - \left( \sum \frac{n}{N} \right) \cdot 100 \quad (A42)$$

where

$L_R$  = fatigue life remaining in the pavement

n = aircraft operations to date for an individual aircraft

N = allowable number of aircraft loads until failure of an individual aircraft

125. The program computes the amount of damage contributed by each aircraft  $n/N$  and then sums these damage ratios to determine the total damage from which the remaining life is calculated. The remaining life can be determined for any point in time by inputting the appropriate number of aircraft operations for each aircraft n up to that point in time. By computing the remaining life at various points in time, the estimated end of the pavement's useful fatigue life can be determined by projecting the relationship of remaining life to time.

126. To accomplish the pavement life analysis for those pavements with PCC layers, a concrete flexural strength was estimated. Based on engineering judgment and some of the generalized relationships available, it was determined that the concrete flexural strength for Test Area 1 on Taxiway 33 was 650 psi, Test Area 4 on Apron 1-A-1 was 700 psi, and Test Area 5 on Apron 1-A was 600 psi.

127. Using the stress and strain information previously computed and documented, the allowable number of aircraft loads was computed for each of the pavement areas. These allowable traffic levels together with the four pass intensity levels of traffic for each of the five pavement sections allowed the computation of the remaining life in each of the five pavements at each of the four pass intensity levels of aircraft traffic; allowable loads for the 13 aircrafts groups were then computed for each of the four pass intensity levels.

128. The computer program AIRPOD designs overlay thicknesses for either AC or PCC pavements using the same concepts as for the pavement life analysis. The materials inputs are the same as those determined for the remaining life analysis, except that properties of the proposed overlay material must be added as imputs. The traffic imput must include the projected number of future loads of each aircraft type. The program considers the amount of life remaining in the existing pavement when computing the overlay thickness.

129. The Air Force system uses an impulse load applied to the pavement surface. Analysis of collected time-domain accelerometer data by discrete Fourier transform techniques provides the phase angle/frequency information needed for pavement evaluation. Knowing the frequency  $f$  and phase angle  $\theta$  a velocity versus wave length dispersion curve can be developed from the relationships.

$$T = \frac{360d}{\theta} \quad (A43)$$

and

$$v = f\lambda \quad (A44)$$

where

$d$  = accelerometer spacing

$\theta$  = phase angle

$v$  = phase velocity

$f$  = frequency

$\lambda$  = wavelength

130. Interpretation of the dispersion curves must be made by the operator to determine velocity values to be used for each layer in the pavement. These velocity values are used with known or assumed material densities  $\gamma$  and Poisson's ratio  $\nu$  to determine the elastic moduli of the material layers. The shear modulus  $G$  is calculated from

$$G = v_s^2 \left( \frac{\gamma}{g} \right) \quad (A45)$$

where

$G$  = shear modulus

$v_s$  = shear wave velocity

$v_s = (V_r/a)$

$V_r$  = Rayleigh wave velocity

$a$  = varies from 0.875 for Poisson's ratio of 0.0 to 0.955 for Poisson's ratio of 0.5

$\gamma$  = unit weight of materials

$g$  = acceleration constant

$E$  = Young's modulus is computed from:  $E = 2(1 + \nu)G$

$\nu$  = Poisson's ratio (assumed)

Corrections are required in the shear wave velocity of subsurface layers to account for variations in the pavement surface. The following general relationship is used for any layer.

$$v_s = \sqrt{\frac{Gg}{\gamma}} \quad (A46)$$

131. Specifically, for layer 2 (base course), the shear wave velocity from the dispersion curve is

$$v'_{s_2} = \sqrt{\frac{G_2 g}{\gamma_2}} \quad (A47)$$

However, to correct for the velocity increase as the wave is propagated into the surface the following expression is used.

$$v_{s_2} = \sqrt{\frac{\gamma_1}{G_1}} \cdot \frac{G_2'}{\gamma_2} v'_{s_2} \quad (A48)$$

where

$v_{s_2}$  = actual shear wave velocity in the base course

$G_1$  = shear modulus for the surface layer

$G_2'$  = shear modulus for the base course using  $v'_{s_2}$

$v'_{s_2}$  = shear wave in the base course from the uncorrected dispersion curve

132. The procedure used is to first calculate shear modulus  $G$  for the surface layer and then to calculate  $G$  for subsurface layers using the uncorrected shear wave velocity. After shear wave velocities are corrected, then they are used to calculate shear modulus  $G$  and Young's modulus  $E$  values for each layer. These values are then used in the computer analysis.

133. The primary component of the Air Force nondestructive pavement evaluation system is the field equipment that collects data pertinent to the strength of the materials composing the pavement system. The field equipment

used by the Air Force is contained in a 1978 Ford parcel delivery van with a custom-engineered cargo area to meet air-transportability requirements, so important to the Air Force for rapid deployment capability. The total vehicle weight for field deployment is approximately 11,000 lb. The vehicle is equipped with an aircraft radio for direct communication with the airfield tower and safety beacons which make it highly visible from the air and ground while operating on the airfield.

134. Contained in the rear of the vehicle is a hydraulically operated impact hammer which provides the impulse energy required to obtain pavement response information through a series of pavement-mounted accelerometers. Operation of the system is by a programmable controller with manual override capability. Hammer weights can be varied from 100 to 500 lb by manual addition of weight to the hammer. The drop height can be varied from 0 to 36 in. The assembly is equipped with grippers that lift the hammer, release it, and then catch the hammer after the first impact to prevent the hammer from striking the pavement more than once.

135. Various types of impact plates are employed to enhance the signal frequency content. Typically, an aluminum plate is used. The impact plate is equipped with a switch which provides information for hydraulic control of the grippers and for triggering the data recording equipment.

136. Up to eight accelerometers are mounted to the pavement on 1/4-in.-diam steel studs 1/4 in. long. A quick-setting epoxy cement is used to attach the mounting studs to the pavement. The accelerometers are then screwed into the studs. Spacing between the accelerometers varies as to pavement type and thickness and requires some operating experience. The mounting operation can be completed in less than 20 min.

137. Each accelerometer is hooked up to a power supply and data acquisition equipment. The data acquisition equipment located in the front portion of the cargo area of the vehicle consists of an HP-9845B desktop computer with CRT display, hard copy printer, and 500-kilobyte memory. Data collected through an HP-6942 multiprogrammer is transferred to the computer for analysis and stored on an HP-9895 floppy disk.

138. In-line filters can be put into the data acquisition system and are designed as gate-type low-pass filters to remove unwanted signals. Filters available to the operator are, 1,000, 2,000, and 5,000 Hz.

139. The computer is primarily used to compute Fast Fourier Transform

(FFT) for phase angle versus frequency and wave velocity versus wavelength (dispersion) plots immediately after the data are obtained. The operator must then decide whether or not the data are acceptable for storage on flexible disks. If they are not, then additional data are collected and analyzed as a separate event or are averaged with previously collected data. When sufficient data are collected for interpretation of the dispersion curve (based on operator experience), the data are stored on a flexible disk and a hard copy made.

140. It is from this hard copy that the operator selects the velocity values that will ultimately be used in the computer analysis for the load-carrying capability of the pavement. The computer analysis on a main-frame computer uses the Air Force-developed PREDICT code.

141. The PREDICT computer code is the second component of the Air Force nondestructive pavement evaluation system. The code uses the field data from the Nondestructive Pavement Testing (NDPT) van, the elastic moduli determined from the field velocity values, to calculate the stresses and strains produced in the pavement as a result of an aircraft wheel load. Stresses and strains are critical locations in the pavement and are compared with fatigue algorithms for the materials to predict the number of cycles to failure for the particular aircraft.

142. The input data required by the PREDICT code are:

- a. Type of aircraft for analysis
- b. Channelized or nonchannelized traffic analysis
- c. Number of material layers composing the pavement
- d. Aircraft wheel load and tire pressure
- e. Concrete split tensile strength
- f. For each material layer:
  - (1) Thickness
  - (2) Elastic modulus
  - (3) Poisson's ratio
  - (4) Soil type
  - (5) Void ratio
  - (6) Degree of saturation
  - (7) Plasticity index

143. The aircraft must be specified and selected from the aircraft available in the computer code aircraft library. The aircraft presently in

the library are the A-10, F-4, F-15, F-16, F-105, F-111, FB-111A, T-38, T-43, B-1, B-52, B-747, C-5, C-9A, C-130, C-141, KC-97, and KC-135.

144. The selection of a channelized or nonchannelized traffic analysis will depend on the location of the pavement on the airfield. Different values of a pass-to-coverage ratio are used for the channelized versus nonchannelized sections.

145. The number of layers composing the pavement must be determined from the as-built drawings or previously obtained destructive testing reports. However, some instances will occur when the NDT data from the dispersion curves may indicate a different number of material layers than the reports. An example of this may be a concrete pavement over a subgrade soil. Destructive tests indicate a two-layer system, but NDT may indicate a third layer that would be a compacted subgrade layer just beneath the concrete surface layer.

146. Concrete split tensile data are obtained from destructive test results. This material property is used in the evaluation process to determine the modulus of rupture of the concrete. The equation is given as

$$MR = 1.02T + 210.5 \quad (\text{A49})$$

where

MR = modulus of rupture, psi

T = split tensile strength, psi

Calculated tensile stresses at the bottom of the concrete are converted to a percentage of the modulus of rupture and compared to a fatigue algorithm to predict the number of cycles.

147. Material layer thickness, soil type, void ratio, degree of saturation, and plasticity index can be obtained with some minor calculations from the destructive testing reports. Poisson's ratio must be selected as a representative value for the specific material.

148. The elastic modulus for each material layer, as stated earlier, is calculated from the dispersion curves developed in the NDT van.

149. The output of the PREDICT code has been minimized to provide an analysis summary for each pavement section input. The output specifies the number of operations for the concrete or AC surface course and the subgrade material. The number of operations were calculated from the predicted tensile

stress or strain in the surface layer and the subgrade compressive strain.

150. To prepare an allowable gross load table in the format shown in Headquarters, Department of the Air Force (1981), a minimum of three runs of the PREDICT code must be made for each airfield feature and each aircraft evaluated, varying the weights of that aircraft. These varying weights are then plotted versus their respective number of allowable operations, as determined by the code. The curve formed by these points is then used to select permissible aircraft weights at the operation or pass intensity levels corresponding with levels I through IV, as specified in Headquarters, Department of the Air Force (1981).

WES DSM Method (Hall and Alexander 1983)

151. The evaluation method for the DSM procedure is based on correlations between the nondestructive DSM measurements and the computed ASWL as determined on a number of inservice airfield pavements representing a range of pavement types and conditions. DSM is a ratio of dynamic load over deflection obtained with the WES 16-kip vibrator (Hall 1978). The ASWL's were computed from existing Corps of Engineers pavement design procedures, using in place pavement strength measurements determined through test pits and direct sampling procedures.

152. The WES 16-kip vibrator is an electrohydraulic steady-state vibratory loading system. The unit is contained in a 36-ft semitrailer along with supporting power supplies and automatic data recording equipment. A 16,000-lb preload is applied to the pavement with a superimposed dynamic load ranging up to 30,000 lb peak-to-peak. The dynamic load can be applied over a frequency range of 5 to 100 Hz, but the standard test frequency is 15 Hz. The dynamic load is measured with a set of three load cells mounted on an 18-in. diam load plate. Velocity transducers which are located on the load plate and at points away from the plate are calibrated to measure elastic deflection. Test results are recorded on X-Y plotters and a digital printer.

153. Data collected with the WES 16-kip vibrator are the DSM and deflection basins. DSM is obtained from the slope (load/deflection) of the dynamic load versus deflection data obtained by sweeping the force to maximum at a constant frequency of 15 Hz. This slope is taken at the higher force levels. Deflection basins are obtained by measuring deflections at distances of

18, 36, and 60 in. away from the center of the load plate. The deflection ratio  $\Delta_{60}/\Delta_{18}$  is used to determine the radius of relative stiffness & for rigid pavements.

154. The conventional theory used to evaluate military airfield flexible pavements is based on a determination of strength parameters, such as the CBR, moisture, density, classification of materials, and other values, using criteria developed from performance studies. To use the proven performance of the conventional methodology, the nondestructive quantity of the DSM was directly correlated (Green and Hall 1975) to the ASWL, as determined from the standard evaluation procedure based on test-pit measurements. The measured DSM for flexible pavements is corrected to a common pavement temperature of 70° F, because deflection measurements on AC are sensitive to temperature. A method adopted from the Asphalt Institute (1969) is used to determine the median temperature of the AC layer. This procedure uses the pavement surface temperature at the time of the test plus the previous 5-day air temperatures. This median pavement temperature is then used with relationships developed by WES to correct the measured DSM to 70° F. The temperature-corrected DSM values are used to determine the ASWL using the correlations developed. The ASWL is then converted to AGAL on any desired aircraft at any level of operations (passes) using existing analytical relationships found in the CBR procedure (Headquarters, Departments of the Navy, Army, and Air Force 1978). Overlay thickness requirements for aircraft loads greater than the existing capacity of the pavement can be determined from similar analysis. Once the allowable load is determined, an effective subgrade CBR can be computed. This CBR along with the existing pavement thickness (thickness from existing records or core borings) can be used with CBR procedure to compute AC overlay thickness. PCC overlays for use over flexible pavements cannot be determined with this evaluation.

155. The methodology for NDT evaluation of rigid pavements using the DSM method uses a correlation between the DSM measured at the slab center to the ASWL as determined from standard evaluation procedure based on test-pit measurements. This standard procedure for rigid pavements is based on the Westergaard analysis using material properties such as thickness, subgrade modulus, and flexural strength (Headquarters, Departments of the Army and Air Force 1979).

156. To determine the allowable loading for aircraft having gears with

different geometries, relationships between the loads of these aircraft and the ASWL are used. These relationships are based upon the equivalency of maximum bending stress in the concrete slab. The radius of relative stiffness  $\lambda$  is used to interrelate the ASWL to the wheel loads of different geometries through a ratio of the AGAL to the ASWL.

157. The radius of relative stiffness  $\lambda$  of a rigid pavement is obtained through deflection basin measurements. A correlation between  $\lambda$  determined from nondestructive deflection basin data and  $\lambda$  determined by the Westergaard theory gives the relationship between a ratio of deflections measured at points 18 and 60 in. from the center of the load plate as a function of  $\lambda$ .

158. The effects of stress repetition levels (aircraft passes) on the AGAL are considered by the use of traffic factors. The traffic factors are a function of the aircraft gear geometry, the lateral distribution of aircraft traffic on the pavement being evaluated, and the traffic volume and are independent of the pavement structure. The AGAL for a specified number of aircraft passes is computed from the equation (Hall 1978)

$$P_G = 0.0189(DSM)(F_L)(T_c) \quad (A50)$$

where

$F_L$  = load factor

$T_c$  = traffic factor

159. Overlays of PCC or AC to strengthen existing PCC pavements are determined from overlay equations from the Corps of Engineers conventional procedure (Headquarters, Departments of the Army and Air Force 1979). These overlay equations consider the condition of the existing slabs, the anticipated degree of cracking to occur in the existing slab, and the structural requirements.

160. The procedure for evaluation of composite pavements is to convert AC overlay and PCC slab to an equivalent thickness of PCC and use the procedure for plain rigid pavement substituting the following equation for the AGAL:  $P_G = 0.0172(DSM)(F_L)(T_c)$ . The radius of relative stiffness  $\lambda$  for a composite pavement cannot be determined from reflection basin measurements. The subgrade modulus  $k$  can be estimated from the subgrade soil classification, and  $\lambda$  can be computed from the Westergaard analysis.

161. Overlays for composite pavements are determined in a manner similar to that for rigid pavements except an equivalent slab concept is used for the composite section.

WES Layered-Elastic Method (Holl and Alexander 1983)

162. The layered-elastic methodology was developed under FAA-sponsored research (Bush 1980b) and was initially developed for light aircraft pavements. It has also been found applicable to heavy aircraft pavements (Alexander 1982). The general approach is to use a linear layered-elastic model with measured deflection basins to predict *in situ* modulus values for a one- to four-layer pavement system. Different NDT loadings are used to describe the nonlinear, stress-dependent modulus of the subgrade. Allowable aircraft loads and overlay thicknesses are determined using limited tensile strain at the bottom of the asphalt layer and vertical compressive strain at the top of the subgrade for flexible pavements. For rigid pavements, a limiting tensile stress at the bottom of the PCC layer is used.

163. The layered-elastic procedure was demonstrated with data from both the WES 16-kip vibrator (previously described) and a FWD. The FWD used by WES is a Dynatest Model 8000 (15 kip). A dynamic force is applied to the pavement surface by dropping a 440-lb weight onto a set of rubber cushions, resulting in an impulse loading. The applied force and pavement deflections are measured with load cells and velocity transducers. The drop height can be varied from 0 to 15.7 in. to produce an impact force from 0 to 15,000 lb. The load is transmitted to the pavement through an 11.8-in.-diam plate. The signal-conditioning equipment displays the resulting pressure in kilopascals and the maximum peak displacement in micrometres. As many as three displacement sensors may be recorded at one time by this data acquisition equipment.

164. FWD data collected were deflection basin measurements. Displacements were measured on the load plate and at distances of 12, 24, 36, and 48 in. away from the center of the load plate. Since this particular model has only two transducers for deflection basin measurement, the four deflection points were obtained by dropping the weight twice at each location and shifting the transducers to the additional spacings.

165. The computer program BISDEF was developed at WES to determine modulus values for pavement layers. BISDEF uses the Shell BISAR (Headquarters,

Department of the Army and Air Force 1979) multilayered linear elastic program. In this procedure, the thicknesses of the layers are determined from historical data or from cores. Poisson's ratios are assumed and a rigid boundary is placed at a depth of 20 ft. Initial modulus values are assumed for each layer as well as an upper and lower limit for the modulus. The layered-elastic program is used to calculate a deflection basin produced by the loading of the NDT device. The calculated basin is compared to the measured basin. If the basins do not agree, the modulus values are changed through an iterative procedure until a set of modulus values is determined, producing a basin from the layered-elastic theory that matches the basin measured with the NDT device. A match is considered adequate when the sum of the absolute values of the differences in the measured and calculated deflections is less than 10 percent. Hence, the average difference for each deflection is less than plus or minus 2.5 percent. For this study, a modulus value of 250,000 psi was assigned to the asphalt layers to account for seasonally higher temperatures than were encountered during the test period.

166. Allowable load-carrying capacities and required overlay thicknesses were evaluated using the WES-developed computer program AIRPAV. For a particular aircraft (gear configuration, load, pass intensity level, etc.), AIRPAV uses the modulus values determined from BISDEF and the BISAR program to compute stresses (for rigid pavement) and strains (for flexible pavement) that will occur in the pavement system. AIRPAV then calculates the limiting stress or strain values based on present Corps of Engineers design and evaluation criteria. The allowable load for the aircraft is determined by comparing the predicted stress or strain to the limiting value.

167. The evaluation of rigid pavements is based on the tensile stress at the bottom of the slab which is determined as follows.

$$\sigma_{All} = \frac{R}{A + B (\log_{10} COV)} \quad (A51)$$

where

R = PCC flexural strength

A = 0.58901

B = 0.35486

COV = aircraft coverages

The horizontal tensile strain at the bottom of the AC and the vertical

subgrade strain are both considered in the evaluation of flexible pavements. The allowable AC strain criteria used is as follows (Heukelom and Klomp 1962):

$$\epsilon_{All(AC)} = 10^{-A} \quad (A52)$$

where

$$A = \frac{N + 2.665 \left( \log_{10} \frac{E_{AC}}{14.22} \right) + 0.392}{5.0}$$

$N = \log_{10}$  (aircraft coverages)

$E_{AC}$  = AC modulus

The allowable subgrade strains are computed using the following.

$$N = 10,000 \left( \frac{A}{\epsilon_{All\_subg}} \right)^B \quad (A53)$$

where

$N$  = repetitions

$A = 0.000247 + 0.000245 \log E_{subgrade}$

$B = 0.0658 (E_{subgrade})^{0.559}$

168. For overlay computations, the required pavement thicknesses are computed by increasing the thickness of the upper layer until the stress or strain criteria are satisfied. AIRPAV accepts as input an initial thickness and uses an iterative procedure to close in on the actual thickness needed to support the aircraft under consideration. AC overlays on AC pavements are simply the difference between the required thickness and the existing AC thickness. Overlays were computed for the PCC pavements using the following.

$$AC \text{ overlay} = 2.5 (Fh_d - C_b h) \quad (A54)$$

$$PCC \text{ (partially bonded)} = \sqrt{h_d^2 - C_r h^2} \quad (A55)$$

$$PCC \text{ unbonded} = 1.4 \sqrt{h_d^{1.4} - C_r h^{1.4}} \quad (A56)$$

where

$F$  = factor projecting the cracking that may be expected in existing PCC pavements

$h_d$  = required thickness of PCC, in.

$C_p$  = condition factor of existing pavement, ranges between 0.75 and 1.00

$h$  = thickness of existing PCC pavement, in.

$C_r$  = condition factor of existing pavement, ranges between 0.35 and 1.00

#### WES Evaluation of Load Transfer

169. The ability of joints in PCC slabs to transfer load is measured with the NDT device. The ratio of deflections measured on each side of the joint (deflection of unloaded slab/deflection of loaded slab) is related to joint efficiency or load transfer. The allowable loads determined at the slab centers can be reduced for poor joint transfer using load-reduction factors. These factors are a function of the deflection ratio.

170. This procedure was developed by first relating the deflection ratios to the percent edge stress. The maximum edge stress condition is a free edge with no load transfer. The edge stress is reduced as more load is transferred across the joint. The design use by the Air Force assumes 75-percent-maximum edge stress (25 percent is carried by adjacent slab). Computations were made with both the ILLISLAB program (Tabatabie and Barenberg 1979) and the WESLIQUID (Chou 1981) (both are finite element programs) for a range of pavement thicknesses and subgrade moduli  $k$ . By computing the allowable percent of design load at different deflection ratios, a relationship was developed between the deflection ratio and load-reduction factors. The procedure provided for reducing the allowable load determined at the slab center to account for the load-transfer capabilities at the joint. The load-reduction factor falls between 0.75 and 1.00.

**APPENDIX B: TEST DATA**

This appendix contains test data collected on the five test area pavements at MacDill AFB during the period 27 October-3 November 1982. The data presented herein were furnished by the following participants using the NDT equipment indicated:

Participant	NDT Equipment
Pavement Consultancy Services, Inc	PCS Falling Weight Deflectometer (FWD)
ARE, Inc.	ARE Dynaflect
Dynatest Consulting, Inc.	Dynatest Model 8000 FWD
ERES	Dynatest Model 8000 FWD
Louis Berger International, Inc	Berger Model 2000 Pavement Profiler
Reinard W. Brandley	Dynatest Model 8000 FWD Brandley Cantilever Beam
Waterways Experiment Station	WES 16-kip Vibrator WES 15-kip FWD (Dynatest)

TEST DATA FROM PAVEMENT CONSULTANCY  
SERVICES, INC.

Data Collected with PCS Falling  
Weight Deflectometer

TABLE 4

MACDILL AIR FORCE BASE TAMPA FLORIDA  
Taxiway 33 Deflection measurements (27-10-82)

POSITION-IDENTIFICATION sect-code	time hh:mm	dist. km	DEFLECTIONS (um/10kN)			Delta 0 60	Delta 0 100	Delta 0 200	FORCE fwd. x10kN	Q-VALUES Q 40 100 200	(-)
			5.9	5.8=	3.7						
CENTRE LINE	1	11.41	0.0	5.9	5.8=	3.7	3.6	10.0	0.943	0.627	0.610
CENTRE LINE	2	11.44	0.023	6.3	6.2<	3.9	3.9	10.0	0.784	0.519	0.619
CENTRE LINE	3	11.45	0.046	5.7>	5.7	4.0	3.9	10.0	1.000	0.702	0.684
CENTRE LINE	4	11.47	0.069	5.5	5.5>	3.7	3.5>	10.0	1.000	0.673	0.636
CENTRE LINE	5	11.49	0.092	6.4<	5.7	3.7	3.6	10.0	0.891	0.578	0.563
CENTRE LINE	6	11.50	0.116	6.1=	5.7	3.6>	3.6	10.0	0.934	0.590	0.590
CENTRE LINE	7	11.52	0.139	6.1	4.6	4.0<	4.0	10.0	1.000	0.656	0.656
CENTRE LINE	8	11.53	0.161	6.3	5.4	3.5	3.3	10.0	0.857	0.556	0.524
CENTRE LINE	9	11.55	0.183	6.9	5.7	3.9	3.9	10.0	0.950	0.650	0.650
CENTRE LINE	10	11.56	0.206	6.0	5.7	3.8=	3.8	10.0	0.950	0.633	0.633
LEFT CL	11	12.02	0.0	6.1	5.8	3.9	3.8	10.0	0.951	0.639	0.623
LEFT CL	12	12.03	0.023	6.3	5.8	3.8	3.8	10.0	0.921	0.603	0.556
LEFT CL	13	12.05	0.046	6.2	6.0	3.8	3.8	10.0	0.968	0.613	0.613=
LEFT CL	14	12.06	0.069	5.6	5.5	3.7	3.6	10.0	0.982	0.661	0.643
LEFT CL	15	12.07	0.092	6.3	5.8	3.6	3.6	10.0	0.921	0.571	0.571
LEFT CL	16	12.09	0.115	6.3	6.3	4.1<	3.9	10.0	1.000	0.651	0.619
LEFT CL	17	12.11	0.137	7.0	6.6	4.4	4.4	10.0	0.943	0.629	0.629
LEFT CL	18	12.12	0.161	6.0	5.7	3.6	3.5	10.0	0.950	0.600	0.583
LEFT CL	19	12.13	0.183	6.2	5.8	3.7	3.7=	10.0	0.935	0.597	0.597
RIGHT CL	20	12.18	0.0	6.2	6.1	4.0	4.0	10.0	0.984	0.645	0.645
RIGHT CL	21	12.19	0.023	6.4	5.9	3.8	3.7	10.0	0.922	0.594	0.578
RIGHT CL	22	12.20	0.046	5.7	5.7	3.7	3.7	10.0	1.000	0.649	0.649
RIGHT CL	23	12.22	0.069	5.8	5.8	3.9	3.7	10.0	1.000	0.672	0.638
RIGHT CL	24	12.23	0.092	5.9	5.9	4.2	3.6	10.0	1.000	0.712	0.610
RIGHT CL	25	12.24	0.116	6.0	6.6	4.3	4.1	10.0	0.971	0.632	0.603
RIGHT CL	26	12.26	0.138	5.7	5.6	3.5	3.5	10.0	0.982	0.614	0.614
RIGHT CL	27	12.27	0.161	5.8	5.7	3.8	3.6	10.0	0.983	0.655	0.621
RIGHT CL	28	12.29	0.184	6.0	5.7	3.6	3.6	10.0	0.950	0.600	0.600

STATISTICS

85-PERCENTILE VALUES (<)  
MEAN VALUES (=)  
15-PERCENTILE VALUES (>)

\*END\*

TABLE 5  
MACDILL AIRFORCE BASE TAMPA FLORIDA  
Taxiway 3-B Deflection measurements (27-10-82)

POSITION-IDENTIFICATION sect-code	Time dist. hh:mm	DEFLECTIONS (um/10kN)			Delta 200	Delta 100	F O R C E fwd. x10kN	Q-VALUES (-)		
		Delta 60	Delta 60	Q 60				Q 100	Q 200	
CENTRE LINE	1	14.67	0.0	29.3	14.3	7.7	4.0	10.0	0.488	0.263
CENTRE LINE	2	14.09	0.051	28.8	16.1	8.5	4.1	10.0	0.559	0.295
CENTRE LINE	3	14.19	0.102	36.8	16.2	8.4	4.0	10.0	0.446	0.228
CENTRE LINE	4	14.12	0.153	27.3	14.6	8.1	3.7	10.0	0.535	0.297
CENTRE LINE	5	14.14	0.204	32.1	15.6	9.2	4.5	10.0	0.517	0.287
3.5M LEFT CL	6	14.21	0.6	34.3	19.0	9.8	4.5	10.0	0.554	0.286(0.131)
3.5M LEFT CL	7	14.23	0.026	33.3	16.9	9.8	4.3	10.0	0.568	0.264
3.5M LEFT CL	8	14.24	0.051	37.1	19.3	9.9	4.6	10.0	0.520	0.267
3.5M LEFT CL	9	14.26	0.077	38.8	18.3	9.4	4.5	10.0	0.472	0.242
3.5M LEFT CL	10	14.27	0.104	33.6	16.8	8.3	4.2	10.0	0.506	0.247
3.5M LEFT CL	11	14.29	0.129	31.4	16.1	7.9	4.1	10.0	0.513	0.252=0.131
3.5M LEFT CL	12	14.31	0.159	32.0	17.4	8.8	4.5	10.0	0.544	0.275
3.5M LEFT CL	13	14.32	0.185	36.1	16.9	8.5	4.4	10.0	0.561	0.282
3.5M LEFT CL	14	14.33	0.211	36.8	19.5	10.3	4.8	10.0	0.530	0.280
3.5M RIGHT CL	15	14.38	0.6	30.5	16.4	8.0	4.2	10.0	0.538	0.262
3.5M RIGHT CL	16	14.40	0.925	34.5	16.4	7.6	4.1	10.0	0.475	0.220
3.5M RIGHT CL	17	14.42	0.050	35.0	15.8	8.0	4.3	10.0	0.480	0.229
3.5M RIGHT CL	18	14.43	0.075	29.8	14.6	6.8	3.9	10.0	0.490	0.228
3.5M RIGHT CL	19	14.48	0.101	38.4	16.2	7.6	4.2	10.0	0.422	0.198
3.5M RIGHT CL	20	14.50	0.126	30.5	14.4	6.9	3.9	10.0	0.472	0.226
3.5M RIGHT CL	21	14.52	0.152	25.6	12.1	5.5	3.4	10.0	0.473	0.215
3.5M RIGHT CL	22	14.53	0.177	30.5	15.3	9.2	4.9	10.0	0.502	0.302
3.5M RIGHT CL	23	14.59	0.262	41.5	18.2	8.9	4.5	10.0	0.439	0.214

### STATISTICS

ES-PERCENTILE VALUES (( )) 37.1 18.3 9.5 4.5  
 MEAN VALUES ( = ) 33.0 16.5 8.4 4.2  
 15-PERCENTILE VALUES ( > ) 28.8 14.6 7.2 3.9

\*END\*

TABLE 11

**MACDILL AIR FORCE BASE TAMPA FLORIDA**  
**Taxiway 3 Deflection Measurements (27-49-82)**

POSITION-IDENTIFICATION sect-code	DEFLECTIONS (um/10kN)						FORCE Q-VALUES (-)			
	time hh:mm	dist. km	0	60	100	200	x10N	60	100	200
CENTRE LINE 1	15.16	0.0	46.9	24.5	11.3	4.8	10.0	0.522	0.241	0.102
CENTRE LINE 2	15.18	0.050	48.8	25.6	12.1	5.4	10.0	0.525	0.248	0.111
CENTRE LINE 3	15.19	0.101	42.9	24.3	12.2	5.0	10.0	0.579	0.290	0.119
CENTRE LINE 4	15.21	0.151	48.5	24.3	11.7	5.1	10.0	0.501	0.241	0.105
CENTRE LINE 5	15.23	0.202	48.9	22.2	11.0	5.3	10.0	0.454	0.225	0.108
CENTRE LINE 6	15.25	0.253	39.4	22.8	10.5	5.3	10.0	0.579	0.266	0.135
CENTRE LINE 7	15.27	0.303	51.8	22.4	11.1	5.1	10.0	0.432	0.214	0.098
3.5M LEFT CL 8	15.31	0.6	82.4	24.4	16.3	5.2	10.0	0.296	0.125	0.063
3.5M LEFT CL 9	15.34	0.625	94.4	25.3	10.0	5.3	10.0	0.248	0.106	0.056
3.5M LEFT CL 10	15.38	0.056	80.7	26.4	11.2	5.8	10.0	0.327	0.139	0.072
3.5M LEFT CL 11	15.40	0.975	81.7	29.6	11.7	5.3	10.0	0.355	0.143	0.065
3.5M LEFT CL 12	15.41	0.100	78.1	26.2	10.4	5.0	10.0	0.335	0.133	0.064
3.5M LEFT CL 13	15.43	0.126	86.4	22.4	10.4	5.0	10.0	0.259	0.120	0.058
3.5M LEFT CL 14	15.45	0.151	89.9	26.8	10.6	5.0	10.0	0.298	0.118	0.056
3.5M LEFT CL 15	15.47	0.176	81.8	24.0	10.5	5.6	10.0	0.293	0.128	0.068
3.5M LEFT CL 16	15.48	0.201	79.5	20.4	9.9	5.2	10.0	0.257	0.113	0.065
3.5M LEFT CL 17	15.50	0.226	76.8	22.8	9.5	5.3	10.0	0.297	0.124	0.069
3.5M LEFT CL 18	15.52	0.251	76.5	22.1	10.9	5.4	10.0	0.289	0.142	0.071
3.5M LEFT CL 19	15.54	0.276	79.7	29.9	8.6	5.1	10.0	0.283	0.122	0.072
3.5M LEFT CL 20	15.55	0.301	71.8	22.2	9.0	5.0	10.0	0.309	0.125	0.070
3.5M RIGHT CL 21	16.01	0.0	78.8	24.8	9.4	4.9	10.0	0.315	0.122	0.062
3.5M RIGHT CL 22	16.03	0.925	82.0	24.3	10.1	5.4	10.0	0.296	0.123	0.066
3.5M RIGHT CL 23	16.06	0.050	79.4	23.6	10.0	5.4	10.0	0.297	0.124	0.066
3.5M RIGHT CL 24	16.08	0.076	83.4	25.1	10.2	5.4	10.0	0.301	0.122	0.065
3.5M RIGHT CL 25	16.10	0.101	83.0	25.3	10.4	5.1	10.0	0.305	0.125	0.061
3.5M RIGHT CL 26	16.12	0.126	89.6	27.2	10.7	5.0	10.0	0.304	0.119	0.056
3.5M RIGHT CL 27	16.14	0.152	92.2	27.9	10.6	5.0	10.0	0.303	0.115	0.054
3.5M RIGHT CL 28	16.16	0.177	94.5	26.4	11.8	5.5	10.0	0.279	0.125	0.058
3.5M RIGHT CL 29	16.18	0.202	82.9	24.3	10.4	5.6	10.0	0.293	0.125	0.068
3.5M RIGHT CL 30	16.20	0.227	66.3	21.6	8.8	5.1	10.0	0.326	0.133	0.077
3.5M RIGHT CL 31	16.22	0.252	76.9	25.8	9.8	5.3	10.0	0.364	0.138	0.075
3.5M RIGHT CL 32	16.24	0.277	72.9	26.3	7.9	4.3	10.0	0.278	0.108	0.066
3.5M RIGHT CL 33	16.26	0.302	72.5	20.8	8.8	5.1	10.0	0.287	0.121	0.070

S T A T I S T I C S  
 85-PERCENTILE VALUES (>)  
 MEAN VALUES (=)  
 15-PERCENTILE VALUES (>)

#END\*

TABLE 17  
MACDILL AIRFORCE BASE TAMPA FLORIDA  
Apron 1-A-1 Deflection Measurements (27-10-62)

POSITION-IDENTIFICATION sect-code	time	dist. hh.mm km	DEFLECTIONS (um/10KN)			Delta 200	Delta 200	FORCE fwd. x10KN	Q-VALUES (-) Q Q Q
			Delta 0	Delta 60	Delta 120				
APRON 1-A-1	1	8.38	0.0	19.0	17.9	12.2	7.5	10.0	0.942 0.642(0.395
AFRON 1-A-1	2	8.40	0.025	19.3	18.7	11.5	5.8	10.0	0.969 0.596 0.301=
AFRON 1-A-1	3	8.43	0.050	22.8	21.8	14.0	7.6=	10.0	0.956 0.614 0.333
AFRON 1-A-1	4	8.45	0.075	42.8	40.3	24.3	12.3	10.0	0.942 0.568 0.287
AFRON 1-A-1	5	8.49	0.0	27.4	27.6	17.8	10.0	10.0	1.007 0.650 0.365
AFRON 1-A-1	6	8.51	0.025	26.6	27.9	17.1	9.4	10.0	1.049 0.643 0.353
AFRON 1-A-1	7	8.53	0.050	26.6	24.6	15.8	7.4	10.0	0.925 0.594 0.279
AFRON 1-A-1	8	8.54	0.075	36.2	35.9	20.4	12.9	10.0	0.992 0.564 0.356=
AFRON 1-A-1	9	8.60	0.0	31.5	30.5	17.9	10.9	10.0	0.968 0.568 0.346
AFRON 1-A-1	10	9.07	0.025	24.9	26.8	14.8	8.3	10.0	0.835 0.594 0.333
AFRON 1-A-1	11	9.69	0.050	29.4	24.2	16.8	7.9	10.0	0.823 0.571=0.238,
AFRON 1-A-1	12	9.10	0.075	32.8	30.4	22.1	12.4	10.0	0.927 0.674 0.378
AFRON 1-A-1	13	9.12	0.0	26.4	18.9	12.1	5.1	10.0	0.716 0.458 0.193
AFRON 1-A-1	14	9.14	0.025	21.9	15.9	11.1	5.5	10.0	0.757 0.529 0.262
APRON 1-A-1	15	9.15	0.050	19.9	16.3	12.3	5.4	10.0	0.819 0.618 0.271
AFRON 1-A-1	16	9.17	0.075	16.6	13.2	9.1	5.0	10.0	0.795 0.548 0.301
AFRON 1-A-1	17	9.19	0.0	22.2	18.3	11.8	4.9	10.0	0.824 0.532 0.221
AFRON 1-A-1	18	9.21	0.025	22.5	15.3	10.3	5.3	10.0	0.686 0.458 0.236
AFRON 1-A-1	19	9.23	0.050	29.7	18.0	12.4	5.3	10.0	0.878 0.599 0.256
AFRON 1-A-1	20	9.25	0.075	19.9	16.6	11.2	5.4	10.0	0.834 0.563 0.271

S T A T I S T I C S

85-PERCENTILE VALUES ( ) 32.2 30.3 19.1 10.5  
MEAN VALUES (+) 25.4 22.7 14.7 7.7  
15-PERCENTILE VALUES ( ) 18.6 15.0 16.4 4.8

\*END\*

TABLE 23

MACDILL AIRFORCE BASE TAMPA FLORIDA  
Apron 1-A Deflection measurements (27-10-82)

POSITION IDENTIFICATION sect-code	time dist. hh:mm	DEFLECTIONS (cm/100N)			FORCE Fwd. Right	Q-VALUES (-) Q Q
		Delta 0	Delta 60	Delta 200		
APRON 1-A	1	9.51	0.069	19.3	14.3	10.9
APRON 1-A	2	9.53	0.015	17.0	14.5	10.9
APRON 1-A	3	9.55	0.039	16.8	15.5	10.9
APRON 1-A	4	9.56	0.045	19.3	16.2	10.9
APRON 1-A	5	9.58	0.066	17.6	15.3	10.9
APRON 1-A	6	10.03	0.006	18.4	15.1	10.9
APRON 1-A	7	10.04	0.015	17.8	15.4	10.9
APRON 1-A	8	10.07	0.039	18.8	16.7	10.9
APRON 1-A	9	10.09	0.045	18.9	17.1	10.9
APRON 1-A	10	10.11	0.066	17.9	15.5	10.9
APRON 1-A	11	10.16	0.039	19.0	17.1	10.9
APRON 1-A	12	10.18	0.045	18.2	16.4	10.9
APRON 1-A	13	10.19	0.066	17.4	15.4	10.9
APRON 1-A	14	10.22	0.066	21.1	18.7	10.9
APRON 1-A	15	10.23	0.015	17.3	15.3	10.9
APRON 1-A	16	10.24	0.039	18.8	17.2	10.9
APRON 1-A	17	10.26	0.045	18.3	15.3	10.9
APRON 1-A	18	10.27	0.066	15.8	14.9	10.9
APRON 1-A	19	10.31	0.066	21.5	18.1	10.9
APRON 1-A	20	10.32	0.015	17.8	16.6	10.9
APRON 1-A	21	10.33	0.039	20.4	17.6	10.9
APRON 1-A	22	10.35	0.045	19.4	16.5	10.9
APRON 1-A	23	10.36	0.060	16.6	15.1	10.9
APRON 1-A	24	10.39	0.060	17.4	16.1	10.9
APRON 1-A	25	10.40	0.015	16.9	14.9	10.9
APRON 1-A	26	10.41	0.030	16.1	14.7	10.9
APRON 1-A	27	10.43	0.045	16.7	14.4	10.9
APRON 1-A	28	10.44	0.060	16.8	15.0	10.9

STATISTICS

85-FERCENTILE VALUES (0)  
MEAN VALUES (=)  
15-FERCENTILE VALUES (1)  
16.6 19.6 19.7 10.1 6.9

\*END\*

TEST DATA FROM ARE, INC.

Data Collected with ARE Dynaflect

MACDILL AIR FORCE BASE  
DYNAFLECT MEASUREMENTS

LOCATION : TAMPA, FL.  
PAVEMENT ID : TAXIWAY 33, AREA 1

PROJECT NO: AF-8  
CLIENT : U.S. AIR FORCE  
DATE : 10/82

RDG NO	STATION	D Y N A F L E C T   R E A D I N G S					TEMP.	TIME	I/E C/M
		#1	#2	#3	#4	#5			
1	0.00	.470	.420	.340	.310	.252	0.	1115	1 1
5	1.00	.330	.300	.237	.213	.186	0.		1 1
9	2.00	.330	.300	.240	.213	.180	0.		1 1
13	3.00	.340	.300	.258	.222	.198	0.	1135	1 1
17	4.00	.390	.360	.320	.267	.234	0.		1 1
21	5.00	.310	.270	.234	.204	.183	0.		1 1
25	6.00	.267	.240	.210	.174	.156	0.	1149	1 1
MEAN =		.348	.313	.263	.229	.198			
STD.DEV =		.065	.060	.048	.045	.033			
COEF.VAR=		18.676	19.064	18.424	19.704	16.800			
#OF PTS =		7							
2	.12	.147	.147	.138	.126	.126	0.		1 2
6	1.12	.162	.162	.153	.141	.135	0.		1 2
10	2.12	.150	.150	.141	.126	.126	0.		1 2
14	3.12	.162	.162	.159	.150	.141	0.		1 2
18	4.12	.189	.189	.186	.171	.165	0.		1 2
22	5.12	.159	.159	.150	.141	.132	0.		1 2
26	6.12	.138	.138	.129	.123	.114	0.		1 2
MEAN =		.158	.158	.151	.140	.134			
STD.DEV =		.016	.016	.018	.017	.016			
COEF.VAR=		10.257	10.257	12.243	12.201	11.954			
#OF PTS =		7							
3	.50	.390	.340	.300	.225	.207	0.		2 1
7	1.50	.330	.300	.231	.204	.180	0.	1127	2 1
11	2.50	.300	.255	.222	.186	.171	0.		2 1
15	3.50	.390	.360	.310	.240	.219	0.		2 1
19	4.50	.400	.370	.330	.261	.249	0.		2 1
23	5.50	.243	.213	.192	.159	.144	0.		2 1
27	6.50	.310	.264	.219	.189	.159	0.		2 1
MEAN =		.338	.300	.258	.209	.190			
STD.DEV =		.059	.059	.054	.035	.037			
COEF.VAR=		17.344	19.697	20.988	16.763	19.411			

MACDILL AIR FORCE BASE  
DYNAFLECT MEASUREMENTS

LOCATION : TAMPA, FL.

PAVEMENT ID : TAXIWAY 33, AREA 1

PROJECT NO: AF-8

CLIENT : U.S. AIR FORCE

DATE : 10/82

RDG NO	STATION	D Y N A F L E C T   R E A D I N G S					TEMP.	TIME	I/E C/M
		#1	#2	#3	#4	#5			
4	.62	.162	.156	.153	.144	.135	0.	2	2
8	1.62	.150	.150	.138	.132	.126	0.	2	2
12	2.62	.156	.156	.153	.141	.132	0.	2	2
16	3.62	.168	.168	.162	.153	.147	0.	2	2
20	4.62	.192	.192	.186	.177	.168	0.	2	2
24	5.62	.135	.135	.132	.117	.111	0.	2	2
28	6.62	.150	.150	.141	.132	.123	0.	2	2
MEAN =		.159	.158	.152	.142	.135			
STD.DEV =		.018	.018	.018	.019	.018			
COEF.VAR=		11.268	11.314	11.924	13.382	13.708			
#OF PTS =		7							

MACDILL AIR FORCE BASE  
DYNAFLECT MEASUREMENTS

LOCATION : TAMPA, FL.  
PAVEMENT : TAXIWAY 3B, AREA 2      PROJECT NO: AF-8  
    CLIENT : U.S. AIR FORCE  
    DATE : 10/82

RDG NO	STATION	D Y N A F L E C T   R E A D I N G S					TEMP.	TIME	I/E C/M
		#1	#2	#3	#4	#5			
1	0.00	.400	.350	.255	.231	.177	0.	259	3
3	1.00	.380	.320	.228	.186	.159	0.		3
5	2.00	.440	.360	.249	.198	.168	0.		3
7	3.00	.410	.350	.237	.189	.150	0.		3
9	4.00	.360	.310	.219	.177	.144	0.	313	3
11	5.00	.340	.264	.186	.156	.129	0.		3
13	6.00	.390	.340	.225	.198	.168	0.		3
15	7.00	.480	.400	.320	.234	.198	0.	321	3
MEAN =		.400	.337	.240	.196	.162			
STD.DEV =		.044	.040	.039	.026	.021			
COEF.VAR=		11.100	11.874	16.100	13.334	13.141			
#OF PTS =		8							
2	.50	.440	.390	.310	.231	.201	0.		4
4	1.50	.430	.380	.300	.231	.192	0.	306	4
6	2.50	.450	.400	.310	.222	.183	0.		4
8	3.50	.420	.360	.249	.186	.153	0.		4
10	4.50	.400	.350	.249	.195	.162	0.		4
12	5.50	.370	.330	.240	.189	.156	0.		4
14	6.50	.460	.410	.300	.237	.201	0.		4
MEAN =		.424	.374	.280	.213	.178			
STD.DEV =		.031	.029	.032	.022	.021			
COEF.VAR=		7.310	7.691	11.419	10.382	11.773			
#OF PTS =		7							
16	.84	.400	.350	.255	.207	.177	0.		5
MEAN =		.400	.350	.255	.207	.177			
STD.DEV =		0.000	0.000	0.000	0.000	0.000			
COEF.VAR=		0.000	0.000	0.000	0.000	0.000			
#OF PTS =		1							

MACDILL AIR FORCE BASE  
DYNAFLECT MEASUREMENTS

LOCATION : TAMPA, FL.  
PAVEMENT ID : TAXIWAY 3, AREA 3

PROJECT NO: AF-8  
CLIENT : U.S. AIR FORCE  
DATE : 10/82

RDG NO	STATION	D Y N A F L E C T   R E A D I N G S					TEMP.	TIME	I/E C/M
		#1	#2	#3	#4	#5			
1	0.00	.790	.570	.360	.237	.180	0.	401	3
3	1.00	.790	.590	.400	.300	.219	0.		3
5	2.00	.800	.570	.370	.243	.216	0.		3
7	3.00	.810	.590	.390	.264	.201	0.		3
9	4.00	.990	.670	.410	.270	.201	0.		3
11	5.00	.960	.630	.390	.267	.201	0.		3
13	6.00	.990	.670	.440	.258	.228	0.	417	3
15	7.00	.900	.600	.390	.246	.210	0.		3
17	8.00	.800	.600	.380	.258	.201	0.		3
19	9.00	.800	.600	.370	.20	.195	0.		3
21	10.00	.830	.600	.400	.300	.210	0.		3
MEAN		.860	.608	.391	.259	.206			
STD.DEV		.063	.035	.022	.026	.013			
COEF.VAR		9.687	5.687	5.657	10.115	6.304			
#OF PTS		11							
2	.50	.900	.590	.400	.243	.219	0.		4
22	.62	.900	.600	.380	.225	.189	0.		4
4	1.50	.990	.700	.460	.320	.240	0.		4
6	2.50	.960	.670	.430	.300	.225	0.		4
8	3.50	.790	.580	.380	.258	.198	0.		4
10	4.50	.580	.490	.370	.252	.228	0.		4
12	5.50	.900	.640	.420	.300	.219	0.		4
14	6.50	.900	.630	.410	.300	.222	0.		4
16	7.50	.810	.600	.380	.258	.207	0.		4
18	8.50	.770	.550	.350	.240	.183	0.		4
20	9.50	.810	.580	.370	.249	.195	0.		4
MEAN		.846	.603	.395	.268	.211			
STD.DEV		.113	.057	.032	.031	.018			
COEF.VAR		13.349	9.505	8.105	11.723	8.572			
#OF PTS		11							

MACDILL AIR FORCE BASE  
DYNAFLECT MEASUREMENTS

LOCATION : TAMPA, FL.  
PAVEMENT ID : APRON 1A1, AREA 4

PROJECT NO: AF-8  
CLIENT : U.S. AIR FORCE  
DATE : 10/82

RDG NO	STATION	D Y N A F L E C T   R E A D I N G S					TEMP.	TIME	I/E C/M
		#1	#2	#3	#4	#5			
26	.55	.450	.430	.390	.350	.310	0.		
	MEAN =	.450	.430	.390	.350	.310			
	STD.DEV =	0.000	0.000	0.000	0.000	0.000			
	COEF.VAR =	0.000	0.000	0.000	0.000	0.000			
	#OF PTS =	1							
1	0.00	.400	.380	.340	.290	.246	0.	1006	A
2	.50	.340	.330	.310	.258	.234	0.		A
3	1.00	.400	.380	.350	.310	.267	0.		A
4	1.50	.500	.490	.450	.390	.350	0.		A
5	2.00	.360	.350	.330	.267	.246	0.		A
	MEAN =	.400	.386	.356	.303	.269			
	STD.DEV =	.062	.062	.055	.053	.047			
	COEF.VAR =	15.411	16.033	15.334	17.392	17.509			
	#OF PTS =	5							
10	.50	.380	.370	.350	.300	.267	0.		B
9	1.00	.430	.420	.390	.370	.320	0.		B
8	1.50	.510	.500	.460	.400	.360	0.		B
7	2.00	.410	.390	.340	.300	.258	0.		B
6	2.50	.340	.340	.330	.261	.231	0.	1017	B
	MEAN =	.414	.404	.374	.326	.287			
	STD.DEV =	.063	.061	.053	.057	.052			
	COEF.VAR =	15.334	15.117	14.224	17.469	18.088			
	#OF PTS =	5							
11	0.00	.430	.410	.380	.310	.285	0.		C
12	.50	.440	.440	.430	.390	.370	0.		C
13	1.00	.580	.500	.400	.300	.261	0.		C
14	1.50	.490	.480	.450	.390	.340	0.		C
15	2.00	.820	.700	.580	.450	.360	0.		C
	MEAN =	.552	.506	.448	.368	.323			
	STD.DEV =	.161	.114	.079	.063	.048			
	COEF.VAR =	29.194	22.516	17.533	17.014	14.802			
	#OF PTS =	5							

MACDILL AIR FORCE BASE  
DYNAFLECT MEASUREMENTS

LOCATION : TAMPA, FL.  
PAVEMENT ID : APRON 1A1, AREA 4

PROJECT NO: AF-8  
CLIENT : U.S. AIR FORCE  
DATE : 10/82

RDG NO	STATION	D Y N A F L E C T   R E A D I N G S					TEMP.	TIME	I/E C/M
		#1	#2	#3	#4	#5			
20	.50	.400	.380	.350	.270	.258	0.		D
19	1.00	.460	.430	.390	.330	.300	0.		D
18	1.50	.410	.400	.370	.320	.270	0.		D
17	2.00	.490	.490	.440	.360	.300	0.		D
16	2.50	.400	.370	.360	.320	.267	0.		D
MEAN =		.432	.414	.382	.320	.279			
STD.DEV =		.041	.048	.036	.032	.020			
COEF.VAR=		9.460	11.659	9.329	10.126	7.051			
#OF PTS =		5							
21	0.00	.530	.490	.450	.400	.360	0.		E
22	.50	.350	.340	.320	.258	.204	0.		E
23	1.00	.560	.500	.420	.310	.273	0.		E
24	1.50	.440	.400	.370	.330	.300	0.		E
25	2.00	.560	.510	.390	.300	.267	0.	1047	E
MEAN =		.488	.448	.390	.320	.281			
STD.DEV =		.091	.075	.049	.052	.057			
COEF.VAR=		18.747	16.659	12.692	16.291	20.138			
#OF PTS =		5							

MACDILL AIR FORCE BASE  
DYNAFLECT MEASUREMENTS

LOCATION : TAMPA, FL.  
PAVEMENT ID : APRON 1A, AREA 5

PROJECT NO: AF-8  
CLIENT : U.S. AIR FORCE  
DATE : 10/82

RDG NO	STATION	D Y N A F L E C T   R E A D I N G S					TEMP.	TIME	I/E	C/M
		#1	#2	#3	#4	#5				
1	0.00	.620	.560	.480	.400	.350	0.	121	E	1
3	.50	.700	.610	.500	.420	.350	0.		E	1
5	1.00	.550	.500	.410	.360	.310	0.		E	1
7	1.50	.760	.630	.490	.400	.330	0.		E	1
9	2.00	.640	.560	.440	.390	.330	0.		E	1
MEAN =		.654	.572	.464	.394	.334				
STD.DEV =		.080	.051	.038	.022	.017				
COEF.VAR=		12.213	8.863	8.150	5.561	5.010				
#OF PTS =		5								
2	.06	.520	.500	.440	.380	.320	0.		E	2
4	.56	.580	.560	.480	.430	.350	0.		E	2
6	1.06	.540	.520	.460	.400	.340	0.		E	2
8	1.56	.510	.490	.440	.380	.320	0.		E	2
MEAN =		.538	.518	.455	.398	.333				
STD.DEV =		.031	.031	.019	.024	.015				
COEF.VAR=		5.759	5.982	4.208	5.945	4.511				
#OF PTS =		4								
10	0.00	.650	.570	.480	.390	.340	0.		I	1
12	.50	.650	.570	.460	.390	.330	0.		I	1
14	1.00	.720	.600	.500	.400	.340	0.		I	1
16	1.50	.750	.640	.530	.430	.350	0.		I	1
18	2.00	.540	.480	.410	.340	.300	0.		I	1
MEAN =		.662	.572	.476	.390	.332				
STD.DEV =		.081	.059	.045	.032	.019				
COEF.VAR=		12.244	10.298	9.465	8.309	5.794				
#OF PTS =		5								
11	.06	.500	.480	.440	.380	.330	0.		I	2
13	.56	.520	.490	.420	.370	.310	0.		I	2
1	1.06	.560	.550	.500	.420	.350	0.		I	2
17	1.56	.570	.540	.460	.380	.300	0.		I	2
19	2.06	.410	.400	.360	.300	.207	0.		I	2
MEAN =		.512	.492	.436	.370	.299				
STD.DEV =		.064	.060	.052	.044	.055				
COEF.VAR=		12.460	12.144	11.874	11.781	18.406				
#OF PTS =		5								

MACDILL AIR FORCE BASE  
DYNAFLECT MEASUREMENTS

LOCATION : TAMPA, FL.  
PAVEMENT ID : APRON 1A, AREA 5

PROJECT NO: AF-8  
CLIENT : U.S. AIR FORCE  
DATE : 10/82

RDG NO	STATION	D Y N A F L E C T   R E A D I N G S					TEMP.	TIME	I/E C/M
		#1	#2	#3	#4	#5			
20	0.00	.560	.510	.440	.370	.320	0.		M 1
22	.50	.540	.500	.440	.370	.320	0.		M 1
24	1.00	.570	.530	.460	.380	.340	0.	142	M 1
26	1.50	.560	.510	.450	.360	.330	0.		M 1
28	2.00	.550	.490	.420	.350	.300	0.		M 1
MEAN	=	.556	.508	.442	.366	.322			
STD.DEV	=	.011	.015	.015	.011	.015			
COEF.VAR	=	2.051	2.920	3.356	3.115	4.606			
#OF PTS	=	5							
21	.06	.490	.480	.430	.360	.310	0.	140	M 2
23	.56	.560	.540	.490	.390	.330	0.		M 2
25	1.06	.560	.540	.490	.400	.340	0.		M 2
27	1.56	.510	.490	.440	.370	.320	0.		M 2
29	2.06	.500	.490	.440	.340	.310	0.		M 2
MEAN	=	.524	.508	.458	.372	.322			
STD.DEV	=	.034	.029	.029	.024	.013			
COEF.VAR	=	6.415	5.806	6.440	6.418	4.049			
#OF PTS	=	5							



TEST DATA FROM DYNATEST CONSULTING, INC.

Data Collected with Dynatest Model 8000  
Falling Weight Deflectometer

Test Area #1: Center slab tests, morning of Oct. 29.

Input File: TA1-1

Date: OCT 29 1982	Temp: 20.6 C.
Roadway: TEST AREA #1 (20°PCC)	Load Radius (mm): 150
Sensor Positions (mm):	0 200 300 600 1200 1800 2400
for d1 d2 d3 d4 d5 d6 d7	
Station	Pressure
d3 d4	d5 d6 d7
68 66	67 68 69
125-106 0000C	1534 73 67
65 60	49 39 31
6.000C	1551 77 67
64 59	49 39 38
275-301 2.000C	1550 69 64
62 57	47 36 28
12.000C	1555 72 65
63 57	47 36 29
JKR-43018.000C	1559 77 70
67 62	52 42 35
18.000C	1557 77 70
68 63	52 42 35
355-6024.000C	852 39 36
35 31	27 23 18
24.000C	1164 53 49
46 42	35 32 26
→ 26.4.000C	1570 68 62
67 57	47 39 34
24.000C	1566 61 64
61 56	46 39 33
→ 50.2.100C	849 42 48
38 35	29 25 23
2.100C	1169 57 52
50 47	36 33 27
2.100C	1562 72 66
63 59	49 40 35
2.100C	1564 78 68
65 61	52 42 36
→ 9200 8.100C	1523 71 63
62 57	45 38 34
8.100C	1516 68 63
62 55	45 37 34
→ 50.14.100C	1527 67 65
53 59	48 49 33
14.100C	1537 68 66
63 61	49 40 33
→ 500.20.100C	1541 71 70
69 63	53 44 37
20.100C	1535 87 78
66 62	54 43 39
→ 650.26.100C	845 39 38
35 32	27 24 21
26.100C	1146 51 48
45 42	35 29 27
26.100C	1539 68 65
61 57	47 39 36
26.100C	1549 69 63
59 55	46 38 34
→ 7100 4.200C	1537 77 71
67 63	52 43 35
4.200C	1548 75 70
66 62	51 43 35
→ 260.16.200C	1517 71 66
63 58	49 38 31
16.200C	1531 72 67
64 61	50 40 33
→ 400.16.200L	1524 71 67
63 59	49 37 29
16.200C	1514 73 66
63 59	48 38 29
→ 550.22.200C	1575 70 64
63 58	46 37 29
22.200C	1520 75 65
63 58	48 36 28
→ 770.28.200C	1558 63 68
64 59	48 38 31
28.200C	1546 67 66
63 58	48 37 29

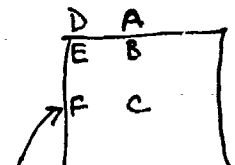
Test Area #1: Corners & Edges, afternoon of Oct. 29.

Input File: TA1-2

Date: OCT 29 1982	Temp: 34 C.
Roadway: TEST AREA #1(20°PCC)	Load Radius (mm): 150
Sensor Positions (mm):	-200 -300 -600 -1000 -2000
for d1 d2 d3 d4 d5 d6 d7	
Station	Pressure
d3 d4	d5 d6 d7
See File TA1-1 Diagram below!	6.000A 1557 98 94
1.000A	85 74 64 83 79
2.000A	1357 90 91
3.000A	84 73 63 81 76
4.000B	1542 97 86
8.000A	80 70 62 68 71
12.000A	1541 94 96
18.000A	79 69 61 77 73
24.000A	1537 65 68 77 83
24.000B	76 66 58 73 69
24.000B	1541 83 76
24.000B	71 63 56 81 74
24.000B	1532 83 76
24.000B	72 66 58 83 77
24.000A	847 55 55
24.000A	45 40 35 48 47
24.000A	1121 72 75
24.000A	68 53 47 65 63
24.000A	1534 101 103
24.000A	78 67 59 85 80
24.000B	1546 97 102
24.000B	76 65 57 83 77
24.000B	845 54 49
24.000B	45 39 35 57 41
24.000B	1125 72 66
24.000B	61 53 45 75 56
24.000B	1536 97 90
24.000B	82 71 62 102 72
24.000B	1536 100 91
24.000B	84 72 62 104 73
12.000D	1468 163 161
71	57 130 123
12.000D	1435 145 155
70	57 124 118
12.000E	1518 173 158
146	128 109 100 86
12.000E	1484 160 149
135	116 100 163 86
12.000F	1522 108 103
96	88 79 100 96
12.000F	1525 106 98
90	83 74 94 91
18.000D	1509 219 217
99	78 67 194 192
18.000D	1513 208 228
86	77 67 187 175
18.000E	1510 153 142
129	112 93 159 129
18.000E	1523 147 136
124	106 91 153 133
18.000F	1533 111 106
10	93 85 104 98
1.00F	1524 102 103
9	90 82 101 96
2.100R	1531 101 111
79	78 60 94 89
1.00A	1541 106 109
1	71 63 92 89
2.100E	1531 135 127
115	98 84 147 63
2.100E	1539 127 123
12	95 81 142 65
4.100A	1515 116 119
73	65 58 100 95
14.100A	1514 110 111
72	63 57 94 88
14.100B	1543 103 91
86	75 65 106 79

14.100B	1534	94	89
84	72	63	182
20.100A	1523	128	133
68	63	56	113
20.100A	1521	123	131
67	62	54	109
20.100B	1522	156	134
125	108	92	162
20.100B	1522	143	125
117	100	85	152
2.100D	1519	142	155
78	64	56	125
2.100E	1523	141	153
78	64	57	122
2.100E	1523	143	133
120	102	87	153
2.100E	1524	140	129
117	99	85	149
2.100F	1500	110	105
99	91	82	104
2.100F	1499	112	104
99	98	81	105
8.100D	856	97	107
43	36	35	86
8.100D	1134	128	141
56	58	44	111
8.100D	1463	167	172
71	63	56	142
8.100D	1474	164	173
71	63	56	142
8.100E	829	81	73
70	60	51	87
8.100E	1111	110	99
92	79	68	115
8.100E	1552	145	136
126	106	91	159
8.100E	1550	149	136
127	107	92	157
8.100F	840	69	65
63	57	59	66
8.100F	1125	92	89
84	79	69	88
8.100F	1538	128	126
113	103	92	116
8.100F	1526	123	119
112	101	91	115
20.100D	1501	332	437
78	69	60	297
20.100D	1500	228	254
114	99	87	205
20.100E	1509	135	132
122	110	99	141
20.100E	1555	176	126
117	105	95	133
20.100F	1502	165	158
164	152	135	160
20.100F	1499	166	158
153	142	127	157
26.100D	846	114	123
38	35	31	98
26.100D	1125	158	170
49	44	40	132
26.100D	1485	218	227
59	54	50	176
26.100D	1474	207	228
61	55	50	177
26.100E	845	117	106
38	84	68	128
26.100E	1131	149	136
124	105	88	161
26.100E	1533	193	179
164	140	116	215
26.100E	1533	194	179
169	140	117	219
26.100F	839	53	53
48	45	40	49
26.100F	1115	71	68
62	57	51	64
26.100F	1557	98	87
85	78	70	88
26.100F	1557	97	74
82	73	68	81
10.200A	1508	92	100
85	74	55	85
10.200A	1513	90	97
83	71	63	82
10.200B	1538	90	85
78	69	62	95
10.200B	1540	93	82
76	68	69	93

16.200A	1523	128	138
64	58	52	111
16.200A	1529	126	136
64	59	53	109
16.200P	1527	123	115
104	98	79	135
10.200B	1525	126	115
187	93	79	134
22.200A	1501	92	99
88	69	62	83
22.200A	1496	93	96
78	68	59	81
22.200B	1527	88	81
75	65	57	93
22.200B	1521	88	80
76	65	57	91
			76



No joint transfer obtained  
during this round of  
tests for point F?

Test Area #1 : Corners  
& Edges (Cont'd), afternoon  
of Oct. 29.

Date: OCT 29 1982 Temp: 31 °C  
Roadway TEST AREA #1(20°PGC)  
Load Radius (mm): 150  
Sensor Positions (mm):  
0 200 300 600 900 -199 -299

Station	Pressure	d1	d2	
d3	d4	d5	d6	d7
4.200D	1527	179	195	
165	145	126	169	163
4.200D	1518	174	189	
162	143	123	165	161
4.200E	1522	144	176	
163	144	125	191	163
4.200E	1527	178	173	
161	142	124	187	166
4.200F	1479	155	147	
141	135	122	146	145
4.200F	1475	144	142	
137	128	119	141	137
16.200D	1534	160	156	
138	126	109	144	140
16.200D	1533	157	161	
140	128	110	142	135
16.200E	1492	153	147	
138	123	108	161	146
16.200E	1466	156	146	
138	124	109	161	146
16.200F	1406	138	134	
130	123	112	132	129
16.200F	1482	138	132	
128	119	110	130	127
28.200D	1516	152	168	
138	138	101	138	133
28.200D	1526	146	188	
135	117	98	134	129
28.200E	1520	159	152	
138	120	104	166	129
28.200E	1519	154	144	
132	117	100	158	132
28.200F	1524	139	144	
137	125	114	140	135
28.200F	1531	142	142	
133	121	110	135	121

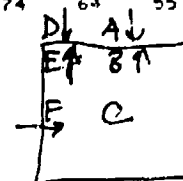
Test Area #1: All loads, money  
of Nov. 1.

Input File: AREA#1

Date: NOV 1 1982 Temp: 30.5 °C  
 Roadway: TEST AREA #1 E20" PCCJ  
 Load Radius (mm): 150  
 Sensor Positions (mm):  
 0 200 305 610 914 1524 2438

Station	Pressure	d1	d2	
d3	d4	d5	d6	d7
2.200C	833	43	42	
39	37	34	29	18
2.200C	1524	73	71	
67	62	56	47	32
2.200C	1530	74	72	
67	62	57	47	31
2.200B	850	65	66	
50	43	38	29	19
2.200B	1535	109	117	
87	74	65	48	31
2.200B	1540	107	114	
83	71	63	46	28
4.100C	838	47	45	
42	40	36	21	19
4.100C	1528	71	79	
73	67	62	51	34
4.100C	1527	80	78	
72	68	61	51	35
4.100B	844	84	87	
35	31	29	25	17
4.100B	1511	135	143	
59	50	47	37	25
4.100B	1514	136	148	
59	54	49	39	27
4.100F	847	78	80	
42	38	33	26	17
4.100F	1512	139	155	
75	67	59	46	31
4.100F	1514	138	150	
74	65	58	45	31
4.100E	841	116	121	
43	40	36	29	20
4.100E	1512	176	194	
91	75	68	53	33
4.100E	1515	179	187	
98	77	69	53	35
6.000C	836	46	41	
39	36	34	27	18
6.000C	1525	74	78	
66	60	55	45	29
6.000C	1531	75	72	
67	61	55	45	30
6.000B	838	64	65	
48	41	37	27	18
6.000B	1510	187	116	
83	71	63	46	29
6.000B	1513	186	110	
82	71	62	46	35
13.200C	833	45	44	
41	37	35	29	20
13.200C	1530	73	74	
78	66	60	49	33
13.200C	1531	74	72	
68	62	57	46	31
13.200B	836	59	60	
52	46	40	31	19
13.200B	1529	100	108	
98	81	68	52	32
13.200B	1532	98	104	
87	79	67	51	30
14.100C	832	42	40	
38	36	32	27	21

14.100C	1528	74	69
66	54	44	31
14.100C	1536	75	70
66	55	44	31
14.100B	835	78	82
36	32	24	17
14.100B	1514	132	143
68	53	38	29
14.100B	1519	133	146
60	53	38	29
15.000C	833	44	42
39	36	27	19
15.000C	1537	79	72
68	55	44	32
15.000C	1548	76	72
68	56	45	31
15.000B	843	68	71
44	38	25	16
15.000B	1523	117	124
76	59	44	29
15.000B	1528	117	124
77	59	45	31
23.200C	830	43	39
37	34	25	17
23.200C	1535	71	67
64	58	41	28
23.200C	1543	74	70
66	59	43	29
23.200B	836	79	91
38	34	24	16
23.200B	1566	139	166
66	58	39	26
23.200B	1512	136	179
63	55	37	26
25.100C	832	43	39
38	34	26	16
25.100C	1526	79	73
65	59	43	28
25.100C	1531	76	74
68	61	45	30
25.100B	836	76	82
30	27	19	13
25.100B	1499	138	157
53	48	35	24
25.100B	1563	133	149
51	48	35	24
25.100F	815	70	76
35	31	22	15
25.100F	1498	125	135
61	54	35	24
25.100F	1496	123	136
60	53	37	26
25.100E	826	82	85
41	37	25	18
25.100E	1509	136	150
80	74	48	32
25.100E	1515	202	140
77	63	46	28
27.000C	821	43	39
37	34	26	15
27.000C	1515	75	69
67	63	44	28
27.000C	1537	76	70
67	63	44	29
27.000B	637	68	70
43	38	26	16
27.000B	1509	114	123
74	64	40	25
27.000B	1513	305	123
74	64	42	29



Wind Tunnel  
 obtained on  
 all corner  
 & edges by  
 placing FWD in  
 the shown  
 direction.

SHUNTVAL IN VOLTS 7.073±5  
STEP 3 "T2"

T2-2-54 *t<sub>1</sub>, 8' Lt of Centaur*  
Station 71-79 LT  
TEST POINT FOR ALL!  

	Ld.(lbs)	9143	13888	13888
Df1(mil)	5.4	5.2	8.7	8.7
Df2(mil)	3.7	3.5	6.1	6.1
Df3(mil)	2.4	2.3	3.9	4.9
Df4(mil)	1.6	1.5	2.7	2.7
Df5(mil)	1.1	1	1.9	1.2
Df6(mil)	0.9	0.8	1.5	1.5
Df7(mil)	4.5	4.3	7.1	7.1
Area(in)	21.4	21.4	21.7	21.8
dsm(kP1)	1679	1759	1683	1683
DSM(kP1)	1370			

T2-2-60  
Station 71-79 LT  
TEST POINT FOR ALL!  

	Ld.(lbs)	18229	18201	23613	23473
Df1(mil)	11.8	11.9	16.3	16.3	
Df2(mil)	8.3	8.4	11.7	11.6	
Df3(mil)	5.4	5.5	7.6	7.6	
Df4(mil)	3.6	3.6	5.1	5.1	
Df5(mil)	2.5	2.6	3.5	3.5	
Df6(mil)	1.9	2.0	2.6	2.6	
Df7(mil)	9.8	9.8	13.6	13.6	
Area(in)	21.8	21.8	22.0	22.0	
dsm(kP1)	1549	1536	1449	1437	
DSM(kP1)	1175				

→ Date Oct 30 1982 Temp 33.6 °C  
Roadway TEST AREAS 2/3 & 4/MODUL  
Time 14:50

Load Radius [Ld] = ~~20m~~ 150mm  
r's=0 12 24 36 48 60 200mm

Results, printed out in  
lbs. & mils for "T2", Test  
Area #2.

Input File: TRP-1

Test Area #2: Summary of  
FWD tests (test drop only)  
Run Oct. 29.

NOTE: A = Cl. 1 Concrete  
near plate.  
B = Cl. 2 Concrete  
near plate.

Date: OCT 29 1982 Temp: 30 C  
Roadway TEST AREA #2 (11" AC)  
Load Radius (mm): 150  
Sensor Positions (mm):  
0 200 300 600 900 1200 1500

(in feet)

Station	Pressure	d1	d2			
d3	d4	d5	d6	d7		
-8 000R	1503	487	348			
382	210	145	102	74		
-100 000R	1482	410	309			
264	186	128	91	57		
-200 000	1480	462	356			
302	290	174	93	58		
-300 000	1480	444	341			
286	199	127	98	68		
-400 000	1454	582	427			
342	202	25	85	61		
-500 000R	1492	457	355			
266	156	32	51	49		
-600 000R	1484	450	351			
296	196	126	90	65		
-700 000R	1470	515	420			
359	155	161	108	77		
50 100R	1507	350	261			
235	164	11	95	64		
150 1000	149	245	293			
357	176	121	86	67		
250	1507	302	258			
222	154	106	75	57		
350 100R	1483	315	275			
239	162	113	96	64		
450 100R	1496	303	261			
225	165	119	86	6		
550 100	1560	314	224			
200	153	116	81	66		
650 100	1486	314	276			
244	183	133	72			
-200R	1442	471	347			
385	186	123	87	66		
-100 200R	1446	475	319			
256	159	103	73	55		
-200 200	1430	447	392			
117	195	124	81	55		
500 100	1456	500	463			
291	184	119	83	52		
-400 100	1464	349	392			
246	164	113	82	61		
-500 200R	1487	360	293			
251	151	97	66	50		
-600 2000	1497	394	341			
233	95	142	191	75		
-700 100	1423	613	486			
394	241	149	100	72		

↑ 15' Left of Centerline

↓ 15' Right of Centerline

Input File: AP#

Test Area #2 : All tests  
run Nov. 1.

Date: NOV 1 1982 Temp: 33 C  
Roadway TEST AREA #2 (11" AC)  
Load Radius (mm): 150  
Sensor Positions (mm):

0 200 305 610 914 1524 2438

(in feet)

Station	Pressure	d1	d2			
d3	d4	d5	d6	d7		
25 000C	829	159	132			
114	81	58	34	19		
25 000C	1470	295	256			
218	154	110	62	35		
25 000C	1482	291	244			
214	151	108	65	34		
75 000C	833	182	152			
133	90	63	34	19		
25 000C	1488	339	293			
258	168	116	61	34		
75 000C	1482	333	284			
248	165	114	61	37		
125 000C	952	202	165			
139	93	63	35	20		
125 000C	1455	373	336			
259	173	119	62	33		
125 000C	1453	363	293			
254	170	118	52	35		
175 000C	817	208	171			
145	94	62	32	18		
175 000C	1442	378	309			
269	178	118	61	35		
175 000C	1444	371	307			
265	175	115	60	35		
225 000C	857	155	137			
117	91	56	33	18		
225 000C	1468	297	254			
223	156	108	59	36		
225 000C	1467	286	247			
217	150	105	57	29		
275 000C	853	173	149			
130	92	65	35	20		
375 000C	1472	323	277			
243	173	122	67	35		
275 000C	1462	317	277			
272	169	122	65	35		
325 000C	819	181	153			
135	92	64	35	28		
325 000C	1450	333	286			
246	173	118	63	35		
325 000C	1457	329	282			
243	169	117	63	36		
375 000C	843	169	143			
125	96	54	33	18		
375 000C	1477	314	265			
235	165	114	61	34		

New Centuries

375.000C	1484	318	261	500.000L	847	381	245
230 161	112	59	33	198 118	74	38	23
425.000C	842	188	141	500.000L	1433	344	448
118 79	54	31	19	362 221	137	65	38
425.000C	1457	327	255	500.000L	1435	527	423
216 147	181	55	33	347 209	132	67	37
425.000C	1458	322	256	600.000L	829	324	234
213 146	102	55	32	183 103	62	33	20
475.000C	853	190	146	600.000L	1433	578	417
123 86	62	35	19	332 192	117	62	40
475.000C	1499	354	271	600.000L	1430	544	406
235 162	119	66	34	320 186	115	62	39
475.000C	1499	346	271	700.000L	850	325	246
124 94	71	40	22	206 126	79	40	25
525.000C	1495	314	269	700.000L	1432	567	438
235 178	133	73	37	363 225	143	70	40
525.000C	1515	308	266	700.000L	1414	549	414
230 176	138	71	38	351 218	142	73	43
575.000C	848	168	138	0.000R	828	302	236
114 82	58	33	18	186 111	74	39	21
575.000C	1487	300	245	0.000R	1440	529	428
214 153	108	58	31	335 203	134	69	37
575.000C	1487	289	242	0.000P	1465	514	418
213 152	108	59	32	331 209	133	70	40
625.000C	847	166	140	100.000R	845	374	228
119 82	57	32	20	172 95	59	32	19
625.000C	1458	307	267	100.000R	1434	615	378
227 157	107	59	35	300 171	106	57	31
625.000C	1460	306	274	100.000P	1440	581	365
224 154	107	67	36	290 164	104	57	31
675.000C	850	170	147	200.000R	839	393	266
129 94	68	35	21	222 118	72	37	21
675.000C	1506	324	292	200.000P	1425	649	439
248 188	129	68	37	377 204	126	63	35
675.000C	1489	313	276	200.000P	1433	615	423
242 175	126	68	38	359 198	124	63	33
0.000L	836	308	231	300.000P	847	346	266
185 118	77	41	24	197 111	67	35	21
0.000L	1460	541	419	300.000R	1442	595	458
338 217	144	73	39	342 198	124	64	36
0.000L	1465	521	411	300.000P	1435	568	432
332 213	142	74	40	328 190	119	62	35
100.000L	844	302	178	400.000R	852	243	196
144 99	68	36	21	165 100	63	35	22
100.000L	1478	497	321	400.000P	1462	431	355
263 183	125	66	35	295 183	118	61	35
100.000L	1465	470	317	400.000R	1461	421	345
259 190	123	67	37	287 178	115	61	59
200.000L	818	291	238	400.000P	1465	422	344
194 120	76	38	22	286 177	115	64	36
200.000L	1484	524	413	400.000R	1458	416	347
347 217	138	70	39	284 176	116	61	37
200.000L	1410	498	403	500.000R	847	334	251
334 205	131	67	35	184 93	52	26	17
300.000L	845	294	213	500.000R	1443	543	394
173 109	70	36	21	298 151	86	42	25
300.000L	1458	516	371	500.000R	1439	522	376
308 198	127	65	37	285 146	83	43	25
300.000L	1446	494	352	600.000P	845	341	260
299 189	123	63	33	209 128	79	40	22
400.000L	814	441	287	600.000R	1425	595	462
221 121	70	35	20	376 231	147	72	38
400.000L	1389	732	497	600.000R	1438	565	442
384 213	127	61	35	361 224	145	75	41
400.000L	1393	699	476	700.000R	838	543	360
366 206	126	63	38	298 148	84	40	23
				700.000R	1383	869	596
				481 257	147	68	40
				700.000R	1398	808	560
				449 243	144	71	40
				1.000r	844	153	136
				112 75	58	29	18
				1.000r	1515	288	244
				202 137	58	31	
				1.000r	1522	275	242
				198 135	92	52	32

Input File: #2-500

Test Area #2: All tests  
run laterally across runway  
at Station #500 on Nov. 1, 1982

NOTE:

r = right of centerline  
l = left of centerline.

Date: NOV 1 1982 Temp: 37 C  
Roadway: ACROSS TAXIWAY (T.A.#2)  
Load Radius (mm): 150  
Sensor Positions (mm):

0 280 305 610 914 1524 2438  
(in ft.) right (r) or left (l) to (L)

Station	Pressure	d <sub>1</sub>	d <sub>2</sub>	d <sub>3</sub>	d <sub>4</sub>	d <sub>5</sub>	d <sub>6</sub>	d <sub>7</sub>
1.000r	849	150	130					
106	72	49	28	19				
1.000r	1511	277	235					
195	133	90	51	32				
1.000r	1512	278	240					
197	134	92	52	32				
4.000r	850	183	152					
127	77	47	25	17				
4.000r	1468	336	277					
236	141	87	45	32				
4.000r	1466	329	270					
231	138	84	45	31				
8.000r	848	235	176					
142	80	48	25	17				
8.000r	1437	430	311					
257	143	86	46	36				
8.000r	1434	416	301					
248	139	82	47	34				
12.000r	850	236	204					
139	70	41	25	18				
12.000r	1437	424	345					
252	127	76	48	35				
12.000r	1436	409	336					
241	120	73	46	34				
16.000r	844	347	232					
162	83	46	27	20				
16.000r	1423	58	377					
276	139	76	47	33				
16.000r	1423	553	363					
264	134	75	47	34				
21.000r	836	434	285					
213	90	47	31	22				
21.000r	1391	691	450					
339	147	77	51	38				
21.000r	1395	643	427					
325	145	76	49	36				
26.000r	813	532	369					
231	84	45	28	23				
26.000r	1381	909	530					
340	131	78	46	39				
26.000r	1385	841	499					
318	127	77	49	40				

31.000r	823	445	312
224	104	55	547
31.000r	1394	714	510
360	170	98	1738
31.000r	1396	681	488
348	167	92	1747
1.000r	862	161	138
112	75	51	20
1.000r	1498	295	241
203	135	92	34
1.000r	1488	293	239
201	133	90	35
4.000r	853	158	128
108	74	51	19
4.000r	1474	289	230
201	133	91	32
4.000r	1475	284	229
198	133	91	33
8.000r	863	204	168
134	79	48	18
8.000r	1514	377	307
239	139	84	44
8.000r	1516	369	296
233	137	83	30
12.000r	857	203	155
127	72	45	24
12.000r	1454	367	281
230	131	82	29
12.000r	1449	356	272
222	126	90	28
16.000r	860	233	166
133	77	46	19
16.000r	1448	410	286
234	135	78	31
16.000r	1450	399	281
228	131	79	32
21.000r	849	335	239
184	90	50	22
21.000r	1422	544	382
295	144	84	33
21.000r	1429	525	371
285	142	84	34
26.000r	857	336	288
219	110	61	23
26.000r	1426	564	468
363	183	105	42
26.000r	557	188	160
121	62	38	18
26.000r	1122	411	323
261	133	80	32
26.000r	1448	540	438
344	176	104	42
26.000r	1439	528	430
338	173	103	40
31.000r	1101	651	429
328	155	67	37
31.000r	1392	789	507
393	189	83	49
31.000r	534	260	175
134	65	33	18
31.000r	1101	565	358
286	137	66	38
31.000r	832	405	277
211	103	51	31
31.000r	1400	728	486
376	180	84	53
31.000r	1401	709	476
368	178	82	35

Input File: TAB-1

Test Area #3: All tests  
Run Oct. 29.

NOTE:

A = Cl. 1 Concrete plate  
B = Cl. 2 — " —

Date: OCT 29 1982 Temp: 32 C  
Roadway: TEST AREA #3 (5.5' AC)  
Load Radius (mm): 150  
Sensor Positions (mm):  
0 200 300 600 900 1200 1500

Station	Pressure	d1	d2	
d3	d4	d5	d6	d7
50 100	1513	718	644	
533 341	211	132	88	
50 100	1509	672	585	
489 333	195	130	88	
150 1000	851	440	366	
305 176	105	67	47	
150 1000	1134	554	459	
535 225	136	90	63	
150 1000	1476	725	631	
596 284	180	110	81	
150 1000	1476	789	596	
489 296	177	121	87	
250 190	1448	603	703	
533 333	210	131	84	
50 100	1471	823	635	
514 314	205	132	90	
350 100	1528	775	676	
593 372	225	136	83	
350 100	1538	731	637	
549 349	215	136	89	
450 100	1500	654	500	
491 288	168	104	71	
450 100	1510	618	544	
459 278	169	108	76	
550 1000	853	557	425	
345 190	106	65	45	
550 1000	1095	693	530	
431 243	141	90	63	
550 1000	1409	913	705	
599 326	187	119	83	
550 1000	1474	897	653	
557 323	198	122	87	
650 1000	1385	965	802	
597 296	165	108	76	
650 1000	1427	862	722	
553 277	172	118	87	
750 100	1431	899	645	
507 280	176	128	82	
750 100	1494	791	595	
459 263	171	118	84	
750 100	1521	626	544	
472 297	182	121	84	
750 100	1521	567	586	
427 274	173	117	84	
950 100	872	475	384	
305 168	92	59	42	
950 100	1125	569	463	
366 211	120	81	61	
950 100	1504	736	624	
500 271	161	106	75	
950 100	1503	718	584	

2458	26	160	108	78
300		804	987	705
526	226	99	53	35
200		1087	1035	745
557	252	121	73	52
200		1397	1274	905
703	321	156	92	67
200		1393	1282	874
669	310	155	96	70
100 200		1385	1289	931
732	330	156	96	73
100 200		1387	1061	781
602	287	153	106	82
200 200		1389	1263	87
622	243	110	76	63
200 200		1392	1043	72
527	225	122	99	72
300 200		1391	1484	105
797	323	149	81	61
200 200		1405	1252	82
681	301	148	92	69
400 200		820	973	66
501	198	80	43	31
400 200		1091	1117	77
594	253	112	66	48
400 200		1411	1391	102
764	334	151	88	63
400 200		1415	1343	98
755	331	154	92	67
500 200		1370	1277	112
811	325	141	90	59
300 200		1393	1371	95
701	309	153	97	72
600 200		1364	1635	116
978	379	173	97	68
600 200		1354	1382	99
771	356	183	113	82
700 200		1401	1223	89
653	304	148	91	68
700 200		1416	1050	78
589	283	158	106	82
800 200		80	74	49
354	140	73	48	39
800 200		1055	838	56
407	182	98	68	56
800 200		1377	1035	72
529	241	128	87	68
800 200		1364	999	68
518	241	133	94	74
900 200		124	1228	83
585	238	107	72	58
900 200		1399	1045	70
510	218	115	83	66
1000 200		1362	1124	78
575	239	114	73	57
1000 200		1346	969	67
504	228	125	87	68
0 000A		1413	1305	94
692	295	141	88	67
0 000A		1426	1103	79
605	281	150	98	76
100 000		1375	1654	118
884	329	124	74	63
0 000A		1304	1239	89
667	273	131	98	76
200 000		1365	1387	170
2706	325	155	92	67
200 000		1375	1084	81
585	322	141	93	83
300 000		837	800	57
475	214	104	68	42
300 000		1105	921	68
535	251	128	82	58
300 000		1422	1154	92
716	328	171	106	73
300 000		1432	1114	86
603	318	170	106	77

4' Rf. of Curbang

400.000B 1387 1534 1154  
 878 35 176 96 68  
 - 400.000B 1400 1301 972  
 742 344 170 104 75  
 500.000B 1389 1604 1062  
 795 328 148 85 62  
 - 500.000B 1406 1282 377  
 639 282 149 99 74  
 600.000A 1391 1442 976  
 754 317 148 92 71  
 - 600.000A 1407 1187 845  
 629 284 150 102 79  
 700.000A 818 801 555  
 392 154 76 54 43  
 700.000A 107 918 645  
 467 200 108 77 61  
 700.000A 1395 1124 815  
 608 266 142 99 78  
 - 700.000A 1389 1077 781  
 579 259 144 102 83  
 800.000 1404 1148 852  
 635 287 170 87 68  
 - 800.000 1405 975 697  
 543 259 132 94 76  
 900.000 1378 1287 868  
 650 248 114 74 68  
 - 900.000 1392 1076 730  
 553 229 121 84 68  
 1000.000 1391 1213 895  
 646 276 132 84 65  
 1000.000 1384 990 709  
 526 241 131 91 73

12' Left of Centerline

Input File: AR#3-1

Test Area #3: All Years  
Run. Nov. 1.

Date: NOV 1 1982 Temp 38 C  
Roadway: TEST AREA #3 (5.5' AC)  
Load Radius (mm): 150  
Sensor Positions (mm):  
0 200 305 610 914 1524 2438  
(in ft.)

Station	Pressure	d1	d2	d3	d4	d5	d6	d7
25.000C	858	503	384	525.000C	1447	896	686	
299 160	92	40	36	525.000C	200	86	48	
25.000C	1469	811	559	525.000C	858	366	249	
490 266	156	67	51	291 131	91	54	31	
25.000C	1472	772	600	425.000C	1504	674	438	
468 259	156	71	42	371 246	170	108	48	
75.000C	861	378	299	425.000C	1506	658	439	
254 158	99	48	23	365 244	171	108	53	
75.000C	1506	648	511	475.000C	851	482	352	
429 265	169	79	11	280 167	102	45	27	
75.000C	1500	626	499	475.000C	1451	870	637	
416 353	160	82	46	496 293	182	78	31	
125.000C	845	372	298	475.000C	1463	828	575	
251 156	99	45	27	473 287	183	78	46	
125.000C	1462	651	519	525.000C	867	391	332	
437 275	173	79	44	280 170	102	43	24	
125.000C	1460	626	490	525.000C	1505	699	682	
420 263	168	88	46	501 303	185	80	54	
175.000C	866	391	323	525.000C	1513	678	573	
279 164	99	42	24	484 295	183	84	48	
175.000C	1527	695	548	575.000C	856	462	347	
529 291	180	75	42	274 151	93	45	23	
175.000C	1522	673	511	575.000C	1478	798	563	
527 280	171	79	43	471 263	165	79	32	
225.000C	860	413	337	575.000C	1454	768	581	
285 176	107	47	30	462 263	167	85	67	
225.000C	1492	721	588	625.000C	174	81	48	
503 300	182	77	50	625.000C	1407	1183	611	
225.000C	579	230	186	506 268	177	85	48	
152 93	58	31	19	625.000C	832	467	352	
225.000C	858	372	289	625.000C	1417	934	645	
241 147	93	44	28	486 257	152	74	46	
225.000C	1133	581	390	675.000C	831	548	390	
327 202	127	60	70	675.000C	1417	938	642	
225.000C	1493	728	545	486 257	152	74	46	
462 283	178	81	47	675.000C	1423	866	607	
275.000C	873	344	285	468 246	154	88	49	
240 151	96	45	24	725.000C	863	363	293	
275.000C	1143	442	371	251 137	87	44	25	
305 193	123	60	34	725.000C	1463	768	567	
275.000C	1543	607	516	428 228	151	76	45	
425 269	172	78	42	725.000C	1463	732	522	
325.000C	864	361	300	410 220	147	78	47	
260 168	108	46	25	725.000C	846	441	343	
325.000C	1137	461	378	270 144	87	44	25	
325 211	136	61	32	825.000C	1438	722	585	
325.000C	1519	628	522	452 248	145	76	43	
448 289	187	82	42	825.000C	1454	700	570	
375.000C	839	553	419	434 245	150	78	43	
337 200	118	44	23	875.000C	871	362	292	
375.000C	1447	952	675	414 258	96	43	24	
567 333	203	98	3	925.000C	1503	657	512	
				216 136	88	44	25	
				393 246	159	79	46	
				925.000C	1502	544	429	
				371 236	155	79	46	
				975.000C	844	359	303	
				236 143	93	15	25	

975.000C	1478	528	508	Date: NOV 1 1982 Temp: 36.5 C
417 254	164	88	45	Roadway: TEST AREA #3 (5.5"AC)
975.000C	1456	581	484	Load Radius (mm): 150
397 244	160	88	46	Sensor Positions (mm):
0.000R	791	1611	681	0 200 305 610 914 1524 2438
467 170	88	38	21	(in ft.)
0.000R	1367	1415	958	Station Pressure d1 d2
700 201	139	78	39	d3 d4 d5 d6 d7
0.000R	1377	1302	878	
656 276	145	74	44	
180.000R	806	843	621	0.000L 800 980 680
463 151	75	44	28	480 183 89 48 22
180.000R	1376	1185	849	0.000L 1370 1318 887
606 256	135	76	47	672 274 140 74 43
100.000R	1381	1186	792	0.000L 1379 1186 826
500 257	143	85	49	616 258 141 74 44
200.000R	600	923	629	180.000L 786 1195 779
427 151	75	42	25	513 169 72 42 29
200.000R	1364	1280	952	180.000L 1370 1445 1014
624 246	129	75	46	680 235 112 74 50
200.000R	1377	1174	803	180.000L 1381 1284 945
384 239	134	81	49	620 229 117 78 49
300.000R	809	986	657	200.000L 815 880 587
169 193	87	38	24	398 143 70 40 26
300.000R	1368	1297	927	200.000L 1396 1234 822
693 296	145	71	43	561 226 116 66 41
300.000R	1366	1201	985	200.000L 1412 1185 799
641 287	148	77	77	548 256 233 66 39
500.000R	794	1810	715	300.000L 810 803 573
500 203	94	37	23	415 158 79 48 25
500.000R	1364	1404	892	300.000L 1436 1179 893
721 295	148	68	40	1506 253 125 64 36
500.000R	1369	1305	849	300.000L 1446 1122 815
565 283	150	75	46	639 258 137 72 48
500.000R	813	796	553	400.000L 794 1047 726
383 152	83	45	25	508 189 78 38 21
500.000R	1372	1262	929	400.000L 1367 1479 996
645 273	147	76	45	738 302 139 61 39
500.000R	1373	1240	869	400.000L 1372 1377 924
647 275	148	79	45	701 302 153 72 46
600.000R	797	1104	802	500.000L 794 1000 656
577 236	108	39	24	436 151 65 32 23
600.000R	1361	1483	974	500.000L 1376 1350 932
813 352	173	74	44	628 244 122 59 41
600.000R	1365	1367	925	500.000L 1388 1243 1408
726 337	175	93	45	595 248 137 74 48
700.000R	806	986	552	600.000L 798 914 614
429 198	97	56	29	412 144 67 36 25
700.000R	1356	1277	848	600.000L 1374 1284 670
629 295	159	83	52	616 244 127 70 44
700.000R	1369	1169	786	600.000L 1373 1192 790
588 283	159	86	49	583 248 138 80 48
800.000R	811	740	528	700.000L 796 831 564
367 157	82	49	26	398 146 66 35 24
800.000R	1375	1077	750	700.000L 1379 1151 782
345 249	148	75	45	561 237 125 68 44
800.000R	1377	988	690	700.000L 1374 1076 747
510 238	140	78	48	541 240 135 77 48
900.000R	804	933	631	800.000L 784 796 556
444 182	84	35	24	389 146 67 35 25
900.000R	1375	1297	884	800.000L 1374 1186 809
519 261	131	64	40	566 234 122 66 45
900.000R	1382	1182	786	800.000L 1379 1072 862
				537 234 130 76 49
				900.000L 808 792 547
				356 127 58 32 23
				900.000L 1386 1061 766
				582 201 104 59 48
				900.000L 1387 981 788
				485 205 113 66 42
				1000.000L 819 653 456
				334 126 58 33 21
				1000.000L 1388 944 659
				496 209 110 62 48
				1000.000L 1398 888 629
				474 211 121 71 45

Input File: AR#3-2  
 (cont'd) [Vol. 1]  
Test Area #3

SHUNTAGE IN VOLTS. 7.07E STEP 3

TRE-2 96  
Station 50-911

BGN T3

Ld.(lbs)	7997	8154	12914	12942
Df1(mil)	22.1	18.9	29.2	21.4
Df2(mil)	10.1	8.8	14.3	10.8
Df3(mil)	3.6	3.3	5.6	5.6
Df4(mil)	1.4	1.6	2.7	2.8
Df5(mil)	.9	.1	1.9	1.9
Df6(mil)	.9	.9	1.6	1.7
Df7(mil)	14.7	12.6	19.9	19.1
Arealain	13.8	14.2	14.7	14.9
dsm(kpsi)	362	431	443	524
DSM(kpsi)	524			

T3 0+62  
10.5 LF. 6  
Centrifuge.

TRE-2 100  
Station 50-911

BGN T3

Ld.(lbs)	17198	17237	22121	22042
Df1(mil)	35.9	35.2	45.2	43.2
Df2(mil)	18.1	18.0	23.9	23.4
Df3(mil)	7.4	7.5	9.0	9.8
Df4(mil)	3.5	3.8	4.1	4.9
Df5(mil)	2.4	2.6	3.2	3.4
Df6(mil)	3.1	2.2	3.7	2.8
Df7(mil)	25.1	14.7	32.7	31.4
Arealain	15.1	15.3	15.6	15.7
dsm(kpsi)	478	490	483	502
DSM(kpsi)	547			

Prev. cart. t3 system = 34.5 L 0230, M82.

Results, printed out in lbs. & mils  
for "T3", Test Area #3.

$d = 150 \text{ mm} (5.91")$

r's = 0", 12", 24", 36", 48", 60" & 100mm

Df1 Df2 Df3 Df4 Df5 Df6 Df7

Input File: AR#4-2

Test Area #4: A few select points from Oct. 30.

Note: E = edge  
I = interior  
C = corner

Date: 19821030 Temp: 24  
Roadway TEST SECT #4 (COMPOSITE)  
Load Radius (mm) 150  
Sensor Positions (mm)

A 200 305 610 914 1219 1524

Station	Pressure	d1	d2	d3	d4	d5	d6	d7
~ Sta. 11 230E	1458	328	335					
239 186	137	107	81					
35A X 11 100I	1459	316	193					
180 152	127	104	84					
11 220E	1453	295	190					
216 168	132	102	71					
12 320I	1524	74	150					
~ Sta. 203 157	124	93	71					
12 230E	1452	287	193					
226 175	125	105	81					
12 180I	1464	326	201					
181 157	132	107	86					
12 220E	1447	243	340					
178 137	112	92	71					
41 320C	1448	479	450					
283 165	125	107	81					
41 230E	1550	378	385					
198 157	170	103	81					
41 220S	1476	330	353					
180 147	114	91	74					
42 230C	1472	447	493					
208 168	135	107	84					
150 D X 41 100I	1459	269	251					
239 203	168	137	109					
31 230E	1479	434	445					
236 191	152	122	97					
~ Sta. 1 100I	1458	205	284					
54 211	123	143	114					
32 320C	1439	976	577					
315 224	133	145	114					
32 220E	1473	784	395					
21 208	165	127	94					
~ Sta. 160I	1468	21	111					
241 175	147	112	99					
32 220F	1452	363	305					
24 196	147	117	91					
Sta. 35D X 180I	1442	244	271					
21 173	140	112	91					

These FWD points were read in by hand from test results which were only printed out. All unneeded "drop" & test points are eliminated from this file.

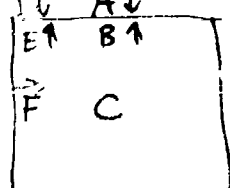
Input File: AREA#4

Test Area #4: All tests run Nov. 1. Planes covered most of the area, so only points from Sta.'s 0'-50' d were run.  
NOTE: T and T+ are Test Point T4, A,B,C,D, E,F are below.

Date: NOV. 1 1982	Temp: 24	Roadway: TEST AREA #4 (COMPOSITE)	Load Radius (mm): 150	Sensor Positions (mm):
0 200	305	610	914	1524
8	14	14	36	65
Station	Pressure	d1	d2	d3
d3	d4	d5	d6	d7
4 000T	527	77	88	
64	55	45	23	15
4 000T	516	77	88	
66	57	47	32	17
4 000T	827	129	131	
111	94	79	52	28
4 000T	830	130	119	
110	96	79	52	28
4 000T	1987	174	157	
146	127	105	69	37
4 000T	1891	173	158	
147	127	107	68	34
4 000T	1455	230	189	
193	158	139	98	45
4 000T	1458	239	209	
193	166	139	98	45
4 000T	536	73	72	
69	64	47	31	16
4 000T	533	80	72	
70	63	46	31	18
4 000T	842	133	117	
113	102	76	58	29
4 000T	841	131	119	
114	104	78	52	29
4 000T	1164	174	158	
152	133	195	69	39
4 000T	1104	174	159	
153	140	195	63	38
4 000T	1478	223	211	
200	183	139	98	48
4 000T	1472	227	212	
201	133	139	98	48
50	105	849	137	127
50 500C	86	64	44	24
50 500C	1164	179	157	
156	138	111	71	27
50 500C	1458	234	218	
203	178	142	92	4
50 500C	1557	233	213	
202	173	141	98	46
50 500B	898	159	166	
121	93	77	43	25
50 500B	1898	203	210	
159	129	132	63	35
50 500B	1452	264	275	
211	111	137	83	47
50 500B	1459	269	273	
208	169	134	83	47

58 4000	845	140	125		20 300B	1112	245	268
117 108	83	53	29		158 129	105	69	39
50 4000	1105	184	166		20 300B	1464	326	332
156 131	109	73	35		209 173	139	87	51
50 4000	1452	246	212		20 300B	1465	327	339
201 171	143	94	48		204 168	136	86	58
50 4000	1453	239	211		20 300C	830	179	178
200 170	141	94	48		150 125	95	61	32
50 4000	829	195	205		20 300C	1087	232	215
118 93	80	53	38		194 159	126	78	39
50 4000	1085	245	265		20 300C	1448	312	288
153 128	104	63	48		258 212	169	104	51
50 4000	1469	325	338		20 300C	1436	307	283
201 166	136	87	50		254 205	166	101	51
50 4000	1471	321	340		20 300C	841	169	168
199 165	134	86	50		143 120	94	59	31
50 4000	843	224	244		20 300C	1092	228	213
119 96	78	50	31		191 158	126	77	39
50 4000	1094	282	304		20 300C	1448	299	287
149 128	96	62	38		254 209	166	102	50
50 4000	1453	370	401		20 300C	1439	302	277
195 157	126	91	51		252 208	165	101	49
50 4000	1458	365	399		20 300C	839	174	162
189 152	122	78	50		143 9	95	59	31
50 2000	831	282	16		20 300C	1093	230	214
141 111	84	54	32		191 159	125	77	39
50 2000	1105	267	221		20 300C	1439	301	289
187 146	111	72	42		251 208	164	100	50
50 2000	1503	351	298		20 300C	1435	307	283
249 196	145	93	55		253 205	166	104	51
50 2000	1508	349	298		20 300D	870	154	144
245 198	144	93	52		136 113	93	60	31
50 2000	824	169	178		20 300D	1157	203	192
136 107	83	51	28		179 147	121	79	41
50 2000	1099	217	219		20 300D	1574	268	247
177 139	102	54	38		238 192	161	105	53
50 2000	1456	296	293		20 300D	1528	270	253
235 185	143	85	50		237 197	161	103	52
50 2000	1456	283	288		20 300E	866	156	182
233 182	141	84	49		171 142	112	66	32
20 1000	858	145	147		20 300E	1131	251	233
132 105	84	51	27		216 177	149	84	41
20 1000	1129	218	201		20 300E	1467	331	304
188 143	114	72	49		285 234	126	118	51
20 1000	1478	406	260		20 300E	1456	330	306
238 191	151	34	50		284 224	125	111	54
20 1000	1469	406	269		20 300E	860	200	190
237 183	158	94	51		153 120	92	55	32
20 1000	839	239	243		20 300E	1112	2	2
143 110	84	52	28		197 149	114	72	41
20 1000	111	304	304		20 300E	1457	331	304
197 149	115	68	36		259 197	152	104	51
20 1000	1440	402	395		20 300E	1463	330	306
259 133	139	91	47		159 197	152	90	54
20 1000	1442	405	397					
265 138	149	89	49					
20 300C	842	158	1					
123 109	88	58	29					
20 300C	1115	207	182					
178 144	112	77	39					
20 300C	1469	279	236					
226 191	155	93	50					
20 300C	1464	272	235					
229 139	154	92	51					
20 300C	843	188	197					
120 99	79	52	31					

↑ ↓ =  
Direction  
of Sensor



Input File: T85-1

Test Area #5: All tests  
run, morning & evening of  
Oct. 29, 1982.

[Centrifuge Tests] = C

Date: OCT 29 1982 Temp: 26.2°C  
Roadway: TEST AREA #5 (10.5" PCC)

Load Radius (mm): 150

Sensor Positions (mm):

0 230 300 600 1200 1800 2400

8 12 74 76 4t 4v

Station Pressure d1 d2

d3 d4 d5 d6 d7

Slab 2

E1 5 0100 1510 232 220

209 163 135 101 44

- 5 0100 1517 231 218

209 182 133 100

8 0300 1529 232 226

215 192 142 89

- 5 0200 1533 235 227

217 193 142 90

12 0300 1340 130 123

116 101 71 42 21

12 0300 1142 111 102

156 135 95 6 39

1 0300 1538 234 227

210 131 127 88 40

- 12 0100 1525 233 227

210 191 126 87 41

7 0400 1523 259 256

238 202 173 79 52

3 0400 1521 267 253

237 300 131 78 51

- 3 0400 1523 267 253

239 201 134 80 53

7 0500 1515 261 260

234 207 143 88 59

- 7 0500 1504 261 250

238 205 141 88 53

- 11 0500 1568 241 234

121 130 129 81 58

- 11 0600 1508 240 232

113 189 129 81 52

14 0700 1524 210 201

134 166 115 74 47

- 12 0700 1527 267 200

127 163 111 73 47

6 0800 1509 248 45

231 202 88

- 6 0800 1514 250

231 203 141 81

10 0900 1545 175 14

11 0900 150 44 36

16 1000 1574 245 231

.59 10 15 53 41

10 0900 1439 273 205

212 121 157 87 55

- 10 0900 1411 261 234

214 186 15 07 55

14 1000 151 209 264

139 165 116 75 50

- 14 1000 1507 267 251

183 144 116 76 50

1 1100 1522 258 270

234 112 151 96 52

- 1 1100 1514 255 251

234 113 151 97 61

- 1 1200 1424 248 271

214 141 131 82 52

E12 - 6 1400 1496 238 230

215 189 138 92 50

5 1500 184 152 147

140 170 72 47 26

1 9 1300 1128 209 196

188 161 106 64 37

9 1300 1451 274 267

251 215 143 55 50

- 9 1300 1500 278 267

252 218 145 96 54

13 1400 1499 248 275

221 197 151 1 66

- 13 1400 1487 242 212

219 195 149 96 66

5 1500 828 134 128

122 176 74 47 1

5 1500 1114 179 170

163 142 98 82 47

5 15 1521 238 235

212 185 127 81 1

- 5 1500 1513 275 274

213 184 128 91 50

9 1600 1509 201 194

182 160 113 75 50

- 9 1600 1513 199 193

179 158 112 72 48

13 1700 1512 220 217

203 176 124 73 50

M17 - 1 1700 1506 224 215

Input File: T85-2

NOTE:

See below for  
location of tests on  
each slab.

[Pos. F Not run w/ Joint  
Efficiency]

Date: OCT 29 1982 Temp: 26.2°C  
Roadway: TEST AREA #5 10.5" PCC  
Load Radius (mm): 150  
Sensor Positions (mm): -200 -300  
0 200 300 600 900 -100 -150

Station Pressure d1 d2

d3 d4 d5 d6 d7

E1 6 08 1464 437 482

12 110 94 374 347

5 0108 1469 417 451

130 114 97 354 325

5 0108 1465 448 392

356 279 214 507 115

5 0108 1454 426 367

334 261 198 473 129

5 0108 1468 229 238

215 189 161 223 213

5 0108 1447 214 214

201 173 148 207 200

5 0108 1455 658 762

113 99 88 572 529

5 0108 1452 64 714

118 105 93 650 519

5 0108 1442 745 616

568 436 372 870 151

5 0108 1430 691 683

556 436 326 780 152

Input File: TA5-2b

Date: OCT 24 1982 Temp: 26 C  
Roadway TEST AREA #5  
Load Radius (mm): 150  
Sensor Positions (mm): -200 -500  
0 200 300 600 900 -100 -200

Station Pressure d1 d2  
d3 d4 d5 d6 d7

5 010F 1475 384 398

383 352 312 374 364

5 010F 1477 374 379

366 339 303 359 379

8 020F 1451 481 558

129 110 95 414 381

8 020F 1463 468 534

132 113 97 395 366

8 020F 1487 461 482

365 287 218 529 129

8 020F 1467 435 388

348 269 204 499 137

12 0300 852 375 424

81 71 58 324 304

12 0300 1123 450 504

128 111 98 389 367

12 0100 1449 546 591

198 168 139 471 454

12 0200 1442 540 598

199 167 137 464 429

12 030E 848 394 352

324 262 203 451 131

12 030E 1113 462 486

373 305 238 553 204

12 030E 1443 543 484

451 365 292 617 283

12 030E 1439 536 483

448 361 279 608 288

12 030F 846 195 192

183 168 149 189 193

12 030F 1117 241 249

226 204 192 234 227

12 030F 1494 747 703

285 253 229 295 297

12 030F 1492 303 301

282 257 227 291 283

3 040F 1462 547 635

126 109 92 462 420

3 040F 1473 526 616

131 112 95 445 482

3 040B 1451 538 465

418 318 237 608 136

3 040B 1470 516 442

396 293 223 580 142

7 0500 1427 980 1129

182 156 138 918 852

7 0500 1425 978 2280

188 152 138 910 821

7 050E 1434 743 665

627 507 386 849 277

7 050E 1431 717 623

598 502 367 803 298

7 050F 1473 511 426

418 389 303 414 405

7 050F 1468 112 405

395 359 314 397 387

11 060A 1485 236 439

176 145 117 339 314

11 060F 1489 385 425

183 151 22 326 304

11 060B 1461 397 341

317 246 122 172 225

11 060E 1462 377 325

296 272 177 434 215  
11 060C 1512 230 223  
209 184 153 217 199  
11 060C 1508 216 209  
145 152 143 202 195  
14 0700 1444 569 631  
213 177 145 506 468  
14 0700 1439 363 621  
214 177 145 494 458  
14 070E 1442 633 569  
530 126 333 786 138  
14 070E 1445 617 553  
520 111 321 825 139  
14 070F 1504 332 321  
324 303 274 324 313  
14 070F 1494 324 321  
312 259 260 312 302  
6 0800 1437 821 1229  
160 137 115 760 691  
6 0800 1436 800 1339  
158 136 115 729 708  
6 080E 1442 766 700  
661 528 420 886 336  
6 080E 1439 728 665  
629 506 398 836 350  
6 080F 1474 433 427  
416 379 379 422 418  
6 080F 1474 416 405  
392 356 315 481 399  
10 090F 832 238 264  
118 96 77 207 191  
10 090P 1100 297 324  
167 175 187 255 238  
10 090R 1458 379 414  
233 186 148 328 395  
10 090R 1468 385 414  
234 187 149 326 304  
10 090E 823 261 226  
208 163 126 295 80  
10 090E 1120 321 281  
257 301 155 360 134  
10 090E 1454 405 358  
217 259 201 460 199  
10 090E 1460 403 355  
724 255 197 453 197  
10 090C 253 125 120  
114 101 87 118 115  
10 090C 1123 161 153  
148 128 108 152 148  
10 090C 15 4 214 206  
196 171 144 203 195  
10 090C 1492 210 204  
192 168 142 201 194  
14 100F 1452 667 722  
240 203 165 574 521  
14 100D 1449 616 648  
247 209 170 603 510  
14 100E 1450 690 652  
577 465 370 781 212  
14 100E 1446 671 627  
571 452 355 768 222  
14 100F 1487 315 321  
304 280 250 302 292  
14 100F 1495 303 300  
288 265 236 288 281  
1 110A 1481 428 502  
243 320 160 466 352  
1 110A 1474 406 458  
243 198 160 359 333  
1 110B 1477 448 398  
368 297 233 504 174  
1 110B 1475 425 375  
349 278 219 476 184  
5 1200 1443 671 771

H2

L3

C4  
G5

K6

N7

F8

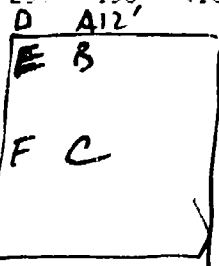
J9

N0

A11

B35

C 12      187 159      136 596 542  
 5 1200      1438 666 771  
 179 152      129 601 536  
 5 120E      1445 703 613  
 583 430      352 638 195  
 5 120E      1432 690 597  
 575 461      347 798 197  
 5 120E      1442 413 395  
 384 345      304 392 279  
 5 120E      1445 37 379  
 365 327      285 374 362  
 9 130R      849 268 299  
 170 133      104 233 216  
 9 130R      1125 329 365  
 241 188      144 285 266  
 9 130R      1455 414 453  
 323 246      190 358 335  
 9 130R      1454 410 452  
 318 249      190 356 333  
 9 130B      832 310 267  
 243 195      137 354 87  
 9 130B      146 494 426  
 386 296      221 556 211  
 9 130B      1453 478 415  
 375 287      212 541 214  
 9 130C      849 146 139  
 171 114      94 137 132  
 9 130C      1478 241 237  
 221 190      156 236 226  
 9 130C      1470 233 231  
 215 184      152 231 217  
 9 130D      832 349 392  
 229 187      149 314 290  
 9 130C      1448 525 575  
 425 336      262 483 449  
 9 130D      1452 525 574  
 427 336      264 471 438  
 9 130E      834 408 360  
 335 267      203 494 110  
 9 130E      1450 591 517  
 493 393      304 685 253  
 9 130E      1445 584 473  
 486 389      304 655 255  
 9 130F      1496 313 313  
 295 263      230 312 303  
 9 130F      1502 305 302  
 285 254      220 301 293  
 13 140R      1475 434 507  
 318 256      197 379 353  
 13 140R      1464 420 474  
 330 255      197 366 336  
 13 140R      1481 397 351  
 326 261      205 434 375  
 13 140E      1477 382 331  
 314 251      196 416 363



↓  
 E 15 F 16 24 17  
 M 14

TEST DATA FROM DRES CONSULTANTS, INC.

Data Collected with Dynatest Model 8000

Falling Weight Deflectometer

Test Area #5: All tests  
run, morning of Nov. 1.

NOTE: See direction of  
Sensor & location of  
test points on Slab below!

Date: NOV 1 1982 Temp: 22.5 C  
Roadway: TEST AREA #5 [10.5" PCC]  
Load Radius (mm): 150  
Sensor Positions (mm):

0 200 305 610 914 1524 2438

1 17 24 30 67 90

Station Pressure d1 d2

d3 d4 d5 d6 d7

Slab

E1 (repeat)

5.010A 1461 501 611

5.010B 88 62 44

5.010C 1461 476 531

5.010D 92 64 38

5.010E 1521 227 224

5.010F 152 105 67

5.010G 1518 219 212

5.010H 174 146 101 66

5.010I 145 479 702

5.010J 99 86 68 37

5.010K 1461 467 536

5.010L 90 63 41

5.010M 1425 773 853

5.010N 113 95 68 45

5.010O 1434 758 1074

5.010P 114 97 71 45

5.010Q 1431 783 1018

5.010R 122 102 71 42

5.010S 1431 777 846

5.010T 124 107 74 44

5.010U 1460 440 519

5.010V 230 173 103 37

5.010W 1474 436 459

5.010X 224 171 102 40

5.010Y 849 256 294

5.010Z 74 58 34 25

5.150A 61 1153 309 349

5.150B 103 82 52 21

5.150C 1547 388 573

5.150D 182 148 119 74

5.150E 1547 367 445

5.150F 184 151 129 79

5.150G 855 249 214

5.150H 61 41 41 21

5.150I 1129 304 211

5.150J 141 115 92 61 34

5.150K 150A 1479 373 420

5.150L 200 160 127 78 44

5.150M 1481 367 414

5.150N 195 157 124 77 43

5.150O 852 128 115

5.150P 109 93 79 55 34

5.150Q 150C 1138 161 152

5.150R 146 124 104 72 45

5.150S 150D 1584 211 205

5.150T 193 165 138 92 39

5.150U 150C 1587 212 202

5.150V 190 163 136 91 58

5.150W 843 228 247

5.150X 96 88 64 42 26

5.150Y 150B 1124 271 298

5.150Z 153 122 97 61 35

5.150A 1473 334 374

5.150B 173 136 83 46

5.150C 1476 329 364

299 173 138 83 45  
5.150D 173 835 484 393  
222 157 125 80 36  
5.150E 1111 463 502  
288 212 168 187 50  
5.150F 1451 555 1433  
403 283 220 141 63  
5.150G 1442 552 1081  
396 282 223 139 64  
5.150H 836 396 440  
198 168 129 80 37  
5.150I 1198 468 496  
267 211 185 187 51  
5.150J 1442 543 584  
357 273 223 139 61  
5.150K 1438 548 601  
359 274 222 137 61  
5.150L 838 321 74  
176 143 111 68 31  
5.150M 1154 382 4  
244 194 155 97 47  
5.150N 1523 461 58  
346 261 284 127 56  
5.150O 1522 459 483  
348 269 285 133 58  
160A 160 850 197 223  
112 87 69 42 23  
9.160A 1487 308 339  
321 174 136 81 43  
9.160B 1496 306 332  
137 172 134 81 44  
9.160C 848 182 9 28  
92 81 67 47 28  
9.160D 1506 185 179  
168 143 121 84 51  
9.160E 1506 185 176  
168 144 121 84 51  
9.160F 847 202 226  
105 84 67 42 25  
9.160G 1491 315 343  
217 168 131 79 43  
9.160H 1495 389 337  
216 167 130 79 45  
13.170C 844 113 108  
103 88 74 53 34  
13.170D 1497 206 190  
183 156 130 87 56  
from 13.170E 1504 281 191  
Oct. 29 182 156 130 86 56  
13.170F 844 336 297  
172 136 115 63 30  
13.170G 1489 416 436  
311 250 198 116 54  
13.170H 1481 420 437  
318 247 194 116 55  
13.170I 848 286 313  
136 109 86 53 28  
13.170J 1472 437 462  
292 224 177 187 51  
13.170K 1481 436 461  
297 227 180 110 54  
13.170L 832 176 236  
144 109 85 50 25  
13.170M 1529 291 318  
278 200 153 92 44  
13.170N 1533 289 311  
259 200 152 88 43  
12.030A 847 251 285  
64 55 47 75 22  
2.030B 148 199 443  
140 115 93 36  
2.030C 1486 399 434  
141 115 96 60 37  
2.030D 842 278 236  
215 169 118 67 27  
2.030E 1466 469 402  
364 270 260 110 47  
2.030F 1476 462 392

J16 (continued)

M17 (continued)

Oct. 29

83 T

355	262	195	118	45		238	186	149	93	43
2 030C		851	128	121	J8	18 00	102	810	1131	124
117	98	82	54	28		118	102	84	54	35
2 030C		1496	225	216		18 000		1495	229	222
206	174	145	91	53		211	182	151	95	47
2 030C		1499	225	213		210 0-00		1515	231	226
203	172	142	90	50		212	183	153	96	49
2 030b		847	147	283		18 030E		840	227	250
66	56	48	37	21		180	91	66	41	24
2 030b		1478	419	476		18 030B		1496	363	399
113	97	84	59	38		224	177	172	83	45
2 030b		1486	418	477	GII	18 030E		498	353	389
118	100	86	61	39		217	170	175	82	45
10 020A		826	275	310		7 110F		322	249	383
77	65	55	39	24		77	67	55	38	23
10 020A		1459	433	492		7 110F		1469	429	381
160	132	107	69	39		135		95	54	37
10 020A		1466	435	493		7		1484	421	47
156	130	106	71	40		139		99	53	37
10 020C		841	128	122		7 110F		833	265	373
118	181	85	56	31		217	183	125	73	35
10 020C		1518	229	219		141	283	1473	43	377
209	181	151	96	54		7 110F		201	116	46
10 020C		1517	229	220		7 110F		1488	428	371
209	181	152	97	55		7 110C		198	117	43
10 020B		847	257	290		7 110C		821	128	121
75	63	53	35	23		117	182	86	55	28
10 020B		1489	402	448		7 110C		1487	421	224
193	157	125	78	43		7 110C		154	103	55
10 020B		1483	394	445		7 110C		1584	231	223
194	158	126	79	45		211	183	155	103	56
10 020F		825	282	321		7 110E		838	257	289
69	59	50	36	22		7 110E		56	40	23
10 020F		1470	436	523		7 110E		1470	425	486
173	141	112	71	31		151	125	103	67	79
10 020F		1485	430	486		7 110E		1474	437	498
172	142	113	73	35		153	123	104	69	40
14 040C		848	239	271		7 110F		824	237	206
68	58	49	35	20		130	151	118	69	27
14 040C		1480	393	443		7 110F		1472	410	364
73	115	94	62	37		314	262	206	121	41
14 040C		1486	384	432		7 110F		1486	410	356
73	115	95	64	38		733	256	203	123	41
70	88	847	252	289		7 110F		842	219	348
56	47	34	19			80	79	57	39	28
14 040E		1476	429	499	L12	7 110F		1488	399	451
51	102	86	61	35		135	117	99	70	39
14 040E		1474	419	479		7 110F		1497	399	454
53	107	90	-	37		135	116	99	71	38
						7 110E		829	442	492

Input File: AP#5-2

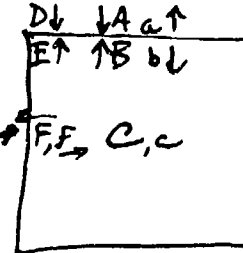
Date: NOV 1 19 Temp: 28.5  
 Friday: TEST H-ERA #5 E11.5"POOD  
 Unit: Radius (mm): 150  
 Outer Fixtures (mm):  
 8 200 70E 610 14 1524 2438

stat:	pressure	d1	d2
d3	d4	d5	d6
6 050C	848	142	132
127	108	89	58
6 050C	1496	240	230
224	191	158	101
6 050C	1584	247	238
224	191	157	101
6 050F	811	262	301
82	71	59	41
6 050F	1441	458	510
147	125	105	72
6 350F	1467	441	499
147	119	106	73
1 070C	846	148	138
172	115	93	59
1 070C	1500	240	252
202	168	109	51
70C	1505	260	247
200	167	107	52
1 070F	846	228	253
101	84	69	46
1 070F	1465	365	401
234	188	151	93
1 070F	1476	357	290

F5

A7

402	314	246	148	67
7 110E		1434	690	708
418	315	245	147	67
12 120C		838	130	122
119	103	88	59	27
12 120C		1498	232	220
212	194	155	103	52
12 120C		1496	231	220
213	194	155	105	52
12 120F		838	254	288
6	57	49	37	21
12 120F		1478	410	455
166	135	109	73	35
12 120F		1482	404	449
164	135	109	75	37



Interior Slab FWD Deflection Results from  
Apron 1-A (10-1/2 in. PCC)

Station	D1*	D2	D3	D4	Area	Wt (lbf)
O15I	8.1**	7.6	6.4	5.4	30.8	25106
K15I	8.5	7.7	6.6	5.5	30.0	23764
G15I	8.9	8.1	6.9	5.8	30.3	23672
C15I	8.8	8.0	6.9	5.7	30.2	24042
L11I	8.2	7.5	6.5	5.4	30.5	23913
H11I	9.5	8.8	7.6	6.5	30.8	23871
D11I	9.6	8.9	7.7	6.4	30.9	23831
M7I	8.9	8.0	6.9	5.7	30.0	23902
I7I	9.0	8.5	7.3	6.2	31.1	23669
F7I	9.8	9.1	7.8	6.7	30.9	23781
N3I	8.1	7.5	6.2	5.2	30.2	23778
J3I	8.9	8.3	7.1	5.9	30.7	23812
F3I	9.1	8.2	7.1	6.0	30.2	24092
B3I	8.7	8.1	6.9	5.7	30.5	23851
Ave.	8.864	8.164	6.993	5.864	30.507	23935

\*D1 = Def. in Center of Plate

D2, D3, D4 = Def. 12, 36, 48 ins. from plate

\*\*Deflection ins. x 10<sup>-3</sup>

Slab Edge (15 ft. side) FWD Deflection Results  
from Apron 1-A (10-1/2 in. PCC)

Slab	Load	D1	D2	LT*	LT adj.**
O15E1	23249	15.8	6.7	42	45
K15E1	23588	15.7	7.3	47	51
G15E1	23204	16.0	7.2	45	49
C15E1	24445	12.5	8.8	70	76
L11E1	23557	14.6	8.7	59	64
H11E1	23507	18.3	5.3	29	31
D11E1	23840	15.2	8.4	56	61
M7E1	23666	12.0	10.1	83	90
I7E1	24081	13.1	11.0	84	91
F7E1	23560	15.7	12.1	77	84
N3E1	23475	13.8	8.7	63	68
J3E1	23688	14.8	10.5	71	77
F3E1	23731	13.9	11.5	83	90
E3E1	23353	16.7	7.8	47	51
Ave.		14.864	8.864	61	66

\*LT = D2/D1

\*\*LT x 1.0857 (Adjustment for slab bending 8.864/8.164)

Slab Edge (12.5 ft. side) FWD Deflection Results  
from Apron 1-A

Slab	Load	D1	D2	LT	LT adj.*
015E2	23663	14.5	6.7	46	50
K15E2	23579	14.1	8.6	61	66
G15E2	23428	16.0	7.8	49	53
C15E2	23495	13.8	8.3	60	65
L11E2	23314	15.4	6.9	45	49
H11E2	23537	18.6	7.8	42	46
D11E2	23406	19.6	5.2	26	28
M7E2	23378	18.4	4.2	23	25
I7E2	23277	18.7	7.3	39	42
F7E2	22938	21.0	6.1	29	31
N3E2	23397	15.9	4.5	28	30
J3E2	23268	17.5	6.5	37	40
F3E2	23562	17.5	6.4	37	40
B3E2	23271	19.9	5.1	26	28
Ave.		17.21	6.53	39	42

\* LT x 8.864/8.164

Slab Corner FWD Deflection Results from  
Apron 1-A

Slab	Load	D1	D2	LT	LT adj.
015C	22584	28.2	16.5	58	63
K15C	22868	22.6	15.4	68	74
G15C	23221	23.9	14.3	60	65
C15C	23557	18.3	14.2	77	84
L11C	23336	18.9	11.1	59	64
H11C	23008	26.8	17.4	65	71
D11C	23179	25.3	4.8	19	21
M7C	22896	22.7	4.9	21	23
I7C	23078	22.1	9.1	41	45
F7C	22961	26.9	5.5	21	23
N3C	22840	27.5	6.9	25	27
J3C	22924	25.8	9.5	37	40
F3C	23307	26.6	10.1	38	41
B3C	22935	28.9	5.3	18	20
Ave.		24.61	10.36	43	47

Interior Slab FWD Deflection Results for  
Apron 1-A-1 (AC/PCC)

Slab	Load	D1	D2	D3	D4	Area
A1	23179	8.5	7.1	6.0	5.0	27.9
A2	23260	8.9	7.5	6.2	5.2	28.0
D1	23627	9.2	7.5	6.4	5.3	27.5
D2	23176	10.6	9.4	8.0	6.6	29.4
C1	23137	12.0	10.0	8.3	6.8	27.7
C2	23316	9.0	7.9	6.9	5.8	29.6
Ave.	23282	9.7	8.2	7.0	5.8	28.35

Longitudinal Edge Joint FWD Deflection Results  
for Apron 1-A-1 (AC/PCC)

Slab	Load	D1	D2	LT	LT adj.*
A1E1	23039	12.9	9.4	73	86
A2E1	23159	11.3	8.9	79	93
D1E1	23829	14.9	7.8	53	63
D2E1	23482	17.6	8.2	47	56
C1E1	23501	17.1	9.3	54	64
C2E1	23403	15.1	10.2	67	79
Ave.		14.8	9.0	62	73

\* LT x 9.7/8.2

Transverse Edge Joint FWD Deflection Results  
for Apron 1-A-1 (AC/PCC)

Slab	Load	D1	D2	LT	LT adj.*
A1E2	23078	11.6	8.5	74	88
A2E2	22980	13.5	6.7	50	59
D1E2	23454	13.0	7.1	54	64
D2E2	23039	10.2	9.2	90	100
C1E2	23198	10.4	9.0	87	100
C2E2	23073	14.3	8.9	62	73
Ave.		12.2	8.2	70	81

\* LT x 9.7/8.2

Corner FWD Deflection Results for Apron 1-A-1  
(AC/PCC)

Slab	Load	D1	D2	LT	LT adj.*
A1C	23498	14.8	11.1	75	89
A2C	24207	13.5	8.0	59	70
D1C	22882	17.3	8.0	46	54
D2C	23002	16.0	15.0	94	100
C1C	23739	12.1	10.5	86	100
C2C	22857	21.1	12.4	59	70
Ave.		15.8	10.8	70	81

\* LT x 9.7/8.2

FWD Deflection Taken at Random Cracks in AC for  
Apron 1-A-1 (AC/PCC)

Slab	Load	D1	D2	LT	LT adj.*
C2E3	23159	10.7	9.3	87	100
C2E4	23411	9.6	9.0	93	100
D1E3	23792	9.6	8.5	88	100
D1E4	23159	9.8	8.5	87	100
A1E3	23935	10.0	8.3	83	98
A1E4	23206	9.1	7.6	84	99
A2E3	23210	9.2	8.1	88	100
A2E4	23030	10.4	8.4	80	95
Ave.		9.8	8.5	86	99

\* LT x 9.7/8.2

**Slab Interior FWD Deflection Results for Taxway 33  
(FCC)**

<b>Slab</b>	<b>Lod</b>	<b>D1</b>	<b>D2</b>	<b>D3</b>	<b>D4</b>	<b>Avg.</b>
67561	24114	3.1	2.0	2.0	2.4	21.0
69961	24506	2.0	2.6	2.3	2.2	21.0
62561	24467	2.2	2.0	2.0	2.6	22.1
45061	24092	3.6	3.3	3.0	2.7	22.0
37561	24146	2.1	2.7	2.4	2.2	20.1
38751	24296	2.9	2.6	2.5	2.3	21.0
39061	24280	2.0	2.6	2.3	2.7	21.0
27561	24216	2.6	2.6	2.4	2.2	21.9
15061	24054	2.0	2.9	2.1	2.1	21.0
7561	24270	2.1	2.0	2.6	2.3	20.9
<b>Avg.</b>	<b>24146</b>	<b>2.02</b>	<b>2.73</b>	<b>2.51</b>	<b>2.32</b>	<b>21.46</b>

Longitudinal Joint FWD Deflection Results for  
Taxiway 33 (PCC)

Slab	Load	D1	D2	LT	LT adj.*
675BE1	24170	4.9	3.0	61	67
600AE1	24655	5.2	2.3	44	49
525BE1	24562	4.7	3.5	73	81
450CE1	24299	7.8	2.5	33	36
375AE1	24047	6.7	1.9	28	31
300BE1	24350	4.5	3.2	71	79
300BE1	24478	4.8	3.9	81	90
225CE1	24148	7.9	2.1	27	30
150AE1	24056	6.6	2.5	37	41
75BE1	24591	5.3	4.0	75	83
Ave,	FWD Plate on Outer Slab A		36		40
	FWD Plate on Inner Slab B		72		80
	FWD Plate on Outer Slab C		30		33 (critical)

\* LT x 3.02/2.73

Transverse Joint FWD Deflection Results for  
Taxiway 33 (PCC)

Slab	Load	D1	D2	LT	LT adj.*
675BE2	25223	6.1	2.0	33	36
600AE2	24591	6.5	2.3	35	39
525BE2	24330	5.8	1.9	33	36
450CE2	24546	4.1	3.5	87	96
375AE2	23924	5.2	3.2	62	69
300BE2	24170	4.7	2.8	59	65
300BE2	23857	6.1	2.3	38	42
225CE2	24050	6.4	3.5	56	62
150AE2	24403	5.7	3.9	67	74
75BE2	24187	8.7	1.8	21	23
Ave.		Plate on Outer Slab A	55	61	
		Plate on Inner Slab B	37	40	
		Plate on Outer Slab C	72	79	

\* LT x 3.02/2.73

Slab Corner FWD Deflection Results for Taxiway 33 (PCC)

Slab	Load	D1	D2	LT	LT adj.*
675BC	24125	8.2	4.0	48	53
600AC	25145	10.4	3.4	33	36
525BC	24039	10.0	4.4	44	49
450CC	24582	7.2	6.2	87	96
375AC	23154	9.4	4.1	43	48
300BC	23442	10.9	2.6	24	27
300BC	23336	14.3	2.0	14	15
225CC	24064	14.7	6.0	41	45
150AC	24683	10.4	8.7	84	93
75BC	23538	20.9	1.9	9	10
Ave.		Plate on Outer Slab A	53	59	
		Plate on Inner Slab B	28	31	
		Plate on Outer Slab C	64	71	

\* LT x 3.02/2.73

FWD Deflections for Taxiway 3B

<u>Position</u>	<u>Load</u>	<u>D<sub>1</sub></u>	<u>D<sub>2</sub></u>	<u>D<sub>3</sub></u>	<u>D<sub>4</sub></u>	<u>D<sub>5</sub></u>	<u>D<sub>6</sub></u>	<u>Area</u>
<b>Centerline</b>								
Sta. 50	25092	11.8*	8.9	6.3	4.5	3.3	2.4	23.8
150	23762	12.4	9.5	6.6	4.5	3.3	2.5	23.7
250	23694	11.0	8.2	5.7	3.9	2.9	2.2	23.3
350	24198	11.5	8.5	6.2	4.4	3.1	2.4	23.7
450	24162	11.8	8.9	6.4	4.5	3.3	2.5	23.9
550	24372	9.9	7.8	6.7	4.3	3.2	2.4	24.9
650	23739	12.2	9.4	6.9	6.0	3.7	2.8	29.5
Averages	24146	11.61						23.97
<b>8-10' Right</b>								
Sta. 100	23717	14.1	9.9	6.1	3.9	2.6	2.1	21.3
300	23146	10.7	12.2	7.6	6.0	3.4	2.6	20.6
600	23955	14.0	11.3	8.0	6.6	4.0	3.0	24.0
Averages	23606	15.70						21.97
<b>8-10' Left</b>								
Sta. 200	23165	19.3	18.1	8.2	6.3	3.7	2.9	20.9
400	24378	17.0	11.9	7.7	6.0	3.5	2.5	21.5
600	23638	15.0	10.8	7.6	6.1	3.7	2.8	22.7
Averages	23727	17.10						21.70
<b>18-20' Right</b>								
Sta. 200	22758	20.7	14.6	7.8	4.9	3.3	2.5	18.6
400	23215	17.6	12.0	7.2	4.6	3.2	2.6	20.7
600	23950	23.3	19.7	9.7	6.2	4.1	3.0	20.6
Averages	23007	21.5						19.97
<b>18-20' Left</b>								
Sta. 100	23310	17.0	12.4	8.2	6.6	3.8	2.7	22.4
300	27629	14.0	14.0	8.3	6.3	3.6	2.8	20.3
600	22636	25.2	13.6	7.3	4.4	2.8	2.2	17.0
Averages	22858	21.03						19.90

\*1 =  $\times 10^{-3}$

FWD Deflection for Taxiway 3

Position	Load	D <sub>1</sub>	D <sub>2</sub>	D <sub>3</sub>	D <sub>4</sub>	D <sub>5</sub>	D <sub>6</sub>	Area
<b>Centerline</b>								
Sta. 950	23179	22.6	15.5	8.8	5.7	3.9	3.0	20.6
650	22266	27.1	17.4	10.9	7.1	4.8	3.4	20.1
750	22112	26.1	16.1	9.7	6.2	4.4	3.2	19.3
850	23579	21.7	16.0	10.4	6.7	4.6	3.4	22.4
550	23070	24.6	16.9	10.9	7.3	4.9	3.4	21.3
450	25011	24.5	17.9	11.0	6.7	4.3	2.9	21.8
350	24509	23.4	18.0	11.9	7.8	5.0	3.4	23.3
250	22552	29.2	18.6	11.7	7.7	5.2	3.6	20.0
150	22470	30.6	18.9	11.4	7.0	4.4	2.9	19.3
50	25058	22.1	16.8	10.9	7.1	4.7	3.3	22.9
Averages	23381	25.19						21.08
<b>10' Right</b>								
Sta. 200	22235	39.5	20.0	9.0	5.1	3.6	2.9	15.6
400	22026	40.9	22.6	10.3	5.6	3.6	2.9	16.5
600	22233	50.2	29.0	13.9	7.2	4.4	3.2	17.1
800	21869	59.9	34.3	14.5	6.6	3.7	2.7	16.4
Averages	22090	45.08						16.55
<b>10' Left</b>								
Sta. 100	22085	50.5	26.3	10.8	5.2	3.5	2.8	15.4
300	22938	45.8	25.9	11.5	6.2	4.1	3.2	16.6
500	21757	55.6	28.1	11.7	5.8	3.7	2.7	15.2
700	22059	45.4	23.6	9.9	5.5	3.8	3.1	15.6
900	22177	43.2	21.9	9.2	4.8	3.2	2.6	15.3
Averages	22203	48.10						15.62

TEST DATA FROM LOUIS BERGER  
INTERNATIONAL, INC.

Data Collected with Model 2000  
Pavement Profiler

## MacDill AFB, Florida

L.B.I.L.

## PAVEMENT DEFLECTION SURVEY

FROM: TO:	<b>AREA #4</b>						Facility:	
						STARTING POINT:		
						DATE: <u>NO 7/15</u> TIME START:		
STATION	READING $r=0$	READING $r=1$	READING $r=2$	READING $r=3$	LOAD KIP	AT TEST POINT		REMARKS: GENERAL CONDITIONS
	1	2	3	4		cracks or rut	patch	
T4A	144	135	114	98	4.49			
T4A	65	63	49	45	2.23			
T4B	58	57	45	41	2.24			
T4B	123	121	96	58	4.48			
T4B	123	122	100	54	4.51			2 Feet back
T4B	62	55	48	37	2.23			" " "
T4C	85	64	50	30	2.23			" " "
T4C	185	134	102	67	4.52			" " "
B41	130	128	118	67	4.49			0
B41	65	62	44	31	2.18			0
B42	67	64	49	31	2.18			50'
B42	142	136	103	61	4.49			50'
B43	158	127	99	62	4.51			100'
REMARKS AND SKETCHES:						UNITS:	TIME FINISH:	

MacDill AFB, Florida PAVEMENT DEFLECTION SURVEY								
FROM: TO: AREA #4								Facility:
PAVEMENT TYPE:								STARTING POINT:
THICKNESS: (INCH)								DATE:
TEMPERATURE: °C TIME:								TIME START:
STATION	READING	READING	READING	READING	RANGE, LOAD KIP	AT TEST POINT		REMARKS: GENERAL CONDITIONS
	$r=0$	$r=1$	$r=2$	$r=3$		$r=4$	cracks or rut	
B43	71	60	44	29	2.19	*		100'
B44	57	52	41	30	2.20	*		150'
B44	117	115	79	60	4.49	*		150'
B45	174	162	118	64	4.53	*		210'
BHS	82	75	55	30	2.21	*		210'
C1A	264	222	163	84	4.51	*	Before Joint	
C1B	253	331	80	52	4.50	*	After Joint	
D1A	200	178	121	75	4.51	*	Before Joint	
D1B	221	254	84	57	4.48	*	After Joint	
D2	260	252	240	150	4.48	*		
D2	123	116	101	68	2.22	*		
REMARKS AND SKETCHES:					UNITS:	TIME FINISH:		
$* = 2 \text{ ft back}$								

MacDill AFB, Florida  
PAVEMENT DEFLECTION SURVEY

L.B.I.I.

FROM: TO:							Facility:	
PAVEMENT TYPE: THICKNESS: INCH AREA TEMPERATURE: °C TIME: 4/							STARTING POINT:	
							DATE: 5-2-72 TIME START: 0800	
STATION	READING	READING	READING	READING	RANGE, LOAD KIP	AT TEST POINT cracks or rut	REMARKS: GENERAL CONDITIONS	
	1 $r=0$	2 $r=$	3 $r=$	4 $r=$				
D3 202	171	137	80	4.46	*		100'	
D3 93	88	68	40	2.19	*		100'	
D41 126	123	116	43	4.48	*		151' before J	
D42 162	140	89	53	4.49	*		151' after J	
D5 132	123	93	87	4.48	*		200'	
D5 166	59	45	38	2.24	*		200'	
C2A 183	162	133	81	4.48	*		Before J	
C2B 199	202	143	87	4.51	*		After J	
T4A 66	72	66	25	2.25	*			
T4A 69	73	64	70	2.19				
T4A 141	138	148	113	4.52			Test point	
T4A 140	158	144	51	4.51	*			
T4A 151	147	129	126	4.51				
T4A 144	145	129	47	UNITS: *			TIME FINISH:	
REMARKS AND SKETCHES:								

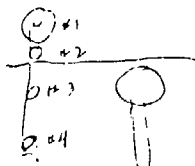
\* = 2 ft. wide - round off

## MacDill AFB, Florida

L.B.I.I.

## PAVEMENT DEFLECTION SURVEY

FROM: TO: AREA #1								Facility:
PAVEMENT TYPE:								STARTING POINT:
THICKNESS: INCH								DATE: TIME START: 9:20
TEMPERATURE: °C TIME:								REMARKS: GENERAL CONDITIONS
STATION	READING $r=1$	READING $r=2$	READING $r=3$	READING $r=4$	RANGE, LOAD KIP	AT TEST POINT		
						cracks or rut	patch	
TIA	46	43	37	27	4.50	*		
TIR	50	44	43	32	4.52	*		
TIC	9	9	8	5	1.08	*		
TIC	19	18	16	11	2.22	*		
TIC	29	28	25	17	3.32	*		
TIC	41	39	34	23	4.53	*		
TID	54	53	47	36	4.49	*	C.L.	4+00 Center
TIE <sup>A</sup>	131	115	92	53	4.51	*	C.L. B.Joint	5+00
TIE <sup>B</sup>	96	109	27	21	4.52		C.L. A.Joint	" "
TIF	44	43	33	27	4.49		C.L.	MID SLAB
TIF <sup>A</sup>	93	73	62	35	4.51		C.L.	B. Joint 4' above on slab
TIF <sup>B</sup>	88	100	31	26	4.52		C.L.	A. Joint 31, 02 on next slab
TIG	40	38	34	22	4.51		C.L.	MID SLAB
REMARKS AND SKETCHES:								UNITS:
								TIME FINISH:



## MacDill AFB, Florida

L.B.I.L.

## PAVEMENT DEFLECTION SURVEY

FROM: TO: <b>AREA #1</b>							Facility:	
PAVEMENT TYPE:							STARTING POINT:	
THICKNESS: INCH							DATE:	
TEMPERATURE: °C TIME:							TIME START:	
STATION	READING	READING	READING	READING	RANGE,	AT TEST POINT	REMARKS: GENERAL CONDITIONS	
	1 $r=0$	2 $r=$	3 $r=$	4 $r=$	LOAD KIP	cracks or rut	patch	
T1A	37	36	31	23	4.53	*	P.C.L.	MID SLAB
T1J <sup>a</sup>	85	63	56	31	4.49	*	B. Joint	long. joint
T1J <sup>b</sup>	80	99	28	22	4.51	*	A. Joint	long. joint
T1K	45	42	35	26	4.54	*	MID SLAB	
T1E <sup>a</sup>	113	86	78	48	4.48	*	F	Free edge
T1K <sup>b</sup>	537	334	157	62	4.50	*	C.L. of shoulder	
T1E <sup>b</sup>	250	139	72	28	2.21	*	C.L. of shoulder	
REMARKS AND SKETCHES:							UNITS:	TIME FINISH:

MacDill AFB, Florida PAVEMENT DEFLECTION SURVEY									L.B.I.I.
FROM: TO: Area #5								Facility:	
PAVEMENT TYPE:								STARTING POINT:	
THICKNESS: INCH								DATE:	
TEMPERATURE: °C TIME:								TIME START: 10:10	
STATION	READING $t=0$	READING $t=$	READING $t=$	READING $t=$	RANGE, LOAD KIP	AT TEST POINT		REMARKS: GENERAL CONDITIONS	
						cracks or rut	patch		
F5C	176	168	137	80	4.49	*		Reat - Center	
F5E	232	203	152	68	4.53	*		Reat - edge	
3A	155	149	120	60	4.51	*		Center	
3C	155	143	118	63	4.52	*		Center	
3E	230	236	172	71	4.52	*		edge Before	
3E	130	107	78	31	2.22	*		edge Before	
3E-J	99	110	39	19	2.21	*		After Joint	
3E-F	235	254	87	44	4.54	*		After Joint	
3I	166	159	126	67	4.53	*		Center	
3I	79	76	61	31	2.20	*		Center	
3I	130	107	73	32	2.20	*		edge	
3I	299	247	178	76	4.52	*		edge	
3I-J	215	244	77	40	4.47	*		After J.	
3I-J	102	113	37	18	2.25 *				
REMARKS AND SKETCHES:						UNITS:	TIME FINISH: "		

## MacDill AFB, Florida

## PAVEMENT DEFLECTION SURVEY

Table 1.

FROM: TO:	(APR 21) 8:15 A.M.						STATION
PAVEMENT TYPE: INCH							STATION
THICKNESS:	TIME:						STATION
TEMPERATURE: °F							REMARKS
STATION	READING 1	READING 2	READING 3	READING 4	FAIRING 10' AIR K.F.	AT TEST POINT 10' AIR K.F.	GENERAL OBSERVATIONS
314	115	118	121	123	119	119	
314	113	114	116	117	113	113	
314	121	122	123	123	121	121	
314	102	104	105	105	103	103	
314	83	84	85	85	83	83	
314	121	122	123	123	121	121	
100	602	604	605	605	604	604	
100	127	128	129	129	127	127	
100	111	111	112	112	111	111	
100	204	205	206	206	204	204	
100	131	132	133	133	131	131	
100	72	72	73	73	72	72	
REMARKS AND SKETCHES:							UNITS:



MacDill AFB, Florida										
PAVEMENT DEFLECTION SURVEY										
FROM: TO:		Area #5								
PAVEMENT TYPE:										
THICKNESS:		INCH								
TEMPERATURE:		°C		TIME:						
STATION	READING r=0	READING r=1"	READING r=2"	READING r=3"	RANGE/ LOAD KIP	AT TEST POINT		REMARKS: GENERAL CONDITIONS		
						cracks or rut	patch			
JUN 217	170	128	52	455	*			Edge -4" from edge		
JUN 241	183	136	53	4.53	*			Edge at edge		
JUN 110	88	62	24	2.19	*			Edge at edge		
JUN 195	163	115	44	4.49	*			on Edge		
JUN 92	74	54	20	3.21	*			on Edge		
JUN 89	73	56	24	3.28	*			Edge -3"		
JUN 176	165	117	51	4.52	*			Edge -3"		
JUN 154	136	104	51	4.53	*			Edge -2"		
JUN 71	63	47	32	2.26	*			Edge -2"		
JUN 144	138	114	61	4.46	*			Center		
JUN 157	148	118	54	4.54	*			Center		
JUN 147	141	114	58	4.58	*			Center		
JUN 154	146	125	60	4.46	*			Center		
REMARKS AND SKETCHES:						UNITS:	TIME FINISH:			

## MacDill AFB, Florida

L.B.I.I.

## PAVEMENT DEFLECTION SURVEY

FROM: TO:	Area 5						Facility:	
						STARTING POINT:		
						DATE:	TIME START: 11:39	
STATION	READING $\epsilon=0$	READING $\epsilon=2$	READING $\epsilon=3$	READING $\epsilon=4$	RANGE, LOAD KIP	AT TEST POINT		REMARKS: GENERAL CONDITIONS
17C	174	170	139	67	4.51	X		Center
17A	155	151	123	62	4.53	X		" "
10A	198	191	154	70	4.53	X		" "
10D	153	144	118	62	4.53	X		" "
10H	300	198	167	89	4.54	X		" "
REMARKS AND SKETCHES:						UNITS:	TIME FINISH: 11:48	

MacDill AFB, Florida PAVEMENT DEFLECTION SURVEY									L.B.T.L.
FROM: TO:									Facility:
PAVEMENT TYPE:									STARTING POINT:
THICKNESS: INCH									DATE:
TEMPERATURE: °C									TIME START: 12:34
STATION	READING 1 r=0	READING 2 r=	READING 3 r=	READING 4 r=	LOAD KSI	AT TEST POINT		REMARKS:	GENERAL CONDITIONS
						cracks or rut	patch		
0	217	151	72	64	4.50				100% 100%
0									210 150
1	174	121	77	52	1.50				
1	75	48	22	22	2.00				
2	93	63	39	28	3.00				
2	210	151	81	51	1.50				
3	225	171	99	69	4.50				
3	92	62	42	32	2.00				
4	81	51	35	21	2.00				
4	187	123	80	53	1.50				
5	151	113	76	47	4.50				
5	71	52	31	22	2.00				
6	76	51	36	21	2.00				
						TIME FINISH:			
REMARKS AND SKETCHES:						00:11:00			

MACDILL AFB, Florida  
PAVEMENT DEFLECTION SURVEY

Job #111

FROM:	TO:		PAVEMENT TYPE:		FACILITY:		
	(W/CY)						
PAVEMENT TYPE:		THICKNESS: INCH		STARTING POINT:			
TEMPERATURE °F		TIME		DATE:			
STATION	READING	READING	READING	READING	TEST	TIME	REMARKS:
1	122	125	123	124	123	12:00	ORIGINAL CONDITIONS
2	125	124	123	124	123		12' ELL LINES
3	97	95	96	98	97	9:00	3'-15' 45° S.
4	203	201	201	202	203		
5	164	161	165	177	168		
6	155	153	154	156	155		
7	72	65	71	71	72		
8	164	165	166	172	162		
9	124	121	123	121	120		
10	62	59	60	63	62		
11	22	21	22	22	22		
12	111	111	111	111	111		
13	123	121	122	121	122		
REMARKS AND SPECIMENS				QUANTITY		TIME TESTED	

## MacDill AFB, Florida

L.D.I.I.

## PAVEMENT DEFLECTION SURVEY

FROM: TO:		122472						Facility:	
PAVEMENT TYPE:								STARTING POINT:	
THICKNESS:	INCH							DATE:	
TEMPERATURE:	°F	TIME:						TIME START:	
STATION	READING #	READING	READING	READING	READING	LOAD	AT TEST POINT		REMARKS: GENERAL CONDITIONS
		1	2	3	4	FT	CRACK OF FT	PATCH	
3	32	66	4	33	2.22				@ Q
5	64	53	34	67	2.03				
7	152	111	74	52	1.48				
1	148	107	68	47	4.50				
1	66	46	36	38	2.03				
0	46	31	34	26	2.01				
0	144	111	75	52	1.47				
11	520	366	226	47	1.47				RIGHT LANE
11	211	151	97	65	2.03				≈ 30' from C.
1	201	145	86	66	2.02				
6	455	324	177	132	1.47				
5	357	251	151	101	1.47				
REMARKS AND SKETCHES:		UNITS:						TIME FINISH:	

MacDill AFB, Florida								
L.B.I.I.								
PAVEMENT DEFLECTION SURVEY								
FROM: TO: AREA 2							Facility:	
PAVEMENT TYPE:							STARTING POINT:	
THICKNESS: INCH							DATE:	
TEMPERATURE: °C TIME:							TIME START:	
STATION	READING	READING	READING	READING	LOAD KIP	AT TEST POINT		REMARKS: GENERAL CONDITIONS
	$x=0$	$x=1$	$x=2$	$x=3$		$x=4$	Cracks or rut	
.5	148	113	66	46	3.33			EIGHT LANE
4	142	108	57	40	2.16			~ 30' from 4
4	353	265	142	85	4.51			
3	373	276	165	106	4.46			
3	152	117	66	49	2.19			
3	168	121	65	41	3.34			
2	355	284	146	87	4.46			
1	327	228	129	81	1.48			
1	142	100	57	37	2.26			
0	134	104	61	39	3.31			
0	303	2410	138	93	1.47			
0	144	159	104	74	4.49			LEFT LANE, 10' off E
REMARKS AND SKETCHES:					UNITS:	TIME FINISH:		

MacDill AFB, Florida PAVEMENT DEFLECTION SURVEY								L.B.I.I.
FROM: TO: AREA 2								Facility:
PAVEMENT TYPE:								STARTING POINT:
THICKNESS: INCH								DATE:
TEMPERATURE: °C TIME:								TIME START:
STATION	READING	READING	READING	READING	LOAD KIP	AT TEST POINT		REMARKS: GENERAL CONDITIONS
	r=0	r=	r=	r=		cracks or rut	patch	
0	80	67	44	32	2.18			LEFT LANE
1	76	59	35	26	2.19			≈ 10' off CL
1	174	153	85	58	4.53			
2	198	156	95	69	4.49			
2	89	70	44	33	2.25			
3	88	67	43	34	2.21			
3	194	151	94	71	4.51			
4	220	161	96	66	4.48			
4	89	65	39	28	2.18			
5	72	53	41	21	2.21			
5	170	129	65	41	4.47			
6	158	131	81	63	4.64			
6	71	58	38	24	2.23			
REMARKS AND SKETCHES:				UNITS				TIME FINISH
7	88	72	47	35	2.17			
7	203	171	112	81	4.54			

## MacDill AFB, Florida

L.B.T.I.

## PAVEMENT DEFLECTION SURVEY

FROM: TO:	<b>AREA 2 PROFILE</b>						Facility:
						STARTING POINT:	
						DATE:	
						TIME START:	
STATION	READING $r=0$	READING $r''$	READING $r'''$	READING $r^4$	LOAD KIP	AT TEST POINT	REMARKS: GENERAL CONDITIONS
1	171	143	82	55	4.42		10' from C.L. 1 P.M. 100% " "
2	164	124	84	56	4.47		5' " "
3	165	118	61	55	4.33	-	C.C.L.
4	182	135	80	57	4.51	(T2)	5' from C.L. (Locate) " "
5	179	60	31	31	2.21	(T2)	" "
REMARKS AND SKETCHES:							TIME FINISH:

MacDill AFB, Florida PAVEMENT DEFLECTION SURVEY									L.B.I.I.	
FROM: TO: AREA # 3							Facility:			
PAVEMENT TYPE:							STARTING POINT:			
THICKNESS: INCH							DATE:			
TEMPERATURE: °C TIME:							TIME START: 2:28			
STATION	READING $t=0$	READING $t=$	READING $t=$	READING $t=$	LOAD KIP	AT TEST POINT		REMARKS: GENERAL CONDITIONS		
						cracks or rut	patch			
0	235	153	77	49	2.00			RIGHT LANE		
0	617	423	191	115	4.46			# 121 #4 C.L.		
1	601	393	197	136	4.53					
1	232	154	80	54	2.22					
2	238	143	70	48	2.19					
2	593	394	176	107	4.44					
3	762	509	232	146	4.52					
3	282	190	91	56	2.31					
4	263	172	86	55	2.23					
4	737	464	222	135	4.52					
5	113	456	226	140	4.50					
5	289	170	88	58	2.24					
REMARKS AND SKETCHES:							UNITS:	TIME FINISH:		

MacDill AFB, Florida									L.B.I.I.
PAVEMENT DEFLECTION SURVEY									
FROM: TO:		Facility:							
PAVEMENT TYPE:		STARTING POINT:							
THICKNESS: INCH		DATE:							
TEMPERATURE: °C		TIME START: 2:37							
STATION	READING $r=0$	READING $r=$	READING $r=$	READING $r=$	LOAD KIP	AT TEST POINT		REMARKS: GENERAL CONDITIONS	
	1	2	3	4	cracks or rut	patch			
6	218	142	78	53	2.03			RIGHT LANE is 12' from C.C.	
6	583	333	195	127	4.51				
7	600	377	184	118	4.49				
7	230	145	76	52	2.20				
8	214	136	73	43	2.23				
8	549	336	172	111	4.50				
9	499	374	178	108	4.48				
9	309	153	74	43	2.37				
10	179	124	66	47	2.21				
10	442	309	146	102	4.50				
REMARKS AND SKETCHES:					UNITS:	TIME FINISH:			

MacDill AFB, Florida PAVEMENT DEFLECTION SURVEY										L.B.I.I.	
FROM: TO: AREA #3								Facility:			
PAVEMENT TYPE:								STARTING POINT:			
THICKNESS: INCH								DATE:			
TEMPERATURE: °C TIME:								TIME START: 2:46			
STATION	READING	READING	READING	READING	LOAD	AT TEST POINT	REMARKS:	GENERAL CONDITIONS			
	1 2.0	2 2.0	3 2.0	4 2.0	KIP						cracks or rut
10	384	233	148	105	4.47			@ C.L.			
10	178	162	65	59	2.24						
9	133	645	60	40	2.21						
9	311	247	101	100	4.48						
8	270	192	139	101	1.50						
8	129	89	62	43	2.21						
7	133	96	57	41	2.21						
7	368	221	129	89	4.48						
6	331	212	176	105	4.47						
6	151	113	72	54	2.21						
5	151	114	75	55	2.24						
5	369	237	182	103	4.47						
REMARKS AND SKETCHES:								UNITS:	TIME FINISH:		

## MacDill AFB, Florida

L.B.I.I.

## PAVEMENT DEFLECTION SURVEY

FROM: TO:		Facility:						
PAVEMENT TYPE:		STARTING POINT:						
THICKNESS: INCH		DATE:						
TEMPERATURE: °C		TIME START: 2.59						
STATION	READING r=0	READING r=2	READING r=3	READING r=4	RANGE, LOAD KIP	AT TEST POINT		REMARKS: GENERAL CONDITIONS
						cracks or rut	patch	
4	451	324	193	136	4.48			@ CL
4	164	122	69	53	2.21			
3	145	109	73	56	2.23			
3	336	261	179	128	4.51			
2	301	213	116	94	4.51			
2	127	94	61	42	2.22			
1	133	114	75	55	2.23			
1	316	266	173	126	4.47			
0	221	263	157	112	4.53			
0	142	104	69	47	2.22			
REMARKS AND SKETCHES:						UNITS:	TIME FINISH:	

**MacBETH AERIAL PHOTOGRAPH**  
**PAVEMENT DEFLECTION SURVEY**

Ref. No. 1

FROM TO: <u>AFCN 405</u>								FACILITY:	
PAVEMENT TYPE:  THICKNESS:      INCH TEMPERATURE      °F      TIME								STANDARD RATIO	
STATION	READING 1	READING 2	READING 3	READING 4	READING 5	READING 6	AVERAGE	<p>GENERAL CONDITIONS</p> 	
	1	12.1	12.0	12.2	12.1	12.0	12.1		
	2	12.5	12.8	12.6	12.7	12.6	12.6		
	3	12.9	12.6	12.8	12.7	12.6	12.7		
	4	12.1	12.0	12.1	12.0	12.1	12.1		
	5	12.6	12.5	12.7	12.6	12.5	12.6		
	6	12.3	12.4	12.5	12.4	12.3	12.4		
	7	12.7	12.6	12.8	12.7	12.6	12.7		
	8	12.5	12.4	12.6	12.5	12.4	12.5		
	9	12.2	12.1	12.3	12.2	12.1	12.2		
	10	12.8	12.7	12.9	12.8	12.7	12.8		
	11	12.6	12.5	12.7	12.6	12.5	12.6		
	12	12.4	12.3	12.5	12.4	12.3	12.4		
	13	12.7	12.6	12.8	12.7	12.6	12.7		
	14	12.5	12.4	12.6	12.5	12.4	12.5		
15	12.3	12.2	12.4	12.3	12.2	12.3			
PENALTY / PENETRATION								TIME INDEX	
TOTAL INDEX								TIME INDEX	

Hebbell Attn. File #10  
TAXABLE PROPERTY TAXES

三

MacDill AFB, Florida PAVEMENT DEFLECTION SURVEY								L.B.I.T.
FROM: TO:	AREA # 2,						Facility:	
PAVEMENT TYPE:								STARTING POINT:
THICKNESS:	INCH						DATE:	
TEMPERATURE:	°C						TIME START:	
STATION	READING #10	READING #2	READING #3	READING #4	LOAD KIP	AT TEST POINT		REMARKS: GENERAL CONDITIONS
T3	101	113	21	25	1.10	CRACKS OFFUT	PATCH	T3
T3	233	116	31	53	2.20			T3
T3	1104	151	132	31	3.33			T3
T3	1751	1416	184	111	4.49			T3
A	110	112	40	34	1.14			T4
B	243	141	116	43	2.24			T4
C	321	127	123	74	1.31			T4
D	1623	421	182	113	4.49			T4
REMARKS AND SKETCHES:								TIME FINISH:

MacDill AFB, Florida L.B.I.I. PAVEMENT DEFLECTION SURVEY								
FROM: TO:		AREA #3					Facility:	
PAVEMENT TYPE:		T3 - PROFILE					STARTING POINT:	
THICKNESS: INCH							DATE:	
TEMPERATURE: °C		TIME:					TIME START: 3:42	
STATION	READING $r=0$	READING $r=$	READING $r=$	READING $r=$	LOAD KIP	AT TEST POINT		REMARKS: GENERAL CONDITIONS
						cracks or rut	patch	
1	460	291	167	105	4.49			LEFT LANE 5' off E
1	183	120	73	38	2.31			" " "
2	127	106	70	45	3.34			on R
2	305	235	154	107	4.49			on E
3	449	316	186	99	4.49			RIGHT LANE, 5' off E
3	192	137	62	53	2.34			" " "
4	226	179	85	53	2.20			" " 10' off R
4	627	407	215	126	4.49			" " "
5	729	465	173	117	4.49			" " 22' off E
5	307	255	85	56	2.24			" " "
6	404	314	129	80	2.20			" " 32' off R
6	1036	723	326	197	4.49			" " "

MacDill AFB, Florida  
PAVEMENT DEFLECTION SURVEY

L.D.L.A.

MacDill AFB, Florida PAVEMENT DEFLECTION SURVEY									
L.D.L.A.									
FROM: <u>APEN AFB</u> TO: _____									
PAVEMENT TYPE: _____									
THICKNESS: INCH _____									
TEMPERATURE: °F _____ TIME: _____									
STATION	READING F=0	READING F=1	READING F=2	READING F=3	READING F=4	MEAN F=1	AT TEST POINT	REMARKS	
71	1038	607	305	210	1150	1150	AT TEST POINT	GENERAL CONDITIONS	
77	4600	337	157	107	2.2	2.2	AT TEST POINT	GENERAL CONDITIONS	
							AT TEST POINT	GENERAL CONDITIONS	
							AT TEST POINT	GENERAL CONDITIONS	
							AT TEST POINT	GENERAL CONDITIONS	
							AT TEST POINT	GENERAL CONDITIONS	
							AT TEST POINT	GENERAL CONDITIONS	
							AT TEST POINT	GENERAL CONDITIONS	
							AT TEST POINT	GENERAL CONDITIONS	
REMARKS AND SKETCHES:								DATE	TIME FINISH

TEST DATA FROM REINARD W. BRANDLEY

Data Collected with Dynatest Model  
8000 Falling Weight Deflectometer  
and Brandley Cantilever Beam

TABLE NO A2

Load Radius 100mm  
no" PCC

## FWD DATA - TEST AREA 7

AFB DILL AFB  
Nov. 1, 1982

Span	Offset	Load	Temp	Deflection in Microns		Distance R from Load mm			
				R=0	R=200	R=305	R=410	R=514	R=624
<u>Span 1000 mm</u>									
0031	4.00	1527	39	74	72	67	62	57	47
0033	6	1528		80	79	73	67	61	51
0037	256	1538		75	71	67	61	55	45
0038	258	1539		74	73	69	64	58	47
0039	6	1528		75	70	66	59	54	44
0042	156	1539		78	72	68	62	56	45
0043	158	1539		73	68	65	59	53	42
0044	6	1528		77	73	66	60	54	44
0045	256	1526		75	69	67	63	56	44
<u>Span 1000 mm</u>									
0037	4.00	823		43	42	39	37	34	29
0039	6	828		47	45	42	40	36	31
0041	254	826		46	41	39	36	34	27
0042	254	833		45	44	41	37	35	29
0043	6	823		42	40	38	36	32	27
0044	156	812		44	42	39	36	33	27
0045	158	826		43	39	37	34	31	25
0046	6	834		43	37	38	34	31	26
0047	254	821		43	39	37	34	30	26
<u>Span 1000 mm</u>									
0031	4.00	1511		108	110	95	73	64	47
0032	6	1513		106	108	60	52	48	35
0033	(6)	1513		107	103	75	66	59	40
0034	(2.5)	1512		107	103	83	71	63	46
0035	(2.5)	1513		79	106	98	80	68	51
0037	(2.5)	1512		102	106	60	53	47	38
0038	(2.5)	1513		101	101	77	67	58	47
0039	(2.5)	1501		107	102	65	57	50	38
0040	(2.5)	1501		105	103	52	31	27	32
0041	(2.5)	1501		105	105	61	54	47	35
0042	(2.5)	1511		104	103	74	64	55	41
<u>Span 1000 mm</u>									
0031	4	801		127	120	90	76	68	53
0033	6	1511		136	145	78	65	61	47

TABLE A 3

A- <sup>en</sup> 2		117AC		FWD DATA - TEST AREA #2.				McD. II ABC			
Load Radius	150mm	18 FT Right of &				Nov 1, 1982					
Str. Line	Load	Deflection in Microns at Distance R from Load - mm								Type	
		KPa	16	R=0	R=200	R=305	Radius	R=914	R=1524	R=2438	
0+00	2:64	828	302	236	186	111	74	39	21	13:304	
	1452	521	415	333	202	134	70	38	38		
1+00	2:72	845	374	228	172	95	59	32	19	13:304	
	1437	698	471	295	167	105	57	31	31		
2+00	2:75	839	393	266	222	118	72	37	21	13:304	
	1424	432	431	368	201	125	63	34	34		
3+00	2:78	847	346	266	167	111	67	35	21	13:304	
	1438	581	441	335	194	122	63	35	35		
4+00	2:82	852	243	196	165	100	63	35	22	13:304	
	1462	422	345	287	178	115	63	34	34		
4+00	2:83	1458	416	347	284	176	116	61	37		
5+00	2:86	847	334	251	184	93	52	26	17	13:304	
	1441	533	385	291	149	84	43	25	25		
6+00	2:89	845	341	260	209	128	79	40	22	13:304	
	1427	580	452	368	228	146	74	38	38		
7+00	2:92	830	543	360	290	148	84	40	23	13:304	
	1387	834	578	465	250	148	70	40	40		

TABLE A4

Area 2 Load Radius		11' NO 150 mm	FWD DATA - TEST AREA #2						Mo D. 11 1982 Nov. 1, 1982	
Stn	Line	Load	0	200	305	410	514	619	724	838
		KPc	lb	"1	"2	"3	"4	"5	"6	"7
0+00	2:45	836	308	221	185	118	77	41	24	
	1462		531	415	335	215	143	73	38	
1+00	2:48	844	302	178	144	99	68	36	21	
	1471		483	319	261	161	124	67	36	
2+00	2:51	818	291	238	194	120	76	38	22	
	1407		511	408	340	211	135	68	37	
3+00	2:54	845	264	213	173	109	70	36	21	
	1448		505	362	304	164	115	64	35	
4+00	2:57	814	441	287	221	121	70	35	20	
	1391		716	486	375	210	127	62	37	
5+00	2:60	847	301	245	198	118	74	38	23	
	1434		530	431	354	215	134	66	37	
6+00	2:63	829	324	234	193	103	62	33	20	
	1431		557	411	326	109	116	62	36	
7+00	2:66	830	325	246	206	126	79	40	25	38.0 °
	1423		556	422	358	222	143	71	41	13:50 am

TABLE A5

Area 2 11' AC  
Radius 150-mm FWD DATA - TEST AREA NO. 2 Mc Dowell AFB  
2' R of Center Line Nov 1, 1982

STA	Line	Load	Deflection in Millions of Millions of Distance R from Load - mm							T <sub>avg</sub> °C
			R=10	R=200	R=305	R=500	R=714	R=1071	R=2438	
0+25	2-3	829	158	182	114	81	58	34	19	33
		1476	293	497	216	152	105	63	35	35
0+75	2-6	823	162	184	133	90	63	34	19	
		1485	336	588	249	167	115	61	35	
1+25	2-9	852	202	165	129	93	63	35	20	
		1454	368	754	256	171	119	62	34	
1+75	2-12	817	208	171	145	94	62	32	18	
		1444	374	806	267	176	117	60	35	
2+25	2-15	857	155	137	117	81	57	33	18	
		1468	290	450	220	153	106	58	33	
2+75	2-18	853	173	148	130	92	65	35	20	111864
		1470	320	576	241	171	121	66	35	
3+25	2-21	819	161	153	125	91	69	35	20	
		1453	331	581	244	171	118	63	35	
3+75	2-24	843	165	143	125	86	59	33	18	
		1460	312	463	433	163	113	60	34	
4+25	2-27	892	180	141	118	79	54	31	15	
		1453	314	454	215	147	102	55	33	
4+75	2-30	853	180	146	123	86	62	35	18	
		1468	320	571	223	161	119	66	35	
5+25	2-33	867	168	142	124	84	71	40	22	
		1505	311	467	227	177	121	72	37	
5+75	2-36	848	162	130	118	82	58	33	18	
		1487	297	493	214	153	108	58	31	
6+25	2-39	847	166	140	114	82	57	32	20	
		1458	307	570	225	155	107	63	36	
6+75	2-42	850	170	147	119	74	68	35	21	
		1474	313	518	245	177	115	35	28	

TABLE A6

Area No. 3 SK "AC"  
Load Radius 150mm

Nov 1, 1982  
FWD DATA  
T/w Center Line.

McDill AFB

STA	Line	Load KPa	Deflection in Millimeters at Distances R from Load - mm								Temp °C
			16	R=0	R=200	R=305	R=610	R=914	R=1514	R=2438	
0+25	3:3	858	503	384	266	160	92	40	36	38	14404
		1470	792	578	415	263	156	69	49	49	
0+15	3:6	861	378	289	254	158	99	48	43	43	14404
		1503	637	505	423	262	168	80	44	44	
1+25	3:9	845	372	288	251	156	99	45	27	14404	14404
		1461	638	505	428	269	171	80	45	45	
1+75	3:12	866	391	323	276	164	99	42	24	24	14404
		1524	684	530	528	285	176	77	43	43	
1+0	3:15	579	230	186	152	83	58	31	19	19	14404
		860	392	313	263	162	100	45	29	29	
		1133	501	380	327	202	127	60	70	70	
		1493	724	562	482	292	179	79	48	48	
2+75	3:21	873	344	285	240	151	90	45	24	24	14404
		1183	442	371	305	193	123	60	34	34	
		1543	607	516	425	264	172	78	42	42	
3+25	3:24	864	361	300	260	162	108	46	25	25	14404
		1137	461	378	345	211	136	61	32	32	
		1516	648	522	448	289	187	82	42	42	
3+75	3:27	939	353	419	337	200	118	44	23	34	14404
		1447	924	681	555	329	201	83	41	41	
4+25	3:30	858	368	249	201	131	91	54	31	31	14404
		1505	666	438	368	245	170	100	55	55	
4+75	3:33	851	402	252	285	127	102	45	27	27	14404
		1457	849	616	785	270	103	75	36	36	
5+25	3:36	867	391	332	290	170	102	43	24	24	14404
		1509	678	588	472	299	184	82	51	51	
5+75	3:39	856	452	347	274	151	93	45	23	23	14404
		1466	901	362	467	263	146	82	50	50	

TABLE A6 cont

Area No 3 5 $\frac{1}{2}$ " AC  
Load Radius 150 mm

Nov 1, 1922  
P.W.D. DATA  
T/W Conditions - Cont.

No Drill AFC

STA	Line	Load KPa	16	Deflection in Microns at Distances R from Load - mm						Temp °C
				R=0	R=200	R=305	R=610	R=914	R=1524	
6+25'	3:42	834	516	382	296	156	95	44	26	
		1412								
6+25'	3:45	832	467	352	271	170	96	48	27	
		1413	815	594	503	273	173	81	46	
6+75'	3:48	831	548	390	264	149	86	43	25	
		1420	898	624	477	257	153	77	47	
7+25'	3:51	863	363	293	240	147	92	45	25	
		1510	644	587	429	245	161	81	46	
7+75'	3:54	846	441	343	251	137	87	44	25	
		1463	750	545	419	224	149	77	46	
8+25'	3:57	844	442	354	270	144	81	41	23	
		1441	711	577	543	246	147	77	43	
8+75'	3:60	871	362	282	241	150	96	43	28	
		1508	649	500	422	262	169	78	42	
9+25'	3:63	862	316	257	216	136	88	44	25	
		1501	556	475	382	241	157	78	46	
9+75'	3:66	844	359	303	236	143	93	45	25	
		1463	610	495	407	249	162	80	46	

ABCD 123

EWU Test 4A74

Last Radius 100mm 18' L of Taxing L.

TADDEI - 27

Page 2 of 11 Date 8/2023

Page 1 / 833

STA	LINE	LBDW KIPS	Deflection in Millions at Distances R from Load - mm								Temp °C
			R=0	R=200	R=300	R=400	R=500	R=600	R=700	R=800	
4+00	2:3	800	980	680	480	183	89	40	22		
		1375	1252	850	644	266	140	74	43		
1400	2:6	786	1165	775	573	109	72	42	29		
		1375	1310	980	650	231	114	76	49		
2+00	2:9	815	980	587	398	143	70	40	26		
		1404	1210	811	555	241	116	66	40		
3+00	2:12	810	803	573	415	158	79	40	25		
		1441	1150	854	629	255	131	66	42		
4+00	2:15	794	1047	720	508	189	78	30	21		
		1370	1326	959	720	302	145	66	42		
5+00	2:18	794	1000	656	436	151	65	32	23		380
		1370	1245	932	612	246	128	67	44		
6+00	2:21	798	914	614	412	144	67	36	25		
		1374	1235	830	600	246	132	75	46		
7+00	2:24	786	831	564	360	146	66	35	24		
		1376	1110	763	551	238	130	73	46		
8+00	2:27	724	796	536	386	146	67	35	25		
		1376	1067	388	552	234	126	71	47		
9+00	2:30	808	792	547	356	127	58	32	23		
		1388	1021	738	494	203	109	62	41		
10+00	2:33	819	653	456	334	126	53	33	21		
		1389	914	644	485	210	115	67	42		

Brugt vedligeholdelse - 5%

TABLE A-3

STA Line	LOAD KPa	FWD TEST DATA							McD-II AFB Nov 1, 1983
		16 R=0	R=200	R=305	R=610	R=114	R=2524	R=2405	
0800 3:09	791	1011	681	467	170	80	38	21	
	1372	1358	818	678	272	142	72	41	
1100 3:12	806	843	601	426	151	75	44	28	30.5°
	1378	1146	821	583	257	139	90	48	1520.4°
2100 3:15	800	923	629	427	151	75	42	25	
	1370	1227	877	594	242	131	78	47	
4100 3:18	809	906	657	469	163	87	38	24	
	1367	1247	906	662	292	146	74	43	
4800 3:51	794	1010	715	508	203	94	37	23	
	1366	1355	870	693	289	149	71	43	
5100 3:184	813	796	553	383	152	93	45	25	
	1372	1251	898	646	274	147	77	45	
6100 3:27	797	1004	802	577	236	108	39	24	
	1363	1425	950	770	343	174	78	46	
7100 3:30	806	906	592	429	190	97	46	29	
	1363	1222	616	669	286	159	84	50	
8100 3:33	811	740	520	367	157	82	40	20	
	1376	1032	720	527	243	140	76	46	
9100 3:36	804	933	631	444	182	84	35	24	
	1378	1239	840	574	253	131	65	44	

PAGE A9

MELT AND WO DATA 11/1/61  
TEST AREA NO. 4, \* ONE POUND TESTS.

Test Location	Position Time °C.	Load Kg.	Difference Hg.	Difference mm.	Percent Error	Load Kg.	Difference Hg.	Difference mm.	Percent Error
T.P. 74	26.0	1936	110	105	1.03	1600	115	110	0.6
T.P. 74	1925*	165	100	100	0.63	135	95	95	0.6
0130 A	1930	129	100	100	0.76	170	100	100	0.5
0130 A	1935*	165	100	100	0.63	125	85	85	0.5
0130 B	1925	190	100	100	0.51	135	100	100	0.4
0130 B	1920	125	100	100	0.63	105	100	100	0.4
0130 C	1935	120	100	100	0.83	135	100	100	0.7
0130 D	1920	120	100	100	0.67	135	100	100	0.7
0130 E	1925	120	100	100	0.83	135	100	100	0.7
0130 F	1925	120	100	100	0.83	135	100	100	0.7
0130 G	1925	120	100	100	0.83	135	100	100	0.7
0130 H	1925	120	100	100	0.83	135	100	100	0.7
0130 I	1925	120	100	100	0.83	135	100	100	0.7
0130 J	1925	120	100	100	0.83	135	100	100	0.7
0130 K	1925	120	100	100	0.83	135	100	100	0.7
0130 L	1925	120	100	100	0.83	135	100	100	0.7
0130 M	1925	120	100	100	0.83	135	100	100	0.7
0130 N	1925	120	100	100	0.83	135	100	100	0.7
0130 O	1925	120	100	100	0.83	135	100	100	0.7
0130 P	1925	120	100	100	0.83	135	100	100	0.7
0130 Q	1925	120	100	100	0.83	135	100	100	0.7
0130 R	1925	120	100	100	0.83	135	100	100	0.7
0130 S	1925	120	100	100	0.83	135	100	100	0.7
0130 T	1925	120	100	100	0.83	135	100	100	0.7
0130 U	1925	120	100	100	0.83	135	100	100	0.7
0130 V	1925	120	100	100	0.83	135	100	100	0.7
0130 W	1925	120	100	100	0.83	135	100	100	0.7
0130 X	1925	120	100	100	0.83	135	100	100	0.7
0130 Y	1925	120	100	100	0.83	135	100	100	0.7
0130 Z	1925	120	100	100	0.83	135	100	100	0.7

TABLE 1A10

Period Averages  
July 1960 - June 1961

Year	Month	Period	Clim.	Definitions in Millions of				Percent of Previous Year			
				1960	1960/61	1961	Period	1960	1961		
<u>Period Averages</u>											
1960	8	1960	1960	8.11	8.93	10.1	1960	107	91	68	
1960	9	1960	1960	8.81	8.83	8.90	1960	104	103	55	
1960	10	1960	1960	8.82	8.50	8.86	1960	107	108	51	
1960	11	1960	1960	8.96	8.98	8.94	1960	107	101	57	
1960	12	1960	1960	8.85	8.19	8.89	1960	102	90	51	
1961	1	1961	1961	8.59	8.10	8.87	1961	117	109	66	
1961	2	1961	1961	8.62	8.96	10.0	1961	106	94	56	
1961	3	1961	1961	8.62	8.96	10.0	1961	106	94	51	
1961	4	1961	1961	8.62	8.96	10.0	1961	106	94	51	
1961	5	1961	1961	8.62	8.96	10.0	1961	106	94	51	
1961	6	1961	1961	8.62	8.96	10.0	1961	106	94	51	
1961	7	1961	1961	8.62	8.96	10.0	1961	106	94	51	
1961	8	1961	1961	8.62	8.96	10.0	1961	106	94	51	
1961	9	1961	1961	8.62	8.96	10.0	1961	106	94	51	
1961	10	1961	1961	8.62	8.96	10.0	1961	106	94	51	
1961	11	1961	1961	8.62	8.96	10.0	1961	106	94	51	
1961	12	1961	1961	8.62	8.96	10.0	1961	106	94	51	
<u>Period Standard Deviations</u>											
1960	8	1960	1960	2.76	3.16	3.77	1960	113	77	43	
1960	9	1960	1960	2.77	2.63	2.73	1960	121	82	42	
1960	10	1960	1960	2.73	2.79	2.82	1960	119	76	41	
1960	11	1960	1960	2.73	2.79	2.77	1960	119	66	38	
1960	12	1960	1960	2.73	2.79	2.77	1960	119	68	37	
1961	1	1961	1961	2.73	2.79	2.77	1961	119	70	39	
1961	2	1961	1961	2.73	2.79	2.77	1961	119	70	39	
1961	3	1961	1961	2.73	2.79	2.77	1961	119	70	39	
1961	4	1961	1961	2.73	2.79	2.77	1961	119	70	39	
1961	5	1961	1961	2.73	2.79	2.77	1961	119	70	39	
1961	6	1961	1961	2.73	2.79	2.77	1961	119	70	39	
1961	7	1961	1961	2.73	2.79	2.77	1961	119	70	39	
1961	8	1961	1961	2.73	2.79	2.77	1961	119	70	39	
1961	9	1961	1961	2.73	2.79	2.77	1961	119	70	39	
1961	10	1961	1961	2.73	2.79	2.77	1961	119	70	39	
1961	11	1961	1961	2.73	2.79	2.77	1961	119	70	39	
1961	12	1961	1961	2.73	2.79	2.77	1961	119	70	39	
<u>Period Standard Deviations</u>											
1960	8	1960	1960	2.45	2.45	2.38	1960	113	121	47	
1960	9	1960	1960	2.45	2.45	2.38	1960	113	121	47	
1960	10	1960	1960	2.45	2.45	2.38	1960	113	121	47	
1960	11	1960	1960	2.45	2.45	2.38	1960	113	121	47	
1960	12	1960	1960	2.45	2.45	2.38	1960	113	121	47	
1961	1	1961	1961	2.45	2.45	2.38	1961	113	121	47	
1961	2	1961	1961	2.45	2.45	2.38	1961	113	121	47	
1961	3	1961	1961	2.45	2.45	2.38	1961	113	121	47	
1961	4	1961	1961	2.45	2.45	2.38	1961	113	121	47	
1961	5	1961	1961	2.45	2.45	2.38	1961	113	121	47	
1961	6	1961	1961	2.45	2.45	2.38	1961	113	121	47	
1961	7	1961	1961	2.45	2.45	2.38	1961	113	121	47	
1961	8	1961	1961	2.45	2.45	2.38	1961	113	121	47	
1961	9	1961	1961	2.45	2.45	2.38	1961	113	121	47	
1961	10	1961	1961	2.45	2.45	2.38	1961	113	121	47	
1961	11	1961	1961	2.45	2.45	2.38	1961	113	121	47	
1961	12	1961	1961	2.45	2.45	2.38	1961	113	121	47	

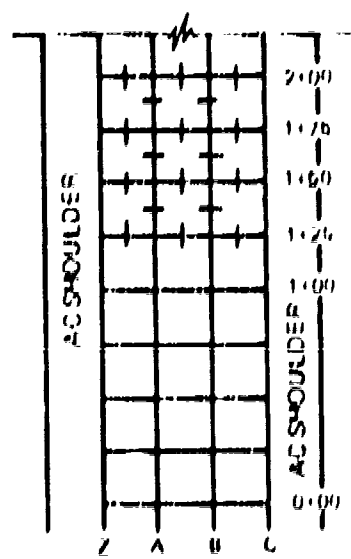
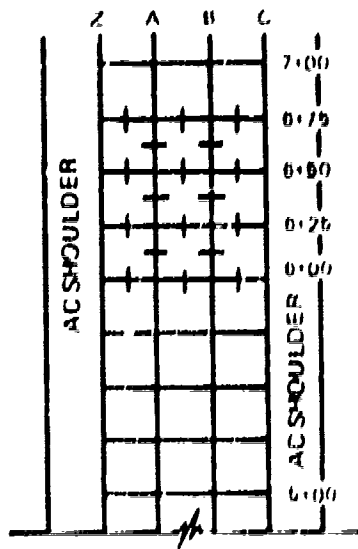
APPENDIX C  
PCC JOINT EFFICIENCY TEST DATA:  
INDEX, PLATES and TABLES

PLATES

<u>Plate No.</u>	<u>Title</u>
C1	Test Area No. 1 - Location Map
C2	Test Area No. 5 - Location Map

TABLES

<u>Table No.</u>	<u>Title</u>
C1	Test Area No. 1 - Joint Testing - Slab Rocking
C2	Test Area No. 5 - Joint Testing - Slab Rocking



LEGEND



JOINT  
NUMBERS

SLAB TESTING  
MCDILL AFB  
11-2-82  
TEST AREA 1

PLATE C1

## TABLE C1 MEDIAN

MANUFACTURER = SCAN Rocking

PICKUP DATE 7-19-62

TEST SITE #1

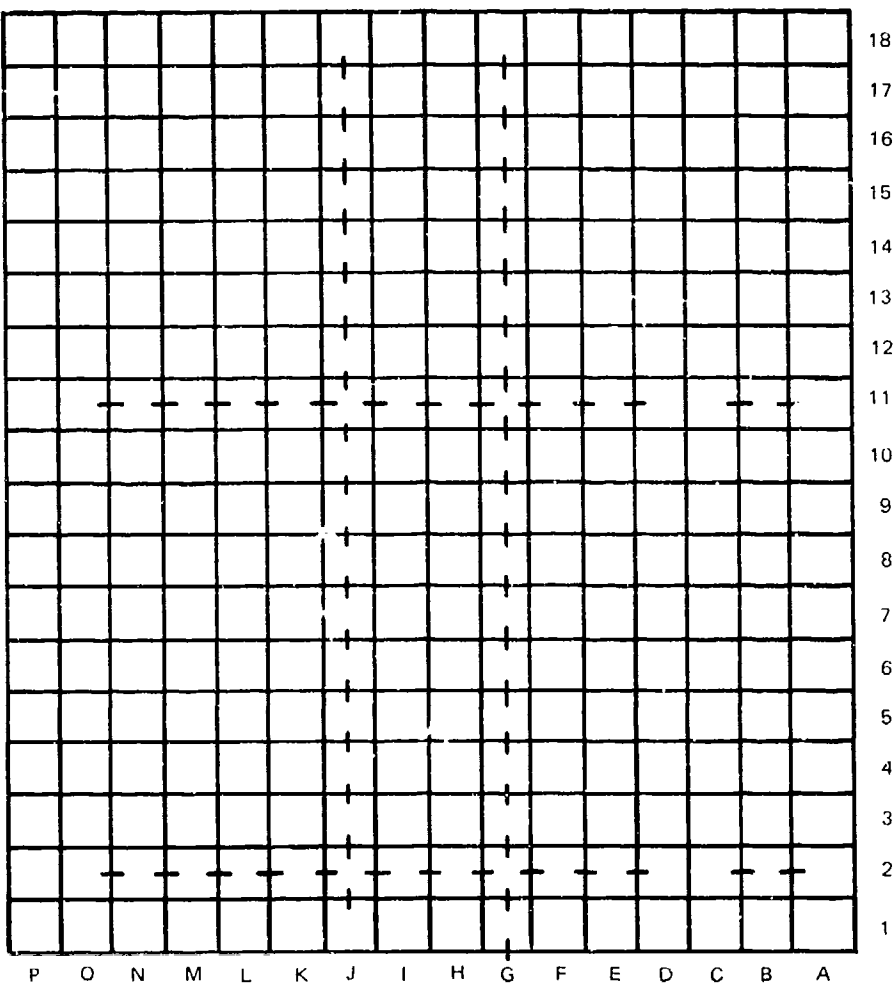
JDMN #	Slab Rocking - inch	
	Wheel #1	Wheel #2
1700 7-10 A	.001	.001
1700 7-10 B	.001	0
1700 7-10 C	.001	.001
1700 7-10 D	.001	.001
1700 7-10 E	.001	.001
1700 7-10 F	.001	.001
1700 7-10 G	.001	.001
1700 7-10 H	.001	.001
1700 7-10 I	.001	.001
1700 7-10 J	.001	.001
1700 7-10 K	.001	.001
1700 7-10 L	.001	.001
1700 7-10 M	.001	.001
1700 7-10 N	.001	.001
1700 7-10 O	.001	.001
1700 7-10 P	.001	.001
1700 7-10 Q	.001	.001
1700 7-10 R	.001	.001
1700 7-10 S	.001	.001
1700 7-10 T	.001	.001
1700 7-10 U	.001	.001
1700 7-10 V	.001	.001
1700 7-10 W	.001	.001
1700 7-10 X	.001	.001
1700 7-10 Y	.001	.001
1700 7-10 Z	.001	.001
1700 7-10 AA	.001	.001
1700 7-10 BB	.001	.001
1700 7-10 CC	.001	.001
1700 7-10 DD	.001	.001
1700 7-10 EE	.001	.001
1700 7-10 FF	.001	.001
1700 7-10 GG	.001	.001
1700 7-10 HH	.001	.001
1700 7-10 II	.001	.001
1700 7-10 JJ	.001	.001
1700 7-10 KK	.001	.001
1700 7-10 LL	.001	.001
1700 7-10 MM	.001	.001
1700 7-10 NN	.001	.001
1700 7-10 OO	.001	.001
1700 7-10 PP	.001	.001
1700 7-10 QQ	.001	.001
1700 7-10 RR	.001	.001
1700 7-10 SS	.001	.001
1700 7-10 TT	.001	.001
1700 7-10 UU	.001	.001
1700 7-10 VV	.001	.001
1700 7-10 WW	.001	.001
1700 7-10 XX	.001	.001
1700 7-10 YY	.001	.001
1700 7-10 ZZ	.001	.001
1700 7-10 AAA	.001	.001
1700 7-10 BBB	.001	.001
1700 7-10 CCC	.001	.001
1700 7-10 DDD	.001	.001
1700 7-10 EEE	.001	.001
1700 7-10 FFF	.001	.001
1700 7-10 GGG	.001	.001
1700 7-10 HHH	.001	.001
1700 7-10 III	.001	.001
1700 7-10 JJJ	.001	.001
1700 7-10 KKK	.001	.001
1700 7-10 LLL	.001	.001
1700 7-10 MLL	.001	.001
1700 7-10 NLL	.001	.001
1700 7-10 OLL	.001	.001
1700 7-10 PLL	.001	.001
1700 7-10 QLL	.001	.001
1700 7-10 RLL	.001	.001
1700 7-10 SLL	.001	.001
1700 7-10 TLL	.001	.001
1700 7-10 ULL	.001	.001
1700 7-10 VLL	.001	.001
1700 7-10 WLL	.001	.001
1700 7-10 XLL	.001	.001
1700 7-10 YLL	.001	.001
1700 7-10 ZLL	.001	.001
1700 7-10 AAAA	.001	.001
1700 7-10 BBBB	.001	.001
1700 7-10 CCCC	.001	.001
1700 7-10 DDDD	.001	.001
1700 7-10 EEEE	.001	.001
1700 7-10 FFFF	.001	.001
1700 7-10 GGGG	.001	.001
1700 7-10 HHHH	.001	.001
1700 7-10 IIII	.001	.001
1700 7-10 JJJJ	.001	.001
1700 7-10 KKKK	.001	.001
1700 7-10 LLLL	.001	.001
1700 7-10 MLLL	.001	.001
1700 7-10 NLLL	.001	.001
1700 7-10 OLLL	.001	.001
1700 7-10 PLLL	.001	.001
1700 7-10 QLLL	.001	.001
1700 7-10 RLLL	.001	.001
1700 7-10 SLLL	.001	.001
1700 7-10 TLLL	.001	.001
1700 7-10 ULLL	.001	.001
1700 7-10 VLLL	.001	.001
1700 7-10 WLLL	.001	.001
1700 7-10 XLLL	.001	.001
1700 7-10 YLLL	.001	.001
1700 7-10 ZLLL	.001	.001
1700 7-10 AAAAA	.001	.001
1700 7-10 BBBBB	.001	.001
1700 7-10 CCCCC	.001	.001
1700 7-10 DDDDD	.001	.001
1700 7-10 EEEEE	.001	.001
1700 7-10 FFFFF	.001	.001
1700 7-10 GGGGG	.001	.001
1700 7-10 HHHHH	.001	.001
1700 7-10 IIIII	.001	.001
1700 7-10 JJJJJ	.001	.001
1700 7-10 KKKKK	.001	.001
1700 7-10 LLLLL	.001	.001
1700 7-10 MLLLL	.001	.001
1700 7-10 NLLLL	.001	.001
1700 7-10 OLLLL	.001	.001
1700 7-10 PLLLL	.001	.001
1700 7-10 QLLLL	.001	.001
1700 7-10 RLLLL	.001	.001
1700 7-10 SLLLL	.001	.001
1700 7-10 TLLLL	.001	.001
1700 7-10 ULLLL	.001	.001
1700 7-10 VLLLL	.001	.001
1700 7-10 WLLLL	.001	.001
1700 7-10 XLLLL	.001	.001
1700 7-10 YLLLL	.001	.001
1700 7-10 ZLLLL	.001	.001

TABLE C1 (cont.)

McDILL AFB

SLAB TESTING  
NOVEMBER 2, 1952  
Test Site No 1

Joint N.	SLAB ROCKING-INCH	
	Wheel #1	Wheel #2
630-675A	.002	.001
630-675B	.001	.002
625-650A	.002	.002
625-650B	.001	.001
600-625 A	.003	.001
600-625 B	.003	.002



LEGEND



2-SLAB  
NUMBER

JOINT  
TESTED

**SLAB TESTING**  
**11-2-82**  
**MCDILL AFB**  
**TEST AREA 5**

PLATE C2

TABLE C2

MacLean AFC

Slab Tearing - Slab Rocking  
Tilometer 2.922  
Tilt Angle = 5

Joint No.	<u>SLAB ROCKING - INCH</u>	
	<u>Wheel #1</u>	<u>Wheel #2</u>
J 1-2	.010	.003
J 2-3	.008	.007
J 3-4	.005	.003
J 4-5	.010	.007
J 5-6	.007	.005
J 6-7	.006	.006
J 7-8	.004	.002
J 8-9	.008	.004
J 9-10	.003	.002
J 10-11	.006	.004
J 11-12	.006	.001
J 12-13	.006	.003
J 13-14	.005	.002
J 14-15	.005	.002
J 15-16	.004	.002
J 16-17	.004	.002
J 17-18	.002	.002
G 17-18	.001	.002
G 16-17	.004	.002
G 15-16	.004	.003
G 14-15	.006	.001
G 13-14	.006	.004
G 12-13	.006	.005
G 11-12	.006	.002
G 10-11	.007	.004
G 9-10	.004	.003
G 8-9	.003	.005
G 7-8	.004	.005
G 6-7	.003	.005
G 5-6	.007	.004
G 4-5	.003	.004
G 3-4	.003	.004
G 2-3	.007	.001
G 1-2	.005	.003
G 0-1	.008	.005

Convair F-106 - Slab Rolling  
November 2, 1962.  
T-61 Case # 12

TABLE C-2 (cont.)

Han Dill AFB

Sort	S L A B		P 2 G E L N G - S U C H	
	Wheel	# 1	Wheel	# 7
2 N-O	.004		.002	
2 M-N	.010		.004	
2 L-M	.006		.003	
2 K-L	.007		.003	
2 J-K	.006		.003	
2 I-J	.006		.003	
2 H-I	.005		.003	
2 G-H	.005		.004	
2 F-G	.005		.003	
2 E-F	.006		.004	
2 D-E	.007		.004	
2 B-C	.004		.005	
2 A-B	.002		.002	
II A-D	.003		.005	
II B-C	.009		.003	
II L-E	.005		.003	
II C-F	.024		.003	
II F-G	.001		.001	
II G-H Conv. 1	.010		.0010	
II G-H Min. 2	.005		.0010	
II H-J	.006		.003	
II I-J	.004		.003	
II J-M	.006		.003	
II K-L	.005		.003	
II L-M	.005		.002	
II M-N	.007		.005	
II N-O	.003		.005	

TEST DATA FROM WATERWAYS EXPERIMENT STATION

Data Collected with WES 16-kip vibrator  
and WES Falling Weight Deflectometer  
(Dynatest 15-kip FWD)

Table 2  
Pavement Condition Rating  
of Test Areas

<u>Test Area</u>	<u>PCI</u>	<u>Rating</u>
1	100	Excellent
2	62	Good
3	46	Fair
4	48	Fair
5	95	Excellent

Table 3  
Test Data - VES 16-Kip Vibrator

Test No.	Station or location	Date	Time	Temperature °F	DSM kips/in.	Corrected DSM kips/in.	Force lb.	Deflection - mils		
								Factor	of plate in.	Distance from center in.
1	A-1 0+12.5	2 Nov 82	14:37	6240			15,047	2.31	1.70	1.44
	A-4 0+87.5			5760			14,663	2.45	1.92	1.62
	A-7 1+02.5			5840			14,864	2.44	1.85	1.52
	A-10 2+17.5			6100			14,514	2.02	1.66	1.37
	A-13 3+12.5			6640			14,280	2.07	1.54	1.26
	A-16 3+87.5			6040			14,910	2.38	1.89	1.57
	A-19 4+62.5			5640			14,463	2.50	2.02	1.67
	A-22 5+17.5			6320			14,895	2.30	1.80	1.53
	A-25 6+12.5			6240			14,732	2.30	1.84	1.54
	A-28 6+87.5			6360			14,854	2.30	1.86	1.57
2	B-2 0+37.5			6400			15,052	2.20	1.75	1.46
	B-5 1+12.5			6280			14,031	2.14	1.71	1.43
	B-8 1+87.5			5400			14,585	2.68	1.73	1.46
	B-11 2+62.5			5560			14,691	2.62	1.57	1.31
	B-14 3+37.5			6880			14,349	2.05	1.57	1.32
	B-17 4+12.5			5440			14,715	2.67	1.80	1.51
	B-20 4+87.5			5240			14,444	2.72	1.77	1.46
	B-23 5+62.5			6920			14,925	2.14	1.70	1.42
	B-26 6+37.5			6560			14,495	2.20	1.71	1.43
	C-3 0+52.5			5400			14,223	2.58	1.92	1.63
	C-6 1+37.5			1421			14,484	2.20	1.76	1.48
	C-9 2+12.5			6360			14,091	2.19	1.68	1.40
	C-12 2+87.5			6000			14,466	2.00	1.65	1.37
	C-15 3+62.5			1423			14,672	2.36	1.80	1.51
	C-18 4+37.5			1424			14,830	2.71	2.11	1.79
	C-21 5+12.5			1425			14,704	2.06	1.58	1.28
	C-24 5+87.5			1426			14,340	3.12	1.83	1.56
	C-27 6+62.5			1427			14,614	2.39	1.85	1.57
2	T-2	0+84.8 ft lf	1 Nov 82	0458	85.8	1860	1.10	2046	4,229	1.47
									9,790	4.08
									14,480	6.63
										4.59
										2.24
										1.37

(Sheet 1 of 6)

(Continued)

Table 7 (Continued)

Test No.	Station ct	Latitude	Elevation	Rate	Time	Surface Temp. °F.	Temperature 15° °F.	Force PSI	Corrected Factor	Temperature Correlation Factor	Deflection, mils		
											Distance of plate, in.	0	16
A-5-16	1 N.W. S2	0.402	90.0		1370	1.12	1534	14,793	9.15	6.06	2.74	1.51	
A-5-16	1 N.W. S2	0.401	1420		1594	15.056	8.95	5.79	2.70	1.65			
A-5-16	1 N.W. S2	0.400	1270		1422	15.686	9.73	5.69	2.73	1.67			
A-5-16	1 N.W. S2	0.399	1356		1523	14.484	9.04	5.75	2.72	1.78			
A-5-16	1 N.W. S2	0.398	1120		1554	14,081	10.48	6.39	2.83	1.84			
A-5-16	1 N.W. S2	0.397	1540		1725	14,706	8.32	4.35	2.03	1.47			
A-5-16	1 N.W. S2	0.396	1250		1400	16,336	9.67	6.13	2.63	1.83			
A-5-16	1 N.W. S2	0.395	1110		1243	14,616	11.15	6.86	3.15	2.03			
A-5-16	1 N.W. S2	0.394	1620		1814	14,330	7.36	4.80	2.45	1.37			
A-5-16	1 N.W. S2	0.393	1670		1870	14,731	7.65	5.22	2.53	1.44			
A-5-16	1 N.W. S2	0.392	1820		2038	14,239	6.56	4.45	2.27	1.33			
A-5-16	1 N.W. S2	0.391	1860		2195	14,618	6.69	5.03	2.39	1.33			
A-5-16	1 N.W. S2	0.390	1859		1859	14,770	7.72	5.11	2.64	1.52			
A-5-16	1 N.W. S2	0.389	1660		1792	14,368	7.90	5.38	2.86	1.64			
A-5-16	1 N.W. S2	0.388	1500		1882	15,030	7.80	5.25	2.73	1.65			
A-5-16	1 N.W. S2	0.387	1886		1870	14,316	7.39	5.18	2.76	1.75			
A-5-16	1 N.W. S2	0.386	1670		1650	14,802	8.71	5.86	2.88	1.76			
A-5-16	1 N.W. S2	0.385	1460		1932	14,721	7.61	5.40	2.69	1.56			
A-5-16	1 N.W. S2	0.384	1710		2210	2509	14,553	5.99	3.52	1.75	1.19		
A-5-16	1 N.W. S2	0.383	1840		2079	14,457	7.11	4.89	2.65	1.63			
A-5-16	1 N.W. S2	0.382	1880		2124	14,739	6.97	4.65	2.62	1.55			
A-5-16	1 N.W. S2	0.381	1550		1751	14,873	8.30	6.19	2.96	1.72			
A-5-16	1 N.W. S2	0.380	1750		1729	14,830	8.37	5.88	3.12	1.78			
A-5-16	1 N.W. S2	0.379	2040		2307	14,478	6.05	4.13	2.09	1.24			
A-5-16	1 N.W. S2	0.378	2260		2531	14,893	5.87	3.84	2.00	1.22			
A-5-16	1 N.W. S2	0.377	1990		2128	14,453	6.76	4.16	2.26	1.40			
A-5-16	1 N.W. S2	0.376	1720		1675	14,074	7.60	5.03	2.75	1.68			
A-5-16	1 N.W. S2	0.375	2040		2285	14,374	6.47	4.49	2.50	1.59			
A-5-16	1 N.W. S2	0.374	2480		2778	14,495	5.48	3.23	1.92	1.43			
A-5-16	1 N.W. S2	0.373	2840		3061	14,513	6.76	4.59	2.45	1.58			
A-5-16	1 N.W. S2	0.372	2960		2128	14,344	6.77	4.71	2.71	1.65			
Center line													
(Continued)													

Table 3 (Continued)

Station Number	Date of Observation	Rate	Time		Surface Temperature °C	RSV in. hrs.	Corrected Force kg.	Temperature Correction Factor	Distance from Center of Plate, m.	Refraction index	Distance from Center of Plate, m.
			1	2							
D-100	1 Nov 62	0.04	100	100	91.0	100	100	1.00	100	100	100
D-105	1 Nov 62	0.05	105	105	91.0	105	105	1.00	105	105	105
D-110	1 Nov 62	0.06	110	110	91.0	110	110	1.00	110	110	110
D-115	1 Nov 62	0.07	115	115	91.0	115	115	1.00	115	115	115
D-120	1 Nov 62	0.08	120	120	91.0	120	120	1.00	120	120	120
D-125	1 Nov 62	0.09	125	125	91.0	125	125	1.00	125	125	125
D-130	1 Nov 62	0.10	130	130	91.0	130	130	1.00	130	130	130
D-135	1 Nov 62	0.11	135	135	91.0	135	135	1.00	135	135	135
D-140	1 Nov 62	0.12	140	140	91.0	140	140	1.00	140	140	140
D-145	1 Nov 62	0.13	145	145	91.0	145	145	1.00	145	145	145
D-150	1 Nov 62	0.14	150	150	91.0	150	150	1.00	150	150	150
D-155	1 Nov 62	0.15	155	155	91.0	155	155	1.00	155	155	155
D-160	1 Nov 62	0.16	160	160	91.0	160	160	1.00	160	160	160
D-165	1 Nov 62	0.17	165	165	91.0	165	165	1.00	165	165	165
D-170	1 Nov 62	0.18	170	170	91.0	170	170	1.00	170	170	170
D-175	1 Nov 62	0.19	175	175	91.0	175	175	1.00	175	175	175
D-180	1 Nov 62	0.20	180	180	91.0	180	180	1.00	180	180	180
D-185	1 Nov 62	0.21	185	185	91.0	185	185	1.00	185	185	185
D-190	1 Nov 62	0.22	190	190	91.0	190	190	1.00	190	190	190
D-195	1 Nov 62	0.23	195	195	91.0	195	195	1.00	195	195	195
D-200	1 Nov 62	0.24	200	200	91.0	200	200	1.00	200	200	200
D-205	1 Nov 62	0.25	205	205	91.0	205	205	1.00	205	205	205
D-210	1 Nov 62	0.26	210	210	91.0	210	210	1.00	210	210	210
D-215	1 Nov 62	0.27	215	215	91.0	215	215	1.00	215	215	215
D-220	1 Nov 62	0.28	220	220	91.0	220	220	1.00	220	220	220
D-225	1 Nov 62	0.29	225	225	91.0	225	225	1.00	225	225	225
D-230	1 Nov 62	0.30	230	230	91.0	230	230	1.00	230	230	230
D-235	1 Nov 62	0.31	235	235	91.0	235	235	1.00	235	235	235
D-240	1 Nov 62	0.32	240	240	91.0	240	240	1.00	240	240	240
D-245	1 Nov 62	0.33	245	245	91.0	245	245	1.00	245	245	245
D-250	1 Nov 62	0.34	250	250	91.0	250	250	1.00	250	250	250
D-255	1 Nov 62	0.35	255	255	91.0	255	255	1.00	255	255	255
D-260	1 Nov 62	0.36	260	260	91.0	260	260	1.00	260	260	260
D-265	1 Nov 62	0.37	265	265	91.0	265	265	1.00	265	265	265
D-270	1 Nov 62	0.38	270	270	91.0	270	270	1.00	270	270	270
D-275	1 Nov 62	0.39	275	275	91.0	275	275	1.00	275	275	275
D-280	1 Nov 62	0.40	280	280	91.0	280	280	1.00	280	280	280
D-285	1 Nov 62	0.41	285	285	91.0	285	285	1.00	285	285	285
D-290	1 Nov 62	0.42	290	290	91.0	290	290	1.00	290	290	290
D-295	1 Nov 62	0.43	295	295	91.0	295	295	1.00	295	295	295
D-300	1 Nov 62	0.44	300	300	91.0	300	300	1.00	300	300	300
D-305	1 Nov 62	0.45	305	305	91.0	305	305	1.00	305	305	305
D-310	1 Nov 62	0.46	310	310	91.0	310	310	1.00	310	310	310
D-315	1 Nov 62	0.47	315	315	91.0	315	315	1.00	315	315	315
D-320	1 Nov 62	0.48	320	320	91.0	320	320	1.00	320	320	320
D-325	1 Nov 62	0.49	325	325	91.0	325	325	1.00	325	325	325
D-330	1 Nov 62	0.50	330	330	91.0	330	330	1.00	330	330	330
D-335	1 Nov 62	0.51	335	335	91.0	335	335	1.00	335	335	335
D-340	1 Nov 62	0.52	340	340	91.0	340	340	1.00	340	340	340
D-345	1 Nov 62	0.53	345	345	91.0	345	345	1.00	345	345	345
D-350	1 Nov 62	0.54	350	350	91.0	350	350	1.00	350	350	350
D-355	1 Nov 62	0.55	355	355	91.0	355	355	1.00	355	355	355
D-360	1 Nov 62	0.56	360	360	91.0	360	360	1.00	360	360	360
D-365	1 Nov 62	0.57	365	365	91.0	365	365	1.00	365	365	365
D-370	1 Nov 62	0.58	370	370	91.0	370	370	1.00	370	370	370
D-375	1 Nov 62	0.59	375	375	91.0	375	375	1.00	375	375	375
D-380	1 Nov 62	0.60	380	380	91.0	380	380	1.00	380	380	380
D-385	1 Nov 62	0.61	385	385	91.0	385	385	1.00	385	385	385
D-390	1 Nov 62	0.62	390	390	91.0	390	390	1.00	390	390	390
D-395	1 Nov 62	0.63	395	395	91.0	395	395	1.00	395	395	395
D-400	1 Nov 62	0.64	400	400	91.0	400	400	1.00	400	400	400
D-405	1 Nov 62	0.65	405	405	91.0	405	405	1.00	405	405	405
D-410	1 Nov 62	0.66	410	410	91.0	410	410	1.00	410	410	410
D-415	1 Nov 62	0.67	415	415	91.0	415	415	1.00	415	415	415
D-420	1 Nov 62	0.68	420	420	91.0	420	420	1.00	420	420	420
D-425	1 Nov 62	0.69	425	425	91.0	425	425	1.00	425	425	425
D-430	1 Nov 62	0.70	430	430	91.0	430	430	1.00	430	430	430
D-435	1 Nov 62	0.71	435	435	91.0	435	435	1.00	435	435	435
D-440	1 Nov 62	0.72	440	440	91.0	440	440	1.00	440	440	440
D-445	1 Nov 62	0.73	445	445	91.0	445	445	1.00	445	445	445
D-450	1 Nov 62	0.74	450	450	91.0	450	450	1.00	450	450	450
D-455	1 Nov 62	0.75	455	455	91.0	455	455	1.00	455	455	455
D-460	1 Nov 62	0.76	460	460	91.0	460	460	1.00	460	460	460
D-465	1 Nov 62	0.77	465	465	91.0	465	465	1.00	465	465	465
D-470	1 Nov 62	0.78	470	470	91.0	470	470	1.00	470	470	470
D-475	1 Nov 62	0.79	475	475	91.0	475	475	1.00	475	475	475
D-480	1 Nov 62	0.80	480	480	91.0	480	480	1.00	480	480	480
D-485	1 Nov 62	0.81	485	485	91.0	485	485	1.00	485	485	485
D-490	1 Nov 62	0.82	490	490	91.0	490	490	1.00	490	490	490
D-495	1 Nov 62	0.83	495	495	91.0	495	495	1.00	495	495	495
D-500	1 Nov 62	0.84	500	500	91.0	500	500	1.00	500	500	500
D-505	1 Nov 62	0.85	505	505	91.0	505	505	1.00	505	505	505
D-510	1 Nov 62	0.86	510	510	91.0	510	510	1.00	510	510	510
D-515	1 Nov 62	0.87	515	515	91.0	515	515	1.00	515	515	515
D-520	1 Nov 62	0.88	520	520	91.0	520	520	1.00	520	520	520
D-525	1 Nov 62	0.89	525	525	91.0	525	525	1.00	525	525	525
D-530	1 Nov 62	0.90	530	530	91.0	530	530	1.00	530	530	530
D-535	1 Nov 62	0.91	535	535	91.0	535	535	1.00	535	535	535
D-540	1 Nov 62	0.92	540	540	91.0	540	540	1.00	540	540	540
D-545	1 Nov 62	0.93	545	545	91.0	545	545	1.00	545	545	545
D-550	1 Nov 62	0.94	550	550	91.0	550	550	1.00	550	550	550
D-555	1 Nov 62	0.95	555	555	91.0	555	555	1.00	555	555	555
D-560	1 Nov 62	0.96	560	560	91.0	560	560	1.00	560	560	560
D-565	1 Nov 62	0.97	565	565	91.0	565	565	1.00	565	565	565
D-570	1 Nov 62	0.98	570	570	91.0	570	570	1.00	570	570	570
D-575	1 Nov 62	0.99	575	575	91.0	575	575	1.00	575	575	575
D-580	1 Nov 62	1.00	580	580	91.0	580	580	1.00	580	580	580
D-585	1 Nov 62	1.01	585	585	91.0	585	585	1.00	585	585	585
D-590	1 Nov 62	1.02	590	590	91.0	590	590	1.00	590	590	590
D-595	1 Nov 62	1.03	595	595	91.0	595	595	1.00	595	595	595
D-600	1 Nov 62	1.04	600	600	91.0	600	600	1.00</			

卷之三

Distance from center line (m)	Series 1 (°C)	Series 2 (°C)	Series 3 (°C)	Series 4 (°C)
-100	15	15	15	15
-50	15	15	15	15
0	30	30	30	30
50	15	15	15	15
100	15	28	28	28

(Segment 2 of 6)

(Cont'd.)

Table 3 (Continued)

Test Area	Test No.	Station or Location	Date	Time	Surface Temperature °F	DSM kips/in.	Corrected DSM Factor	Temperature Correction Factor	Corrected Force kips/in.	Deflection from Center		
										0	18	36
4	5	1518	101.0	2580	1.16	2993	14.348	5.48	4.54	3.27	2.26	
	6	1520		2620		3039	14.611	5.47	4.42	3.20	2.32	
	7	1521		2160		2506	14.618	6.56	5.56	3.99	2.77	
J-6		1524		1780		2065	14.529	7.51	5.14	3.15	2.12	
	9	1532		2300		2668	14.737	6.26	5.23	3.59	2.43	
10		1542		2360		2738	14.739	6.12	5.11	3.40	2.32	
J-11		1544		1940		2250	14.432	7.04	5.64	3.74	2.56	
12		1546		2300		2668	14.966	6.34	5.22	3.62	2.53	
J-13		1547		1330		1543	14.618	10.09	7.99	4.93	3.40	
J-14		1549		1720		1995	14.571	8.07	6.90	5.33	4.18	
15		1551		1910		2216	14.535	7.46	6.25	4.45	3.32	
16		1552		2000		2320	14.735	7.19	6.04	4.46	3.08	
5	A-1	0838		2620			14.322	5.32	3.95	2.80	2.10	
E-1		0840		2780			14.184	5.05	4.21	3.06	2.17	
I-1		0840		2400			14.557	6.04	4.48	3.11	2.07	
N-1		0841		2740			14.779	5.38	4.54	3.27	2.35	
N-3		0844		2800			14.462	5.16	4.03	2.92	2.20	
J-3		0853		2520			14.574	5.59	4.55	3.23	2.31	
F-3		0855		2500			14.593	5.79	4.29	2.99	2.03	
B-3		0855		2900			14.416	4.95	4.01	2.75	1.97	
G-5		0900		2220			14.937	6.62	5.19	3.77	2.81	
K-5		0901		2380			14.619	5.80	4.46	3.09	2.21	
O-5		0903		2720			14.575	5.30	4.03	2.92	2.16	
M-7		0907		2720			14.482	5.23	4.23	2.94	2.08	
I-7		0909		2520			14.350	5.64	4.35	3.20	2.34	
F-7		0909		2360			14.650	5.76	4.43	3.09	2.14	
D-9		0920		2380			14.300	5.87	4.73	3.35	2.22	
F-9		0922		2480			14.301	5.55	4.62	3.34	2.43	
J-9		0923		2620			14.492	5.40	4.25	3.12	2.33	
O-11		0929		2760			14.893	5.24	4.20	3.17	2.44	
K-11		0939		2700			14.620	5.29	4.09	2.97	2.15	
G-11		0931		2400			14.051	5.68	4.31	3.11	2.16	

(Continued)

(Sheet 5 of 6)

Table 3 (Concluded)

Test Area	Test No.	Station or Location		Time	Temperature °F	DSN kips/in.	Corrected DSN Factor	Temperature Correction Factor	Deflection, mils		
		Date	Time						0	18	36
5	C-11	2 Nov 82	0931	2380	14,674	6.01	3.72	2.64			
	A-13	0933	2340	14,664	6.05	5.10	3.60	2.49			
	E-13	0934	2740	14,464	5.27	4.38	3.22	2.40			
	I-13	0934	2440	14,581	5.96	4.97	3.48	2.31			
	M-13	0935	2760	14,401	5.07	4.12	2.97	2.26			
	N-15	0937	2720	14,595	5.17	4.03	2.92	2.13			
	J-15	0933	2520	15,087	5.88	4.73	3.40	2.50			
	F-15	0939	2580	14,584	5.53	4.28	3.06	2.16			
	B-15	0939	2720	14,522	5.27	4.18	3.02	1.99			
	C-17	0941	2720	14,530	5.26	4.52	5.63	2.18			
	G-17	0943	2700	14,748	5.41	4.49	3.34	2.47			
	K-17	0944	2200	14,545	6.55	5.38	4.09	2.96			
	O-17	0945	2900	14,863	5.06	4.09	3.00	2.17			
	L-18	0948	2600	14,952	5.69	4.78	3.60	2.72			
	M-18	0949	2740	14,619	5.30	4.32	3.12	2.28			

(Sheet 6 of 6)

**Table 4**  
**Test Data With 16-kip Vibratory St. Joint Tests**

Test Area	Test No.	Station or Location	Date	Temp. °F	DST	Surface Elevation ft	Blade Elev./in.	Force lb	Reflected Plane, in. in. Plate, in.	Reflection, in.	
										Instantaneous Center of Plate, in.	Final Center of Plate, in.
1	TJ-1	C3-C2	2 Nov 62	1152	69.1	4720	14,770	2.93	2.32	0.79	
	TJ-2	C12-C11		1158		4700	14,872	3.47	2.16	0.61	
	TJ-3	C21-C26		1200		5720	14,403	2.64	1.62	0.69	
	TJ-4	A22-A23		1216		3620	14,735	4.20	1.93	0.66	
	TJ-5	A13-A14		1211		5800	14,575	2.40	2.09	0.81	
	TJ-6	A6-A5		1213		4900	14,743	2.62	2.35	0.83	
	TJ-7	B2-B1		1215		3760	14,582	3.03	1.59	0.79	
	TJ-8	B11-B10		1218		5520	14,523	2.55	1.89	0.74	
	TJ-9	B20-B19		1219		3600	14,597	4.08	1.58	0.79	
	TJ-10	B26-B25		1220		4560	14,325	3.06	1.45	0.66	
	TJ-11	A1-B1		1224		3660	14,368	3.82	1.77	0.67	
	TJ-12	B5-A5		1226		4080	14,479	4.11	1.98	0.69	
	TJ-13	B8-C8		1227		3650	14,854	3.71	1.58	0.63	
	TJ-14	C12-A17		1229		5040	14,525	7.86	1.88	0.67	
	TJ-15	A16-B16		1230		3840	14,697	3.67	1.39	0.45	
	TJ-16	C18-B18		1232		3700	14,281	3.78	1.47	0.48	
	TJ-17	B20-C20		1233		3620	14,156	4.09	1.35	0.43	
	TJ-18	B23-A23		1236		5700	14,493	2.47	1.75	0.71	
	TJ-19	B26-C26		1237		4900	14,928	4.65	2.18	0.58	
2	TJ-1	J15-J16		1019		2100	14,566	1.98	1.66	0.84	
						10,099	6.55	3.83	0.84		
						14,566	6.71	3.59	0.83		
	TJ-2	J17-J18		1021		1790	14,493	7.54	4.97	0.66	
	TJ-3	J9-C19		1023		2660	14,378	6.78	2.71	0.85	
	TJ-4	J6-J7		1025		1610	14,747	8.76	5.77	0.79	
	TJ-5	J3-J4		1026		1770	14,641	7.89	6.46	0.81	
	TJ-6	G5-G6		1029		1570	14,647	8.76	5.86	0.67	
	TJ-7	G8-G7		1030		1850	14,717	7.51	6.77	0.83	
	TJ-8	G11-G10		1031		1760	14,906	7.91	6.13	0.77	
	TJ-9	G14-G13		1032		1760	14,457	7.92	6.65	0.59	
	TJ-10	G17-G16		1033		2399	14,617	6.27	5.15	0.83	
	TJ-11	A1-B1		1039		1740	14,691	7.87	5.93	0.56	
	TJ-12	L1-L1		1040		1470	14,769	10.15	3.69	0.46	
	TJ-13	G1-H1		1040		1580	14,606	8.17	5.97	0.71	
	TJ-14	L1-J1		1041		1770	14,763	7.81	4.86	0.62	
	TJ-15	H1-H1		1049		1680	14,823	8.67	4.66	0.47	
	TJ-16	G11-H11		1048		1310	14,611	10.08	4.78	0.47	
	TJ-17	G11-H11		1049		1560	14,715	8.67	5.17	0.69	
	TJ-18	E11-H11		1049		1960	14,618	7.13	5.43	0.76	
	TJ-19	G11-H11		1041		1960	14,661	7.10	5.11	0.47	
3	J1	J2-J4		1052		1840	14,569	7.22	5.46	0.76	
	J2	J2		1056		2560	14,772	5.61	4.75	0.85	
	J3	J2-J2		1057		1890	14,416	7.14	5.04	0.69	
	J4	J2-J1		1058		1760	14,757	7.87	4.88	0.62	
	J5	J3-J7		1058		1680	14,527	7.96	5.56	0.70	
	J6	J2-J1		1104		1470	14,426	9.09	3.81	0.62	
	J7	J3-J2		1105		1190	14,466	9.10	7.67	0.76	

**Table 5**  
**Test Data - Falling Weight Deflectometer**

TEST AREA	TEST NO.	TEST DATE	TEST TIME	SURFACE TEMPERATURE °F	FORCE IN. 1 lb.	DEFLECTION, IN.		
						1/4	1/2	3/4
A-1	9-17-5	3-Nov-52	91.0		14,428	1.77	1.57	**
					14,769	1.73	1.56	**
					14,428	1.73	**	1.13
					14,476	1.73	**	1.14
A-4	9-17-5				14,587	2.01	1.73	**
					14,587	2.01	1.73	**
					14,506	1.89	**	1.61
					14,571	1.91	**	1.30
A-7	10-2-5	10-20	91.3		14,365	2.01	1.69	**
					14,460	2.05	1.73	**
					14,360	2.05	**	1.50
					14,317	2.01	**	1.18
A-10	7-17-5		91.0		14,476	2.05	1.54	**
					14,380	2.01	1.65	**
					14,269	2.05	**	1.57
					14,396	2.01	**	1.18
A-13	9-12-5				14,317	2.13	1.57	**
					14,412	2.09	1.57	**
					14,464	2.17	**	1.45
					14,396	2.05	**	1.18
A-16	9-17-5				14,317	2.20	1.61	**
					14,369	2.17	1.69	**
					14,253	2.17	**	1.55
					14,385	2.20	**	1.26
A-19	6-6-5		92.0		14,285	2.17	1.81	**
					14,333	2.13	1.85	**
					14,333	2.09	**	1.61
					14,317	2.17	**	1.62
A-22	5-17-5				14,365	1.97	1.69	**
					14,396	2.05	1.65	**
					14,317	2.01	**	1.57
					14,380	1.93	**	1.54
A-25	9-12-5				14,285	1.89	1.46	**
					14,285	1.77	1.54	**
					14,285	1.69	**	1.50
					14,301	1.81	**	1.42
A-28	6-6-5				14,333	1.73	1.50	**
					14,380	1.73	1.46	**
					14,285	1.69	**	1.46
					14,333	1.69	**	1.38
B-2	9-17-5				14,126	1.89	1.57	**
					14,176	1.89	1.59	**
					14,301	1.89	**	1.46
					14,253	1.85	**	1.46
B-5	10-2-5				14,476	1.85	1.65	**
					14,333	1.65	1.73	**
					14,333	1.01	**	1.57
					14,369	1.91	**	1.61

(Continued)

(Sheet 1 of 15)

Table 5 (Continued)

Test Area	Test No.	Station or Location	Date	Time	Surface Temperature °F	Force 1b	Deflection, mils				
							Distance from center of Plate, in.				
1	B-8	1+87.5	3 Nov 82		92.0	14,253	1.73	1.57	--	1.30	--
						14,333	1.73	1.57	--	1.30	--
						14,301	1.73	--	1.42	--	1.18
						14,349	1.77	--	1.50	--	1.14
B-11		2+62.5				14,158	1.61	1.50	--	1.22	--
						14,126	1.65	1.54	--	1.26	--
						14,206	1.69	--	1.54	--	1.10
						14,174	1.73	--	1.46	--	1.14
B-14		3+37.5				14,301	1.85	1.57	--	1.30	--
						14,333	1.69	1.54	--	1.30	--
						14,333	1.77	--	1.42	--	1.18
						14,365	1.73	--	1.42	--	1.22
B-17		4+12.5				14,317	1.81	1.77	--	1.38	--
						14,269	1.77	1.85	--	1.42	--
						13,936	1.81	--	1.46	--	1.22
						14,285	1.73	--	1.50	--	1.26
B-20		4+87.5				14,444	1.81	1.61	--	1.38	--
						14,460	1.85	1.65	--	1.38	--
						14,460	1.81	--	1.38	--	1.22
						14,460	1.81	--	1.42	--	1.18
B-23		5+62.5				14,365	1.73	1.42	--	1.22	--
						14,380	1.61	1.46	--	1.14	--
						14,301	1.65	--	1.30	--	1.06
						14,301	1.65	--	1.26	--	1.06
B-26		6+37.5				14,333	1.65	1.50	--	1.26	--
						14,365	1.65	1.50	--	1.26	--
						14,380	1.69	--	1.34	--	1.10
						14,365	1.65	--	1.38	--	1.10
C-3		0+62.5				14,237	1.89	1.69	--	1.42	--
						14,253	1.89	1.54	--	1.42	--
						14,269	1.89	--	1.69	--	1.34
						15,159	1.97	--	1.77	--	1.38
C-6		1+37.5				14,110	1.85	1.77	--	1.34	--
						14,222	1.85	1.85	--	1.30	--
						14,301	1.85	--	1.54	--	1.14
						14,222	1.81	--	1.50	--	1.14
C-9		2+12.5				14,094	1.65	1.54	--	1.26	--
						14,126	1.77	1.61	--	1.30	--
						14,237	1.69	--	1.26	--	1.18
						14,110	1.73	--	1.26	--	1.30
C-12		2+87.5			93.0	14,253	1.97	1.65	--	1.46	--
						14,349	1.93	1.69	--	1.46	--
						14,333	1.93	--	1.85	--	1.30
						14,380	1.93	--	1.61	--	1.18
C-15		3+62.5				14,444	1.81	1.61	--	1.34	--
						14,476	1.81	1.61	--	1.34	--
						14,221	1.81	--	1.54	--	1.22
						14,476	1.81	--	1.57	--	1.26

(Continued)

(Sheet 2 of 15)

Table 5 (Continued)

Test Area	Test No.	Station or Location	Date	Time	Surface Temperature °F	Force lb	Deflection, mils				
							0	12	24	36	48
1	C-18	4+37.5	3 Nov 82		93.0	14,174	2.20	1.81	--	1.54	--
						14,269	2.13	1.85	--	1.54	--
						14,349	2.20	--	1.61	--	1.38
						14,301	2.24	--	1.77	--	1.38
C-21	5+12.5					14,476	1.65	1.50	--	1.22	--
						14,492	1.57	1.18	--	1.26	--
						14,285	1.61	--	1.34	--	1.10
						14,460	1.61	--	1.26	--	1.14
C-24	5+87.5					13,983	1.97	1.50	--	1.18	--
						14,237	1.89	1.54	--	1.22	--
						14,285	1.93	--	1.42	--	1.10
						14,269	1.93	--	1.38	--	1.10
C-27	6+62.5		11:30			14,142	1.97	1.50	--	1.30	--
						14,333	1.97	1.61	--	1.30	--
						13,999	1.97	--	1.46	--	1.14
						14,078	1.97	--	1.42	--	1.26
2	T-2	0+84 8 ft lf	2:10	97.0		4,036	2.17	1.50	--	0.63	--
						4,052	2.24	1.54	--	0.63	--
						3,988	2.32	--	0.94	--	0.47
						4,020	2.28	--	0.94	--	0.47
						8,755	5.08	3.54	--	1.42	--
						8,771	5.04	3.54	--	1.42	--
						8,740	5.31	--	2.28	--	1.06
						8,740	5.31	--	2.28	--	1.06
						14,174	8.62	6.06	--	2.44	--
						14,253	8.70	6.10	--	2.52	--
						14,206	8.74	--	3.90	--	1.77
						14,190	8.66	--	3.86	--	1.77
A-0+00	≈22 ft lf		98.0			13,983	14.80	8.62	--	3.15	--
						14,094	14.09	8.62	--	3.19	--
						14,047	13.70	--	5.08	--	2.20
						--	--	--	--	--	--
A-1+00						14,110	12.13	8.15	--	2.87	--
						14,126	12.09	8.15	--	2.91	--
						14,047	12.52	--	4.84	--	2.01
						14,110	12.32	--	4.84	--	2.05
A-2+00			97.0			14,158	16.38	9.41	--	2.68	--
						14,126	15.63	9.25	--	2.72	--
						14,126	15.43	--	4.96	--	1.93
						14,158	15.31	--	5.04	--	1.93
A-3+00						14,078	14.57	9.02	--	2.87	--
						14,094	14.45	9.06	--	2.83	--
						14,031	15.75	--	4.92	--	--
						14,031	14.92	--	4.80	--	1.89
A-4+00						14,078	20.08	10.35	--	2.72	--
						14,126	18.90	10.08	--	2.80	--
						14,126	18.19	--	4.80	--	1.93
						14,110	18.74	--	4.96	--	1.93

(Continued)

(Sheet 3 of 15)

Table 5 (Continued)

Test Area	Test No.	Station or Location	Date	Time	Surface Temperature °F	Force lb	Deflection, mils				
							0	12	24	36	48
2	A-5+00	≈22 ft 1f	3 Nov 82		97.0	14,063	15.24	7.72	--	1.73	--
						14,078	15.00	7.72	--	1.69	--
						14,031	16.77	--	3.50	--	1.26
						14,031	15.79	--	3.43	--	1.30
A-6+00		≈22 ft 1f				14,063	19.92	10.31	--	2.83	--
						14,078	18.27	10.09	--	2.80	--
						14,063	17.68	--	4.80	--	2.01
						14,078	17.28	--	4.84	--	2.01
A-700						13,729	17.28	10.39	--	2.99	--
						14,047	17.28	10.83	--	3.03	--
						13,935	18.70	--	5.31	--	1.93
						14,031	17.80	--	5.28	--	2.01
B-0+00		≈12 ft 1f				14,963	10.28	6.97	--	2.83	--
						--	--	--	--	--	--
						14,174	10.24	--	4.41	--	1.93
						14,190	10.24	--	4.41	--	1.97
B-0+50						14,078	9.90	6.46	--	2.68	--
						14,094	9.84	6.46	--	2.68	--
						14,063	11.02	--	4.09	--	1.89
						14,047	10.16	--	4.13	--	1.93
B-1+00						14,206	9.37	5.87	--	2.52	--
						14,126	8.98	5.94	--	2.56	--
						14,142	10.00	--	3.86	--	1.81
						--	--	--	--	--	--
B-1+50						14,190	8.11	5.75	--	2.56	--
						14,221	7.99	5.75	--	2.68	--
						14,190	8.03	--	3.82	--	1.89
						14,253	7.91	--	3.86	--	1.65
B-2+00						14,237	9.12	6.65	--	2.68	--
						14,221	9.69	6.50	--	2.60	--
						14,206	9.80	--	4.09	--	1.77
						14,253	9.76	--	4.13	--	1.85
B-2+50						13,872	11.61	6.77	--	2.68	--
						14,015	11.18	6.81	--	2.72	--
						14,041	11.16	--	4.33	--	1.93
						14,176	11.18	--	4.33	--	1.93
B-3+00						14,158	9.69	5.95	--	1.73	--
						14,206	9.37	4.02	--	1.77	--
						14,174	9.41	--	6.46	--	2.52
						14,206	9.53	--	6.50	--	2.44
B-3+50						13,999	10.51	6.30	--	2.64	--
						14,063	10.29	6.34	--	2.66	--
						14,063	9.96	--	3.70	--	1.61
						14,094	9.96	--	3.98	--	1.69
B-4+00						14,190	9.65	6.56	--	2.44	--
						14,158	9.51	6.51	--	2.44	--
						14,126	9.41	--	4.06	--	1.77
						14,142	9.49	--	4.09	--	1.81
B-4+50						14,158	9.33	6.06	--	2.28	--
						14,190	9.09	6.06	--	2.30	--
						14,110	8.94	--	3.70	--	1.50
						14,174	8.94	--	3.66	--	1.61

(Continued)

(Sheet 4 of 15)

Table 5 (Continued)

Test Area	Test No.	Station or Location	Date	Time	Surface Temperature °F	Force lb	Deflection, mils				
							0	12	24	36	48
Z	B-5+00	212 ft 11	3 Nov 82	97.0	14,094	9.21	5.39	--	1.54	--	
						14,206	9.29	5.43	--	1.61	--
						14,126	9.69	--	2.80	--	1.14
						14,190	9.45	--	2.83	--	1.14
	B-5+50					14,063	8.31	5.63	--	2.44	--
						14,206	8.15	5.67	--	2.48	--
						14,206	8.11	--	3.78	--	1.77
						14,190	8.03	--	3.74	--	1.77
	B-6+00					14,158	7.40	5.47	--	2.28	--
						14,301	7.36	5.63	--	2.36	--
B	B-6+50			98.0	14,142	7.44	--	3.54	--	1.69	
						14,237	7.52	--	3.58	--	1.73
						--	10.83	7.01	--	2.80	--
						13,999	10.59	7.01	--	2.76	--
						13,983	10.39	--	4.33	--	2.05
						14,063	10.47	--	4.37	--	2.09
	B-7+00					14,094	10.08	7.20	--	2.80	--
						14,253	10.20	7.32	--	2.87	--
						14,158	10.59	--	4.76	--	2.09
						14,237	10.35	--	4.72	--	2.09
C	C-0+00	Center Line		98.0	14,126	9.02	5.04	--	2.24	--	
						14,110	8.78	5.12	--	2.20	--
						14,078	9.33	--	3.43	--	1.61
						--	--	--	--	--	--
	C-1+00					14,158	6.77	4.65	--	2.05	--
						14,206	6.81	4.65	--	2.01	--
						14,237	6.77	--	3.39	--	1.65
						14,237	6.89	--	3.07	--	1.46
	C-2+00					14,110	8.39	4.76	--	1.97	--
						14,158	8.23	5.08	--	2.20	--
C	C-3+00			98.0	14,110	8.90	--	3.31	--	1.61	
						14,094	8.58	--	3.27	--	1.69
						14,047	11.22	5.91	--	2.44	--
						14,094	10.43	5.91	--	2.48	--
						14,094	9.92	--	3.70	--	1.73
						14,078	9.72	--	3.74	--	1.73
	C-4+00					14,078	9.49	5.35	--	2.20	--
						--	--	--	--	--	--
						14,015	10.59	--	3.46	--	1.54
						14,047	9.96	--	3.46	--	1.54
C	C-5+00			98.0	13,983	8.11	4.53	--	1.81	--	
						13,999	7.83	--	1.85	--	
						14,094	7.56	--	2.91	--	1.42
						14,094	7.40	--	2.91	--	1.42
	C-6+00					13,967	9.72	4.88	--	2.13	--
						14,047	9.49	4.88	--	2.20	--
						14,047	11.50	--	3.27	--	1.61
						14,015	10.31	--	3.31	--	1.61
	C-7+00					14,110	9.49	6.30	--	2.87	--
						14,110	9.17	6.22	--	2.87	--
				2:50	14,094	9.09	--	4.13	--	2.01	
						14,063	8.98	--	4.17	--	2.01

(Continued)

(Sheet 5 of 15)

Table 5 (Continued)

Test Area	Test No.	Station or Location	Date	Time	Surface Temperature °F	Force lb	Deflection, mils			
							0	12	24	36
2	D-0+00	≈12 ft rt	3 Nov 82		97.0	14,190	9.06	6.22	--	2.44
						14,317	9.09	6.46	--	2.44
						14,301	9.02	--	3.82	--
						14,333	9.13	--	3.82	--
						14,349	10.00	6.61	--	2.36
						14,349	9.96	6.65	--	2.36
						14,206	10.12	--	3.78	--
						14,301	9.96	--	3.86	--
						14,253	8.58	5.43	--	1.97
						14,237	8.39	5.35	--	2.05
D	D-1+00					14,237	8.27	--	3.23	--
						14,158	8.31	--	3.58	--
						14,142	11.22	7.28	--	2.52
						14,174	11.10	7.36	--	2.56
						14,174	11.77	--	4.02	--
						14,174	11.42	--	4.09	--
						14,206	10.55	6.85	--	2.32
						14,269	10.35	6.69	--	2.40
						14,269	10.39	--	3.90	--
						14,285	10.31	--	3.86	--
D	D-2+00					14,110	8.50	5.75	--	2.09
						14,269	8.43	5.83	--	2.17
						14,174	8.86	--	3.27	--
						14,253	8.62	--	3.35	--
						14,174	11.38	7.09	--	2.40
						14,190	10.79	7.01	--	2.44
						14,142	10.43	--	3.82	--
						14,221	10.39	--	3.90	--
						14,158	10.31	6.61	--	2.44
						14,206	10.28	6.57	--	2.40
D	D-3+50					14,142	10.55	--	3.94	--
						14,158	10.47	--	3.94	--
						14,094	9.33	5.51	--	2.28
						14,158	9.06	5.43	--	2.20
						14,158	8.86	--	3.31	--
						14,190	8.82	--	3.39	--
						14,221	9.33	6.38	--	2.56
						14,269	9.29	6.54	--	2.60
						14,174	9.53	--	4.02	--
						14,221	9.41	--	4.06	--
D	D-4+00					14,174	9.13	5.12	--	1.73
						14,190	8.90	5.08	--	1.73
						14,126	8.70	--	2.95	--
						14,158	8.62	--	3.03	--
						14,063	9.17	6.26	--	2.64
						14,174	9.02	6.46	--	2.76
						14,126	9.84	--	4.17	--
						14,126	9.21	--	4.13	--
										2.05

(Continued)

(Page 6 of 15)

Table 5 (Continued)

Test Area	Test No.	Station or Location	Date	Time	Surface Temperature °F	Force 1b	Deflection, mils						
							0	12	24	36			
2	D-6+00	≈12 ft rt	3 Nov 82	97.0	14,110	9.92	6.10	--	2.52	--			
						14,174	9.25	6.10	--	2.56			
						14,126	8.82	--	3.78	--			
						14,206	8.86	--	3.82	--			
	D-6+50				14,047	10.20	6.50	--	2.48	--			
						14,110	10.20	6.57	--	2.48			
						14,063	10.59	--	3.98	--			
						14,078	10.31	--	3.98	--			
	D-7+00				14,110	12.56	8.03	--	2.76	--			
						14,158	12.20	7.91	--	2.80			
						14,174	11.97	--	4.61	--			
						14,174	11.97	--	4.69	--			
E	E-0+00	≈22 ft rt		97.0	14,126	12.76	8.11	--	2.83	--			
						14,094	12.68	7.99	--	2.83			
						14,047	12.95	--	4.80	--			
						--	--	--	--	--			
	E-1+00				14,063	13.43	7.68	--	2.20	--			
						14,142	12.80	7.56	--	2.24			
						14,142	12.72	--	3.94	--			
						14,158	12.64	--	3.94	--			
	E-2+00				14,078	12.91	8.11	--	2.64	--			
						14,158	12.95	8.15	--	2.72			
						14,094	13.27	--	4.53	--			
						14,094	13.07	--	4.53	--			
E	E-3+00				14,047	16.89	8.90	--	2.60	--			
						14,078	15.47	8.74	--	2.64			
						14,078	14.76	--	4.53	--			
						14,110	14.61	--	4.37	--			
	E-4+00				14,047	10.28	7.01	--	2.32	--			
						14,110	10.79	7.17	--	2.44			
						14,047	11.54	--	4.09	--			
						14,094	11.06	--	4.09	--			
E	E-5+00				14,063	12.52	7.52	--	1.97	--			
						14,110	12.09	7.32	--	1.89			
						14,110	12.05	--	3.39	--			
						14,126	11.97	--	3.43	--			
	E-6+00				14,047	15.47	9.88	--	3.23	--			
						14,078	15.35	9.84	--	3.27			
						14,031	16.61	--	5.43	--			
						14,047	16.34	--	5.51	--			
E	E-7+00				13,904	23.46	11.54	--	2.87	--			
						13,951	21.46	11.02	--	2.95			
						14,047	20.55	--	5.20	--			
						14,078	20.31	--	5.16	--			
	T-3				92.0	3,957	9.57	4.25	--	0.75			
						3,909	9.33	4.13	--	0.75			
						3,988	11.02	--	1.38	--			
						3,941	10.12	--	1.42	--			

(Continued)

(Sheet 7 of 15)

Table 5 (Continued)

Test Area	Test No.	Station or Location	Date	Time	Surface Temperature °F	Force lb	Deflection, mils				
							Distance from Center of Plate, in.				
							0	12	24	36	48
3	T-3	≈22 ft rt	3 Nov 82		92.0	8,708	18.50	9.09	--	1.69	--
						8,724	18.46	9.17	--	1.61	--
						8,708	19.65	--	3.15	--	1.22
						8,724	19.13	--	3.15	--	1.22
						14,078	27.72	14.61	--	2.56	--
						14,047	27.68	14.76	--	2.60	--
						14,047	29.13	--	5.08	--	1.85
						14,047	28.82	--	5.16	--	1.89
	A-0+50	≈12 ft lf				14,094	27.99	15.04	--	2.83	--
						14,110	24.40	14.76	--	2.91	--
						14,078	26.42	--	5.03	--	1.93
						14,126	25.98	--	5.03	--	1.89
	A-1+50					13,983	29.25	15.43	--	3.35	--
						13,999	27.72	15.28	--	3.54	--
						14,047	26.97	--	6.22	--	2.48
						14,078	26.97	--	6.46	--	2.52
	A-2+50					13,983	27.95	15.91	--	4.02	--
						13,983	27.68	15.83	--	4.13	--
						14,047	29.09	--	7.52	--	2.56
						13,983	28.39	--	7.28	--	2.30
	A-3+50					14,063	29.57	16.26	--	3.54	--
						14,470	28.23	15.83	--	3.50	--
						13,951	27.40	--	6.42	--	2.24
						14,063	27.09	--	6.38	--	2.20
	A-4+50					13,872	21.34	11.61	--	4.17	--
						13,999	21.50	11.02	--	4.21	--
						13,872	22.87	--	5.98	--	3.07
						13,904	22.28	--	6.06	--	3.07
	A-5+50					13,983	27.56	14.88	--	3.39	--
						13,935	26.42	14.53	--	3.39	--
						13,951	25.79	--	6.34	--	2.32
						13,951	25.47	--	6.34	--	2.32
	A-6+50					13,872	28.62	14.80	--	2.99	--
						13,904	28.03	14.76	--	3.11	--
						13,856	30.59	--	5.79	--	2.17
						13,920	29.29	--	5.79	--	2.20
	A-7+50					13,920	26.97	13.19	--	2.76	--
						13,888	25.55	12.87	--	2.80	--
						13,920	25.51	--	5.08	--	2.01
						13,920	25.91	--	5.18	--	2.05
	A-8+50					13,872	24.84	13.90	--	2.64	--
						13,904	25.00	13.46	--	2.60	--
						13,872	27.17	--	5.28	--	1.85
						13,920	25.67	--	5.24	--	1.89
	A-9+50					13,840	27.56	14.41	--	3.15	--
						13,888	26.85	14.29	--	3.11	--
						13,840	26.34	--	5.04	--	2.17
						13,856	26.18	--	6.02	--	2.20

(Continued)

(Sheet 8 of 15)

Table 5 (Continued)

Test	Test No.	Station or Location	Date	Time	Surface Temperature °F	Force	Deflection, mils					
							16	20	24	36	48	Distance from center of plate, in.
6-12-63	C-0-60	Center line	3 Nov 62	3:43	94.1	13,824	15.34	10.47	--	3.67	--	
						14,031	15.55	10.63	--	3.78	--	
						15,078	16.18	--	6.34	--	2.49	
						14,647	15.85	--	6.22	--	2.20	
	C-1-60				92.0	16,063	17.48	11.10	--	4.17	--	
						14,078	17.12	10.98	--	4.21	--	
						13,824	16.13	--	6.46	--	2.52	
						13,983	16.61	--	6.61	--	2.80	
	C-2-60					14,047	16.16	10.26	--	3.31	--	
						14,094	16.10	10.12	--	3.35	--	
						14,156	16.73	--	5.79	--	2.20	
						14,078	16.50	--	5.71	--	2.24	
	C-3-60					14,064	16.73	11.02	--	4.21	--	
						13,999	16.20	10.91	--	4.21	--	
						13,967	16.02	--	6.30	--	2.60	
						14,015	15.91	--	6.28	--	2.52	
	C-4-60					13,951	23.39	13.90	--	4.21	--	
						13,935	23.27	13.78	--	4.06	--	
						13,933	24.25	--	7.05	--	2.68	
						12,994	23.54	--	6.97	--	2.72	
	C-5-60			31.6		14,031	26.03	12.01	--	3.90	--	
						14,015	19.80	11.85	--	3.90	--	
						13,951	11.37	--	6.38	--	2.52	
						13,920	19.96	--	6.44	--	2.56	
	C-6-60					16,915	20.09	11.16	--	4.13	--	
						16,047	19.34	11.21	--	4.13	--	
						14,067	20.94	--	6.57	--	2.95	
						13,999	20.28	--	6.54	--	2.91	
	C-7-60					14,076	17.28	10.63	--	3.43	--	
						14,067	16.97	10.63	--	3.54	--	
						14,047	16.77	--	5.31	--	2.69	
						14,110	16.77	--	5.43	--	2.17	
	C-8-60					13,300	15.39	8.82	--	3.25	--	
						12,542	15.41	8.78	--	3.43	--	
						13,792	15.94	--	5.39	--	2.40	
						13,792	15.63	--	5.31	--	2.44	
	C-9-60					14,035	18.78	10.12	--	3.11	--	
						14,094	18.11	10.16	--	3.07	--	
						14,063	17.60	--	5.24	--	2.13	
						14,110	17.48	--	5.12	--	2.13	
	C-10-60			4:30	90.8	13,808	15.71	9.53	--	3.31	--	
						14,015	15.94	9.65	--	3.43	--	
						14,031	16.54	--	5.51	--	2.44	
						14,047	16.22	--	5.51	--	2.40	
	B-0-60	~12 TT TU			92.0	13,935	30.31	15.43	--	3.11	--	
						13,935	28.46	15.04	--	3.15	--	
						13,792	27.32	--	6.06	--	2.09	
						13,920	27.13	--	5.91	--	2.13	

(Continued)

(Sheet 9 of 15)

Table 5 (Continued)

Test Area	Test No.	Station or Location	Date	Time	Surface Temperature °F	Force lb	Deflection, mils			
							0	12	24	36
3	B-1+00	~12 ft rt	3 Nov 82		92.0	13,860	25.39	14.33	--	3.27
						13,904	24.96	14.21	--	3.31
						13,920	27.48	--	6.14	--
						13,935	26.30	--	6.22	--
	B-2+00					13,920	31.38	15.31	--	2.83
						13,935	29.88	16.00	--	2.83
						13,935	29.49	--	5.47	--
						13,935	29.02	--	5.39	--
	B-3+00					13,888	31.50	17.09	--	3.31
						13,888	30.98	17.13	--	3.33
4	B-4+00					13,872	33.94	--	6.89	--
						13,920	32.72	--	6.73	--
						13,951	34.29	18.07	--	3.62
						13,888	30.67	16.65	--	3.46
						13,792	31.30	--	7.68	--
						13,904	31.14	--	7.76	--
	B-5+00					13,935	32.32	17.36	--	3.35
						13,935	31.18	16.91	--	3.43
						13,935	30.43	--	6.97	--
						13,888	30.04	--	7.13	--
4	B-6+00					13,904	36.55	20.75	--	4.02
						13,935	30.67	17.48	--	4.02
						13,920	32.28	--	7.72	--
						13,888	31.14	--	7.87	--
	B-7+00					14,031	25.55	13.66	--	3.31
						13,983	24.72	13.54	--	3.35
						13,999	24.37	--	6.10	--
						13,983	24.13	--	6.18	--
	B-8+00					13,888	24.41	12.91	--	2.81
4						13,935	24.13	12.95	--	2.99
						13,920	25.75	--	5.47	--
						13,920	24.84	--	5.55	--
	B-9+00					13,856	27.60	13.90	--	2.56
						13,856	26.46	13.58	--	2.68
						13,872	25.47	--	5.16	--
						13,856	26.62	--	5.24	--
	B-10+00					13,792	23.62	11.57	--	2.60
						13,983	22.60	11.61	--	2.68
						13,920	23.98	--	4.76	--
4	T-4				0	13,967	25.24	--	4.76	--
						4,338	1.77	1.42	--	1.02
						4,290	1.69	1.42	--	0.98
						4,306	1.73	--	1.18	--
						4,338	1.69	--	1.18	--
						8,771	3.31	2.91	--	2.05
						9,010	3.39	2.95	--	2.13
						8,946	3.39	--	2.68	--
						9,137	3.50	--	2.52	--
										1.65

(Continued)

(Sheet 10 of 15)

Table 5 (Continued)

Test Area	Test No.	Station or Location	Date	Time	Surface Temperature °F	Force 1b	Deflection, mils				
							Distance from Center of Plate, in.				
							0	12	24	36	48
4	T-4		3 Nov 82		86.0	14,063	5.08	4.57	--	3.27	--
						14,126	5.12	4.57	--	3.31	--
						14,078	5.04	--	3.90	--	2.52
						14,126	5.08	--	3.82	--	2.60
1						14,221	5.79	5.04	--	3.46	--
						14,285	5.83	5.16	--	3.58	--
						14,206	5.83	--	4.29	--	2.87
						14,285	5.83	--	4.33	--	2.99
2						14,221	6.10	5.16	--	3.62	--
						14,221	6.02	5.16	--	3.54	--
						14,190	5.87	--	4.41	--	3.03
						14,221	5.87	--	4.25	--	2.83
J-3						14,031	7.87	4.76	--	3.15	--
						14,047	7.83	4.65	--	3.03	--
						14,078	7.83	--	3.94	--	2.44
						14,063	7.83	--	3.90	--	2.48
4			5:45			14,094	7.36	5.94	--	4.25	--
						14,126	7.32	5.98	--	4.33	--
						14,126	7.36	--	5.24	--	3.58
						14,126	7.36	--	5.24	--	3.35
5						14,078	5.79	4.84	--	3.27	--
						14,174	5.83	4.88	--	3.35	--
						14,142	5.91	--	4.29	--	2.80
						14,190	5.87	--	4.29	--	2.72
6						14,126	5.43	4.45	--	3.07	--
						14,142	5.43	4.45	--	3.11	--
						14,126	5.39	--	3.78	--	2.46
						14,158	5.31	--	3.82	--	2.48
7						13,935	7.95	5.20	--	3.46	--
						13,951	7.83	5.20	--	3.43	--
						13,967	8.43	--	4.41	--	2.91
						13,983	8.27	--	4.45	--	2.95
J-8						14,031	8.11	5.94	--	3.43	--
						14,047	8.07	5.94	--	3.50	--
						14,015	8.07	--	4.41	--	2.64
						14,031	8.03	--	4.45	--	2.60
9						13,983	7.72	6.10	--	3.70	--
						14,094	7.64	6.22	--	3.86	--
						14,063	7.76	--	4.92	--	2.95
						14,078	7.64	--	4.84	--	2.99
10						14,174	6.10	5.08	--	3.50	--
						14,206	6.06	5.20	--	3.58	--
						14,237	6.14	--	4.45	--	2.83
						14,237	6.10	--	4.45	--	2.80
J-V						14,094	6.34	5.98	--	3.50	--
						13,951	6.22	5.83	--	3.43	--
						14,031	6.30	--	4.69	--	2.72
						14,094	6.22	--	4.69	--	2.76

(Continued)

(Sheet 11 of 15)

Table 5 (Continued)

Test Area	Test No.	Station or Location	Date	Time	Surface Temperature °F	Force lb	Deflection, mils						
							Distance from Center of Plate, in.						
4	12	J-13	3 Nov 82	6:30	86.0	14,126	7.52	5.67	--	3.50	--		
						14,174	7.72	5.71	--	3.50	--		
						14,110	7.68	--	4.57	--	2.72		
						14,158	7.80	--	4.57	--	2.72		
						14,047	12.48	5.28	--	3.43	--		
						14,078	12.44	5.28	--	3.43	--		
						13,872	12.24	--	4.13	--	2.56		
						14,047	12.36	--	4.13	--	2.56		
						14,174	7.36	6.30	--	4.37	--		
						14,285	7.44	6.38	--	4.45	--		
14	15	14	15	6:30	86.0	14,221	7.40	--	5.55	--	3.58		
						14,206	7.44	--	5.51	--	3.54		
						14,047	7.60	6.38	--	4.45	--		
						14,142	7.64	6.46	--	4.45	--		
						14,078	7.56	--	5.28	--	3.62		
						14,094	7.56	--	5.28	--	3.39		
						14,174	6.30	5.28	--	3.74	--		
						14,126	6.34	5.24	--	3.70	--		
5	A-1	E-1	I-1	M-1	N-3	J-3	F-3	14,078	--	4.57	--	2.99	
								14,094	--	4.57	--	2.95	
								14,809	5.00	4.65	--	3.54	--
								14,746	4.96	4.65	--	3.50	--
								14,746	4.96	--	4.25	--	3.11
								14,714	5.00	--	4.37	--	3.15
								14,619	5.71	4.80	--	3.70	--
								14,571	5.51	4.76	--	3.66	--
								14,571	5.51	--	4.17	--	2.95
								14,603	5.71	--	4.21	--	2.99
A-1	E-1	I-1	M-1	N-3	J-3	F-3	C29	14,635	6.02	5.43	--	3.90	--
								14,539	5.94	5.47	--	3.94	--
								14,555	5.94	--	4.61	--	3.27
								14,555	5.79	--	4.65	--	3.27
								14,698	5.31	4.84	--	3.43	--
								14,651	5.20	4.88	--	3.43	--
								14,651	5.35	--	3.86	--	2.83
								14,619	5.31	--	4.06	--	2.76
								14,619	5.28	4.29	--	2.95	--
								14,365	5.24	4.29	--	2.95	--
E-1	I-1	M-1	N-3	J-3	F-3	C29	(Sheet 12 of 15)	14,508	4.92	--	3.46	--	2.52
								14,571	4.84	--	3.50	--	2.48
								14,524	5.28	4.80	--	3.31	--
								14,619	5.35	4.72	--	3.31	--
								14,651	5.35	--	4.25	--	2.80
								14,651	5.35	--	4.21	--	2.80
								14,714	5.20	4.88	--	3.50	--
								14,698	5.20	4.84	--	3.50	--
								14,666	5.20	--	4.21	--	3.03
								14,603	5.24	--	4.21	--	2.99

(Continued)

(Sheet 12 of 15)

Table 5 (Continued)

Test Area	Test No.	Station or Location	Date	Time	Surface Temperature °F	Force lb	Deflection, inches				
							Distance from Center of Plate, in.				
							0	12	24	36	48
5	B-3		3 Nov 82		81.0	14,619	5.16	4.41	--	3.97	--
						14,603	5.12	4.53	--	3.23	--
						14,555	5.16	--	3.90	--	2.60
						14,635	5.04	--	3.90	--	2.56
	G-5					14,444	5.98	5.39	--	3.90	--
						14,508	6.02	5.43	--	3.90	--
						14,555	5.98	--	4.72	--	3.23
						14,476	5.94	--	4.72	--	3.23
	K-5					14,539	5.31	4.65	--	3.22	--
						14,492	5.35	4.72	--	3.27	--
						14,555	5.28	--	3.98	--	2.68
						14,555	5.39	--	3.98	--	2.68
	O-5				82.0	14,508	4.92	4.37	--	2.87	--
						14,523	4.88	4.37	--	2.80	--
						14,539	4.96	--	3.74	--	2.60
						14,476	4.80	--	3.74	--	2.36
	M-7					14,444	4.92	4.45	--	3.03	--
						14,476	4.92	4.45	--	3.15	--
						14,428	5.12	--	3.70	--	2.68
						14,476	5.00	--	3.74	--	2.64
	I-7					14,444	5.04	4.57	--	3.27	--
						14,396	5.08	4.61	--	3.27	--
						14,412	5.08	--	4.02	--	2.91
						14,444	5.08	--	3.94	--	2.91
	F-7					14,253	5.67	4.96	--	3.35	--
						14,285	5.79	5.09	--	3.35	--
						14,333	5.55	--	4.25	--	2.86
						14,317	5.61	--	4.25	--	2.80
	D-9					14,253	5.71	5.16	--	3.23	--
						14,253	5.71	5.16	--	3.21	--
						14,174	5.83	--	4.29	--	2.99
						14,221	5.83	--	4.61	--	2.87
	F-9				83.0	14,396	5.39	4.88	--	3.39	--
						14,396	5.47	4.88	--	3.43	--
						14,365	5.35	--	4.06	--	2.80
						14,380	5.35	--	4.09	--	2.83
	J-9					14,365	5.04	4.53	--	3.54	--
						14,365	5.00	4.61	--	3.58	--
						14,285	5.08	--	3.94	--	3.23
						14,349	5.08	--	4.09	--	3.19
	O-11					14,333	4.61	4.29	--	3.07	--
						14,380	4.69	4.29	--	3.11	--
						14,333	4.53	--	3.82	--	2.80
						14,412	4.61	--	3.78	--	2.80
	K-11				84.0	14,285	5.51	4.21	--	3.23	--
						14,221	5.35	4.37	--	3.19	--
						14,206	5.28	--	3.82	--	2.44
						14,199	5.28	--	4.06	--	2.72
	G-11					14,190	4.92	4.88	--	3.27	--
						14,237	4.99	4.92	--	3.27	--
						14,253	5.09	--	4.05	--	2.72
						14,206	4.99	--	4.02	--	2.72

(Continued)

(Sheet 13 of 15)

Table 5 (Continued)

Test Area	Test No.	Station or Location	Date	Type	Surface Temperature °F	Time 10	Reflected Heat Distance from Platform (ft)				
							16	12	8	4	0
S-C-11	3-Nov-82	86.0			14,189	5.28	**	**	3.5	**	
					14,428	5.28	4.94	**	3.5	**	
					14,444	5.39	**	4.53	**	2.72	
					14,460	5.35	**	4.61	**	2.87	
A-13					14,174	6.18	5.20	**	3.45	**	
					14,221	6.16	5.28	**	3.53	**	
					14,126	6.10	**	4.45	**	2.95	
					14,158	6.16	**	4.59	**	2.87	
E-13		85.0			14,378	5.08	4.95	**	3.11	**	
					14,692	5.09	4.49	**	3.12	**	
					14,612	5.09	**	3.78	**	2.64	
					14,612	5.04	**	3.86	**	2.66	
I-13					14,396	5.67	4.84	**	3.31	**	
					14,313	5.51	4.88	**	3.21	**	
					14,349	5.83	**	4.69	**	2.76	
					14,285	5.61	**	4.21	**	2.76	
H-13					14,158	6.88	6.37	**	3.31	**	
					14,174	6.96	6.45	**	3.25	**	
					14,206	5.03	**	3.95	**	2.87	
					14,158	6.96	**	3.99	**	2.91	
B-15					14,676	6.86	6.21	**	3.62	**	
					14,598	6.72	6.25	**	3.6	**	
					14,571	6.76	**	3.74	**	2.57	
					14,581	6.84	**	3.74	**	2.56	
J-15					14,217	5.20	4.49	**	3.07	**	
					14,237	5.29	4.45	**	3.07	**	
					14,190	5.28	**	3.86	**	2.56	
					14,271	5.31	**	3.86	**	2.50	
I-15					14,206	5.08	4.57	**	3.13	**	
					14,158	4.96	4.67	**	3.11	**	
					14,301	5.06	**	4.79	**	2.66	
					14,190	5.00	**	4.96	**	2.50	
B-15		86.0			14,460	5.28	4.65	**	3.31	**	
					14,476	5.28	4.69	**	3.33	**	
					14,444	5.35	**	4.21	**	2.68	
					14,444	5.24	**	4.13	**	2.70	
C-17					14,365	5.24	4.45	**	3.11	**	
					14,347	5.35	4.53	**	3.11	**	
					14,285	5.39	**	3.70	**	2.52	
					14,253	5.31	**	3.82	**	2.52	
G-17					14,206	5.08	4.53	**	3.12	**	
					14,190	5.08	4.61	**	3.13	**	
					14,285	5.00	**	3.74	**	2.68	
					14,190	4.96	**	3.76	**	2.60	
E-17					14,389	5.20	4.04	**	3.50	**	
					14,444	5.28	4.04	**	3.53	**	
					14,349	5.35	**	3.99	**	2.80	
					14,365	5.41	**	4.09	**	2.83	
L-18					14,361	4.86	4.21	**	2.91	**	
					14,369	4.84	4.25	**	2.91	**	
					14,301	4.88	**	3.58	**	2.44	
					14,678	4.92	**	3.66	**	2.49	

(Continued)

(Collect 1-17-15)

Table 5 (Concluded)

Test Area	Test No.	Station or Location	Date	Time	Surface Temperature °F	Force lb	Deflection, mils						
							0	12	24	36			
S	H-18		3 Nov 82	86.0	14,317	4.72	4.29	--	3.03	--			
						4.65	4.21	--	3.03	--			
						4.76	--	3.46	--	2.52			
						4.69	--	3.62	--	2.52			
	J-6			87.0	4,211	1.50	1.34	--	1.10	--			
						1.57	1.42	--	0.94	--			
						1.54	--	1.14	--	0.75			
						1.38	--	1.14	--	0.79			
S	H-18		3 Nov 82	91.0	9,153	3.07	2.95	--	2.01	--			
						3.15	2.83	--	2.01	--			
						3.07	--	2.40	--	1.77			
						3.15	--	2.44	--	1.77			
	J-6				14,206	4.76	4.45	--	2.87	--			
						4.76	4.41	--	2.87	--			
						4.76	--	3.62	--	2.64			
						4.80	--	3.58	--	2.64			

(Sheet 15 of 15)

Table 6  
Test Data - Falling Weight Deflectometer - Joint Tests

Test Area	Test No.	Station or Location	Date	Time	Surface Temperature °F	Force lb	Deflection, mils			Deflection Ratio
							0	12	36	
1	TJ-1	C3-C2	3 Nov 82		91.0	14,349	2.80	2.24	1.69	0.80
						14,316	2.68	2.20	1.65	0.82
	TJ-2	C12-C11			90.0	14,412	2.68	2.44	1.69	0.91
						14,412	2.68	2.36	1.65	0.88
	TJ-3	C21-C20			90.0	14,459	2.52	1.81	1.38	0.72
						14,444	2.52	1.77	1.38	0.70
	TJ-4	A22-A23			87.0	14,428	2.87	1.93	1.50	0.67
						14,476	2.87	1.93	1.54	0.67
	TJ-5	A13-A14			86.5	14,476	2.48	2.20	1.54	0.89
						14,492	2.48	2.20	1.50	0.89
	TJ-6	A4-A5				14,380	2.60	2.36	1.77	0.90
						14,555	2.60	2.36	1.77	
	TJ-7	B2-B1			88.0	14,492	5.39	1.10	0.91	0.20
						14,476	5.39	1.06	0.87	0.20
	TJ-8	B11-B10			87.0	14,460	3.27	1.42	1.06	0.43
						14,396	3.19	1.38	1.06	0.43
	TJ-9	B20-B19			87.0	14,237	5.24	1.38	1.10	0.26
						14,221	5.28	1.54	1.10	0.29
	TJ-10	B26-B25			87.0	14,523	3.66	1.26	1.02	0.34
						14,317	3.62	1.34	0.98	0.37
	LJ-11	A1-B1			88.0	14,444	2.91	2.17	1.54	0.75
						14,539	2.91	2.17	1.50	0.75
	LJ-12	B5-A5			88.0	14,444	3.86	1.69	1.22	0.44
						14,317	3.66	1.57	1.18	0.43
	LJ-13	B8-C8			88.0	14,396	4.13	1.34	0.98	0.32
						14,460	4.13	1.34	1.02	0.32
	LJ-14	C12-B12			89.0	14,301	3.27	1.93	1.42	0.59
						14,428	3.19	1.89	1.42	0.59
	LJ-15	A16-B16			89.0	14,476	4.69	1.26	1.02	0.27
						14,364	4.69	1.30	1.06	0.27
	LJ-16	C18-B18			89.0	14,333	5.35	1.54	1.22	0.29
						14,365	5.28	1.54	1.18	0.29
	LJ-17	B20-C20			89.0	14,365	5.39	1.22	1.02	0.23
						14,396	5.43	1.22	0.98	0.23
	LJ-18	B23-A23			90.0	14,285	2.87	1.77	1.34	0.62
						14,396	2.87	1.69	1.30	0.56
	LJ-19	B26-C26			90.0	14,285	2.56	2.09	1.46	0.82
						14,428	2.56	2.05	1.42	0.80
5	TJ-1	J15-J16			87.0	14,285	9.09	5.51	3.19	0.61
						14,317	8.98	5.39	3.15	0.60
	TJ-2	J12-J13			87.0	14,253	11.46	3.11	2.17	0.27
						14,269	11.50	3.03	2.17	0.26

(Continued)

Table 6 (Concluded)

Test Area	Test No.	Station or Location	Date	Time	Surface Temperature °F	Force lb	Deflection, mils			Deflection Ratio	
							0	12	36		
5	TJ-3	J9-J10	3 Nov 82	0930	87.0	14,269	8.31	7.28	4.09	0.88	
						14,317	8.27	7.24	4.02	0.88	
	TJ-4	J6-J7			87.0	14,237	12.95	3.11	2.24	0.24	
						14,237	12.91	3.11	2.17	0.24	
	TJ-5	J3-J4			87.0	14,349	10.00	6.22	3.66	0.62	
						14,396	9.96	6.26	3.62	0.63	
	TJ-6	G5-G4			87.0	14,285	13.94	3.03	2.09	0.22	
						14,269	15.94	3.03	2.09	0.22	
	TJ-7	G8-G7			86.0	14,349	11.65	6.69	3.62	0.57	
						14,380	11.69	6.73	3.70	0.58	
	TJ-8	G11-G10			86.0	14,333	11.97	4.61	2.87	0.39	
						14,221	11.85	4.57	2.87	0.39	
	TJ-9	G14-G13			86.2	14,253	11.02	5.71	3.46	0.52	
						14,301	10.91	5.75	3.43	0.53	
	TJ-10	G17-G16			86.0	14,317	7.36	5.39	3.19	0.73	
						14,380	7.32	5.39	3.15	0.74	
	LJ-11	A1-B1			78.0	14,587	13.03	3.70	2.24	0.28	
						14,603	12.91	3.35	2.13	0.26	
	LJ-12	E1-F1			79.0	14,682	16.54	2.91	1.97	0.18	
						14,635	16.42	2.95	2.01	0.18	
	LJ-13	G1-H1			79.0	14,746	14.53	4.45	2.83	0.31	
						14,682	14.45	4.53	2.87	0.31	
	LJ-14	I1-J1			79.0	14,619	15.63	4.17	2.76	0.27	
						14,555	15.51	4.21	2.80	0.27	
	LJ-15	M1-N1			80.0	14,555	12.80	2.72	1.97	0.21	
						14,571	12.72	2.72	1.97	0.21	
	LJ-16	C11-B11			84.0	14,269	13.98	3.46	2.24	0.25	
						14,206	13.78	3.50	2.28	0.25	
	LJ-17	G11-F11			84.0	14,365	13.31	3.43	2.28	0.26	
						14,365	13.03	3.43	2.24	0.26	
	LJ-18	K11-J11			83.0	14,253	13.23	3.66	2.44	0.28	
						14,253	13.31	3.70	2.32	0.28	
	LJ-19	O11-N11			0900	83.3	14,269	12.99	2.36	1.77	0.18
						14,253	13.11	2.36	1.77	0.18	

Table 7  
Air Temperature Data

Date 1982	Maximum Temperature °F	Minimum Temperature °F
20 Oct	85	68
21 Oct	84	69
22 Oct	84	70
23 Oct	72	63
24 Oct	68	56
25 Oct	72	52
26 Oct	75	53
27 Oct	78	58
28 Oct	81	62
29 Oct	82	65
30 Oct	83	68
31 Oct	82	71
1 Nov	84	68
2 Nov	84	66
3 Nov	83	71